Synthetic hydrogels as instructive microenvironments for human mesenchymal stromal cell expansion

By

Ngoc Nhi T. Le

A dissertation submitted in partial fulfillment of

the requirements for the degree of

Doctor of Philosophy

(Materials Science)

at the

UNIVERSITY OF WISCONSIN-MADISON

2019

Date of final oral examination: August 30th, 2019

The dissertation is approved by the following members of the Final Oral Committee:

- William L. Murphy, Harvey D. Spangler Professor, Biomedical Engineering (Chair)
- Randolph Ashton, Assistant Professor, Biomedical Engineering
- Padma Gopalan, Professor, Materials Science & Engineering
- Hau D. Le, Assistant Professor, Surgery
- Wan-Ju Li, Associate Professor, Biomedical Engineering
- Sean P. Palecek, Milton J. and A. Maude Shoemaker Professor, Chemical & Biological Engineering

Abstract

Human mesenchymal stromal cells (hMSCs) are appealing for cell therapies because they possess potent immunomodulatory properties, secrete cytokines and growth factors (GFs) to support tissue regeneration, and can differentiate into various cell types for tissue replacement; however, hMSCs constitute <0.01% of bone marrow mononuclear cells, therefore *in vitro* expansion is needed to generate sufficient numbers for clinical and research applications. Current hMSC biomanufacturing processes exist for generating small numbers of cells for research and initial clinical studies; however, widespread therapeutic utility will require materials and processes designed specifically to address the challenges of commercial scale up. Current small-scale hMSC biomanufacturing processes are plagued with low reproducibility, high cost, and poor understanding of how *in vitro* culture parameters affect cell behavior and subsequently *in vivo* efficacy. To address these challenges, we have developed enhanced throughput screening methods and benchtop amenable hydrogel screening array technologies to systematically probe how culture parameters (namely substrate stiffness, substrate adhesivity, GF regulation, and media formulation) affect hMSC behavior *in vitro*. Using this screening approach, we developed customized hydrogel substrates with tunable stiffness, adhesivity, and GF regulation capabilities for functional hMSC expansion in serum-containing and serum-free media. We performed multivariate analysis of the screening results to gain insight into how culture parameters independently and combinatorially affect hMSC behavior and use those insights to develop materials for enhanced hMSC expansion. We developed hydrogel substrates with tunable stiffness and adhesivity to increase hMSC expansion and modulate differential GF secretion. Finally, we developed substrates with added GF sequestering functionality to sequester

exogenous recombinant GFs supplemented into the growth media as well as endogenous hMSC-secreted GFs to enhance hMSC expansion without the need for induction via additionally supplemented GFs. Taken together, the screening method, platforms, and customized substrates identified from this approach represent adaptable tools and processes that allow systematic study of how culture parameters affect hMSC behavior. The concepts discussed in this thesis work can more broadly be applied to develop customized processes for more efficient, cost-effect hMSC biomanufacturing.

Dedication and Acknowledgements

To dad, mom, sis, and Kev.

Con trao tất cả tình thương của con cho ba, mẹ, chị, và em.

Thank you so much to my thesis advisor, Bill Murphy, for the unwavering show of support, wisdom, understanding, and guidance. Above all, thank you so much for encouraging me to approach my training in a holistic, application- and impact-driven way. I'll never be able to find the words to sufficiently describe how you've changed my life.

I'm so thankful to my current and former colleagues in the Bioninspired Materials Lab for helping me find my way, teaching me the fundamentals of research, and sharing your personal and professional time and life with me.

Thank you so much to my committee members, Padma Gopalan, Wan-Ju Li, Hau Le, Randolph Ashton, and Sean Palecek for generously sharing your time, insight, advice, and mentorship. Thank you for working on an unusual timeline to help me on my way!

I've been so blessed to have many funding and professional opportunities that have opened doors and expanded my mind and heart. The Gates Millennium Scholars Program (GMSP) has supported me for the last 10 years and provided me with a national, powerful, network of like-minded minorities who've become lifelong friends and mentors. The University of Wisconsin-Madison Graduate Engineering Research Scholars (GERS) Program has created an incredibly diverse, inclusive, and loving community of friends. Specifically, thank you to GERS for the second family I've found in Kelly, Doug, Dinh, Chandler, Heidi, Richard, and Jose. The National Science Foundation Graduate Research Fellowship Program and the National Science Foundation Engineering Research Center for Cell Manufacturing Technologies (CMaT) have both provided

me with an international network of research collaborators and mentors. The Wisconsin Alumni Research Foundation has helped me learn academic tech transfer and commercialization. The gener8tor, Doyenne, and StartingBlock teams took a major chance on me and gave me a way to learn venture capital and startup mentoring. Special thanks to Diana Rhoads and Ray Vanderby for making the Materials Science Program such an incredibly phenomenal program and training.

Finally, I've been so incredibly blessed to have received so much love and kindness from family, friends, and strangers who've all come into my life and made all the difference. In lieu of listing all your names, I'll come give you the biggest hug of 2019!

Table of Contents

List of Figures and Tables

Chapter 1 – Introduction

1.1. Background and Significance

Human mesenchymal stromal cells (hMSCs) are appealing candidates for cell therapies and tissue engineering because they possess potent immunomodulatory properties, secrete cytokines and growth factors (GFs) to support tissue regeneration, and can differentiate into various cell types for tissue replacement [1-3]. hMSCs constitute 0.001-0.01% of bone marrow mononuclear cells, therefore *in vitro* expansion is needed to generate sufficient numbers for clinical and research applications [3]. While biomanufacturing methods currently exist for generating sufficient cell supply for initial clinical studies, widespread clinical applicability will require new materials and methods designed specifically to address the challenges of commercial scale up: low reproducibility, high cost, and high labor and time requirements [4, 5]. Here, we propose the development of customized chemically-defined substrates for hMSC culture in order to improve our understanding of how *in vitro* culture parameters affect cell behavior and subsequently use these materials to control for desired biomanufacturing outputs (e.g. increased expansion rates or growth factor secretion). Through this approach, we will focus the work to demonstrate the ability to use materials engineering as means for increasing biomanufacturing reproducibility and reducing cost.

In current cell biomanufacturing protocols, hMSCs are expanded on tissue culture polystyrene (TCPS) in growth media containing fetal bovine serum (FBS) supplement. Here, the TCPS is a permissive support substrate that enables hMSC adhesion while soluble factors in the growth media are instructive and regulate hMSC function and growth. While it is widely accepted that soluble signals (e.g. growth factors and cytokines) are major regulatory players, research has

demonstrate that hMSC behavior can also be influenced by insoluble substrate signals such as GF-sequestering capabilities of the extracellular matrix as well as stiffness and adhesion-promoting properties of the microenvironment [6-18].

Regulation of cell behavior involves complex relationships between soluble factors, immobilized cell adhesive signals, and mechanical signals found in the cell's microenvironment [6-19]. While the effects of soluble signals on hMSC behavior in culture have been widely studied, there is less known about the effects of substrate properties on hMSC function and even less is understood about the positive feedback loops activated as cells sense and respond to their extracellular microenvironment. The microenvironment and the cell's response to extracellular signals is dynamic and interdependent. While soluble and mechanical signals can individually instruct hMSC behavior, the signaling pathways they activate often converge to synergistically regulate hMSC function and serve as feedback loops for each other. As cells receive extracellular signals, intracellular signaling pathways are activated and inactivated to enable cellular responses that span from changes in gene expression to differential GF and enzyme secretion that dynamically remodel their microenvironment [10, 11, 13, 14, 20-26].

In the past two decades, researchers have demonstrated that cells sense and respond to changes in matrix stiffness by modulating cytoskeletal assembly and contractility (a concept referred to as "mechanosensing") via activation of intracellular signaling pathways involved in survival, growth and differentiation [9, 13, 14]. Substrate stiffness, cell adhesion molecule affinity, and cell adhesion molecule density have been shown to influence hMSC survival, expansion, GF secretion, and differentiation [9-12, 14-18, 27, 28]. For example, several studies have demonstrated that soft substrates promote hMSC adipogenic commitment while stiff substrates promote hMSC proliferation and osteogenic commitment [13, 15, 29]. We and others

have demonstrated increased hMSC attachment, spreading, and proliferation with increasing substrate stiffness and adhesivity [10, 11, 13, 14, 20, 21]. These studies demonstrated controlled hMSC behavior by regulating mechanosensing: hMSCs cultured on surfaces that promoted high cytoskeletal tension possessed well-defined focal adhesion and were more well-spread, proliferative, and likely to undergo osteogenic differentiation [9-13].

To address the challenges associated with TCPS use, we and others have developed a variety of biomimetic synthetic surfaces for controllable cell adhesion to enable mechanistic understanding of interactions at the cell-materials interface. Examples include self-assembled monolayers (SAMs) or poly (ethylene glycol) (PEG) hydrogels presenting immobilized RGD or IKVAV peptides (adhesion-promoting molecules derived from fibronectin and laminin, insoluble proteins found in the ECM)[18, 30-32]. These non-fouling surfaces resist non-specific protein adsorption and serve as bioinert blank templates whereby bioactivity can be conferred by covalently immobilizing bioreactive molecules to the surface. In addition to adhesion, synthetic surfaces can also be designed to mimic the GF-regulating capability of the ECM by selectively sequestering specific growth factors (GFs) at 2-dimentional (2D) interfaces. For example, SAMs presenting RGD in combination with HEPpep or TYRSRKY (peptides derived from the heparin-binding domain of basic fibroblast growth factor, FGF2) enabled controlled hMSC adhesion and increased expansion in heparin-containing, serum-free medium supplemented with recombinant FGF2 [30-32]. In recent years, as the mechanosensing mechanisms have been more clearly elucidated, we and others have also developed biomimetic synthetic culture surfaces of varying stiffness and presenting adhesion-promoting peptides in order to examine the combinatorial influences of both adhesivity and mechanical stiffness on cell behavior [13, 33]. In order to more fully recapitulate the functions of the ECM, research is shifting towards combining several

elements of the aforementioned surfaces to develop culture substrates capable of providing a comprehensive array of adhesion, mechanical, and GF-regulating signals to the cells.

In this thesis, we utilize high throughput screening techniques to develop chemically-defined, customized biomaterials for cell culture to study the effects of substrate stiffness, adhesivity, and GF regulation on hMSC adhesion, survival, and proliferation during *in vitro* culture. We use these techniques and screening hydrogel array platforms to examine the mechanisms by which the cells interact with their environment. Finally, we also use these insights to develop culture substrates that amplify hMSC responses to extracellular signals to enhance hMSC expansion without the need for additionally supplemented GFs.

The proposed work is innovative as it enables understanding of how *in vitro* culture parameters affect hMSC behavior and establishes a role for biomaterials as inductive substrates capable of not only modulating cell behavior but also serving as mediators of GF signaling to further amplify and catalyze substrate-induced behavioral changes. Additionally, this work demonstrates the potential for developing and using instructive biomaterials substrates as a method for regulating hMSC behavior without the need for supplemented GFs, potentially leading to increased biomanufacturing efficiency, speed, and cost reduction.

In chapter 3, we develop differential wettability patterning techniques for hydrogel array formation and demonstrate the ability to use this array for examining the influence of substrate stiffness and adhesivity on hMSC behavior. This enhanced-throughput method is benchtop amenable and can be performed without the need for liquid handling systems, characteristics that are particularly important for low barrier-to-adoption of the screening technique and enabling technology transfer to other academic and industrial collaborators.

In chapter 4, we examine the influence of culture parameters (namely culture media formulation, substrate stiffness, and substrate adhesivity) on hMSC adhesion and expansion. We use design of experiment (DOE) to develop a screening method that enables the examination of 144 different substrate compositions to identify customized hydrogel substrates that enables hMSC expansion in serum-containing and serum-free culture. Using this screening data, we perform multivariate analysis (MVA) to determine the individual and combinatorial effects of culture parameters on hMSC expansion.

In chapter 5, we use the aforementioned screening methods and MVA insights to develop GF-sequestering materials that amplify substrate stiffness-induced changes in hMSC behavior. These GF-sequestering substrates are autocatalytic; stiffness increase hMSC expansion and VEGF secretion while VEGF-sequestering capabilities built into the substrate amplified and further promoted increased GF signaling and hMSC expansion. With this autocatalytic, GF-sequestering biomaterial, we demonstrate the use of the substrate to both induce and further escalate the cell response. Additionally, we further build on the concept of biomimicry previously established in our lab to explore the concept of endogenous GF regulation as a method for reducing the need for exogenously supplemented GF.

In future studies, the screening methods and techniques developed in this thesis can serve as a tool to customize materials substrate for desired optimizing cell biomanufacturing outputs of not only hMSCs, but also several other cell types. In Chapter 6 of this work, we've preliminarily demonstrated the ability to use these methods for customizing materials for pluripotent cell culture and pluripotency maintenance, endothelial cell tubulogenesis, and mouse-derived MSC derivation – all possible without additional supplemented GFs.

1.2 References

[1] M. Rodrigues, L.G. Griffith, A. Wells, Growth factor regulation of proliferation and survival of multipotential stromal cells, Stem Cell Research & Therapy 1(4) (2010) 32-32.

[2] M.F. Pittenger, A.M. Mackay, S.C. Beck, R.K. Jaiswal, R. Douglas, J.D. Mosca, M.A. Moorman, D.W. Simonetti, S. Craig, D.R. Marshak, Multilineage Potential of Adult Human Mesenchymal Stem Cells, Science 284(5411) (1999) 143-147.

[3] G. Chamberlain, J. Fox, B. Ashton, J. Middleton, Concise Review: Mesenchymal Stem Cells: Their Phenotype, Differentiation Capacity, Immunological Features, and Potential for Homing, STEM CELLS 25(11) (2007) 2739-2749.

[4] N.c.M. Consortium, Achieving Large-Scale, Cost-Effective, Reproducible Manufacturing of High-Quality Cells: A Technology Roadmap to 2025, National cell Manufacturing Consortium, http://www.cellmanufacturingusa.org, 2016.

[5] A. Aijaz, M. Li, D. Smith, D. Khong, C. LeBlon, O.S. Fenton, R.M. Olabisi, S. Libutti, J. Tischfield, M.V. Maus, R. Deans, R.N. Barcia, D.G. Anderson, J. Ritz, R. Preti, B. Parekkadan, Biomanufacturing for clinically advanced cell therapies, Nat Biomed Eng 2(6) (2018) 362-376.

[6] Y. Sun, C.S. Chen, J. Fu, Forcing stem cells to behave: a biophysical perspective of the cellular microenvironment, Annual review of biophysics 41 (2012) 519-42.

[7] S. Gobaa, S. Hoehnel, M. Roccio, A. Negro, S. Kobel, M.P. Lutolf, Artificial niche microarrays for probing single stem cell fate in high throughput, Nature methods 8(11) (2011) 949-55.

[8] D.E. Discher, D.J. Mooney, P.W. Zandstra, Growth factors, matrices, and forces combine and control stem cells, Science 324(5935) (2009) 1673-1677.

[9] A.J. Engler, L. Bacakova, C. Newman, A. Hategan, M. Griffin, D.E. Discher, Substrate Compliance versus Ligand Density in Cell on Gel Responses, Biophysical journal 86(1) (2004) 617-628.

[10] J.T. Koepsel, S.G. Loveland, M.P. Schwartz, S. Zorn, D.G. Belair, N.N. Le, W.L. Murphy, A chemically-defined screening platform reveals behavioral similarities between primary human mesenchymal stem cells and endothelial cells, Integrative biology : quantitative biosciences from nano to macro 4(12) (2012) 1508-21.

[11] K.A. Kilian, M. Mrksich, Directing stem cell fate by controlling the affinity and density of ligand-receptor interactions at the biomaterials interface, Angewandte Chemie 51(20) (2012) 4891-5.

[12] J. Lee, A.A. Abdeen, D. Zhang, K.A. Kilian, Directing stem cell fate on hydrogel substrates by controlling cell geometry, matrix mechanics and adhesion ligand composition, Biomaterials 34(33) (2013) 8140-8.

[13] N.N.T. Le, S. Zorn, S.K. Schmitt, P. Gopalan, W.L. Murphy, Hydrogel arrays formed via differential wettability patterning enable combinatorial screening of stem cell behavior, Acta Biomaterialia (2015).

[14] A.K. Jha, K.E. Healy, Controlling Osteogenic Stem Cell Differentiation via Soft, PLOS ONE 9(6) (2014) 1-11.

[15] A.A. Abdeen, J.B. Weiss, J. Lee, K.A. Kilian, Matrix Composition and Mechanics Direct Proangiogenic Signaling from Mesenchymal Stem Cells, Tissue Engineering. Part A 20(19-20) (2014) 2737-2745.

[16] D.S. Benoit, K.S. Anseth, Heparin functionalized PEG gels that modulate protein adsorption for hMSC adhesion and differentiation, Acta Biomater 1(4) (2005) 461-70.

[17] D.G. Belair, N.N. Le, W.L. Murphy, Design of growth factor sequestering biomaterials, Chem Commun (Camb) 50(99) (2014) 15651-68.

[18] W.L. Murphy, T.C. McDevitt, A.J. Engler, Materials as stem cell regulators, Nat Mater 13(6) (2014) 547-557.

[19] O.Z. Fisher, A. Khademhosseini, R. Langer, N.A. Peppas, Bioinspired materials for controlling stem cell fate, Accounts of chemical research 43(3) (2010) 419-28.

[20] S.K. Schmitt, W.L. Murphy, P. Gopalan, Crosslinked PEG mats for peptide immobilization and stem cell adhesion, Journal of Materials Chemistry B 1(9) (2013) 1349.

[21] S. Lin, N. Sangaj, T. Razafiarison, C. Zhang, S. Varghese, Influence of physical properties of biomaterials on cellular behavior, Pharmaceutical research 28(6) (2011) 1422-30.

[22] M.M.L. Deckers, M. Karperien, C. van der Bent, T. Yamashita, S.E. Papapoulos, C.W.G.M. Löwik, Expression of Vascular Endothelial Growth Factors and Their Receptors during Osteoblast Differentiation, Endocrinology 141(5) (2000) 1667-1674.

[23] I.A. Potapova, G.R. Gaudette, P.R. Brink, R.B. Robinson, M.R. Rosen, I.S. Cohen, S.V. Doronin, Mesenchymal Stem Cells Support Migration, Extracellular Matrix Invasion, Proliferation, and Survival of Endothelial Cells In Vitro, STEM CELLS 25(7) (2007) 1761-1768.

[24] H. Mayer, H. Bertram, W. Lindenmaier, T. Korff, H. Weber, H. Weich, Vascular endothelial growth factor (VEGF-A) expression in human mesenchymal stem cells: Autocrine and paracrine role on osteoblastic and endothelial differentiation, Journal of Cellular Biochemistry 95(4) (2005) 827-839.

[25] T. Furumatsu, Z.N. Shen, A. Kawai, K. Nishida, H. Manabe, T. Oohashi, H. Inoue, Y. Ninomiya, Vascular Endothelial Growth Factor Principally Acts as the Main Angiogenic Factor in the Early Stage of Human Osteoblastogenesis, Journal of Biochemistry 133(5) (2003) 633-639.

[26] S.B. Traphagen, I. Titushkin, S. Sun, K.K. Wary, M. Cho, Endothelial invasive response in a co-culture model with physically-induced osteodifferentiation, Journal of Tissue Engineering and Regenerative Medicine 7(8) (2013) 621-630.

[27] F.P. Seib, M. Prewitz, C. Werner, M. Bornhauser, Matrix elasticity regulates the secretory profile of human bone marrow-derived multipotent mesenchymal stromal cells (MSCs), Biochem Biophys Res Commun 389(4) (2009) 663-7.

[28] R.A. Marklein, D.E. Soranno, J.A. Burdick, Magnitude and presentation of mechanical signals influence adult stem cell behavior in 3-dimensional macroporous hydrogels, Soft Matter 8(31) (2012) 8113-8120.

[29] A.J. Engler, S. Sen, H.L. Sweeney, D.E. Discher, Matrix Elasticity Directs Stem Cell Lineage Specification, Cell 126(4) (2006) 677-689.

[30] G.A. Hudalla, J.T. Koepsel, W.L. Murphy, Surfaces That Sequester Serum-Borne Heparin Amplify Growth Factor Activity, Advanced Materials 23(45) (2011) 5415-5418.

[31] G.A. Hudalla, N.A. Kouris, J.T. Koepsel, B.M. Ogle, W.L. Murphy, Harnessing endogenous growth factor activity modulates stem cell behavior, Integrative Biology 3(8) (2011) 832-842.

[32] G.A. Hudalla, W.L. Murphy, Immobilization of Peptides with Distinct Biological Activities onto Stem Cell Culture Substrates Using Orthogonal Chemistries, Langmuir 26(9) (2010) 6449-6456.

[33] S. Musah, P.J. Wrighton, Y. Zaltsman, X. Zhong, S. Zorn, M.B. Parlato, C. Hsiao, S.P. Palecek, Q. Chang, W.L. Murphy, L.L. Kiessling, Substratum-induced differentiation of human pluripotent stem cells reveals the coactivator YAP is a potent regulator of neuronal specification, Proceedings of the National Academy of Sciences 111(38) (2014) 13805-13810.

Chapter 2- Literature Review

2.1 Preface

Advances in chemically-defined biomaterials and media development have enabled detailed characterization of the complex effects of biochemical and biophysical signals on cell behavior. This review will examine what has been published regarding human mesenchymal stromal cells (hMSCs) response to biochemical and biophysical signals during *in vitro* culture and how these known behavioral insights have been used to design biomaterials for improved biomanufacturing of hMSCs for cell therapeutics.

2.2 Abstract

Human mesenchymal stromal cells (hMSCs) are appealing candidates for cell therapies and tissue engineering because they can differentiate into various mesodermal cells types for tissue replacement, possess potent immunomodulatory properties to regulate immune function, and secrete an array of paracrine factors capable of supporting tissue regeneration [1-3]. As hMSC constitute only 0.001-0.001% of the bone marrow mononuclear cells, *in vitro* expansion through cell biomanufacturing is needed in order to generate sufficient numbers of cells needed for clinical applications [3]. While small-scale biomanufacturing methods currently exist for generating sufficient cell supply for initial clinical studies, widespread clinical applicability will require new materials and methods designed specifically to address the challenges of commercial scale up: low reproducibility, high cost, and high labor and time requirements [4, 5]. In this chapter, we examined the previous literature regarding hMSC behavior *in vivo* and during *in vitro* culture in order to gauge the current understanding of how culture parameters affect cell behavior. We

subsequently explored how these insights have been used to develop new innovative materials for controlling cell behavior to improve cell biomanufacturing.

2.3 Introduction

In vivo, the decision for a stem cell to either self-renew or differentiate is tightly regulated by biochemical and biophysical signals provided by the stem cells' microenvironment (Figure 2.1). Researchers extensively study the extracellular matrix (ECM) in the stem cell's microenvironment because it possesses key properties crucial for regulating both biochemical and biophysical signals- namely ability to promote cell adhesion and organization, provide mechanical forces to regulate migration and other cell functions, and regulate growth factor availability and activity. A key objective in stem cell bioengineering is the design of *in vitro* conditions that mimic the *in vivo* stem cell niche in order to provide cues that regulate cell survival and growth. Though the exact underlying mechanisms of niche regulation are incompletely understood, several essential interactions between the cell and its microenvironment have been uncovered and recapitulated *in vitro* [6-19].

In current cell biomanufacturing protocols, hMSCs are expanded on tissue culture polystyrene (TCPS) in growth media containing fetal bovine serum (FBS) supplement. Here, the TCPS is a permissive support substrate that enables hMSC adhesion while soluble factors in the growth media are instructive and regulate hMSC function and growth. While it is widely accepted that soluble signals (e.g. growth factors and cytokines) are major regulatory players, research has demonstrate that hMSC behavior can also be influenced by insoluble substrate signals such as GF-sequestering capabilities of the extracellular matrix as well as stiffness and adhesion-promoting properties of the microenvironment [6-8, 10-12, 14, 20-25].

In the last two decades, researchers have demonstrated that cells sense and respond to changes in matrix stiffness by modulating cytoskeletal assembly and contractility (a concept referred to as "mechanosensing") [10, 20]. There is ample evidence that biophysical signals provided by changing culture substrate stiffness and adhesivity can be used to modulate hMSC behavior. Additionally, not only are hMSCs able to respond to extracellular cues, they are able to respond to and actively change their microenvironment through GF production, protein and enzyme secretion that actively remodel the surrounding extracellular matrix, and alter expression of intracellular signaling proteins to change the intracellular response [9-19].

Despite this understanding, when hMSCs are expanded *in vitro*, routine biomanufacturing culture protocols disregard the role of biophysical cues and rely entirely on biochemical regulation, using cost-prohibitively high concentrations of supplemented growth factors (GF) to control hMSC behavior. In this review, we will examine the state of the art in hMSC biomanufacturing to gauge our current understanding of hMSC behavior during *in vitro* culture, then we will assess the state of the industry by reviewing innovations that use these insights to improve biomanufacturing processes.

2.4 hMSC biomanufacturing: state of the industry

2.4.1 hMSC culture on TCPS in FBS-containing media

Traditionally, hMSCs are cultured on uncoated TCPS. in serum-containing (SC) media (most commonly, growth medium is supplemented with FBS). In this culture system, the TCPS surface mimics some functions of the ECM by enabling nonspecific protein adsorption and cell adhesion while the FBS provides soluble signals. Here, TCPS substrates are considered permissive: passive

plastic enables adhesion to promote survival while the growth stimulating cues are provided through supplemented soluble factors found in the culture media. In these culture systems, researcher treat biochemical and biophysical extracellular cues as independent parallel signals.

In addition to demonstrated culture-adapted changes in hMSC behavior, TCPS and FBS reliance pose technical challenges that reduce the ability to parse the mechanisms that regulate hMSC growth and function *in vitro*. The reliance on TCPS raises concerns due to its supraphysiologically high stiffness as well as the inability to gain clear understanding of the mechanisms by which cells interact with their environment due to the nonspecific protein adsorption at the cell-material interface. TCPS allows nonspecific protein adsorption in uncontrolled orientations, thereby it's difficult to gain clear understanding of the mechanisms engaged at the cell-material interface [26]. Meanwhile, reliance on FBS raises several concerns: xenogenic contamination, large batch-to-batch variability, and inconsistency in price and supply due to FBS availability being linked to the demands in the beef market.

While TCPS and FBS-containing media culture system supports hMSC expansion, it's been demonstrated that prolonged *in vitro* adherent cell culture on TCPS increases cellular stress and senescence [27]. First and foremost, hMSCs cultured on TCPS have decreased proliferation rate, telomere length, and differentiation potential, all changes that have been associated with decreased hMSC mechanosensitivity due to cytoskeletal coarsening and stiffening [27]. Bone marrow is ~300 Pa while TCPS modulus is six orders of magnitude higher than bone marrow and five orders of magnitude higher than any soft tissue [28, 29]. Maloney *et al.* has demonstrated prolonged *in vitro* hMSC culture over >13 passages on stiff substrates result in actin stress fiber coarsening and bundling, increased whole-cell stiffening, and reduced whole-cell mechanical compliance [27].

2.4.2 Chemically-defined substrates for hMSC culture

Several chemically-defined natural and synthetic substrates have been developed in attempt to replace TCPS and improve efficiency and reproducibility of hMSC biomanufacturing processes, but these have limited success. Naturally-derived materials (e.g. Matrigel, fibrin, collagen, gelatin, fibronectin, vitronectin) can not only serve to promote adhesion and hMSC survival, but also are able to regulate soluble factor signaling to instruct hMSC behavior. However, customization of natural materials is typically limited to concentration and molecular weight, with limited control over structure, organization, and GF regulation. For example, fibrin matrices naturally contain heparin, a heterogenous and highly sulfated glycosaminoglycan (GAG) that can promiscuously bind to and regulate the activity of hundreds of different growth factors, yet there's limited ability to control heparin structure and GF binding specificity [23, 30-34]. To overcome these challenges, researchers have developed chemically-defined, synthetic coatings (e.g. CellStart, Synthemax, StemAdhere) for TCPS that contain recombinant proteins and synthetic peptides (e.g. fibronectin, vitronectin, RGD, IKVAV) in order to enable precise control over concentration, orientation, and activity of moieties that mimic known cell-substrate interactions [35-38]. Researchers have also created synthetic hydrogels (*e.g.* PEG, PLGA, PLLA, methacrylated polymers) with immobilized bioactive moieties to enable the added ability to culture hMSCs in both 2D and 3D. Nonetheless, these synthetic surfaces often times contain a limited number of proteins and are designed to either 1) promote well-defined adhesion or 2) regulate specific growth factors. Few of these chemically-defined, synthetic substrates mimic the complex biochemical and biophysical signals provided by the stem cell niche. These oversimplified synthetic cell microenvironments lead to hMSC adhesion and growth rates that are often lower than what can be achieved on TCPS and FBS systems. Additionally, the proprietary nature of

several of these substrates prevent the ability to parse out mechanisms of specific cell-substrate interactions. Our lab and several others have created poly(ethylene glycol) (PEG) hydrogels with incorporated adhesion ligands, growth factor-sequestering peptides, and degradable crosslinkers as well as the ability to regulate substrate stiffness [33, 35-37, 39-45]. Hydrogels composed of synthetic polymers such PEG as are promising alternatives to protein-coated TCPS. The PEG backbone is "bioinert" as it resists non-specific protein binding and does not contain cell-signaling molecules, thereby serving as a blank template. PEG is amenable to functionalization with peptides, GFs, and glycoasminoglycans, which allows the user to design biomimetic hydrogel substrates with precise control over the cell-material interactions. Additionally, PEG hydrogels can be formed to possess stiffness values that mimic soft tissues such as brain, fat, and muscle (0.5 – 50 kPa shear modulus).

The work in this thesis builds upon this prior knowledge to examine the effects of systematic, independent and combinatorial control over these substrate properties to develop customizes materials for enhanced hMSC function.

2.4.3 Technical and logistical challenges with FBS reliance

In addition to logistical challenges of using TCPS, reliance on FBS has its own unique issues. Many researchers have developed and commercialized chemically defined, xeno-free (XF), serum-free (XF) hMSC culture media to resolve some of the issues associated with FBS-reliance in hMSC biomanufacturing (Table 1) [46, 47]. Despite the development and commercialization of these XF SF culture systems, there are still major hurdles to large-scale, efficient hMSC biomanufacturing of cell therapeutics. First and foremost, several cell behaviors in culture have been shown to be serum-dependent, but serum-dependence of cell behaviors in culture, namely adhesion and

proliferation, are not well-studied because of the undefined nature of serum, and thus these behaviors are poorly understood. To create SF hMSC cell lines, hMSCs are often transitioned through subculture directly from SC media into SF media. These protocols operate under the assumption that there is no effect from the previous culture in serum. As such, attempts to develop SF media and cell banks have been plagued with performance issues commonly resulting in poor adhesion, low expansion rates, and phenotypic changes relative to what can be achieved with hMSCs cultured on TCPS in FBS-containing media [47-50].

Secondly, several commercially-available SF media formulations are proprietary and optimized for use with proprietary culture substrates [47-49]. Studies evaluating performance of SF systems reveal the need for concurrent optimization of both the media formulation and the substrate in order to achieve hMSC growth comparable to levels achieved in SC culture systems [47, 50-53]. For example, comparisons of hMSC growth in Mesencult-XF medium performed by Miwa et al. and Hartman et al. demonstrated that the Mesencult-XF system supported attachment when cultured using both the Mesencult-XF medium and the manufacturer's proprietary attachment substrate but did not support attachment when the medium was used in combination with fibronectin-coated TCPS [52, 53]. These two studies suggest that the performance of the medium could be improved by optimizing the culture substrate [47]. Unknown media compositions limit the ability to study the individual effects of media components and elucidate mechanistic understanding, problems that are originally associated with FBS use. A key scientific advantage to working with a defined, published media formulations is the ability to omit, reduce, or increase the concentrations of the individual components to study their individual and combinatorial effects on cellular behavior and function. This ability to modulate the media composition is critical to understanding cell function and enables mechanistic insight

[54]. Finally, hMSC behavior in response to extracellular biochemical and biophysical cues in both SC and SF culture is generally poorly understood, resulting in lack of control over biomanufacturing cell quality and their subsequent efficacy *in vivo*. [3, 46, 47].

2.4.4 Cost of hMSC biomanufacturing

Compounding with the technical challenges associated with poor understanding and control of hMSC behavior *in vitro* is a second hurdle to large-scale hMSC biomanufacturing for cell therapeutics: the prohibitively high cost. The cell culture, sera, reagents market is expected to reach $7.1 billion by 2023, with the largest growth seen in development of defined media and substrates [47, 55-57]. Regardless of SF or SC culture, stem cell growth and differentiation protocols traditionally rely on supraphysiologically high concentrations of recombinant GF supplements [39]. The majority of these protocols are expensive and have difficulty in gaining regulatory approval for clinical application because they often require numerous GFs at a variety of concentrations and combinations at various timescales. The requirement for high concentrations of GF used in stem cell bioprocessing is still extremely cost inhibitive, with academic and industrial labs reporting that materials cost accounted for ~36% of their overall biomanufacturing cost and can contribute up to as high as 70% of the total cost of goods (COGs) for hMSC biomanufacturing. From that cost, more than 20% of the total materials COGs is attributed to the media [58].

Discoveries in the past two decades revealed that substrates are indeed instructive and synergistic with the soluble factors found in the media [6-8, 10-12, 14, 20-25]. Not only are hMSCs able to sense extracellular cues, they are able to respond through altered expression of intracellular signaling and cell surface proteins, GF production, and protein and enzyme secretion to

dynamically change their microenvironment [9-19]. Substrate stiffness, adhesion signals, and GF regulation all provide instructive cues to regulate cell behavior and these extracellular signals are interdependent and potentially convergent. While there are a number of studies demonstrate that biomaterials can *influence* cell fate decisions, few examples to date have observed that biomaterials alone can *induce* stem cell self-renewal (i.e. expansion) or differentiation in chemically-defined cell culture environments. Our lab and others have started exploring the development of inductive, GF regulating cell culture substrates that are able to induce changes in hMSC behavior and sequester the subsequent differentially-secreted GFs to further amplify those behavior changes (Figure 2.2) [39, 40]. The work in this thesis builds upon the prior discoveries in our lab to examine the potential of using customized biomaterials to either reduce the amount of or completely mitigate the need for supplemented GFs to control hMSC behavior (Figure 2.3).

2.5 Stem cell behavior during in vitro culture

In vivo, stem cell survival and fate decisions to either self-renew or differentiate are regulated by complex interactions with local microenvironments, termed the stem cell "niches" (Figure 2.1) [29, 59, 60]. To harness the full potential of stem cells, an understanding of how the cells respond to microenvironmental cues is needed. A key aspect in stem cell engineering is the ability to recreate the niches *in vitro* in order to mimic and understand the role of *in vivo* cues that direct stem cell fate decisions [59, 60]. The exact underlying mechanisms of niche regulation are incompletely understood; however, several essential interactions between the cell and its microenvironment have been uncovered and recapitulated *in vitro* and studied. Here, we review the literature on hMSC behavior in response to *in vitro* signals and focus on the potential underlying mechanisms that regulate hMSC growth.

It is widely accepted that soluble signals (such as GFs and cytokines) are major regulatory players in both the *in vivo* and *in vitro* stem cell microenvironments [61]. Stem cell behavior can also be influenced by a variety of insoluble signals including biomolecules immobilized by the ECM as well as biophysical properties of the microenvironment itself [61-63].Recent studies indicates that regulation of stem cell behavior involves complex and coexisting relationships between soluble factors, insoluble adhesive signals, and mechanical signals contained in and dynamically regulated by the stem cell niche [61, 64]. A study by Anderson *et al.* demonstrated that varying spatial and temporal regulation of soluble factors (retinoic acid) in combination with the identities of insoluble adhesion-promoting polymeric matrices enabled combinatorial control over stem cell attachment, survival, and proliferation [65].

2.5.1 Demonstration of hMSC mechanosensitivity

Over the past two decades, several studies have provided evidence of the *in vitro* microenvironment's ability to control stem cell fate through regulation of cytoskeletal tension and integrin-mediated adhesion [61, 66]. Studies of single-cell mechanics demonstrated hMSC are inherently viscoelastic bodies and their mechanical properties are regulated by the organization of the actin cytoskeleton and forces generated through actomyosin contractility [67].

In a landmark study, Engler *et al.* demonstrated that polyacrylamide (PAAm) gels of varying substrate elasticity were able to induce hMSC differentiation towards various lineages in 2D cell culture, even in the absence of soluble inductive signals. Additionally, hMSCs committed to lineages specified by the matrix elasticity: cells seeded on soft matrices mimicking brain tissue expressed neurogenic markers while cells seeded on matrices with elasticity similar to muscle and

bone expressed myogenic and osteogenic markers, respectively [66]. Engler *et al.* also showed a positive correlation between the substrate elasticity and the intracellular cytoskeletal contractility, indicating that cells senses and responded to changes in matrix stiffness by modulation of cytoskeletal assembly and organization (a concept referred to as "mechanosensing") [61, 66]. In the presence of inhibitors that block non muscle myosin II-mediated cytoskeletal contractility, and subsequently cytoskeletal tension, cell commitment in response to matrix elasticity was diminished [66].

Others have demonstrated the importance of mechanosensing during lineage specification and commitment of adult stem cells. Huebsch *et al.*'s study of mouse and human MSC mechanosensitivity in both 2D and 3D cell culture on numerous naturally-existing ECM proteins revealed that the relationship between matrix elasticity and stem cell fate specification was neither species nor substrate composition dependent. Huebsch *et al.* also investigated the underlying mechanism of mechanosensitivity and showed that MSC mechanosensing of substrates is mediated by cytoskeletal-associated adhesion complex signaling [68]. Other groups have shown MSC osteogenic commitment when patterned on substrates that promoted cell spreading and cytoskeletal tension by controlling cell shape [69-72].

2.5.2 Phenotypic indicators of hMSC mechanosensing

Phenotypic-based biophysical characteristics can be directly correlated to where and how force transduction occurs through the cell [62, 64, 66, 69-74]. For example, hMSCs cultured on stiffer substrates express higher levels of adhesion molecules to enable stronger attachment to surface; thereby, focal adhesion complexes are more prominent and larger in cells on stiffer surfaces. hMSC on stiffer substrates also increase actin synthesis, F-actin polymerization, and form

organized actomyosin cytoskeletal to provide large amounts of resistive forces necessary to deform the microenvironment and assist cells in migration. A common sign of cell mechanosensing on stiff surfaces is organized, distinct F-actin stress fibers indicative of high cytoskeletal tension. This higher counterforce is a major contributing factor to the well-spread, elongated morphology typical of cells cultured on stiffer substrates [11, 12, 14, 20, 21, 67, 73, 75-77]. We and others have demonstrated similar of hMSC stem cell fate by modulating cytoskeletal tension with varying density and affinity of adhesion promoting peptides presented on PEG hydrogel culture surfaces [14, 38, 62, 78, 79]. hMSCs cultured on hydrogel surfaces that promoted high cytoskeletal tension (via high substrate stiffness, cell adhesion molecule affinity, or cell adhesion molecule density) resulted in well-spread cells that possessed highly-organized f-actin stress fibers and large, well-defined focal adhesions. Additionally, hMSCs on stiffer substrates possessed higher proliferation rates. Alternately, substrates that promoted low cytoskeletal tension resulted in rounded cells with diffused actin and small, unstable focal adhesions, with low proliferative capacity [11, 12, 14, 20, 21]. In many of these studies, substrate-induced stem cell fate specification was negated in the presence of inhibitors that block actomyosin contractility and, subsequently, cytoskeletal tension.

2.5.3 Intracellular signaling during hMSC mechanosensing

Extracellular signals regulate hMSC function via signal transduction through the cell that eventually leads to gene expression changes in the nucleus. Several studies have also unearthed several key components in the intracellular signaling cascade required for mechanotransduction from the cytoskeleton into the nucleus. Phenotypically, cells cultured on stiffer substrates have larger nuclear-to-cytoplasmic ratios with large nuclei that are elongated and aligned along the direction of force transduction. hMSC phenotypic assessment is commonly used for high

throughput screening and previous studies have demonstrated hMSC biophysical characteristics (cell size, spreading, cytoskeletal organization, nuclear-to-cytoplasmic ratio, etc.) are indicators of *in vitro* hMSC functions [14, 66, 80-90].

At the single protein level, some intracellular signaling proteins are mechanosensitive and mechanical stress induces conformational changes to regulate their activity. For example, p130Cas proteins are highly involved in integrin-mediated signaling and play important roles in cell migration, survival, and proliferation. Mechanical stretch exposes tyrosine and serine/threonine binding sites on p130Cas, which then can be phosphorylated and activated by several effector proteins (i.e. growth factors, such as VEGF and FGF-2, or hormones and other signaling proteins). Activated p130Cas serves as scaffold molecule in focal adhesion complexes to spatially regulate effector proteins that bridge cell-surface integrins to the F-actin cytoskeleton [75].

In addition to phenotypic changes associated with cytoskeletal organization and cell shape, mechanical forces applied to the cell are transduced throughout the cytoplasm and into the nucleus to alter gene expression. This signal transduction occurs through both soluble protein signaling and protein complexes that physical link the F-actin cytoskeleton in the cytoplasm through the nuclear envelop and into the nuclear interior [76]. The nucleus contains various elements (namely components of the nuclear membrane and nuclear lamina) that help facilitate this interaction. Much like the cell membrane, the nuclear envelope also has mechanosensing machinery. The nuclear membrane contains a transmembrane linker of nucleoskeleton and cytoskeleton (LINC)-complex that spans both the inner and outer nuclear membrane (INM and ONM, respectively) and serve as a bridge through the perinuclear space. The cytoplasmic portion of the LINC-complex is composed of nesprin, a protein that contains an ONM-embedded Klarsicht, ANC-1 Syne homology (KASH) domain, C-tail-anchored membrane proteins which are targeted specifically to the outer membrane

of the nuclear envelope. The KASH domain binds to F-actin in the cytoplasm and also binds to Sad1p, UNC-84 (SUN)-domain containing proteins in the perinuclear space. SUN proteins span the INM and also bind to the lamins (intermediate filaments) in the nuclear lamina such that the KASH/SUN interaction mediates direct linkage between the cyto- and nucleoskeletons. Tension provided through these nesprin-KASH/SUN bridges in turn provide tension to the nuclear envelope and prevent nuclear envelope ruffling more commonly seen in cells cultured on softer substrates [73, 76, 77]. The intermediate filaments of the nuclear lamina also contain chromatin binding domains that bind to specific DNA sequences on chromatin to facilitate chromatin organization [91].

Talele *et al.* and others have also demonstrated that stem cell mechanosensing can also lead to changes in gene expression by changing the localization of transcriptional co-activators yes-associated protein (YAP) and Tafazzin (TAZ), downstream mediators of gene regulation and biological functions of the signaling through the evolutionally conserved Hippo signaling pathway [92-94]. *In vitro*, the Hippo pathway is a major regulatory mechanism associated with cell contact inhibition and YAP and TAZ translocation into the nucleus has been demonstrated to be a key event in regulating stem cell self-renewal and differentiation gene expression. In hMSCs cultured on stiff surfaces *in vitro*, YAP and TAZ co-localizes in the nucleus, where they regulate gene expression that leads to low self-renewal and reduced lineage differentiation potential. However, on soft substrates, YAP and TAZ remain in the cytoplasm and are degraded and inactivated. This *in vitro* YAP and TAZ translocation in response to stiffness mimics how hMSCs respond to *in vivo* pro-fibrotic environments of scars and tumors. hMSCs found in stiff, fibrotic environments have been demonstrated to convert into highly contractile myofibroblasts (MFs) that possess well-organized α-smooth muscle actin (α-SMA, an isoform of actin)-

containing stress fibers. Different actin isoforms promote different levels of actin organization and changes in actin isoform is one mechanism by which cells can dynamically alter cytoskeletal function to respond to extracellular signals. Transient MSC-to-MF activation is common in wound healing, but persistent MF activation leads to excessive production and contraction of collagen-rich ECMs that increases microenvironmental stiffness and turns soft tissues into stiff scar tissue. As scar tissue continues to form, increasing tissue stiffness promotes further mechanical activation MSC-to-MF transition. Even prior to MF activation, hMSCs that possess α-SMA incorporation into pre-existing stress fibers have higher overall actin organization, cytoskeletal tension, and YAP/TAZ nuclear localization [92].

2.5.4 Combinatorial microenvironmental cues regulate hMSC behavior

While the majority of these previous studies have examined effects of individual microenvironmental cues on hMSC behavior, we and others have demonstrated that microenvironmental cues act combinatorially to regulate hMSC function. Our preliminary study of 2D hMSC culture in SC media demonstrated potential synergies between adhesivity and substrate stiffness that would otherwise have been undetectable in a screening format not suited for systematic, combinatorial experiments [14, 95]. The synergy between adhesion and stiffness was demonstrated with hMSC expansion, where on hydrogel surfaces of high adhesivity (4 mM CRGDS), hMSCs expand regardless of hydrogel spot stiffness; however, hydrogels presenting lower adhesivity required substrates with higher substrate stiffness [14]. These results are consistent with previously reported trends suggesting that low cytoskeletal tension in response to low cell adhesion ligand density could be compensated by high cytoskeletal tension produced from high substrate stiffness [10, 11]. Additionally, these trends suggest some baseline level of

cytoskeletal tension was required for hMSC proliferation on hydrogel substrates and that multiple substrate signals could be engineered to work in synergy to promote mechanosensing and regulate cell behavior [11, 21].

Others have also demonstrated synergy between soluble and insoluble cues to amplify downstream signaling pathways. hMSC-secreted vascular endothelial growth factor (VEGF) and hepatocyte growth factor (HGF) synergistically upregulated Ras-related C3 botulinum toxin substrate 1 (Rac) activity and downregulate Ras homolog gene family, member A (RhoA) activity which led to increase in adhesive junction-associated proteins, Cadherin 5, type 2 (VE-cadherin) concentrations, and filamentous actin (F-actin) remodeling. This ultimately resulted in improved endothelial cell viability and reduce endothelial permeability [96]. In non-induced hMSCs, VEGF and soft 2 kPa PEGDM culture substrates independently increased fetal liver kinase 1 (VEGF receptor 2, Flk-1) and eNOS (endothelial genes) expression and PECAM (endothelial-specific functional protein) production but did not promote hMSC capillary-like tube formation. Synergy between VEGF and cues from 2 kDa PEGDM also increased hMSC insulin-like growth factor (IGF) expression and Akt signaling to further amplify Flk-1, eNOS, and PECAM expression and additionally promoted tube formation that was not seen with either cues alone [97]. The synergistic effects of VEGF and soft substrates increased VEGF autocrine signaling via increased downstream Akt signaling and subsequently Flk-1expression.

2.5.5 hMSC secretome profiles during in vitro culture

Routine hMSC culture protocols rely on supraphysiological concentrations of supplemented GFs to stimulate cell growth and differentiation; however; there is ample evidence hMSCs produce critical GFs necessary for effectively regulating their own growth and

differentiation. For example, fibroblast growth factor 2 (FGF-2), also known as basic fibroblast growth factor (bFGF), is a mitogenic GF routinely supplemented in hMSC growth media to promote cell survival and proliferation; hMSCs have been shown to secrete FGF-2 during proliferation [16, 98]. High concentrations of supplemented vascular endothelial growth factor A ("VEGF") are known to enhance osteoblast differentiation; hMSCs have been shown to secrete detectable levels of VEGF in routine culture and endogenous VEGF is secreted in increasing quantities during osteogenic differentiation [15-19]. Transforming growth factor beta 1 (TGF-β1) is known to induce hMSC chondrogenic differentiation and recent studies have confirmed increased endogenous TGF-β1 secretion as chondrogenesis progresses [99, 100]. Bone morphogenetic protein 2 (BMP-2) is supplemented into osteogenic medium to induce osteogenesis, but has also been shown to be secreted by hMSCs in amounts that increase as hMSCs undergo osteogenic differentiation[101-103].

FBS-supplementation provides approximately 2-50 pg/mL FGF-2 and 5-350 pg/mL VEGF, and 90-1,500 pg/mL of active TGF-β1 to stimulate hMSC proliferation; however, the concentrations provided vary significantly depending on FBS lot and manufacturer, quantification method, as well as time in culture (because of GF's short half-life) [16, 104-107]. As such, there is need for high concentrations of recombinant GF supplementation to ensure sufficient bioactive GF concentration. For example, protocols for VEGF-mediated hMSC growth use 10 – 100X higher concentrations (20-100 pg/mL) of VEGF than what's physiologically relevant (0.2-2 pg/mL) in order to stimulate proliferation and survival [16, 19, 108-112]. Previous studies have also demonstrated that 5-200 ng/mL VEGF pre-treatment prior to or co-delivered during transplantation decreases stress-associated apoptosis and increased viability, resulting in improved transplanted hMSC survival and engraftment [16, 19, 108-112].

Studies have demonstrated hMSCs cultured on TCPS in FBS-containing media secrete bioactive and detectable levels of several GFs and cytokines [16, 19, 22, 109-124]. In routine 2D monolayer culture and 3D spheroid culture, hMSCs have been shown to secrete approximately 4-30 pg/mL of FGF-2, 80-3,500 pg/mL of VEGF, and 125-4,000 pg/mL TGFβ1 during expansion [16, 98, 110, 125, 126]. Additionally, while hMSC differentiation protocols routinely require high concentrations of GFs supplemented to the FBS-containing growth media, there is sufficient evidence that hMSCs secrete detectable levels of GFs required for further catalyzing their differentiation. For example, chondrocyte differentiation protocols routinely use 0.5-10 ng/mL supplemented TGF-β1; however, as hMSCs undergo chondrogenic differentiation, the amount of endogenous TGF-β1 secreted can be as high as 1 ng/mL per day and this is accompanied by a 3-fold increase in TGF-β1 receptor expression, indicative of autocrine signaling [99, 100]. For osteogenic differentiation, 10-25 ng/mL supplemented VEGF is used to induce differentiation and promote mineralization; however, as hMSCs undergo osteogenic differentiation, the amount of endogenous VEGF secreted increases 3-fold over the course of 3 weeks to as high as 250 pg/mL per day. This increased hMSC-secreted VEGF is also accompanied by increased VEGF receptors 1 and 2 (VEGFR1 and VEGFR2) expression, indicative that the positive feedback mechanism based on amplified autocrine signaling is not specific to one GF signaling pathway [15-19].

In addition to the effects of both recombinant and cell-secreted GFs on hMSC behavior *in vitro*, it is increasingly clear that inherent signals that are always present in the environment of the cell can also have a substantial influence on stem cell phenotype[127, 128]. Recent studies have implicated various biomaterial properties, presented to stem cells at the outset of cell culture, as critical instructive elements of the stem cell environment. For example, substrate mechanical

stiffness, nanometer-scale topography, and simple chemical functionality each impact hMSC expansion and differentiation [21, 66, 129-133]. This is in contrast to the traditional view that biomaterials simply provide a permissive context in which soluble GFs do the heavy lifting of induced stem cell differentiation. As a result, stem cell differentiation and associated tissue morphogenesis are typically induced via soluble GF supplements.

2.5.6 hMSC mechanosensing leads to differential secretome profiles

Matrix mechanics has been shown to influence cell growth and differentiation but the relationship between mechanics and GF production is not well understood [22, 81, 96, 134-139]. For example, hMSCs cultured on stiff substrates secrete up to 4X more VEGF than those cultured on soft substrates [22, 134]. Previous studies attempting to examine this relationship have predominantly relied on culture media supplemented with FBS, resulting in increased background noise (attributed to the poorly-characterized nature as well as the potentially confounding and conflicting signals from the numerous components of serum) that could mask small but significant changes in GF secretion as well as reduced reproducibility of results (due to serum's large batch-to-batch variability) [140].

Only a small number of published studies have examined hMSC GF secretion in response to substrate stiffness; however, the results were inconsistent and contradictory [22, 28, 81, 82, 85, 96, 134-139]. Seib *et al.* showed hMSCs cultured on stiffer substrates (20 kPa vs 2 kPa hydrogels formed with PEG diacrylate, thiol-modified hyaluronic acid, and gelatine) produced higher concentrations of GFs and cytokines due to increased Rho-associated protein kinase (ROCK) signaling pathway activation that increase myosin- and F-actin-mediated cytoskeletal tension. Independent of time (over 18 days of culture) and donor (6 different donors), hMSCs cultured on

20 kPa stiff substrates produced higher levels of VEGF and μPA than hMSCs cultured on 2 kPa soft substrates [82]. Abdeen *et al.* cultured hMSC in DMEM + 10% FBS on fibronectin-coated polyacrylamide hydrogels of 0.5, 10, and 40 kPa stiffness and corroborated Seib et al.'s observation of stiffness-mediated increase in VEGF expression [22]. Contradictory to these results, Marklein *et al.* claimed a temporal-dependence in correlation between stiffness and GF secretion when hMSCs were cultured in 3D, with an overall conclusion that increasing substrate stiffness resulted in decreased VEGF secretion [134, 135]. Still others have demonstrated hMSCs cultured on 2 kPa PEG-NB or 20 kPa alginate all produced lower levels of VEGF than hMSCs cultured on TCPS [28, 85].

The existing studies have predominantly relied on culture media supplemented with FBS with varying substrates. These contradictory results might be due to several factors: 1) lack of reproducibility due to FBS variability, 2) temporal differences, and 3) differences in culture substrate chemistry. Nonnis *et al*. examined the effects of FBS on the hMSC secretome and revealed that increasing FBS concentration in culture media did not affect total protein concentration (both human and bovine) in the secretome, but did cause a significant reduction in relative concentrations of secreted human protein and thereby decreased the detection sensitivity and accuracy needed for characterizing hMSC protein production [141]. Nonnis et al. and others have demonstrated bovine contaminants in the secretome reduced the total portion of human proteins identified by mass spectrometry, whereby reducing FBS supplementation (from 5% to 0%) in the media resulted in a 2X increase the total amount of hMSC-secreted proteins detected by mass spectrometry and also allowed detection of less abundant human proteins that were previously masked [141, 142]. Still others have demonstrated that serum deprivation increased

activation of several apoptotic pathways, decreased MAPK and ERK1/2 phosphorylation, and decreased hMSC proliferation [143].

While previous studies have demonstrated increasing hMSC spreading can be induced via both increased stiffness and substrate adhesivity, there has been no demonstrated relationship between mechanosensing of changing adhesivity and differential GF secretion [11, 12, 14, 20, 21]. Markelein *et al.* and *Seib et al.* both noted a possible correlation between cell spreading and GF secretion with increased VEGF secretion on substrates that promote high cell spreading, but this qualitative assessment was not characterized or further examined [22, 134, 135].

As a result of this dependence on supraphysiological concentrations (~100 ng/ml) of recombinant GF supplements [144-147], stem cell biomanufacturing processes are plagued by inordinately high costs and undue regulatory burden. A recent study indicated that over half the cost of hMSC biomanufacturing for clinical cell therapy was attributable to recombinant GF supplements used during cell expansion [46]. Reducing, or potentially mitigating altogether, the required supplemented GFs routinely used in hMSC expansion and differentiation can significantly reduce the cost of biomanufacturing, thereby increasing the feasibility for clinical applications. For example, Corning Life Sciences estimated reducing FBS supplementation from 10% to 5% in routine hMSC growth media results in a cost savings of 33% per 500-mL bottle of medium. Further reduction from 10% to 2% FBS results in a cost savings over ~53% [148].

2.5.7 Demonstration of hESC mechanosensing

While this thesis predominantly focuses on hMSC behavior, the concepts of mechanosensing and substrate-mediated changes in stem cell behaviors are not limited to hMSCs. Human embryonic stem cells (hESCs) exhibit infinite self-renewal, and are pluripotent

(capable of differentiating to endodermal, mesodermal, and ectodermal lineages) [149]. Due to their defining self-renewal and pluripotent properties, hESC serve as a promising cell source for cell therapies, drug screening, disease modeling, and for understanding human development [149, 150]. Understanding of the mechanisms that control hESC self-renewal and differentiation is crucial for realizing and optimizing hESC use in numerous therapeutic applications [150, 151].

Like hMSCs, the hESC cell fate decision between self-renewal and differentiation require tightly regulated intrinsic and extrinsic biochemical and biophysical cues. Several transcription factors (namely Oct4, Sox2, and Nanog) have been identified as important intrinsic regulators and numerous key extrinsic regulatory cues (such as growth factor signaling and adhesion to the ECM and supporting cells) have also been identified [61]. Recent studies have also indicated that there is significant crosstalk between intrinsic and extrinsic regulatory pathways as well as biochemical and biophysical cues [150].

In the last decade, many discoveries have enabled enhanced understanding of biochemical regulation of hESC cell fate decisions; however, the biophysical regulation of hESC cell fate decision via cell-cell and cell-matrix interaction are poorly understood and significantly less is known about the former than the latter [151-153]. Previous studies have demonstrated hESC mechanosensing and matrix stiffness direct cell lineage. In a similar manner to hMSC mechanosensing, hESCs mechanosensing is tissue and substrate stiffness dependent: stiffer substrates promote pluripotency maintenance and while soft substrates promote differentiation[93, 94, 154, 155]. Zoldan *et al.* reported that substrates with high, intermediate, and low elastic moduli promote mesoderm, endoderm, and ectoderm differentiation, respectively. After 14 days of culture on substrates of very high stiffness (> 6 Mpa as determined by tensile testing), hESCs remain undifferentiated, express high levels of pluripotency-associated

genes, and express low levels of lineage-specific markers [155]. hESCs on stiff scaffolds (1.5-6 Mpa), had upregulated FOXF1, MEOX1, and KDR (genes correlated with mesodermal tissue morphogenesis towards muscle, blood vessels, heart, cartilage, and bone). hESCs on scaffold with intermediate stiffness (0.1-1 Mpa) had upregulated GSC, SOX17, Brachyury, and MIXL1 (genes correlated with endodermal tissue morphogenesis towards digestive system, exocrine systems, lungs, and epithelium). hESCs on soft scaffolds (<0.1 Mpa) had upregulated SOX1 and ZIC1 (genes correlated with trophectoderm development, anterior/posterior axis specification, stem cell maintenance, and neurogenesis).

2.5.8 Phenotypic indicators of hESC mechanosensing

Similar to hMSCs, hESCs also possess phenotypic changes as a result of mechanosensing; however, the results have been somewhat confounding and, at times, contradictory. While Keung *et al.* demonstrated that hESC spreading increased after culture on substrates with higher stiffness, Eroshenko *et al.* reported no correlation between stiffness and cell spreading [156, 157]. While Musah *et al.* demonstrated increased hESC proliferation after culture on substrates with higher stiffness, Keung *et al.* saw no correlation between stiffness and proliferation [93, 94, 156]. Additionally, while there were demonstrated losses in pluripotency on all soft substrates, there were temporal differences as to when hESCs stopped expressing pluripotency markers [156]. Keung *et al.* suggested loss of pluripotency markers within 3 days after transition to substrates with softer stiffness, but Sun *et al.* suggested loss can be seen as early as within 1-2 days, and Erochenko *et al.* reported that pluripotency marker loss couldn't be observed until 4 days after stiffness changes [154, 156-158]. These contradictory results could be due to the same experimental limitations that we see in hMSCs. The majority of these studies

were either conducted in ill-defined culture conditions that are dependent on long-term use of animal proteins or Rho- associated protein kinase (ROCK) inhibitor Y-27632s. Several studies used Matrigel for cell attachment [155, 156], knock-out media for cell culture[157], or Y-27632 for cell survival and attachment [93, 94, 154]. ROCK inhibitor prevents myosin phosphorylation and thereby blocks actomyosin-mediated contractility and changes in cytoskeletal tension. The long-term effects of ROCK inhibitor on hESC culture has not been fully elucidated and this reliance on ROCK inhibitor potential reduces hMSC mechanosensing sensitivity.

Nonetheless, these studies reveal that hESC mechanosensing of substrate stiffness during *in vitro* cell culture mimics the cellular response to stiffness changes during gastrulation. During embryogenesis, cells are affected by or generate force. During gastrulation, blastula epiblast cells ingress and change their shape and motility, which changes the cellular forces in the developing embryo and leads to mechanical stress patterning in the following way:

1. Epiblast cells converge at midline
2. Epiblast cells ingress at primitive streak
3. Rate of cell movement along the top of the blastula exceeds the rate of cell movement at the ingression, which causes epiblast cells to compress into bottle-shaped cells at the primitive streak
4. First cells to ingress differentiates into endoderm
5. Mesoderm arises from cells ingressing and migrating at later stage
6. Cells that remain at surface differentiated into ectoderm

The mechanical stress patterning in the embryo influences cell differentiation and development through force profiles that mimic how cells sense matrix stiffness during 2D culture: 1) by passively constraining movement of tissues and cells, cells move slower and exert

higher traction forces and 2) cells increase cortical stiffness by changing amount and pattern of polymerized cytoskeletal actin [93, 94, 154, 155].

2.5.9 Intracellular signaling during hESC mechanosensing

Finally, similar to hMSCs, hESC mechanotransduction is epithelial cadherin (E-cadherin)-mediated and relies on actomyosin contractility to alter cytoskeletal tension and subsequently regulate hESC self-renewal by modulating expression of pluripotency genes. E-cadherin, a transmembrane cell surface glycoprotein, mediates cell-cell adhesions to provide a link between the intracellular actin network and signaling pathways of neighboring cells and these cell-cell adhesions have been demonstrated to be important in both hESC survival and self-renewal. E-cadherin is normally distributed on the hESC cell surface and its co-expression with various pluripotency cell surface markers (such as SSEA-4 and TRA-1-60) and transcription factors (such as Oct4, Nanog, and Sox2) have been commonly used to identify pluripotent hESCs. Induction of hESC differentiation results in drastic loss of E-cadherin expression as well as the downregulation of the aforementioned pluripotency cell surface markers and transcription factors [150].

Not only is E-cadherin an indicator of pluripotency, but it also is capable of modulating hESC cell fate decisions. Various studies have indicated that upregulation of E-cadherin enhances hESC self-renewal while inhibition results in rapid loss of expression of the core transcriptional circuitry that regulates pluripotency (Oct4, Nanog, and Sox2) [150]. Recent discoveries suggest that E-cadherin-mediate signaling is a convergence point between biochemical and biophysical signaling pathways for that regulate hESC cell fate decisions. Cell-cell signaling has been demonstrated to alter intercellular signal transduction pathways as well as

cell response to soluble growth factor signaling from the extracellular microenvironment to modulate the expression and activity of the core transcription factors. Despite recent advances in understanding cell-cell mediated regulation of hESC self-renewal, the signaling events downstream of E-cadherin that connect it to the core transcription circuitry is poorly understood.

Recent studies propose that the E-cadherin mediated adhesions interact with the actin networks in the cytoskeleton to transduce forces and mechanotransduce from the cell membrane to the nucleus. It is well established that E-cadherin is directly anchored to the actin network and that interaction plays an important role in both stabilizing E-cadherin expression as well as strengthening E-cadherin-mediated cell-cell adhesions [152, 159, 160]. Non-muscle myosin II (NMMII) is an actin-binding motor protein that regulates contractile functions and force production in numerous cells, including hMSCs [150]. Studies indicate that a positive feedback loop between NMMII-mediated actomyosin contractility and E-cadherin regulates both hESC survival and self-renewal. For example, in response to mechanical and enzymatic dissociation, hESC cell-cell contacts are disrupted and E-cadherin expression at the cell surface is loss. Loss of cell-cell contact weakens the E-cadherin interactions with the actin network and results in hyperactivation of NMMII-dependent actomyosin contractility. Actomyosin hyperactivation further decreases E-cadherin stability at the cell surface by increasing E-cadherin endocytosis and degradation. This results in the inability to re-establish cell-cell adhesion and, consequently, dissociation-induced hESC cell death through biochemical and biophysical mechanisms that are not completely understood [150-152, 159]. While actomyosin hyperactivation reduces survival of dissociated hESC, long-term inhibition or complete depletion of NMMII (and subsequently reduction in actomyosin contractility) in hESC colonies results in reduction of Oct4 and Sox2 expression and complete ablation of Nanog expression [150, 151]. Ectopic over-expression of E-

cadherin in hESC colonies with NMMII depletion was able to completely restore Oct4, Sox2, and Nanog expression [153]. These results demonstrate that mechanotransduction through actomyosin contractility not only plays a role in generating and transmitting signals that affect cell survival, it is also a participates in E-cadherin-mediated hESC self-renewal.

Preliminary attempts to gain mechanistic insight into E-cadherin-mediated hESC self-renewal have revealed that E-cadherin and actomyosin co-regulation is needed to affect the core transcriptional circuitry. In response to well-established hESC cell-cell adhesions, E-cadherin clustering at the plasma membrane causes the release of α-catenin dimers, proteins that are known to bind to E-cadherin associated adaptor proteins. α-catenin dimers also interact with formin, a protein that nucleates and polymerize new F-actin. Formin also binds to profilin, a protein that regulates the activity of actin monomers, and also directly competes with Arp2/3, a protein complex that nucleates new F-actin along the sides of pre-existing F-actin. Both of these formin-mediated interactions result in changes in actin network assembly dynamics and, subsequently, alter intra- and intercellular mechanotransduction. This mechanotransduction pathway is speculated to be one mechanism by which information is transduced from cell-cell contacts to the core transcriptional circuitry to modulate hESC self-renewal [153].

A handful of other studies have also alluded to this E-cadherin-actomyosin mechanotransduction signaling pathway. Gharechachi *et al.* revealed that actomyosin hypercontractility and loss of E-cadherin resulted in altered expression of several transcriptional regulation proteins that have known functions in chromatin remodeling to alter DNA accessibility and, consequently, global gene expression [161]. The hESC self-renewal promoting activity of the core transcription circuitry is primarily attributed to their ability to upregulate pluripotency-associated genes while suppressing the genes that encode lineage-specific

transcription factors. Previous studies have indicated that the core transcription circuitry not only modulating their own transcription promoters, but also they form regulatory loops with chromatin regulators to change the chromatin architecture and, consequently, alter access to DNA to silence lineage specific genes [150].

Despite these attempts to understand the signaling mechanisms for E-cadherin-mediated mechanotransduction, major molecular components have yet to be identified and comprehension of the spatiotemporal dynamics remain largely based off speculation. The KASH/SUN bridge demonstrated in hMSC mechanosensing provides a potential route through which E-cadherin signaling can be used to mediate hESC self-renewal by direct regulation of chromatin structure and organization. In fact, a previous study using mouse ESCs (mESCs) demonstrated that differentiated mESCs displayed higher expression of nesprin isoform 1 (nesprin-1) and lamins than undifferentiated mESCs. In addition, forced over-expression of nesprin resulted in modulation of mESC self-renewal [162]. Due to marked differences between mouse and human ESCs, the results of this study cannot be used as a direct indicator of hESC singaling pathways. Nonetheless, it can be used as a guiding hypothesis for additional investigation of the interplay between mechanotransduction and hESC self-renewal.

2.7 Biomaterials for growth factor sequestering

In order to accelerate advances in stem cell biomanufacturing and cell therapeutics, there is a particular need for biomaterials that actively control GF signaling and mitigate the reliance on costly GF supplements. One can envision an “autocatalytic” process, in which stem cells can amplify their own expansion or differentiation by secreting their own GF stimulants (Figure 1). However, standard cell culture conditions feature a very low surface area/volume ratio, and cell-

produced GFs are rapidly diluted due to convective currents [163].

One intriguing and very common natural mechanism to address this challenge involves GF binding to the ECM [164]. The ECM contains many insoluble proteins and proteoglycans that can regulate both endogenous and exogenous GF signaling. Several prior studies have suggested that the positive influence of natural ECMs (e.g. Matrigel, heparin, collagen) and ECM-derived glycoproteins (e.g. vitronectin, fibronectin) in stem cell culture may actually be due to their ability to bind and localize cell-secreted GFs near the cell population. The ECM is capable of sequestering soluble GFs and releasing them upon enzymatic degradation for cell-demanded signaling as well as regulate insoluble GF signaling by irreversibly binding GFs. Both soluble and insoluble GF signaling elicits different effects on hMSCs, therefore, it's important to consider the sequestering context when discussing the effects of GF regulation on hMSC behavior [24, 165-167]. Additionally, there's been demonstrated synergy between multiple GFs that are able to activate converging signaling pathways, therefore the complexity of the signaling environment will dictate the GF effects [43, 120-124, 168-171].

2.7.1 Effects of VEGF on hMSC behavior

In this work, we will examine the literature discussing effects of VEGF and VEGF sequestering on hMSC behavior during 2D *in vitro* culture. VEGF was chosen as a model system because of its demonstrated significance both *in vitro* and *in vivo*. *In vitro*, VEGF supplementation in the growth media has been shown to promote hMSC survival, proliferation, migration, and osteoblast mineralization during late osteogenesis [15, 17, 18, 96, 108, 109, 112, 168, 172-179]. There is conflicting hypothesis regarding the intracellular signaling pathways involved in VEGF-mediated hMSC proliferation. Some suggest VEGF promotes hMSC

proliferation via VEGF receptor 2 (VEGFR2)-mediated PKC, PI3K/Akt, and MAPK/ERK pathway activation while others suggest that hMSCs do not contain cell-surface VEGFRs but instead is mediated by platelet derived growth factor (PDGF), HGF, and neuropilin (Nrp) receptors [96, 168, 172-179]. *In vivo*, VEGF has been shown to promote hMSC adipogenesis and osteogenesis, angiogenesis via enhancing endothelial cell organization, increase hMSC and endothelial cell survival by decreasing autocrine and paracrine apoptotic signals, and stimulate hMSC and endothelial cell proliferation via decreasing expression of cell cycle inhibitors and pro-apoptotic factors while increasing pro-survival factors [108, 109, 112, 172-174, 176, 179-182].

It's been reported that <1% of transplanted hMSCs survive and engraft 24 hours after transplantation because of the stress from rapid into the hypoxic, highly inflammatory environment. VEGF priming (pre-treatment) during hMSC culture has been shown to promote survival and engraftment through multiple, synergistic pathways [17, 18, 168, 172-179]. Pons *et al.* demonstrated that 24 hour priming hMSCs via media supplementation with VEGF (20 ng/10^6 cells) during culture on TCPS in 10% FBS-containing media is sufficient to observe increased hMSC proliferation and survival after transplantation in infarcted mice myocardiums. Increased hMSC proliferation (observed via BrdU incorporation) was accompanied by increased cyclin B1 (regulator of S/G2 cell entry during mitosis) production, decreased $p16^{INK}$ (cell cycle inhibitor) production, and increased Akt phosphorylation that resulted in increased Bcl-xL (anti-apoptotic survival protein kinase) and decreased Bax (pro-apoptotic protein) production. Even without priming, bolus co-injection of hMSCs with soluble VEGF was sufficient to increase hMSC survival up to 28 days post injection [109]. Penna *et al.* demonstrated that VEGF priming in hMSC *in vitro* culture (~100 ng/10^6 cells/day of supplemented soluble VEGF) increased hMSC

proliferation through increased Akt, PKCε, and Erk 1/2 phosphorylation. Without priming, co-delivery of VEGF during 3D microcarrier culture and transplantation resulted in sustained VEGF release and also increased cell survival *in vivo* by increased total Erk 1/2 protein expression and phosphorylation, sustained Akt phosphorylation increase, increased Bcl-2 (anti-apoptotic survival protein kinase) biosynthesis, and reduced cleaved caspase-3 (a pro-apoptotic protease enzyme) [112].

2.7.2 Natural and synthetic biomaterials for GF Sequestering

Several natural-based biomaterials (e.g. collagen, silk, agarose, alginate, hyaluronan, gelatin) have been utilized for hMSC culture and delivery, but these scaffolds have been primarily developed to provide structural and mechanical support without consideration of the material's role in GF regulation [183-202].

Other natural biomaterials (e.g. fibrin, Matrigel, heparin-containing scaffolds) have also been used for hMSC culture, but these scaffolds are ill-defined and promiscuously bind hundreds of different GFs, thereby it's difficult to control and parse out the effects of individual signaling pathways[193, 202-207]. For example, proteomic studies indicate that Matrigel includes >1,500 unique proteins and each ECM-derived glycoprotein may bind promiscuously to several GFs with high affinity [208]. Hubbell and coworkers recently showed that the 12-14th type III repeats of fibronectin can bind with high affinity to 16 distinct GFs [209]. Peng *et al.* and Benoit *et al.* showed heparin carries a high degree of negative charge from its sulfation profile and can regulate a wide range of positively-charged GFs and proteins that control hMSC adhesion, proliferation, and differentiation (e.g. FGF-2, BMP, fibronectin, and numerous proteins found in FBS) [23, 210].

Several synthetic scaffolds have been developed for hMSC culture and some have been customized with GF sequestering capabilities (Table 2) [33, 35-45, 169, 207, 211-224] [170, 171, 202, 225-228].

Benoit *et al.* demonstrated increased hMSC proliferation and osteogenic differentiation in heparin-crosslinked PEG hydrogels presenting supplemented recombinant FGF-2 [23]. Parmar *et al.* demonstrated increased encapsulated hMSC chondrogenic differentiation in collagen hydrogels presenting heparin-binding peptides [229]. While these studies demonstrate the potential utility of GF-sequestering substrates for hMSC culture, few characterize the endogenous GF sequestering, and none examine the potential synergistic effects of substrate stiffness.

Our lab has developed PEG-norbornene functionalized degradable and non-degradable hydrogels as well as polymer-coated TCPS surfaces with immobilized adhesion-promoting peptides [225-228]. We have also created alkanethiol self-assembled monolayers with immobilized adhesion-promoting peptide and heparin-binging peptides for hMSC culture and demonstrated the ability to sequester serum-borne heparin and subsequently heparin-binding GFs to increase hMSC proliferation [39, 230].

Again, these synthetic scaffolds enable promiscuous binding, which has its own utility, but is not amenable to studies that parse out the effects of individual biophysical and biochemical signals.

2.7.3 Biomaterials for specific VEGF sequestering

We and others have developed synthetic scaffolds to specifically sequester VEGF [43, 169, 215-218]. Using mimicry of known protein-protein interaction, we and others have isolated peptide sequences from the active binding domains and created VEGF binding peptides that have

high affinity and specificity for VEGF. Leppänen *et al.* first used this approach to study the binding domain between VEGF and the extracellular domain of VEGFR2 to identify VEGFR2 amino acid residues that bind VEGF isoform A (EFAYLIDFNWEYPASK) and isoform C (RTELNVGIDFNWEYPASK). Our lab developed D-substituted amino acid variants of the VEGF isoform A-binding peptide (VEGF-binding peptide, VBP) with a terminal N-terminus cysteine ($EF_dA_dY_dL_d$IDFNWEYPASKC) as well as branched and dimerized versions of VBP to improve VEGF affinity, specificity, and peptide serum stability to protect against protease degradation [43, 169, 231]. Work previously published in our lab and others have shown the ability to use terminal cysteine modifications to covalently immobilize peptides into PEG-norbornene hydrogel networks using thiolene click chemistry [42, 232].

Our previous work has demonstrated the ability to use VBP-containing hydrogels ("VBP hydrogels") to sequester, localize, and provide sustained release of recombinant VEGF, serum-borne VEGF, and cell-secreted VEGF from activated platelets to promote endothelial cell survival and morphogenesis [43, 218, 231, 233]. In this thesis work, we build upon the previous discoveries to develop VEGF-sequestering hydrogel substrates for enhanced hMSC survival and proliferation without the need for additionally supplemented VEGF in the *in vitro* SC and SF growth media.

2.8 Biomaterials for combinatorial control of biochemical and biophysical signaling

A small number of prior studies have examined the direct combinatorial effects of substrate stiffness and endogenous GF regulation on hMSC growth and differentiation. Some studies incorporated heparin into culture matrices to sequester endogenous GF and influence behavior of various cells and others have specifically examined these effects on hMSCs [23, 24, 229].

Jha *et al.* demonstrated increased cardiac progenitor cell (CPC) proliferation and cardiac differentiation in heparin-containing hyaluronic-based hydrogels with increasing stiffness (0-1 kPa) and increasing RGD density (0-380 μM). Increasing both adhesivity and stiffness resulted in increased CPC proliferation and tubular network formation, but stiffness had a greater effect than adhesivity. Increasing heparin concentration in the hydrogels also increased binding and retention of supplemented TGFβ1 and CPC-secreted angiogenic cytokines. Nonetheless, Jha *et al.* demonstrated the ability to create chemically-defined networks with systematic and independent control over stiffness, adhesivity, and GF sequestering, but did not evaluate the combinatorial effects of these parameters [234].

2.9 High Throughput Screening

In vivo, the decision for cell growth and function is tightly and combinatorially regulated by a complex array of biochemical and biophysical signals provided by the microenvironment. Though the exact underlying mechanisms of niche regulation are incompletely understood, several essential interactions between the cell and its microenvironment have been uncovered and recapitulated to promote hMSC expansion during *in vitro* cell culture: cell-matrix interactions, cell-cell interactions, and soluble factor signaling [1-3, 46, 47]. Chemically well-defined cell culture substrates can allow researchers to parse out the effects of specific signals on stem cell behavior [235]. However, attempts to investigate synergistic or antagonistic effects of combinations of signals produce thousands of potential signal combinations, leading to difficult and costly experiments [7, 21]. Screening array platform technologies with chemically-defined substrates offer the ability to rapidly and concurrently examine multiple variables.

Currently existing hydrogel platforms for screening the influence of stiffness on cell behavior rely on low-throughput techniques using bulk hydrogels, plated hydrogel arrays in cell culture dishes or elastomeric wells, or arrays formed using expensive liquid handling systems. These methods have limitations, including high materials and equipment cost and the potential for deformation via "buckling" when hydrogels swell against the constrained dimensions of the well [7, 236-239]. Our lab and others have previously developed hydrogel array systems for 2D and 3D stem cell culture and screening, but these systems required liquid handling systems and the resulting surfaces were not flat or uniform enough to be compatible with standard imaging-based, label-free characterization to allow for high content assessment of cell behavior without disrupting hMSC growth in culture [7, 236, 237, 240-242].

2.10 Tables and Figures

Table 2.1. Commercially-available defined culture media

Name	Manufacturer	Xeno-Free	Serum-Free	Chemically-Defined	Intellectual Property
StemPro MSC SFM XenoFree	Thermo Fisher Scientific	Yes	Yes	--	Trade secret
StemPro MSC SFM	Thermo Fisher Scientific	Yes	No	--	Trade secret
Mesencult-XF	Stem Cell Technologies	Yes	Yes	Yes	Trade secret
PRIME-XVTM MSC Expansion SFM	Irvine Scientific	No	Yes	--	Trade secret
Cellgro Stemgro hMSC medium	CellGenix	No	Yes	--	Trade secret
Therapeak MSCGM-CD Medium	Lonza	Yes	Yes	Yes	Trade secret
Stemgro hMSC medium	Corning	Yes	Yes	Yes	Trade secret
RoosterNourish	Roosterbio	Yes	No	No	Trade secret
MSC Nutristem XF Medium	Biological Industries	Yes	Yes	Yes	Trade secret
PPRF-msc6	Pharmaceutical Production Research Facility	Yes	Yes	No	Formulation published
Mosaich MSC Serum-Free medium (BD-SF)	Becton Dickinson (BD) Biosciences	--	Yes	Yes	Trade secret
HEScGRO	Merck Millipore	Yes	Yes	Yes	Trade secret
Mesenchymal stem cell growth medium DXF	PromoCell	Yes	Yes	Yes	Trade secret
MesenGro	StemRD	--	--	Yes	Trade secret
MSC Qualified Plus	Compass Biomedical	Yes	--	--	Trade secret
MSC-GroTM (SF, complete)	Vitro Biopharma	--	Yes	--	Trade secret
MSCGS-ACF (MSC supplements)	Stem Cell Research	--	Yes	--	Trade secret
mTeSR	Stem Cell Technologies	--	Yes	--	Trade secret
RS-NovoTM and GEM-Novo	Kerry Bio-Sciences	Yes	Yes	Yes	Trade secret
SPE-IV	Abecell-Bio	--	Yes	--	Trade secret
Stemline MSC expansion medium	Sigma Aldrich	Yes	Yes	Yes	Trade secret
Stem X Vivo	R&D Systems	--	Yes	--	Trade secret
STK2	Two Cells Co	Yes	Yes	Yes	Trade secret
Ultrasor G (lyophilized)	Pall Biosepra	--	Yes	--	Trade secret

Table 2.2. Biomaterials for VEGF Sequestering

Matrix	GF Sequestering Moiety	Target	Characteristic Effect	Reference
Fibrin	Heparin	Multiple GFs	--	[207]
Fibrin	Anti-thrombin-mimicking peptide $ATIII_{121-134}$	Multiple GFs	--	[211, 212]
Fibrin	Fibronectin-mimicking peptide α_2PI_{1-8} -FN III_{12-14}	Multiple GFs	Enhanced morphogenesis	[213, 214]
Nanofibers	Heparin-binding peptide amphiphiles	Heparin and multiple heparin-binding GFs	Enhanced morphogenesis, vascularization, tubulogenesis, and survival	[219-224]
PEG	RTELNVGIDFNWEYPASK, $EF_dA_dY_dL_dIDFNWEYPASK$ and $(EF_dA_dY_dL_dIDFNWEYPASK)_2K$	VEGF isoform A and isoform C	Anti-Angiogenic	[169, 215-218]
PEG	$EF_dA_dY_dL_dIDFNWEYPASKC$ (VBP-C)	VEGF isoform A	Anti- Angiogenic[a] and Pro-Angiogenic [b]	[43, 169]
PEG	$(EF_dA_dY_dL_dIDFNWEYPASK)_2KC$ (VBP_2-C)	VEGF isoform A	Anti- Angiogenic [a] and Pro- Angiogenic [b]	[43]

[a] Anti-Angiogenic function demonstrated upon sequestering of soluble VEGF
[b] Pro-Angiogenic function demonstrated upon sustained release of bound VEGF

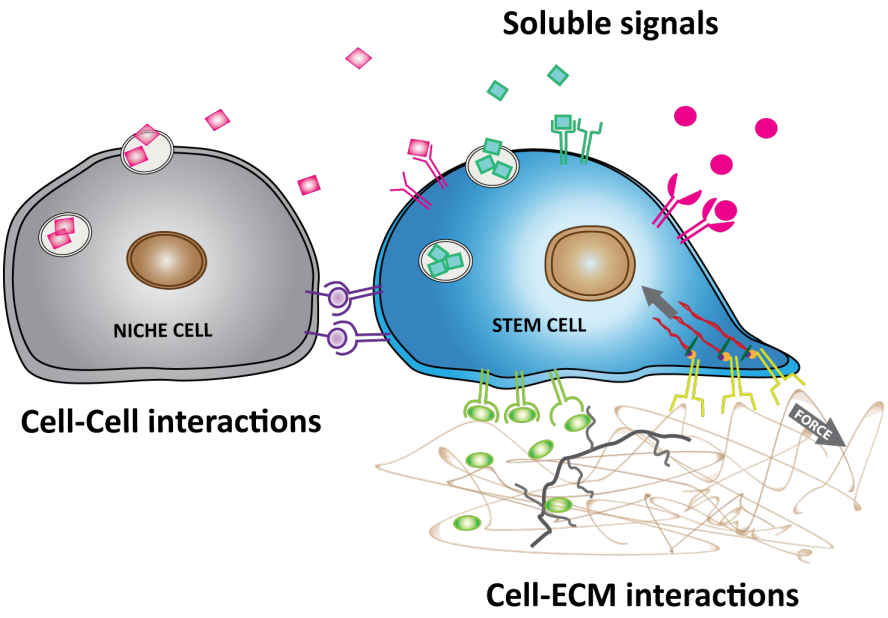

Figure 2.1 Networks of intrinsic and extrinsic biochemical and biophysical cues from the stem cell niche regulate stem cell self-renewal and differentiation.

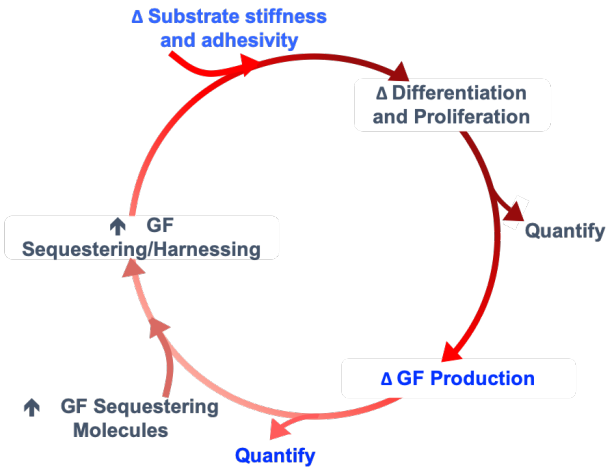

Figure 2.2. Autocatalytic culture substrates provide positive feedback loops to both induce changes in hMSC behavior and amplify the effects without the need for additionally supplemented growth factors. Modulating substrate stiffness and integrin-binding peptide concentration induces changes in hMSC behaviour. Upon proliferation or differentiation, cells generate GFs that are sequestered to the matrix, which further enhances growth and differentiation. Here, control of substrate properties in combination with harnessing cell-secreted endogenous GFs will cyclically autocatalyze growth and differentiation, all without the needed for additionally supplement GFs.

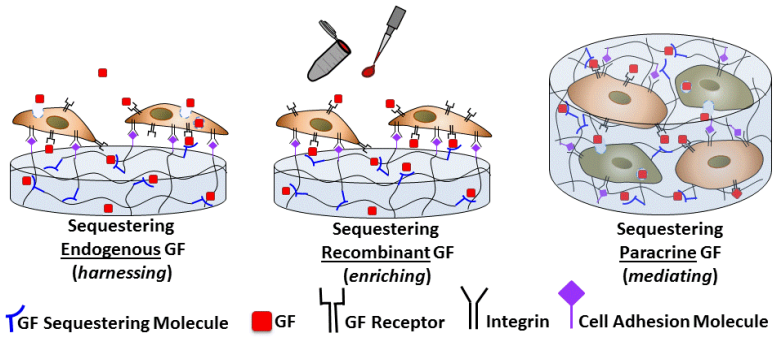

Figure 2.3. Schematic representation of sequestering and regulation of endogenous, recombinant, and paracrine GFs using substrates presenting sequestering molecules for harnessing, enriching, and mediating GF signaling.

2.11 References

[1] M. Rodrigues, L.G. Griffith, A. Wells, Growth factor regulation of proliferation and survival of multipotential stromal cells, Stem Cell Research & Therapy 1(4) (2010) 32-32.

[2] M.F. Pittenger, A.M. Mackay, S.C. Beck, R.K. Jaiswal, R. Douglas, J.D. Mosca, M.A. Moorman, D.W. Simonetti, S. Craig, D.R. Marshak, Multilineage Potential of Adult Human Mesenchymal Stem Cells, Science 284(5411) (1999) 143-147.

[3] G. Chamberlain, J. Fox, B. Ashton, J. Middleton, Concise Review: Mesenchymal Stem Cells: Their Phenotype, Differentiation Capacity, Immunological Features, and Potential for Homing, STEM CELLS 25(11) (2007) 2739-2749.

[4] N.c.M. Consortium, Achieving Large-Scale, Cost-Effective, Reproducible Manufacturing of High-Quality Cells: A Technology Roadmap to 2025, National cell Manufacturing Consortium, http://www.cellmanufacturingusa.org, 2016.

[5] A. Aijaz, M. Li, D. Smith, D. Khong, C. LeBlon, O.S. Fenton, R.M. Olabisi, S. Libutti, J. Tischfield, M.V. Maus, R. Deans, R.N. Barcia, D.G. Anderson, J. Ritz, R. Preti, B. Parekkadan, Biomanufacturing for clinically advanced cell therapies, Nat Biomed Eng 2(6) (2018) 362-376.

[6] Y. Sun, C.S. Chen, J. Fu, Forcing stem cells to behave: a biophysical perspective of the cellular microenvironment, Annual review of biophysics 41 (2012) 519-42.

[7] S. Gobaa, S. Hoehnel, M. Roccio, A. Negro, S. Kobel, M.P. Lutolf, Artificial niche microarrays for probing single stem cell fate in high throughput, Nature methods 8(11) (2011) 949-55.

[8] D.E. Discher, D.J. Mooney, P.W. Zandstra, Growth factors, matrices, and forces combine and control stem cells, Science 324(5935) (2009) 1673-1677.

[9] S.K. Schmitt, W.L. Murphy, P. Gopalan, Crosslinked PEG mats for peptide immobilization and stem cell adhesion, Journal of Materials Chemistry B 1(9) (2013) 1349.

[10] A.K. Jha, K.E. Healy, Controlling Osteogenic Stem Cell Differentiation via Soft, PLOS ONE 9(6) (2014) 1-11.

[11] K.A. Kilian, M. Mrksich, Directing stem cell fate by controlling the affinity and density of ligand-receptor interactions at the biomaterials interface, Angewandte Chemie 51(20) (2012) 4891-5.

[12] J.T. Koepsel, S.G. Loveland, M.P. Schwartz, S. Zorn, D.G. Belair, N.N. Le, W.L. Murphy, A chemically-defined screening platform reveals behavioral similarities between primary human mesenchymal stem cells and endothelial cells, Integrative biology : quantitative biosciences from nano to macro 4(12) (2012) 1508-21.

[13] S. Lin, N. Sangaj, T. Razafiarison, C. Zhang, S. Varghese, Influence of physical properties of biomaterials on cellular behavior, Pharmaceutical research 28(6) (2011) 1422-30.

[14] N.N.T. Le, S. Zorn, S.K. Schmitt, P. Gopalan, W.L. Murphy, Hydrogel arrays formed via differential wettability patterning enable combinatorial screening of stem cell behavior, Acta Biomaterialia (2015).

[15] M.M.L. Deckers, M. Karperien, C. van der Bent, T. Yamashita, S.E. Papapoulos, C.W.G.M. Löwik, Expression of Vascular Endothelial Growth Factors and Their Receptors during Osteoblast Differentiation, Endocrinology 141(5) (2000) 1667-1674.

[16] I.A. Potapova, G.R. Gaudette, P.R. Brink, R.B. Robinson, M.R. Rosen, I.S. Cohen, S.V. Doronin, Mesenchymal Stem Cells Support Migration, Extracellular Matrix Invasion, Proliferation, and Survival of Endothelial Cells In Vitro, STEM CELLS 25(7) (2007) 1761-1768.

[17] H. Mayer, H. Bertram, W. Lindenmaier, T. Korff, H. Weber, H. Weich, Vascular endothelial growth factor (VEGF-A) expression in human mesenchymal stem cells: Autocrine and paracrine

role on osteoblastic and endothelial differentiation, Journal of Cellular Biochemistry 95(4) (2005) 827-839.

[18] T. Furumatsu, Z.N. Shen, A. Kawai, K. Nishida, H. Manabe, T. Oohashi, H. Inoue, Y. Ninomiya, Vascular Endothelial Growth Factor Principally Acts as the Main Angiogenic Factor in the Early Stage of Human Osteoblastogenesis, Journal of Biochemistry 133(5) (2003) 633-639.

[19] S.B. Traphagen, I. Titushkin, S. Sun, K.K. Wary, M. Cho, Endothelial invasive response in a co-culture model with physically-induced osteodifferentiation, Journal of Tissue Engineering and Regenerative Medicine 7(8) (2013) 621-630.

[20] A.J. Engler, L. Bacakova, C. Newman, A. Hategan, M. Griffin, D.E. Discher, Substrate Compliance versus Ligand Density in Cell on Gel Responses, Biophysical journal 86(1) (2004) 617-628.

[21] J. Lee, A.A. Abdeen, D. Zhang, K.A. Kilian, Directing stem cell fate on hydrogel substrates by controlling cell geometry, matrix mechanics and adhesion ligand composition, Biomaterials 34(33) (2013) 8140-8.

[22] A.A. Abdeen, J.B. Weiss, J. Lee, K.A. Kilian, Matrix Composition and Mechanics Direct Proangiogenic Signaling from Mesenchymal Stem Cells, Tissue Engineering. Part A 20(19-20) (2014) 2737-2745.

[23] D.S. Benoit, K.S. Anseth, Heparin functionalized PEG gels that modulate protein adsorption for hMSC adhesion and differentiation, Acta Biomater 1(4) (2005) 461-70.

[24] D.G. Belair, N.N. Le, W.L. Murphy, Design of growth factor sequestering biomaterials, Chem Commun (Camb) 50(99) (2014) 15651-68.

[25] W.L. Murphy, T.C. McDevitt, A.J. Engler, Materials as stem cell regulators, Nat Mater 13(6) (2014) 547-557.

[26] S. VandeVondele, J. Voros, J.A. Hubbell, RGD-grafted poly-L-lysine-graft-(polyethylene glycol) copolymers block non-specific protein adsorption while promoting cell adhesion, Biotechnol Bioeng 82(7) (2003) 784-90.

[27] J.M. Maloney, D. Nikova, F. Lautenschlager, E. Clarke, R. Langer, J. Guck, K.J. Van Vliet, Mesenchymal stem cell mechanics from the attached to the suspended state, Biophys J 99(8) (2010) 2479-87.

[28] V.V. Rao, M.K. Vu, H. Ma, A.R. Killaars, K.S. Anseth, Rescuing mesenchymal stem cell regenerative properties on hydrogel substrates post serial expansion, Bioengineering & Translational Medicine (2018).

[29] M. Raab, J.-W. Shin, D.E. Discher, Matrix elasticity in vitro controls muscle stem cell fate in vivo, Stem Cell Research & Therapy 1(5) (2010) 38-38.

[30] H. Liu, Z. Zhang, R.J. Linhardt, Lessons learned from the contamination of heparin, Nat Prod Rep 26(3) (2009) 313-21.

[31] A.W. McMahon, R.G. Pratt, T.A. Hammad, S. Kozlowski, E. Zhou, S. Lu, C.G. Kulick, T. Mallick, G. Dal Pan, Description of hypersensitivity adverse events following administration of heparin that was potentially contaminated with oversulfated chondroitin sulfate in early 2008, Pharmacoepidemiol Drug Saf 19(9) (2010) 921-33.

[32] J.Y. van der Meer, E. Kellenbach, L.J. van den Bos, From Farm to Pharma: An Overview of Industrial Heparin Manufacturing Methods, Molecules 22(6) (2017).

[33] J.R. Bishop, M. Schuksz, J.D. Esko, Heparan sulphate proteoglycans fine-tune mammalian physiology, Nature 446 (2007) 1030.

[34] A.W. Xie, W.L. Murphy, Engineered biomaterials to mitigate growth factor cost in cell biomanufacturing, Current Opinion in Biomedical Engineering 10 (2019) 1-10.

[35] J.L. Drury, D.J. Mooney, Hydrogels for tissue engineering: scaffold design variables and applications, Biomaterials 24(24) (2003) 4337-4351.

[36] B.V. Slaughter, S.S. Khurshid, O.Z. Fisher, A. Khademhosseini, N.A. Peppas, Hydrogels in regenerative medicine, Adv Mater 21(32-33) (2009) 3307-3329.

[37] M. Jafari, Z. Paknejad, M.R. Rad, S.R. Motamedian, M.J. Eghbal, N. Nadjmi, A. Khojasteh, Polymeric scaffolds in tissue engineering: a literature review, Journal of Biomedical Materials Research Part B: Applied Biomaterials 105(2) (2017) 431-459.

[38] E. Ruoslahti, Ruoslahti E. RGD and other recognition sequences for integrins. Annu Rev Cell Dev Biol 12: 697-715, 1996.

[39] G.A. Hudalla, N.A. Kouris, J.T. Koepsel, B.M. Ogle, W.L. Murphy, Harnessing endogenous growth factor activity modulates stem cell behavior, Integrative Biology 3(8) (2011) 832-842.

[40] G.A. Hudalla, W.L. Murphy, Immobilization of Peptides with Distinct Biological Activities onto Stem Cell Culture Substrates Using Orthogonal Chemistries, Langmuir 26(9) (2010) 6449-6456.

[41] A.G. Arroyo, M.L. Iruela-Arispe, Extracellular matrix, inflammation, and the angiogenic response, Cardiovascular research 86(2) (2010) 226-235.

[42] B.D. Fairbanks, M.P. Schwartz, A.E. Halevi, C.R. Nuttelman, C.N. Bowman, K.S. Anseth, A Versatile Synthetic Extracellular Matrix Mimic via Thiol-Norbornene Photopolymerization, Adv Mater 21(48) (2009) 5005-5010.

[43] M.W. Toepke, N.A. Impellitteri, S.K. Lan Levengood, D.S. Boeldt, I.M. Bird, W.L. Murphy, Regulating specific growth factor signaling using immobilized branched ligands, Advanced healthcare materials 1(4) (2012) 457-460.

[44] H. Davids, A. Ahmed, A. Oberholster, C. van der Westhuizen, M. Mer, I. Havlik, Endogenous heparin levels in the controlled asthmatic patient, South African Medical Journal; Vol 100, No 5 (2010) (2010).

[45] M.W. Mosesson, Fibrinogen and fibrin structure and functions, Journal of Thrombosis and Haemostasis 3(8) (2005) 1894-1904.

[46] K. Crapnell, R. Blaesius, A. Hastings, D.P. Lennon, A.I. Caplan, S.P. Bruder, Growth, differentiation capacity, and function of mesenchymal stem cells expanded in serum-free medium developed via combinatorial screening, Exp Cell Res 319(10) (2013) 1409-18.

[47] S. Jung, K.M. Panchalingam, L. Rosenberg, L.A. Behie, Ex Vivo Expansion of Human Mesenchymal Stem Cells in Defined Serum-Free Media, Stem Cells International 2012 (2012) 21.

[48] L.G. Chase, S. Yang, V. Zachar, Z. Yang, U. Lakshmipathy, J. Bradford, S.E. Boucher, M.C. Vemuri, Development and characterization of a clinically compliant xeno-free culture medium in good manufacturing practice for human multipotent mesenchymal stem cells, Stem Cells Transl Med 1(10) (2012) 750-8.

[49] L.G. Chase, U. Lakshmipathy, L.A. Solchaga, M.S. Rao, M.C. Vemuri, A novel serum-free medium for the expansion of human mesenchymal stem cells, Stem Cell Research & Therapy 1(1) (2010) 8-8.

[50] C. Tekkatte, G.P. Gunasingh, K.M. Cherian, K. Sankaranarayanan, "Humanized" stem cell culture techniques: the animal serum controversy, Stem cells international 2011 (2011) 504723-504723.

[51] K.Y. Tan, K.L. Teo, J.F.Y. Lim, A.K.L. Chen, S. Reuveny, S.K.W. Oh, Serum-free media formulations are cell line–specific and require optimization for microcarrier culture, Cytotherapy 17(8) (2015) 1152-1165.

[52] P.J. Dolley-Sonneville, L.E. Romeo, Z.K. Melkoumian, Synthetic Surface for Expansion of Human Mesenchymal Stem Cells in Xeno-Free, Chemically Defined Culture Conditions, PLoS ONE 8(8) (2013) e70263.

[53] H. Miwa, Y. Hashimoto, K. Tensho, S. Wakitani, M. Takagi, Xeno-free proliferation of human bone marrow mesenchymal stem cells, Cytotechnology 64(3) (2012) 301-308.

[54] I. Hartmann, T. Hollweck, S. Haffner, M. Krebs, B. Meiser, B. Reichart, G. Eissner, Umbilical cord tissue-derived mesenchymal stem cells grow best under GMP-compliant culture conditions and maintain their phenotypic and functional properties, Journal of Immunological Methods 363(1) (2010) 80-89.

[55] A. DePalma, Confluent Trends in Cell Culture Media, Genetic Engineering & Biotechnology News 36(3) (2016) 16-19.

[56] Cell Culture Media, Sera, and Reagents Market - Global Industry Analysis, Size, Share, Growth, Trends, and Forecast 2015 - 2023, 2015. http://www.transparencymarketresearch.com/cell-culture-media-sera-reagents-market.html. (Accessed May 9 2017).

[57] S. Ding, P. Kingshott, H. Thissen, M. Pera, P.-Y. Wang, Modulation of human mesenchymal and pluripotent stem cell behavior using biophysical and biochemical cues: A review, Biotechnology and Bioengineering 114(2) (2017) 260-280.

[58] A. Oikonomopoulos, W.K. van Deen, A.-R. Manansala, P.N. Lacey, T.A. Tomakili, A. Ziman, D.W. Hommes, Optimization of human mesenchymal stem cell manufacturing: the effects of animal/xeno-free media, Scientific Reports 5 (2015) 16570.

[59] Y.Y. Lipsitz, W.D. Milligan, I. Fitzpatrick, E. Stalmeijer, S.S. Farid, K.Y. Tan, D. Smith, R. Perry, J. Carmen, A. Chen, C. Mooney, J. Fink, A roadmap for cost-of-goods planning to guide economic production of cell therapy products, Cytotherapy 19(12) (2017) 1383-1391.

[60] S. Gobaa, S. Hoehnel, M.P. Lutolf, Substrate elasticity modulates the responsiveness of mesenchymal stem cells to commitment cues, Integrative Biology 7(10) (2015) 1135-1142.

[61] A. Ranga, M.P. Lutolf, High-throughput approaches for the analysis of extrinsic regulators of stem cell fate, Current Opinion in Cell Biology 24(2) (2012) 236-244.

[62] Y. Sun, C.S. Chen, J. Fu, Forcing stem cells to behave: a biophysical perspective of the cellular microenvironment, Annu Rev Biophys 41 (2012) 519-542.

[63] J.T. Koepsel, P.T. Brown, S.G. Loveland, W.-J. Li, W.L. Murphy, Combinatorial screening of chemically defined human mesenchymal stem cell culture substrates, J Mater Chem 22(37) (2012) 19474-19481.

[64] S. Kobel, M.P. Lutolf, High-throughput methods to define complex stem cell niches, BioTechniques 48(4) (2010) ix-xxii.

[65] D.E. Discher, D.J. Mooney, P.W. Zandstra, Growth Factors, Matrices, and Forces Combine and Control Stem Cells, Science 324(5935) (2009) 1673.

[66] D.G. Anderson, S. Levenberg, R. Langer, Nanoliter-scale synthesis of arrayed biomaterials and application to human embryonic stem cells, Nature Biotechnology 22(7) (2004) 863-866.

[67] A.J. Engler, S. Sen, H.L. Sweeney, D.E. Discher, Matrix Elasticity Directs Stem Cell Lineage Specification, Cell 126(4) (2006) 677-689.

[68] S.C. Tan, W.X. Pan, G. Ma, N. Cai, K.W. Leong, K. Liao, Viscoelastic behaviour of human mesenchymal stem cells, BMC Cell Biol 9 (2008) 40.

[69] N. Huebsch, P.R. Arany, A.S. Mao, D. Shvartsman, O.A. Ali, S.A. Bencherif, J. Rivera-Feliciano, D.J. Mooney, Harnessing traction-mediated manipulation of the cell/matrix interface to control stem-cell fate, Nat Mater 9(6) (2010) 518-26.

[70] R. McBeath, D.M. Pirone, C.M. Nelson, K. Bhadriraju, C.S. Chen, Cell Shape, Cytoskeletal Tension, and RhoA Regulate Stem Cell Lineage Commitment, Developmental Cell 6(4) (2004) 483-495.

[71] X. Yao, R. Peng, J. Ding, Effects of aspect ratios of stem cells on lineage commitments with and without induction media, Biomaterials 34(4) (2013) 930-939.

[72] K.A. Kilian, B. Bugarija, B.T. Lahn, M. Mrksich, Geometric cues for directing the differentiation of mesenchymal stem cells, Proceedings of the National Academy of Sciences 107(11) (2010) 4872.

[73] I.L. Kim, S. Khetan, B.M. Baker, C.S. Chen, J.A. Burdick, Fibrous hyaluronic acid hydrogels that direct MSC chondrogenesis through mechanical and adhesive cues, Biomaterials 34(22) (2013) 5571-5580.

[74] S. Cho, J. Irianto, D.E. Discher, Mechanosensing by the nucleus: From pathways to scaling relationships, J Cell Biol 216(2) (2017) 305-315.

[75] P.C. Dingal, D.E. Discher, Combining insoluble and soluble factors to steer stem cell fate, Nat Mater 13(6) (2014) 532-7.

[76] P. Defilippi, P. Di Stefano, S. Cabodi, p130Cas: a versatile scaffold in signaling networks, Trends Cell Biol 16(5) (2006) 257-63.

[77] G.R. Fedorchak, A. Kaminski, J. Lammerding, Cellular mechanosensing: getting to the nucleus of it all, Prog Biophys Mol Biol 115(2-3) (2014) 76-92.

[78] J. Lammerding, K. Wolf, Nuclear envelope rupture: Actin fibers are putting the squeeze on the nucleus, J Cell Biol 215(1) (2016) 5-8.

[79] S.X. Hsiong, T. Boontheekul, N. Huebsch, D.J. Mooney, Cyclic arginine-glycine-aspartate peptides enhance three-dimensional stem cell osteogenic differentiation, Tissue engineering. Part A 15(2) (2009) 263-272.

[80] K.A. Kilian, M. Mrksich, Directing Stem Cell Fate by Controlling the Affinity and Density of Ligand–Receptor Interactions at the Biomaterials Interface, Angewandte Chemie International Edition 51(20) (2012) 4891-4895.

[81] L.-S. Wang, J. Boulaire, P.P.Y. Chan, J.E. Chung, M. Kurisawa, The role of stiffness of gelatin–hydroxyphenylpropionic acid hydrogels formed by enzyme-mediated crosslinking on the differentiation of human mesenchymal stem cell, Biomaterials 31(33) (2010) 8608-8616.

[82] M. Sun, G. Chi, P. Li, S. Lv, J. Xu, Z. Xu, Y. Xia, Y. Tan, J. Xu, L. Li, Y. Li, Effects of Matrix Stiffness on the Morphology, Adhesion, Proliferation and Osteogenic Differentiation of Mesenchymal Stem Cells, Int J Med Sci 15(3) (2018) 257-268.

[83] F.P. Seib, M. Prewitz, C. Werner, M. Bornhäuser, Matrix elasticity regulates the secretory profile of human bone marrow-derived multipotent mesenchymal stromal cells (MSCs), Biochemical and Biophysical Research Communications 389(4) (2009) 663-667.

[84] E.H. Schwab, M. Halbig, K. Glenske, A.-S. Wagner, S. Wenisch, E.A. Cavalcanti-Adam, Distinct Effects of RGD-glycoproteins on Integrin-Mediated Adhesion and Osteogenic Differentiation of Human Mesenchymal Stem Cells, International Journal of Medical Sciences 10(13) (2013) 1846-1859.

[85] A.S. Rowlands, P.A. George, J.J. Cooper-White, Directing osteogenic and myogenic differentiation of MSCs: interplay of stiffness and adhesive ligand presentation, American Journal of Physiology - Cell Physiology 295(4) (2008) C1037.

[86] T.H. Qazi, D.J. Mooney, G.N. Duda, S. Geissler, Biomaterials that promote cell-cell interactions enhance the paracrine function of MSCs, Biomaterials 140 (2017) 103-114.

[87] J.S. Park, J.S. Chu, A.D. Tsou, R. Diop, Z. Tang, A. Wang, S. Li, The Effect of Matrix Stiffness on the Differentiation of Mesenchymal Stem Cells in Response to TGF-β, Biomaterials 32(16) (2011) 3921-3930.

[88] W.C. Lee, H. Shi, Z. Poon, L.M. Nyan, T. Kaushik, G.V. Shivashankar, J.K. Chan, C.T. Lim, J. Han, K.J. Van Vliet, Multivariate biophysical markers predictive of mesenchymal stromal cell multipotency, Proc Natl Acad Sci U S A 111(42) (2014) E4409-18.

[89] K.Y. Lee, E. Alsberg, S. Hsiong, W. Comisar, J. Linderman, R. Ziff, D. Mooney, Nanoscale Adhesion Ligand Organization Regulates Osteoblast Proliferation and Differentiation, Nano Letters 4(8) (2004) 1501-1506.

[90] J. Lam, T. Segura, The modulation of MSC integrin expression by RGD presentation, Biomaterials 34(16) (2013) 3938-3947.

[91] J.E. Frith, R.J. Mills, J.E. Hudson, J.J. Cooper-White, Tailored Integrin–Extracellular Matrix Interactions to Direct Human Mesenchymal Stem Cell Differentiation, Stem Cells and Development 21(13) (2012) 2442-2456.

[92] D.A. Starr, H.N. Fridolfsson, Interactions between nuclei and the cytoskeleton are mediated by SUN-KASH nuclear-envelope bridges, Annual review of cell and developmental biology 26 (2010) 421-444.

[93] N.P. Talele, J. Fradette, J.E. Davies, A. Kapus, B. Hinz, Expression of α-Smooth Muscle Actin Determines the Fate of Mesenchymal Stromal Cells, Stem Cell Reports 4(6) (2015) 1016-1030.

[94] S. Musah, S.A. Morin, P.J. Wrighton, D.B. Zwick, S. Jin, L.L. Kiessling, Glycosaminoglycan-Binding Hydrogels Enable Mechanical Control of Human Pluripotent Stem Cell Self-Renewal, ACS Nano 6(11) (2012) 10168-10177.

[95] S. Musah, P.J. Wrighton, Y. Zaltsman, X. Zhong, S. Zorn, M.B. Parlato, C. Hsiao, S.P. Palecek, Q. Chang, W.L. Murphy, L.L. Kiessling, Substratum-induced differentiation of human pluripotent stem cells reveals the coactivator YAP is a potent regulator of neuronal specification, Proceedings of the National Academy of Sciences 111(38) (2014) 13805-13810.

[96] A.L. Smith Callahan, Combinatorial Method/High Throughput Strategies for Hydrogel Optimization in Tissue Engineering Applications, Gels 2(2) (2016).

[97] Y. Yang, Q.H. Chen, A.R. Liu, X.P. Xu, J.B. Han, H.B. Qiu, Synergism of MSC-secreted HGF and VEGF in stabilising endothelial barrier function upon lipopolysaccharide stimulation via the Rac1 pathway, Stem Cell Res Ther 6 (2015) 250.

[98] K. Wingate, M. Floren, Y. Tan, P.O.N. Tseng, W. Tan, Synergism of Matrix Stiffness and Vascular Endothelial Growth Factor on Mesenchymal Stem Cells for Vascular Endothelial Regeneration, Tissue Engineering. Part A 20(17-18) (2014) 2503-2512.

[99] I. Aizman, D. Vinodkumar, M. McGrogan, D. Bates, Cell Injury-Induced Release of Fibroblast Growth Factor 2: Relevance to Intracerebral Mesenchymal Stromal Cell Transplantations, Stem Cells and Development 24(14) (2015) 1623-1634.

[100] B. Johnstone, T.M. Hering, A.I. Caplan, V.M. Goldberg, J.U. Yoo, In VitroChondrogenesis of Bone Marrow-Derived Mesenchymal Progenitor Cells, Experimental Cell Research 238(1) (1998) 265-272.

[101] P.T. Lee, W.-J. Li, Chondrogenesis of Embryonic Stem Cell-Derived Mesenchymal Stem Cells Induced by TGFβ1 and BMP7 Through Increased TGFβ Receptor Expression and Endogenous TGFβ1 Production, Journal of Cellular Biochemistry (2016) n/a-n/a.

[102] Z. Huang, E.R. Nelson, R.L. Smith, S.B. Goodman, The sequential expression profiles of growth factors from osteoprogenitors [correction of osteroprogenitors] to osteoblasts in vitro, Tissue engineering 13(9) (2007) 2311-20.

[103] B.S. Kim, K.S. Kang, S.K. Kang, Soluble factors from ASCs effectively direct control of chondrogenic fate, Cell proliferation 43(3) (2010) 249-61.

[104] J.S. Lee, A. Wagoner-Johnson, W.L. Murphy, Modular Peptide Growth Factors for Substrate-Mediated Stem Cell Differentiation, Angew. Chem.-Int. Edit. 48(34) (2009) 6266-6269.

[105] S.A. Khan, J. Joyce, T. Tsuda, Quantification of active and total transforming growth factor-β levels in serum and solid organ tissues by bioassay, BMC Research Notes 5(1) (2012) 1-9.

[106] T. Oida, H.L. Weiner, Depletion of TGF-β from fetal bovine serum, Journal of Immunological Methods 362(1–2) (2010) 195-198.

[107] X. Zheng, H. Baker, W.S. Hancock, F. Fawaz, M. McCaman, E. Pungor, Proteomic Analysis for the Assessment of Different Lots of Fetal Bovine Serum as a Raw Material for Cell Culture. Part IV. Application of Proteomics to the Manufacture of Biological Drugs, Biotechnology Progress 22(5) (2006) 1294-1300.

[108] G. Villegas, B. Lange-Sperandio, A. Tufro, Autocrine and paracrine functions of vascular endothelial growth factor (VEGF) in renal tubular epithelial cells, Kidney Int 67(2) (2005) 449-57.

[109] D. Krakora, P. Mulcrone, M. Meyer, C. Lewis, K. Bernau, G. Gowing, C. Zimprich, P. Aebischer, C.N. Svendsen, M. Suzuki, Synergistic effects of GDNF and VEGF on lifespan and disease progression in a familial ALS rat model, Mol Ther 21(8) (2013) 1602-10.

[110] J. Pons, Y. Huang, J. Arakawa-Hoyt, D. Washko, J. Takagawa, J. Ye, W. Grossman, H. Su, VEGF improves survival of mesenchymal stem cells in infarcted hearts, Biochemical and Biophysical Research Communications 376(2) (2008) 419-422.

[111] P.R. Amable, M.V.T. Teixeira, R.B.V. Carias, J.M. Granjeiro, R. Borojevic, Protein synthesis and secretion in human mesenchymal cells derived from bone marrow, adipose tissue and Wharton's jelly, Stem Cell Research & Therapy 5(2) (2014) 53-53.

[112] P.R. Amable, M.V.T. Teixeira, R.B.V. Carias, J.M. Granjeiro, R. Borojevic, Gene expression and protein secretion during human mesenchymal cell differentiation into adipogenic cells, BMC Cell Biology 15(1) (2014) 46.

[113] C. Penna, M.-G. Perrelli, J.-P. Karam, C. Angotti, C. Muscari, C.N. Montero-Menei, P. Pagliaro, Pharmacologically active microcarriers influence VEGF-A effects on mesenchymal stem cell survival, Journal of Cellular and Molecular Medicine 17(1) (2013) 192-204.

[114] J.S. Elman, M. Li, F. Wang, J.M. Gimble, B. Parekkadan, A comparison of adipose and bone marrow-derived mesenchymal stromal cell secreted factors in the treatment of systemic inflammation, Journal of Inflammation 11(1) (2014) 1.

[115] K. Ogata, M. Osugi, T. Kawai, Y. Wakayama, K. Sakaguchi, S. Nakamura, W. Katagiri, Secretomes of mesenchymal stem cells induce early bone regeneration by accelerating migration

of stem cells, Journal of Oral and Maxillofacial Surgery, Medicine, and Pathology 30(5) (2018) 445-451.

[116] K. Ogata, W. Katagiri, H. Hibi, Secretomes from mesenchymal stem cells participate in the regulation of osteoclastogenesis in vitro, Clin Oral Investig 21(6) (2017) 1979-1988.

[117] W. Katagiri, T. Kawai, M. Osugi, Y. Sugimura-Wakayama, K. Sakaguchi, T. Kojima, T. Kobayashi, Angiogenesis in newly regenerated bone by secretomes of human mesenchymal stem cells, Maxillofac Plast Reconstr Surg 39(1) (2017) 8.

[118] K. Ogata, M. Matsumura, M. Moriyama, W. Katagiri, H. Hibi, S. Nakamura, Cytokine Mixtures Mimicking Secretomes From Mesenchymal Stem Cells Improve Medication-Related Osteonecrosis of the Jaw in a Rat Model, JBMR Plus 2(2) (2018) 69-80.

[119] S. Barreto, A. Gonzalez-Vazquez, A.R. Cameron, B. Cavanagh, D.J. Murray, F.J. O'Brien, Identification of the mechanisms by which age alters the mechanosensitivity of mesenchymal stromal cells on substrates of differing stiffness: Implications for osteogenesis and angiogenesis, Acta Biomater 53 (2017) 59-69.

[120] A.L. Russell, R. Lefavor, N. Durand, L. Glover, A.C. Zubair, Modifiers of mesenchymal stem cell quantity and quality, Transfusion 58(6) (2018) 1434-1440.

[121] J.A. Zimmermann, T.C. McDevitt, Pre-conditioning mesenchymal stromal cell spheroids for immunomodulatory paracrine factor secretion, Cytotherapy 16(3) (2014) 331-45.

[122] Y.M. Li, T. Schilling, P. Benisch, S. Zeck, J. Meissner-Weigl, D. Schneider, C. Limbert, J. Seufert, M. Kassem, N. Schutze, F. Jakob, R. Ebert, Effects of high glucose on mesenchymal stem cell proliferation and differentiation, Biochem Biophys Res Commun 363(1) (2007) 209-15.

[123] B.R. Weil, A.M. Abarbanell, J.L. Herrmann, Y. Wang, D.R. Meldrum, High glucose concentration in cell culture medium does not acutely affect human mesenchymal stem cell growth

factor production or proliferation, Am J Physiol Regul Integr Comp Physiol 296(6) (2009) R1735-43.

[124] S. Proksch, G. Bittermann, K. Vach, R. Nitschke, P. Tomakidi, E. Hellwig, hMSC-Derived VEGF Release Triggers the Chemoattraction of Alveolar Osteoblasts, Stem Cells 33(10) (2015) 3114-24.

[125] Y.C. Jiang, H.L. Jiao, M.S. Lee, T. Wang, L.S. Turng, Q. Li, W.J. Li, Endogenous biological factors modulated by substrate stiffness regulate endothelial differentiation of mesenchymal stem cells, J Biomed Mater Res A 106(6) (2018) 1595-1603.

[126] H. Kagiwada, T. Yashiki, A. Ohshima, M. Tadokoro, N. Nagaya, H. Ohgushi, Human mesenchymal stem cells as a stable source of VEGF-producing cells, Journal of Tissue Engineering and Regenerative Medicine 2(4) (2008) 184-189.

[127] K.D. Salazar, S.M. Lankford, A.R. Brody, Mesenchymal stem cells produce Wnt isoforms and TGF-β1 that mediate proliferation and procollagen expression by lung fibroblasts, American Journal of Physiology - Lung Cellular and Molecular Physiology 297(5) (2009) L1002-L1011.

[128] A.S. Khalil, A.W. Xie, W.L. Murphy, Context clues: the importance of stem cell-material interactions, ACS chemical biology 9(1) (2014) 45-56.

[129] W.L. Murphy, T.C. McDevitt, A.J. Engler, Materials as stem cell regulators, Nature Materials Accepted (2014).

[130] M.J. Dalby, N. Gadegaard, R. Tare, A. Andar, M.O. Riehle, P. Herzyk, C.D. Wilkinson, R.O. Oreffo, The control of human mesenchymal cell differentiation using nanoscale symmetry and disorder, Nat Mater 6(12) (2007) 997-1003.

[131] R.J. McMurray, N. Gadegaard, P.M. Tsimbouri, K.V. Burgess, L.E. McNamara, R. Tare, K. Murawski, E. Kingham, R.O. Oreffo, M.J. Dalby, Nanoscale surfaces for the long-term

maintenance of mesenchymal stem cell phenotype and multipotency, Nat Mater 10(8) (2011) 637-44.

[132] E.K. Yim, E.M. Darling, K. Kulangara, F. Guilak, K.W. Leong, Nanotopography-induced changes in focal adhesions, cytoskeletal organization, and mechanical properties of human mesenchymal stem cells, Biomaterials 31(6) (2010) 1299-306.

[133] D.S.W. Benoit, M.P. Schwartz, A.R. Durney, K.S. Anseth, Small functional groups for controlled differentiation of hydrogel-encapsulated human mesenchymal stem cells, Nature Materials 7(10) (2008) 816-823.

[134] K. Saha, Y. Mei, C.M. Reisterer, N.K. Pyzocha, J. Yang, J. Muffat, M.C. Davies, M.R. Alexander, R. Langer, D.G. Anderson, R. Jaenisch, Surface-engineered substrates for improved human pluripotent stem cell culture under fully defined conditions, Proceedings of the National Academy of Sciences of the United States of America 108(46) (2011) 18714-9.

[135] F.P. Seib, M. Prewitz, C. Werner, M. Bornhauser, Matrix elasticity regulates the secretory profile of human bone marrow-derived multipotent mesenchymal stromal cells (MSCs), Biochem Biophys Res Commun 389(4) (2009) 663-7.

[136] R.A. Marklein, D.E. Soranno, J.A. Burdick, Magnitude and presentation of mechanical signals influence adult stem cell behavior in 3-dimensional macroporous hydrogels, Soft Matter 8(31) (2012) 8113-8120.

[137] C.J. Cunningham, E. Redondo-Castro, S.M. Allan, The therapeutic potential of the mesenchymal stem cell secretome in ischaemic stroke, J Cereb Blood Flow Metab 38(8) (2018) 1276-1292.

[138] J. Rezaie, M.S. Mehranjani, R. Rahbarghazi, M.A. Shariatzadeh, Angiogenic and Restorative Abilities of Human Mesenchymal Stem Cells Were Reduced Following Treatment With Serum From Diabetes Mellitus Type 2 Patients, J Cell Biochem 119(1) (2018) 524-535.

[139] K.C. Murphy, J. Whitehead, D. Zhou, S.S. Ho, J.K. Leach, Engineering fibrin hydrogels to promote the wound healing potential of mesenchymal stem cell spheroids, Acta Biomater 64 (2017) 176-186.

[140] H.R. Hofer, R.S. Tuan, Secreted trophic factors of mesenchymal stem cells support neurovascular and musculoskeletal therapies, Stem Cell Res Ther 7(1) (2016) 131.

[141] L. Solmesky, S. Lefler, J. Jacob-Hirsch, S. Bulvik, G. Rechavi, M. Weil, Serum Free Cultured Bone Marrow Mesenchymal Stem Cells as a Platform to Characterize the Effects of Specific Molecules, PLoS ONE 5(9) (2010) e12689.

[142] S. Nonnis, E. Maffioli, L. Zanotti, F. Santagata, A. Negri, A. Viola, S. Elliman, G. Tedeschi, Effect of fetal bovine serum in culture media on MS analysis of mesenchymal stromal cells secretome, EuPA Open Proteomics 10 (2016) 28-30.

[143] M.C. Pellitteri-Hahn, M.C. Warren, D.N. Didier, E.L. Winkler, S.P. Mirza, A.S. Greene, M. Olivier, Improved Mass Spectrometric Proteomic Profiling of the Secretome of Rat Vascular Endothelial Cells, Journal of Proteome Research 5(10) (2006) 2861-2864.

[144] J.L. Berlier, S. Rigutto, A. Dalla Valle, J. Lechanteur, M.S. Soyfoo, V. Gangji, J. Rasschaert, Adenosine triphosphate prevents serum deprivation-induced apoptosis in human mesenchymal stem cells via activation of the MAPK signaling pathways, Stem Cells 33(1) (2015) 211-8.

[145] G. Chen, D.R. Gulbranson, Z. Hou, J.M. Bolin, V. Ruotti, M.D. Probasco, K. Smuga-Otto, S.E. Howden, N.R. Diol, N.E. Propson, R. Wagner, G.O. Lee, J. Antosiewicz-Bourget, J.M. Teng,

J.A. Thomson, Chemically defined conditions for human iPSC derivation and culture, Nature methods 8(5) (2011) 424-9.

[146] E.S. Lippmann, M.C. Estevez-Silva, R.S. Ashton, Defined human pluripotent stem cell culture enables highly efficient neuroepithelium derivation without small molecule inhibitors, Stem cells (2013).

[147] T.E. Ludwig, V. Bergendahl, M.E. Levenstein, J. Yu, M.D. Probasco, J.A. Thomson, Feeder-independent culture of human embryonic stem cells, Nature methods 3(8) (2006) 637-46.

[148] S. Zhu, M. Rezvani, J. Harbell, A.N. Mattis, A.R. Wolfe, L.Z. Benet, H. Willenbring, S. Ding, Mouse liver repopulation with hepatocytes generated from human fibroblasts, Nature (2014).

[149] J.A. Ryan, Reducing Cell Culture Costs By Reducing Serum Levels, in: A. Laboratory (Ed.) Application Notes, www.AmericanLaboratory.com, www.AmericanLaboratory.com, 2006.

[150] K. Takahashi, K. Tanabe, M. Ohnuki, M. Narita, T. Ichisaka, K. Tomoda, S. Yamanaka, Induction of Pluripotent Stem Cells from Adult Human Fibroblasts by Defined Factors, Cell 131(5) (2007) 861-872.

[151] L. Li, S.A.L. Bennett, L. Wang, Role of E-cadherin and other cell adhesion molecules in survival and differentiation of human pluripotent stem cells, Cell Adh Migr 6(1) (2012) 59-70.

[152] D. Li, J. Zhou, F. Chowdhury, J. Cheng, N. Wang, F. Wang, Role of mechanical factors in fate decisions of stem cells, Regenerative medicine 6(2) (2011) 229-240.

[153] M. Ohgushi, M. Matsumura, M. Eiraku, K. Murakami, T. Aramaki, A. Nishiyama, K. Muguruma, T. Nakano, H. Suga, M. Ueno, T. Ishizaki, H. Suemori, S. Narumiya, H. Niwa, Y. Sasai, Molecular Pathway and Cell State Responsible for Dissociation-Induced Apoptosis in Human Pluripotent Stem Cells, Cell Stem Cell 7(2) (2010) 225-239.

[154] D. Li, J. Zhou, L. Wang, M.E. Shin, P. Su, X. Lei, H. Kuang, W. Guo, H. Yang, L. Cheng, T.S. Tanaka, D.E. Leckband, A.B. Reynolds, E. Duan, F. Wang, Integrated biochemical and mechanical signals regulate multifaceted human embryonic stem cell functions, The Journal of cell biology 191(3) (2010) 631-644.

[155] Y. Sun, L.G. Villa-Diaz, R.H.W. Lam, W. Chen, P.H. Krebsbach, J. Fu, Mechanics Regulates Fate Decisions of Human Embryonic Stem Cells, PLoS ONE 7(5) (2012) e37178.

[156] J. Zoldan, E.D. Karagiannis, C.Y. Lee, D.G. Anderson, R. Langer, S. Levenberg, The influence of scaffold elasticity on germ layer specification of human embryonic stem cells, Biomaterials 32(36) (2011) 9612-9621.

[157] A.J. Keung, P. Asuri, S. Kumar, D.V. Schaffer, Soft microenvironments promote the early neurogenic differentiation but not self-renewal of human pluripotent stem cells, Integrative biology : quantitative biosciences from nano to macro 4(9) (2012) 1049-1058.

[158] N. Eroshenko, R. Ramachandran, V.K. Yadavalli, R.R. Rao, Effect of substrate stiffness on early human embryonic stem cell differentiation, Journal of Biological Engineering 7 (2013) 7-7.

[159] Y. Sun, J. Fu, Mechanobiology: a new frontier for human pluripotent stem cells, Integrative Biology 5(3) (2013) 450-457.

[160] G. Chen, D.R. Gulbranson, Z. Hou, J.M. Bolin, V. Ruotti, M.D. Probasco, K. Smuga-Otto, S.E. Howden, N.R. Diol, N.E. Propson, R. Wagner, G.O. Lee, J. Antosiewicz-Bourget, J.M.C. Teng, J.A. Thomson, Chemically defined conditions for human iPSC derivation and culture, Nat Meth 8(5) (2011) 424-429.

[161] H. Ichikawa, N. Nakata, Y. Abo, S. Shirasawa, T. Yokoyama, S. Yoshie, F. Yue, D. Tomotsune, K. Sasaki, Gene pathway analysis of the mechanism by which the Rho-associated

kinase inhibitor Y-27632 inhibits apoptosis in isolated thawed human embryonic stem cells, Cryobiology 64(1) (2012) 12-22.

[162] J. Gharechahi, M. Pakzad, S. Mirshavaladi, M. Sharifitabar, H. Baharvand, G.H. Salekdeh, The effect of Rho-associated kinase inhibition on the proteome pattern of dissociated human embryonic stem cells, Molecular BioSystems 10(3) (2014) 640-652.

[163] E.R. Smith, X.-Y. Zhang, C.D. Capo-Chichi, X. Chen, X.-X. Xu, Increased expression of Syne1/nesprin-1 facilitates nuclear envelope structure changes in embryonic stem cell differentiation, Dev Dyn 240(10) (2011) 2245-2255.

[164] E.W. Young, D.J. Beebe, Fundamentals of microfluidic cell culture in controlled microenvironments, Chemical Society reviews 39(3) (2010) 1036-48.

[165] G.A. Hudalla, W.L. Murphy, Biomaterials that regulate growth factor activity via bioinspired interactions, Advanced functional materials 21(10) (2011) 1754-1768.

[166] J.E. Rundhaug, Matrix metalloproteinases and angiogenesis, Journal of Cellular and Molecular Medicine 9(2) (2005) 267-285.

[167] N. Ferrara, Binding to the extracellular matrix and proteolytic processing: two key mechanisms regulating vascular endothelial growth factor action, Molecular biology of the cell 21(5) (2010) 687-690.

[168] E. Davis George, R. Senger Donald, Endothelial Extracellular Matrix, Circulation Research 97(11) (2005) 1093-1107.

[169] S. Pennock, A. Kazlauskas, Vascular endothelial growth factor A competitively inhibits platelet-derived growth factor (PDGF)-dependent activation of PDGF receptor and subsequent signaling events and cellular responses, Mol Cell Biol 32(10) (2012) 1955-66.

[170] D.G. Belair, W.L. Murphy, Specific VEGF sequestering to biomaterials: influence of serum stability, Acta biomaterialia 9(11) (2013) 8823-8831.

[171] G.A. Hudalla, W.L. Murphy, Biomaterials that Regulate Growth Factor Activity via Bioinspired Interactions, Advanced Functional Materials 21(10) (2011) 1754-1768.

[172] G.A. Hudalla, W.L. Murphy, Chemically well-defined self-assembled monolayers for cell culture: toward mimicking the natural ECM, Soft Matter 7(20) (2011) 9561-9571.

[173] Y. Bai, P. Li, G. Yin, Z. Huang, X. Liao, X. Chen, Y. Yao, BMP-2, VEGF and bFGF synergistically promote the osteogenic differentiation of rat bone marrow-derived mesenchymal stem cells, Biotechnol Lett 35(3) (2013) 301-308.

[174] M.W. Parker, P. Xu, H.-F. Guo, C.W. Vander Kooi, Mechanism of Selective VEGF-A Binding by Neuropilin-1 Reveals a Basis for Specific Ligand Inhibition, PLOS ONE 7(11) (2012) e49177.

[175] Stephen G. Ball, C. Bayley, C A. Shuttleworth, Cay M. Kielty, Neuropilin-1 regulates platelet-derived growth factor receptor signalling in mesenchymal stem cells, Biochemical Journal 427(Pt 1) (2010) 29-40.

[176] S.P. Yun, M.Y. Lee, J.M. Ryu, C.H. Song, H.J. Han, Role of HIF-1α and VEGF in human mesenchymal stem cell proliferation by 17β-estradiol: involvement of PKC, PI3K/Akt, and MAPKs, American Journal of Physiology - Cell Physiology 296(2) (2009) C317-C326.

[177] S.P. Yun, M.Y. Lee, J.M. Ryu, C.H. Song, H.J. Han, Role of HIF-1alpha and VEGF in human mesenchymal stem cell proliferation by 17beta-estradiol: involvement of PKC, PI3K/Akt, and MAPKs, Am J Physiol Cell Physiol 296(2) (2009) C317-26.

[178] S.G. Ball, C.A. Shuttleworth, C.M. Kielty, Vascular endothelial growth factor can signal through platelet-derived growth factor receptors, J Cell Biol 177(3) (2007) 489-500.

[179] S.H. Lee, Y.J. Lee, C.H. Song, Y.K. Ahn, H.J. Han, Role of FAK phosphorylation in hypoxia-induced hMSCS migration: involvement of VEGF as well as MAPKS and eNOS pathways, Am J Physiol Cell Physiol 298(4) (2010) C847-56.

[180] L.G.G. Melanie Rodrigues, Alan Wells, Growth factor regulation of proliferation and survival of multipotential stromal cells, Stem Cell Research & Therapy 1(32) (2010) 12.

[181] M.L. Ponce, S. Koelling, A. Kluever, D.E. Heinemann, N. Miosge, G. Wulf, K.H. Frosch, N. Schutze, M. Hufner, H. Siggelkow, Coexpression of osteogenic and adipogenic differentiation markers in selected subpopulations of primary human mesenchymal progenitor cells, J Cell Biochem 104(4) (2008) 1342-55.

[182] D. Fukumura, A. Ushiyama, D.G. Duda, L. Xu, J. Tam, V. Krishna, K. Chatterjee, I. Garkavtsev, R.K. Jain, Paracrine regulation of angiogenesis and adipocyte differentiation during in vivo adipogenesis, Circ Res 93(9) (2003) e88-97.

[183] A.D. Berendsen, B.R. Olsen, Regulation of adipogenesis and osteogenesis in mesenchymal stem cells by vascular endothelial growth factor A, Journal of Internal Medicine 277(6) (2015) 674-680.

[184] B.P. Chan, T.Y. Hui, C.W. Yeung, J. Li, I. Mo, G.C.F. Chan, Self-assembled collagen–human mesenchymal stem cell microspheres for regenerative medicine, Biomaterials 28(31) (2007) 4652-4666.

[185] U. Nöth, K. Schupp, A. Heymer, S. Kall, F. Jakob, N. Schütze, B. Baumann, T. Barthel, J. Eulert, C. Hendrich, Anterior cruciate ligament constructs fabricated from human mesenchymal stem cells in a collagen type I hydrogel, Cytotherapy 7(5) (2005) 447-455.

[186] R.D. Sumanasinghe, S.H. Bernacki, E.G. Loboa, Osteogenic Differentiation of Human Mesenchymal Stem Cells in Collagen Matrices: Effect of Uniaxial Cyclic Tensile Strain on Bone

Morphogenetic Protein (BMP-2) mRNA Expression, Tissue Engineering 12(12) (2006) 3459-3465.

[187] L. Meinel, V. Karageorgiou, R. Fajardo, B. Snyder, V. Shinde-Patil, L. Zichner, D. Kaplan, R. Langer, G. Vunjak-Novakovic, Bone Tissue Engineering Using Human Mesenchymal Stem Cells: Effects of Scaffold Material and Medium Flow, Annals of Biomedical Engineering 32(1) (2004) 112-122.

[188] G.H. Altman, R.L. Horan, H.H. Lu, J. Moreau, I. Martin, J.C. Richmond, D.L. Kaplan, Silk matrix for tissue engineered anterior cruciate ligaments, Biomaterials 23(20) (2002) 4131-4141.

[189] Y. Wang, U.-J. Kim, D.J. Blasioli, H.-J. Kim, D.L. Kaplan, In vitro cartilage tissue engineering with 3D porous aqueous-derived silk scaffolds and mesenchymal stem cells, Biomaterials 26(34) (2005) 7082-7094.

[190] L. Meinel, V. Karageorgiou, S. Hofmann, R. Fajardo, B. Snyder, C. Li, L. Zichner, R. Langer, G. Vunjak-Novakovic, D.L. Kaplan, Engineering bone-like tissue in vitro using human bone marrow stem cells and silk scaffolds, Journal of Biomedical Materials Research Part A 71A(1) (2004) 25-34.

[191] L. Meinel, S. Hofmann, V. Karageorgiou, L. Zichner, R. Langer, D. Kaplan, G. Vunjak-Novakovic, Engineering cartilage-like tissue using human mesenchymal stem cells and silk protein scaffolds, Biotechnology and Bioengineering 88(3) (2004) 379-391.

[192] L. Meinel, R. Fajardo, S. Hofmann, R. Langer, J. Chen, B. Snyder, G. Vunjak-Novakovic, D. Kaplan, Silk implants for the healing of critical size bone defects, Bone 37(5) (2005) 688-698.

[193] J.R. Mauney, T. Nguyen, K. Gillen, C. Kirker-Head, J.M. Gimble, D.L. Kaplan, Engineering adipose-like tissue in vitro and in vivo utilizing human bone marrow and adipose-derived mesenchymal stem cells with silk fibroin 3D scaffolds, Biomaterials 28(35) (2007) 5280-5290.

[194] G. Im, II, Y.-W. Shin, K.-B. Lee, Do adipose tissue-derived mesenchymal stem cells have the same osteogenic and chondrogenic potential as bone marrow-derived cells?, Osteoarthritis and Cartilage 13(10) (2005) 845-853.

[195] S. Hofmann, S. Knecht, R. Langer, D.L. Kaplan, G. Vunjak-Novakovic, H.P. Merkle, L. Meinel, Cartilage-like Tissue Engineering Using Silk Scaffolds and Mesenchymal Stem Cells, Tissue Engineering 12(10) (2006) 2729-2738.

[196] S. Hofmann, H. Hagenmüller, A.M. Koch, R. Müller, G. Vunjak-Novakovic, D.L. Kaplan, H.P. Merkle, L. Meinel, Control of in vitro tissue-engineered bone-like structures using human mesenchymal stem cells and porous silk scaffolds, Biomaterials 28(6) (2007) 1152-1162.

[197] R.L. Mauck, X. Yuan, R.S. Tuan, Chondrogenic differentiation and functional maturation of bovine mesenchymal stem cells in long-term agarose culture, Osteoarthritis and Cartilage 14(2) (2006) 179-189.

[198] C.Y. Charles Huang, P.M. Reuben, G. D'Ippolito, P.C. Schiller, H.S. Cheung, Chondrogenesis of human bone marrow-derived mesenchymal stem cells in agarose culture, The Anatomical Record Part A: Discoveries in Molecular, Cellular, and Evolutionary Biology 278A(1) (2004) 428-436.

[199] A.R. Finger, C.Y. Sargent, K.O. Dulaney, S.H. Bernacki, E.G. Loboa, Differential Effects on Messenger Ribonucleic Acid Expression by Bone Marrow–Derived Human Mesenchymal Stem Cells Seeded in Agarose Constructs Due to Ramped and Steady Applications of Cyclic Hydrostatic Pressure, Tissue Engineering 13(6) (2007) 1151-1158.

[200] H.A. Awad, M. Quinn Wickham, H.A. Leddy, J.M. Gimble, F. Guilak, Chondrogenic differentiation of adipose-derived adult stem cells in agarose, alginate, and gelatin scaffolds, Biomaterials 25(16) (2004) 3211-3222.

[201] J.S. Wayne, C.L. McDowell, K.J. Shields, R.S. Tuan, In Vivo Response of Polylactic Acid–Alginate Scaffolds and Bone Marrow-Derived Cells for Cartilage Tissue Engineering, Tissue Engineering 11(5-6) (2005) 953-963.

[202] P. Angele, B. Johnstone, R. Kujat, J. Zellner, M. Nerlich, V. Goldberg, J. Yoo, Stem cell based tissue engineering for meniscus repair, Journal of Biomedical Materials Research Part A 85A(2) (2008) 445-455.

[203] S.M. Willerth, S.E. Sakiyama-Elbert, Combining Stem Cells and Biomaterial Scaffolds for Constructing Tissues and Cell Delivery, StemJournal 1(1) (2019) 1-25.

[204] P.A. Janmey, J.P. Winer, J.W. Weisel, Fibrin gels and their clinical and bioengineering applications, J R Soc Interface 6(30) (2009) 1-10.

[205] A.A. Worster, B.D. Brower-Toland, L.A. Fortier, S.J. Bent, J. Williams, A.J. Nixon, Chondrocytic differentiation of mesenchymal stem cells sequentially exposed to transforming growth factor-β1 in monolayer and insulin-like growth factor-I in a three-dimensional matrix, Journal of Orthopaedic Research 19(4) (2001) 738-749.

[206] I. Catelas, N. Sese, B.M. Wu, J.C.Y. Dunn, S. Helgerson, B. Tawil, Human Mesenchymal Stem Cell Proliferation and Osteogenic Differentiation in Fibrin Gels in Vitro, Tissue Engineering 12(8) (2006) 2385-2396.

[207] O. Gurevich, A. Vexler, G. Marx, T. Prigozhina, L. Levdansky, S. Slavin, I. Shimeliovich, R. Gorodetsky, Fibrin Microbeads for Isolating and Growing Bone Marrow–Derived Progenitor Cells Capable of Forming Bone Tissue, Tissue Engineering 8(4) (2002) 661-672.

[208] S.M. Willerth, P.J. Johnson, D.J. Maxwell, S.R. Parsons, M.E. Doukas, S.E. Sakiyama-Elbert, Rationally designed peptides for controlled release of nerve growth factor from fibrin matrices, Journal of Biomedical Materials Research Part A 80A(1) (2007) 13-23.

[209] C.S. Hughes, L.M. Postovit, G.A. Lajoie, Matrigel: a complex protein mixture required for optimal growth of cell culture, Proteomics 10(9) (2010) 1886-90.

[210] M.M. Martino, J.A. Hubbell, The 12th-14th type III repeats of fibronectin function as a highly promiscuous growth factor-binding domain, FASEB journal : official publication of the Federation of American Societies for Experimental Biology 24(12) (2010) 4711-21.

[211] Y. Peng, L.E. Tellier, J.S. Temenoff, Heparin-based hydrogels with tunable sulfation & degradation for anti-inflammatory small molecule delivery, Biomater Sci 4(9) (2016) 1371-80.

[212] S.J. Kridel, W.W. Chan, D.J. Knauer, Requirement of Lysine Residues Outside of the Proposed Pentasaccharide Binding Region for High Affinity Heparin Binding and Activation of Human Antithrombin III, Journal of Biological Chemistry 271(34) (1996) 20935-20941.

[213] S.T. Olson, K.R. Srinivasan, I. Björk, J.D. Shore, Binding of high affinity heparin to antithrombin III. Stopped flow kinetic studies of the binding interaction, Journal of Biological Chemistry 256(21) (1981) 11073-11079.

[214] M.M. Martino, F. Tortelli, M. Mochizuki, S. Traub, D. Ben-David, G.A. Kuhn, R. Müller, E. Livne, S.A. Eming, J.A. Hubbell, Engineering the Growth Factor Microenvironment with Fibronectin Domains to Promote Wound and Bone Tissue Healing, Science Translational Medicine 3(100) (2011) 100ra89.

[215] M.M. Martino, J.A. Hubbell, The 12th–14th type III repeats of fibronectin function as a highly promiscuous growth factor-binding domain, The FASEB Journal 24(12) (2010) 4711-4721.

[216] V.-M. Leppänen, A.E. Prota, M. Jeltsch, A. Anisimov, N. Kalkkinen, T. Strandin, H. Lankinen, A. Goldman, K. Ballmer-Hofer, K. Alitalo, Structural determinants of growth factor binding and specificity by VEGF receptor 2, Proceedings of the National Academy of Sciences of the United States of America 107(6) (2010) 2425-2430.

[217] C. Piossek, K.-H. Thierauch, J. Schneider-Mergener, R. Volkmer-Engert, M.F. Bachmann, T. Korff, H.G. Augustin, L. Germeroth, Potent inhibition of angiogenesis by D,L-peptides derived from vascular endothelial growth factor receptor 2, Thromb Haemost 90(09) (2003) 501-510.

[218] C. Piossek, J. Schneider-Mergener, M. Schirner, E. Vakalopoulou, L. Germeroth, K.-H. Thierauch, Vascular Endothelial Growth Factor (VEGF) Receptor II-derived Peptides Inhibit VEGF, Journal of Biological Chemistry 274(9) (1999) 5612-5619.

[219] D.G. Belair, N.N. Le, W.L. Murphy, Regulating VEGF signaling in platelet concentrates via specific VEGF sequestering, Biomaterials Science 4(5) (2016) 819-825.

[220] L.W. Chow, R. Bitton, M.J. Webber, D. Carvajal, K.R. Shull, A.K. Sharma, S.I. Stupp, A bioactive self-assembled membrane to promote angiogenesis, Biomaterials 32(6) (2011) 1574-1582.

[221] H.-d. Guo, G.-h. Cui, J.-j. Yang, C. Wang, J. Zhu, L.-s. Zhang, J. Jiang, S.-j. Shao, Sustained delivery of VEGF from designer self-assembling peptides improves cardiac function after myocardial infarction, Biochemical and Biophysical Research Communications 424(1) (2012) 105-111.

[222] L.W. Chow, L.-j. Wang, D.B. Kaufman, S.I. Stupp, Self-assembling nanostructures to deliver angiogenic factors to pancreatic islets, Biomaterials 31(24) (2010) 6154-6161.

[223] R. Mammadov, B. Mammadov, S. Toksoz, B. Aydin, R. Yagci, A.B. Tekinay, M.O. Guler, Heparin Mimetic Peptide Nanofibers Promote Angiogenesis, Biomacromolecules 12(10) (2011) 3508-3519.

[224] K. Rajangam, H.A. Behanna, M.J. Hui, X. Han, J.F. Hulvat, J.W. Lomasney, S.I. Stupp, Heparin Binding Nanostructures to Promote Growth of Blood Vessels, Nano Letters 6(9) (2006) 2086-2090.

[225] K. Rajangam, M.S. Arnold, M.A. Rocco, S.I. Stupp, Peptide amphiphile nanostructure-heparin interactions and their relationship to bioactivity, Biomaterials 29(23) (2008) 3298-3305.

[226] J.D. Krutty, A.D. Dias, J. Yun, W.L. Murphy, P. Gopalan, Synthetic, Chemically Defined Polymer-Coated Microcarriers for the Expansion of Human Mesenchymal Stem Cells, Macromolecular Bioscience 19(2) (2019) 1800299.

[227] S.K. Schmitt, D.J. Trebatoski, J.D. Krutty, A.W. Xie, B. Rollins, W.L. Murphy, P. Gopalan, Peptide Conjugation to a Polymer Coating via Native Chemical Ligation of Azlactones for Cell Culture, Biomacromolecules 17(3) (2016) 1040-1047.

[228] S.K. Schmitt, A.W. Xie, R.M. Ghassemi, D.J. Trebatoski, W.L. Murphy, P. Gopalan, Polyethylene Glycol Coatings on Plastic Substrates for Chemically Defined Stem Cell Culture, Advanced Healthcare Materials 4(10) (2015) 1555-1564.

[229] A.D. Dias, J.M. Elicson, W.L. Murphy, Microcarriers with Synthetic Hydrogel Surfaces for Stem Cell Expansion, Adv Healthc Mater 6(16) (2017).

[230] P.A. Parmar, S.C. Skaalure, L.W. Chow, J.P. St-Pierre, V. Stoichevska, Y.Y. Peng, J.A. Werkmeister, J.A. Ramshaw, M.M. Stevens, Temporally degradable collagen-mimetic hydrogels tuned to chondrogenesis of human mesenchymal stem cells, Biomaterials 99 (2016) 56-71.

[231] G.A. Hudalla, J.T. Koepsel, W.L. Murphy, Surfaces That Sequester Serum-Borne Heparin Amplify Growth Factor Activity, Advanced Materials 23(45) (2011) 5415-5418.

[232] N.A. Impellitteri, M.W. Toepke, S.K. Lan Levengood, W.L. Murphy, Specific VEGF sequestering and release using peptide-functionalized hydrogel microspheres, Biomaterials 33(12) (2012) 3475-3484.

[233] M. Parlato, S. Reichert, N. Barney, W.L. Murphy, Poly(ethylene glycol) Hydrogels with Adaptable Mechanical and Degradation Properties for Use in Biomedical Applications, Macromolecular Bioscience 14(5) (2014) 687-698.

[234] D.G. Belair, M.J. Miller, S. Wang, S.R. Darjatmoko, B.Y.K. Binder, N. Sheibani, W.L. Murphy, Differential regulation of angiogenesis using degradable VEGF-binding microspheres, Biomaterials 93 (2016) 27-37.

[235] A.K. Jha, K.M. Tharp, J. Ye, J.L. Santiago-Ortiz, W.M. Jackson, A. Stahl, D.V. Schaffer, Y. Yeghiazarians, K.E. Healy, Enhanced survival and engraftment of transplanted stem cells using growth factor sequestering hydrogels, Biomaterials 47 (2015) 1-12.

[236] O.Z. Fisher, A. Khademhosseini, R. Langer, N.A. Peppas, Bioinspired materials for controlling stem cell fate, Accounts of chemical research 43(3) (2010) 419-28.

[237] L. Jongpaiboonkit, W.J. King, W.L. Murphy, Screening for 3D environments that support human mesenchymal stem cell viability using hydrogel arrays, Tissue Engineering: Part A 15(2) (2009) 11.

[238] A. Ranga, M.P. Lutolf, High-throughput approaches for the analysis of extrinsic regulators of stem cell fate, Current opinion in cell biology 24(2) (2012) 236-44.

[239] W.J. King, L. Jongpaiboonkit, W.L. Murphy, Influence of FGF2 and PEG hydrogel matrix properties on hMSC viability and spreading, Journal of Biomedical Materials Research Part A 93A(3) (2010) 1110-1123.

[240] L. Jongpaiboonkit, W.J. King, G.E. Lyons, A.L. Paguirigan, J.W. Warrick, D.J. Beebe, W.L. Murphy, An adaptable hydrogel array format for 3-dimensional cell culture and analysis, Biomaterials 29(23) (2008) 3346-3356.

[241] M.J. Wilson, Y. Jiang, B. Yañez-Soto, S. Liliensiek, W.L. Murphy, P.F. Nealey, Arrays of topographically and peptide-functionalized hydrogels for analysis of biomimetic extracellular matrix properties, Journal of Vacuum Science and Technology. B, Nanotechnology & microelectronics : materials, processing, measurement, & phenomena : JVST B 30(6) (2012) 06F903.

[242] E.H. Nguyen, M.R. Zanotelli, M.P. Schwartz, W.L. Murphy, Differential effects of cell adhesion, modulus and VEGFR-2 inhibition on capillary network formation in synthetic hydrogel arrays, Biomaterials 35(7) (2014) 2149-61.

[243] A. Khademhosseini, R. Langer, J. Borenstein, J.P. Vacanti, Microscale technologies for tissue engineering and biology, Proceedings of the National Academy of Sciences of the United States of America 103(8) (2006) 2480-2487.

Chapter 3- Hydrogel arrays formed via differential wettability patterning enable combinatorial screening of stem cell behavior

Ngoc Nhi T. Le[a], Stefan Zorn [b], Samantha K. Schmitt [a], Padma Gopalan [a,c,d], William L. Murphy[a,b,c,e*]

[a] Materials Science Program, University of Wisconsin-Madison, Madison, WI USA

[b] Department of Biomedical Engineering, University of Wisconsin-Madison, Madison, WI USA

[c] Department of Material Science and Engineering, University of Wisconsin-Madison, Madison, WI USA

[d] Department of Chemistry, University of Wisconsin-Madison, Madison, WI USA

[e] Department of Orthopedics and Rehabilitation, University of Wisconsin-Madison, Madison, WI USA

* Corresponding author can be contacted at Wisconsin Institute for Medical Research II, 1111 Highland Avenue Room 5405, Madison, WI USA 53705. Phone: (608)265-9978; Email: wlmurphy@wisc.edu

3.1. Preface

The aim of this work was to develop hydrogel arrays for screening that would meet the following criteria: 1) benchtop amenable and suitable for formation without the need for liquid handling systems to increase potential translatability and accessibility, 2) flat and compatible with standard high content imaging techniques for label-free data acquisition approaches that are more suitable for enhanced throughput screening, and 3) enable independent and combinatorial control of substrate stiffness, substrate adhesivity, growth factor regulation capabilities, and

media composition in order to enable examination of combinatorial effects of culture parameters on cell behavior. This study was performed using substrate-mediated hMSC phenotypic changes as a model system but can also be broadly applied to identify customized substrates for culture of other cell types and other cell behaviors.

Additionally, we provide additional information in the appendix to inform the reader of patenting and commercialization efforts regarding this and other array platforms developed for screening the effects of substrate parameters on cell behavior.

3.2. Abstract

Here, we have developed a novel method for forming hydrogel arrays using surfaces patterned with differential wettability. Our method for benchtop array formation is suitable for enhanced-throughput, combinatorial screening of biochemical and biophysical cues from chemically defined cell culture substrates. We demonstrated the ability to generate these arrays without the need for liquid handling systems and screened the combinatorial effects of substrate stiffness and immobilized cell adhesion peptide concentration on human mesenchymal stromal cell (hMSC) behavior during short-term 2-dimensional cell culture. Regardless of substrate stiffness, hMSC initial cell attachment, spreading, and proliferation were linearly correlated with immobilized CRGDS peptide concentration. Increasing substrate stiffness also resulted in increased hMSC initial cell attachment, spreading, and proliferation; however, examination of the combinatorial effects of CRGDS peptide concentration and substrate stiffness revealed potential interplay between these distinct substrate signals. Maximal hMSC proliferation seen on substrates with either high stiffness or high CRGDS peptide concentration suggests that some baseline level of cytoskeletal tension was required for hMSC proliferation on hydrogel substrates and that

multiple substrate signals could be engineered to work in synergy to promote mechanosensing and regulate cell behavior.

3.3. Statement of Significance

Our novel array formation method using surfaces patterned with differential wettability offers the advantages of benchtop array formation for 2-dimensional cell cultures and enhanced-throughput screening without the need for liquid handling systems. Hydrogel arrays formed via our method are suitable for screening the influence of chemical (e.g. cell adhesive ligands) and physical (stiffness, size, shape, and thickness) substrate properties on stem cell behavior. The arrays are also fully compatible with commercially available micro-array add-on systems, which allows for simultaneous control of the insoluble and soluble cell culture environment. This study used hydrogel arrays to demonstrate that synergy between cell adhesion and mechanosensing can be used to regulate hMSC behavior.

3.4. Introduction

It is widely accepted that soluble signals (such as growth factors and cytokines) are major regulatory players in both the *in vivo* and *in vitro* stem cell microenvironments; however, stem cell behavior can also be influenced by a variety of insoluble signals, including biomolecules immobilized in the extracellular matrix as well as biophysical properties of microenvironment [1-3]. Recent studies indicate that regulation of stem cell behavior involves complex relationships between soluble factors, immobilized cell adhesive signals, and mechanical signals contained in, and dynamically regulated by, the stem cell microenvironment. Chemically well-defined cell culture substrates can allow researchers to parse out the effects of specific signals on stem cell behavior [4]. However, attempts to investigate synergistic or antagonistic effects of combinations of signals produce thousands of potential signal combinations, leading to difficult and costly experiments [2, 5]. Here, we designed hydrogel arrays for enhanced-throughput, combinatorial screening of biochemical and biophysical cues from chemically defined cell culture substrates. Current hydrogel platforms for screening the influence of stiffness on cell behavior rely on low-throughput techniques using bulk hydrogels, plated hydrogel arrays in cell culture dishes or wells, or arrays formed using expensive liquid handling systems. These methods have limitations, including high materials and equipment cost and the potential for deformation via "buckling" when hydrogels swell against the constrained dimensions of the well [2, 6-9]. Here, we demonstrated the ability to generate arrays for enhanced-throughput screening without the need for liquid handling systems and our arrays comprise free-standing hydrogel spots, which reduces the likelihood of hydrogel deformation via buckling. Using these arrays, we screened the combinatorial effects of substrate stiffness and immobilized cell adhesion peptide concentration on human mesenchymal stromal cell (hMSC) behavior during short-term cell culture. hMSC

adhesion was chosen as a model biological outcome to demonstrate the utility of hydrogel arrays, as recent studies have extensively detailed the influence of substrate properties on hMSC behavior [10-12] [5, 13-17].

Over the past two decades, many researchers have demonstrated a positive correlation between the substrate stiffness and the intracellular cytoskeletal tension, indicating that cells sense and respond to changes in matrix stiffness by modulating cytoskeletal assembly and contractility (a concept referred to as "mechanosensing")[11, 12]. We and others have also demonstrated control of hMSC behavior by regulating mechanosensing: hMSCs cultured on surfaces that promoted high cytoskeletal tension (via high substrate stiffness, cell adhesion molecule affinity, or cell adhesion molecule density) resulted in well-spread cells that possessed highly-organized f-actin stress fibers and large and well-defined focal adhesions, while substrates that promoted low cytoskeletal tension resulted in rounded cells with diffused actin and small, unstable focal adhesions.[5, 11, 13, 18].

3.5. Materials and methods

3.5.1 Differential wettability pattering and glass silanization

Gold-coated glass slides (TA134, EMF Corporation) were cleaned via sonication in ethanol for 1 minute and dried with air. Hydrophobic SAM formation on gold-coated glass slides were prepared by immersion in a 1 mM solutions of HS-$(CH_2)_{11}$-O-$(CH_2)_2$-$(CF_2)_5$-CF_3 (fluorinated alkanethiols, ProChimia Surfaces) in ethanol for ≥2 hours. Polydimethylsiloxane (PDMS) elastomeric stencils for determining the pattern for selective etching of hydrophilic SAM regions were fabricated using soft lithography as previously described [18] using a 1:10 ratio of curing agent to base. Gold-coated glass slides with the hydrophobic SAM were cleaned with ethanol,

dried with air, and covered with the PDMS elastomeric stencil. Exposed regions of the hydrophobic SAM (regions not covered by the PDMS elastomeric stencil) were etched by oxygen plasma treatment at 40 sccm and 50 W for 1 minute. The PDMS elastomeric stencil was removed and the selectively etched gold-coated slides were cleaned with ethanol and immersed in a 0.1 mM solution of $HS–C_{11}–(O–CH_2–CH_2)_3–OH$ (PEG-terminated alkanethiols, ProChimia Surfaces) in ethanol solution for ≥2 hours so that hydrophilic alkanethiol SAM layer could form in the etched regions. Hydrophobic and hydrophilic SAM formation on the gold-coated slides were confirmed by static contact angles measurements at room temperature using a contact angle goniometer (DataPhysics Contact Angle System, OCA). A drop of distilled water (3 μL) was placed on the surface and the static contact angle was measured for 3 different samples at 5 different places on each sample and the contact angles were averaged.

Silanized glass coverslips were prepared via liquid-phase silanization. Silanization was performed with slight modifications from procedures previously described [19, 20]. Glass coverslips were cleaned via sonication in acetone for 30 minutes, rinse with ethanol, and dried with air. Clean glass coverslips were activated by oxygen plasma treatment at 40 sccm and 50 W for 5 minutes to increase the number of activated hydroxyl groups on the surface. Immediately after activation, glass coverslips were immersed in a solution of 2.5 v./v.% 3-mercaptopropyl trimethoxysilane (3-MPTS, Sigma Aldrich) in toluene for 2 hours, thoroughly rinsed with ethanol, dried with air, cured under nitrogen atmosphere at 100 °C for 1 hour, and treated with 10 mM DTT in PBS for 30 minutes at 37°C to increase free thiols available for thiolene reaction with PEG-NB.

3.5.2. Hydrogel array formation

Norbornene-functionalized PEG (PEG-NB, 20 kDa molecular weight, 8-arm with tripentaerythritol core, JenKem Technology) was synthesized and characterized as previously described [21-23]. Dimethylaminopyridine (DMAP), pyridine, dichloromethane (DCM), 5-Norbornene-2-carboxylic acid, N,N′-dicyclohexylcarbodiimide (DCC), diethyl ether, hexane, SNAKESKIN dialysis tubing (MWCO 3.5K), deuterated chloroform ($CDCl_3$), and tetramethylsilane (TMS) were purchased from Sigma Aldrich.

Briefly, eight-arm PEG-OH, DMAP and pyridine (Sigma Aldrich) were dissolved in anhydrous DCM in one reaction vessel and DCC and 5-norbornene-2-carboxylic acid were dissolved in another. The PEG and norbornene solutions were combined and stirred overnight to covalently couple the 5-norbornene-2-carboxylic acid to the PEG-OH. The PEG-NB product was filtered through a medium fritted Buchner funnel to remove urea salts formed during the reaction. The filtrate was then precipitated in 900 mL cold diethyl ether and 100 mL hexane. The solids were collected on qualitative grade filter paper and air dried overnight. The PEG-NB product was purified by dialysis against 4L of dH2O at 4°C for 72 hours (with water change every 8 hours) to remove residual norbornene acid, filtered through a 0.45 μm nylon filter to remove particulates and impurities, and subsequently freeze dried.

Norbornene functionalization of >90% was confirmed with 1H nuclear magnetic resonance spectroscopy. Samples were prepared at 6 mg/mL in $CDCl_3$ with TMS internal standard. Free induction decay (FID) spectra were obtained using spectroscopy services provided by the National Magnetic Resonance Facility at Madison on a Bruker Instruments Avance III 500i spectrometer at 400 MHz and 27°C.

Linear CRGDS, linear CRDGS, cyclic (RGDfC), and matrix metalloproteinase (MMP)-degradable peptide crosslinker KCGGPQGIWGQGCK were purchased from GenScript USA. Linear PEG-dithiol (PEG-DT, 3.4 kDa) was purchased from Laysan Bio. Note that the "f" notation denotes a D-amino acid.

Hydrogel precursor solutions were prepared by combining PEG-NB (4-8 wt/wt %), PEG-DT (0.5-1 mole ratio of thiol-to-norbornene), peptides (1-4 mM), and 0.5 wt/wt% Irgacure 2959 photoinitiator (CIBA/BASF) and diluted to desired concentrations with phosphate buffered saline (PBS, pH 7.4) immediately prior to hydrogel array formation. For cell encapsulation studies, cells were suspended at the desired concentration in growth medium and added to the remaining hydrogel precursor solution components in place of the PBS that was used for dilution. All encapsulation studies utilized the MMP-degradable crosslinker in place of the non-degradable PEG-DT crosslinker. Hydrogel precursor solutions were spotted onto the hydrophilic regions of the patterned gold-coated slides using a micropipette, the DTT-treated silanized glass coverslip was used to sandwich the hydrogel precursor solutions between the coverslip and the patterned gold-coated slide. Hydrogel precursor solutions were crosslinked by UV-initiated photopolymerization with 365 nm wavelength light for 2 seconds at 90 mW/cm^2, with the light penetrating through the glass coverslip. The gold-coated slide was separated from the coverslip, which enabled the glass-immobilized hydrogel spots to cleanly detach from the gold-coated slide. The resulting glass-immobilized hydrogel spots, collectively referred to as the "hydrogel array", were allowed to swell to equilibrium overnight at room temperature in PBS, sterilized by immersion in 70% ethanol for ≥ 1 hour, thoroughly washed with PBS to remove any remaining unreacted components, and immersed in cell growth medium at 37 °C until use.

3.5.3. Hydrogel array characterization

Hydrogel mass equilibrium swelling ratios [21, 23], shear storage moduli [21], and mesh size calculations (calculated using empirical equilibrium swelling data and Flory–Rehner theory) were determined as previously reported [21, 24-26]. To characterize surface roughness, hydrogels were allowed to swell to equilibrium in PBS overnight at room temperature then imaged on a BioScope Catalyst BioAFM (Bruker) with a Zeiss optical microscope. Tapping atomic force microscopy (AFM) was performed in ScanAsyst mode in water using ScanAsyst Fluid+ tips (Bruker). At least 3 images of 2.5 μm by 2.5 μm or larger in area were scanned at different locations on the hydrogels and these images were used to calculate height data. The root mean square (RMS) roughness was calculated using Nanoscope Analysis software (Bruker) for 3 images per sample and averaged.

To demonstrate controllable microsphere encapsulation and peptide immobilization, we formed hydrogel arrays with varying concentrations of 2 μm fluorescent red carboxylate-modified polystyrene latex beads (Sigma Aldrich) and CRGDS peptides in the hydrogel precursor solution. Immediately following hydrogel array formation, the N-terminal amine on CRGDS peptides were labeled using Alexa-Fluor 488 5-sulfodichlorophenol (SDP) ester (Invitrogen) as previously described [21]. Briefly, hydrogel arrays were immersed overnight in a solution of SDP ester in PBS (pH 7.4) with at 2-fold molar excess of SDP ester to CRGDS, rinsed with PBS, soaked in PBS for 6 hours with PBS change every 2 hours to remove unreacted SDP ester. Fluorescently-labeled arrays were imaged using a Nikon Eclipse Ti microscope (Nikon) and relative fluorescence intensities of each hydrogel spot in the array were obtained using the threshold feature in NIS Elements software (Nikon).

3.5.4. Cell culture

Bone marrow-derived hMSCs (Lonza) were expanded in 10% fetal bovine serum (FBS, Invitrogen) in minimum essential medium, alpha (αMEM, MediaTech) supplemented with 1% penicillin/streptomycin (Invitrogen) on tissue culture polystyrene plates at 37 °C in a 5% CO_2 atmosphere until 70% confluence. Passage 7 hMSC were harvested using trypsin (Invitrogen), resuspended in 10% FBS in αMEM, and seeded at 2000 cells/cm^2 on sterilized hydrogel arrays. After 24 hours, unattached cells were removed by gently replacing the culture media. Cells on hydrogel arrays were maintained at 37 °C in a 5% CO_2 atmosphere and culture media was replaced every 3 days.

3.5.5. Data acquisition and analysis

Samples were placed in a heated environmental chamber and imaged on the Nikon Eclipse Ti microscope (Nikon) at the desired times. Immunofluorescence staining for vinculin and F-actin were conducted using the FAK100 focal adhesion staining kit (Millipore) per the manufacturer's instructions with 1:200 dilutions of both the TRITC-conjugated phalloidin and primary mouse anti-vinculin monoclonal antibody components included in the kit. Alexa-Fluor 488 goat anti-mouse IgG secondary antibody (Invitrogen) was used at 1:200 dilution. Live/dead stain (Invitrogen) was performed per the manufacturer's instructions. Nuclear counterstain was performed using 1:5000 dilution of diamidino-2-phenylindole (DAPI, Life Technologies).

Cell number was manually determined using NIS Elements software (Nikon), cell area of single cells were determined using NIS Elements's threshold and automated measurement features, and cell proliferation was quantified as previously reported by normalizing cell number at day 4 (C_4) to cell number at day 1 (C_1), where normalized cell number greater than 1 was used

to indicate proliferation [18]. Focal adhesion length was determined using NIS Element's threshold and automated measurement features to define regions on the periphery of single cells stained with mouse anti-vinculin monoclonal antibody. Focal adhesion density was determined by normalizing the number features stained with mouse anti-vinculin monoclonal antibody to the cell area. Encapsulated cell concentration was determined by counting cells at 3 focal planes 50 μm apart in distance. Cell viability was determined by comparing the total number of calcein positive to total DAPI positive cells. Statistical analysis was performed using Student's t-test (2-tailed, α=0.05) or ANOVA with post-hoc Tukey (HSD or Kramer depending on sample size variability) tests as indicated. All error bars denote standard deviation. All Pearson's product-moment correlation coefficients (R^2) were calculated using Excel's Analysis ToolPak.

3.6. Results and discussion

3.6.1. Differential wettability patterning and hydrogel array formation

Since cell structural measures (e.g. cell area and morphology) and perturbations (e.g. proliferation and cytoskeletal organization) have been demonstrated to be accurate qualitative measures of hMSC mechanosensing in response to substrate stiffness and ligand density, we examined these properties here using automated data collection techniques that augmented the enhanced-throughput capability of our array-based screening system [11, 12, 15, 24]. Hydrogel arrays were formed using gold-coated glass slides patterned with alkanethiolate self-assembled monolayers (SAMs), and differential wettability was used to define the geometry and confine the contents of each spot in the array (Figure 3.10). Gold-coated glass slides with a fully formed hydrophobic SAM composed of fluorinated alkanethiolates were covered with elastomeric stencils and etched using oxygen plasma to selectively destroy exposed regions of the hydrophobic

SAM [27]. The gold-coated slides were subsequently immersed in solutions containing poly(ethylene glycol) (PEG)-terminated alkanethiols to replace the etched regions with a hydrophilic PEG alkanethiolate SAM (Figure 3.10a). Differential wettability of SAMs resulting from this removal and replacement method were confirmed using static contact angle measurements (Figure 3.10b).

Hydrogel precursor solutions (0.75 μL per 2.4 mm diameter, 150 μm thick hydrogel spot) containing norbornene-functionalized PEG (PEG-NB) and PEG-dithiol (PEG-DT) were deposited onto the hydrophilic regions on the patterned gold-coated slide using either a single-channel micropipettor, multichannel micropipettor, or a single-channel repeat pipettor. The wettability patterning was designed with dimensions compatible with an 8-channel micropipette, allowing for deposition of multiple solutions simultaneously. A 150 μm PDMS spacer was places on regions of the patterned gold slide and a silanized glass slide was placed atop the entire patterned gold slide to sandwich the precursor solution (Figure 3.10c,d and 3.S1a). UV-initiated crosslinking was used to form hydrogel spots via radically-mediated thiol-norbornene (term "thiolene") photopolymerization, a step-growth reaction mechanism that enabled rapid gelation time and resulted in homogeneous polymer network formation (Figure 3.10e and Figure 3.12a) [22, 23]. The silanes on the silanized glass slide possessed terminal thiols that were capable of participating in thiolene reaction with the norbornene groups on PEG-NB, thereby enabling covalent immobilization of the hydrogels to the glass slide upon polymerization. The result was an array of hydrogel spots upon a glass slide (Figure 3.10f). The dimensions of the hydrogel spots could be altered by changing the pattern on the elastomeric stencil used for SAM patterning (to define the X and Y dimensions) and by using a polydimethylsiloxane (PDMS) elastomeric spacer between the patterned SAM and the silanized glass slides (to define the Z dimension of the resulting

hydrogel spot) (Figure 3.10g,h). Note that the silanized glass slides promote non-specific cell adhesion which could contribute to the soluble factors presented in the microenvironment and influence cell behavior during long-term cell culture. We are currently developing a passivation procedure to address this in our design process.

The lack of a liquid handling system does limit the throughput on this array formation method because of the time required for deposition of hydrogel precursor solution for each spot in the array. We use small volumes (0.75 μL) to generate each hydrogel spot to reduce the materials cost; however, due to the small volumes, evaporation concerns limited array sizes to what can be feasibly produced within a 5-minute timeframe. Within a 5-minute timeframe, we can feasibly generate an array for 2D culture comprised 80 spots formed using up to 16 different hydrogel precursor solutions. For 3D encapsulation studies, arrays sizes are limited by evaporation, cell viability in suspension, and cell settling once the hydrogel precursor solution has been deposited onto the patterned gold slide. Arrays formed for 3D encapsulation experiments in this manuscript were formed within 2 minutes and contained 20 spots formed using up to 5 different hydrogel precursor solutions.

Previous studies have indicated that natural and synthetic compliant surfaces with topographical features typically ≥ 100 nm in height can be used to modulate integrin-mediated stem cell attachment, cytoskeletal structure, proliferation, migration, and differentiation [28-31]. As the hydrogel array formation procedure required glass-immobilized hydrogel detachment from the patterned gold-coated slide, it was plausible that this detachment could have contributed to the formation of nano- or micron-sized features on our hydrogel surface. Therefore, we used hydrated atomic force microscopy (AFM) to examine the resulting hydrogel surface roughness and root mean square (RMS) roughness of all hydrogels formed. Regardless of concentration of PEG-NB

or PEG-DT crosslinker in the precursor solution, the surface roughnesses were similar in value and did not seem to correlate with changing PEG-NB or PEG-DT concentration (Figure 3.11). This indicates that the detachment procedure and changes in hydrogel composition minimally influence surface nanotopography. Additionally, height of features found on our hydrogel surfaces (6.6-15.1 nm) are lower than the feature sizes commonly used in prior studies of surface topography effects, which suggests minimal contribution of surface topography to observed differences in hMSC behavior (Figure 3.11b).

3.6.2. Changing composition of each hydrogel spot

The composition of each hydrogel spot in the arrays could be also systematically and independently altered (Figure 3.12). Thiolene photopolymerization offered the advantage of facile ligand incorporation into the polymer network as long as the ligand contained a thiol capable of participating in thiolene reaction with PEG-NB (Figure 3.12a). We utilized cysteine-terminated CRGDS peptide and, by changing the molar ratio of peptide to norbornene functional groups, we could systematically and independently change the concentration of the peptides immobilized in each hydrogel spot in the array (Figure 3.12b,c). The resulting relative CRGDS concentrations in the hydrogel spots were directly correlated to the concentration of CRGDS in the hydrogel precursor solution (R^2=0.9845).

The array formation procedure also allowed for encapsulation of micron-sized materials and cells (Figure 3.12b and Figure 3.14). By adding the material or cells into the precursor solution, those components could be encapsulated within and uniformly distributed throughout the hydrogel spots upon photopolymerization (Figure 3.S2). As the mesh size of typical hydrogel networks generated were 6-12 nm (Figure 3.13a), micron-sized components were not able to freely diffuse

through and out of the network, thereby enabling their entrapment and encapsulation. We demonstrated the ability to change the density of encapsulated materials or cells by varying the concentration of fluorescently-tagged microspheres (from 0 to 2.5 w/v %) or cells (from 250,000 to 1 million cells/mL) in the hydrogel precursor solution (Figure 3.12b,d and Figure 3.14a-c). The resulting concentrations of encapsulated materials in the hydrogel spots were directly correlated to the concentrations of materials added to the hydrogel precursor solutions (R^2=0.9855 and 0.9655 for microspheres and cells, respectively). At the concentrations typically used for cell encapsulation studies (500,000 and 1 million cells/mL), the empirical cell number encapsulated in the hydrogels is 75 and 69% of the desired cell number. Note that, due to the small volumes of viscous fluids, low-resolution microscopy, and automated measurement techniques used to enable enhance throughput screening with the hydrogel arrays, minor technical errors could result in significant variability in the resulting encapsulated cell concentration. Consistent with other workflows utilizing screening techniques, results from enhanced throughput screens with our hydrogel arrays should be confirmed with follow-up experiments using large-scale culture.

We also demonstrated that the array formation procedure enabled hMSC encapsulation with cell viability consistent with those previous published for encapsulation in PEG hydrogels (70-90% viable cells at 24 hours after encapsulation, Figure 3.14d-e) [8, 32, 33]. Additionally, increasing concentration of CRGDS (which has been used to promote hMSC adhesion to hydrogel surfaces through interactions with $\alpha_v\beta_3$ and $\alpha_5\beta_1$ integrins on the cell surface) did not significantly affect hMSC viability (Figure 3.14e) [33-35].

The hydrogel spot stiffness (as measured by shear storage modulus) was controllably altered by varying either the concentration of PEG-NB or PEG-DT crosslinker in the precursor solution. These results were consistent with those previously reported [36]. Hydrogel shear

modulus was directly correlated to both PEG-NB monomer concentration and PEG-DT crosslinker density (with 50%-100% density corresponding to 0.5-1 mole ratio of thiol-to-norbornene) in the precursor solution, and these results were confirmed by determining equilibrium mass swelling ratio (Figure 3.12e and Figure 3.13b).

3.6.3. hMSC adhesion and proliferation on hydrogel array

For hMSC adhesion studies, we generated arrays containing hydrogel spots with stiffness values ranging from 1.8 to 10.9 kPa and varying immobilized CRGDS peptide concentrations from 0 to 4 mM. The arrays generated comprised several isolated hydrogel spots where each hydrogel spot possessed a unique CRGDS concentration and stiffness value. As the PEG hydrogel is bio-inert and does not permit cell adhesion, the inclusion of RGD-containing peptides was designed to promote hMSC integrin-mediated cell adhesion and enable integrin-mediated mechanosensing [14, 21, 22, 37, 38]. Note that total peptide concentration was maintained at 4 mM by supplementing the hydrogel precursor solution with a "scrambled", non-bioactive CRDGS peptide (whereby "0 mM CRGDS" hydrogels contain 4 mM CRDGS scrambled peptide). The stiffness range was chosen to reflect the reported stiffness values of various soft tissues, including fat and muscle tissue [39, 40]. Following hydrogel array formation, hMSCs were seeded onto the hydrogel spots and cultured for up to 8 days (Figure 3.15a). hMSC initial cell attachment, spreading, and proliferation were linearly correlated with immobilized CRGDS concentration (Figure 3.15b-d and Figure 3.S3a-d) regardless of the hydrogel spot stiffness. After 1 day of culture, minimal hMSCs were attached to hydrogel spots that did not contain CRGDS (4 mM "scrambled" CRDGS), indicating that initial cell adhesion was mediated by the bioactivity of the immobilized peptide. Increased CRGDS concentration resulted in increased hMSC attachment, spreading, and

proliferation with maximal values on hydrogel spots presenting 4 mM CRGDS. These results are consistent with previously reported relationships [12, 13, 18, 24, 41], and confirmed that hydrogel arrays can be used to screen for the effects of peptide density and identity on hMSC behavior.

Increasing hydrogel spot stiffness (from 1.8 to 10.9 kPa) also resulted in increased hMSC initial cell attachment, spreading, and proliferation; however, maximal values for these cell behaviors were achieved on hydrogel spots with the highest CRGDS concentration and intermediate stiffness values Figure 3.15b-d). In particular, maximal hMSC initial cell attachment was seen on hydrogel spots of 8.2 kPa stiffness while maximal cell spreading and proliferation were both seen on hydrogel spots of 5.4 kPa stiffness. As previous studies have reported that hMSC integrin-mediated mechanosensing is directly correlated to cytoskeletal tension, we examined focal adhesion formation and cytoskeletal structure to assess the influence of hydrogel spot stiffness on cytoskeletal tension [10, 12, 13, 15, 16, 18, 38]. Immunofluorescence staining for vinculin (a component of focal adhesions) and F-actin (an important component of stress fibers in adherent cultured cells) qualitatively revealed diffuse F-actin and focal adhesion in hMSCs seeded on softer hydrogels spots (3.3 kPa or less), while those seeded on stiffer hydrogels spots (5.4 kPa or greater) expressed well-defined stress fibers terminated by prominent focal adhesions (Figure 3.16a). hMSCs expression of F-actin stress fibers terminated by prominent focal adhesions has been previously directly correlated to both substrate stiffness and cytoskeletal tension [10, 15, 16, 18]. Independent of CRGDS concentration and substrate stiffness, hMSCs cultured on all substrates used in this study present mature focal adhesions (≥5 μm in length, Figure 3.16) [31]. Independent of substrate stiffness, hMSC focal adhesion density appeared to be linearly correlated to CRGDS concentration (R^2= 0.8852, Figure 3.16b). Additionally, independent of CRGDS concentration, focal adhesion length appeared to be correlated with substrate stiffness (Figure

3.16c). These trends are consistent with those previously reported and further support that hydrogel spot stiffness can be used to modulate hMSC cytoskeletal tension [42, 43]. Combined, these results suggested that hydrogel arrays produced here may be used to screen for the effects of substrate stiffness on hMSC mechanosensing.

Interestingly, examination of the combinatorial effects of CRGDS concentration and hydrogel spot stiffness revealed potential interplay between these distinct substrate signals. The synergy between adhesion and stiffness is most clearly demonstrated with hMSC proliferation (Figure 3.15d). At 4 mM CRGDS, hMSCs proliferate regardless of hydrogel spot stiffness; however, hydrogel spots presenting 1 and 2 mM CRGDS required stiffness values greater than 1.8 and 3.3 kPa, respectively. These results are consistent with previously reported trends suggesting that low cytoskeletal tension in response to low cell adhesion ligand density could be compensated by high cytoskeletal tension produced from high substrate stiffness [12, 13]. Additionally, these trends suggest some baseline level of cytoskeletal tension was required for hMSC proliferation on hydrogel substrates and that multiple substrate signals could be engineered to work in synergy to promote mechanosensing and regulate cell behavior [5, 13]. It is worthwhile to note that, as we modified both PEG-NB concentration and crosslinking density to control stiffness, it is unclear the extent to which stiffness influences surface polymer chain mobility and subsequently the ability for the cells to access the cell adhesive ligands. Increasing stiffness could potentially decrease polymer chain mobility, reduce the effective CRGDS density accessible to the cells, and actively limit integrin clustering which subsequently impacts hMSC cytoskeletal reorganization and mechanosensing. Previous studies indicated that integrin clustering regulates cell adhesion, spreading, and proliferation and are dependent on both concentration and spatial distribution of cell adhesive ligands [31, 44]. Increasing PEG-NB concentration and crosslinking density could

reduce polymer chain mobility to decrease the number of favorable conformations of the CRGDS ligand during integrin clustering, thereby limiting the cluster size and distribution on the cell surface. Additionally, increasing crosslinking density could decrease potential sites for CRGDS covalently attachment and subsequently reduce effective CRGDS density [31]. Previous studies have also suggested that integrin clustering and mechanosensing is dependent on the flexibility of the anchor points to which cells adhere to the surface [31, 38, 44]. By increasing crosslinking density to increase substrate stiffness, we could have potentially decreased anchor point flexibility and limited hMSC integrin clustering, leading to increase hMSC spreading on stiffer substrates.

3.6.4. hMSC adhesion on hydrogels presenting peptides with varying ligand-receptor affinity

We cultured hMSCs on hydrogels spots presenting 0-4 mM of the linear CRGDS or the cyclic (RGDfC) peptide to determine the influence of ligand-receptor affinity on cell behavior (Figure 3.17). Previous studies have indicated that the cyclic peptide possesses higher affinity for $\alpha_v\beta_3$ integrins than the linear peptide [34, 35]. Note that total peptide concentration was maintained at 4 mM by supplementing the hydrogel precursor solutions with the non-bioactive CRDGS peptide. Following hydrogel array formation, hMSCs were seeded onto the hydrogel spots and cultured for up to 3 days (Figure 3.17a). While changing the immobilize peptide identity did not significantly change the hydrogel spot stiffness or the linear correlation between both initial hMSC attachment or spreading and immobilized RGD-containing peptide concentration (Figure 3.S4), hMSCs initial attachment and spreading on hydrogels presenting cyclic (RGDfC) was higher than on hydrogels presenting equivalent concentrations of CRGDS (Figure 3.17b). These results are consistent with those previously reported for comparison of hMSC attachment and spreading on SAMs presenting linear vs. cyclic RGD-containing peptides [13] and suggest

that hydrogels with varying immobilized peptides identity could be used to screen for the effects of changing ligand-receptor affinity on hMSC mechanosensing.

It is worthwhile to note that previous studies have suggested that more low-affinity ligands must be presented to the cells in order to achieve the same integrin clustering, stable attachments, and cell spreading when compared to higher affinity ligands [31]. Consistent with these suggestions, low concentrations of cyclic (RGDfC) promoted similar or higher levels of hMSC initial attachment and spreading than high concentrations of CRGDS (Figure 3.17b,c).

3.7. Conclusion

In conclusion, we have developed a method for forming hydrogel arrays using surfaces patterned with differential wettability. The proof-of-concept study presented here confirmed that our hydrogel array formation procedure is capable of producing hydrogel spots with properties that can be systematically and independently varied and that these arrays can be used for stem cell culture and screening for the effects of various chemical and mechanical substrate properties on stem cell behavior. While we and others have previously developed other hydrogel array systems for stem cell culture and screening [2, 6, 7, 21, 37, 45], our current array system offers the unique advantage of benchtop array formation for both 2- and 3-dimensional cell cultures and enhanced-throughput screening without the need for liquid handling systems [7]. Our method is also suitable for screening the influence of substrate size, shape, and thickness on stem cell behavior via our ability to control the XYZ dimensions. Additionally, hydrogel arrays formed using our method are compatible with commercially-available micro-array add-on systems, thereby enabling attachment of wells for each individual spots to offer control over the soluble medium presented to each spot in the array (Figure 3.18). Our hydrogel array system therefore can be used to identify and optimize

substrate properties and culture conditions for stem cell culture. This capability is particularly important in stem cell engineering, as there is a need for optimization of chemically well-defined cell culture substrates for stem cell expansion, differentiation, and tissue assembly.

3.8. Acknowledgements

The authors acknowledge the following funding sources: the National Institutes of Health (grant no. R01HL093282), the National Science Foundation (grant no. 1306482), the National Science Foundation Graduate Research Fellowships Program (grant no. DGE-0718123), the University of Wisconsin-Madison Graduate Engineering Research Scholars, and the Gates Millennium Scholars Program. The authors also acknowledge support from staff and the use of equipment at the Materials Science Center (National Science Foundation grant no. 1121288) and services from the National Magnetic Resonance Facility at the University of Wisconsin-Madison.

3.9. Figures

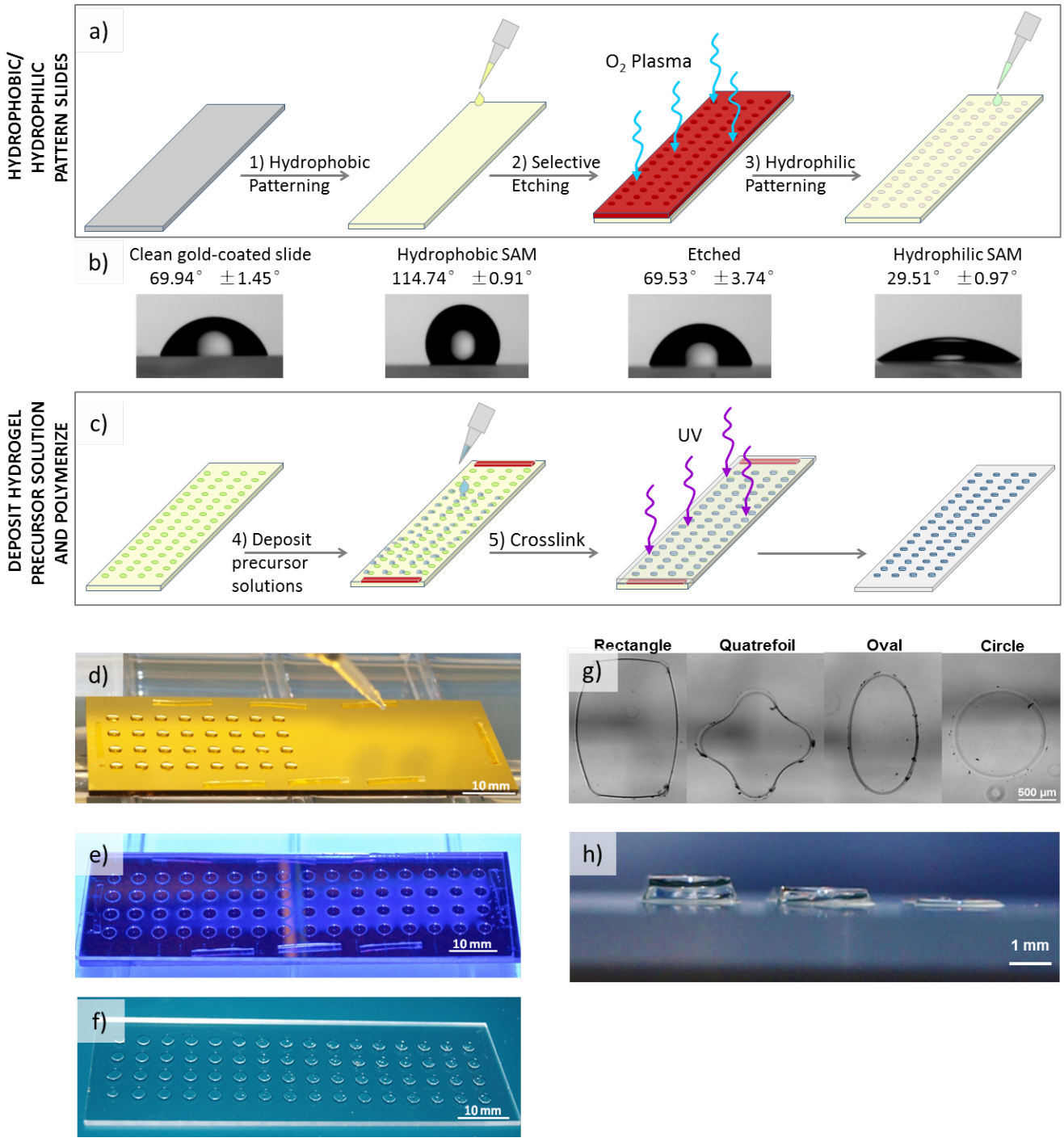

Figure 3.10. Hydrogel array formation procedure and outputs. a-b) Hydrogels arrays were formed on gold-coated glass slides patterned with SAMs with differential wettability. c-e) Hydrogel precursor solutions deposited onto the hydrophilic SAM regions of the patterned slide

were crosslinked via UV-initiated photopolymerization to form hydrogel spots. F) The resulting array is composed of hydrogel spots immobilized on a glass slide. g-h) The array formation procedure allows for the formation of hydrogel spots of various size, shape, and height.

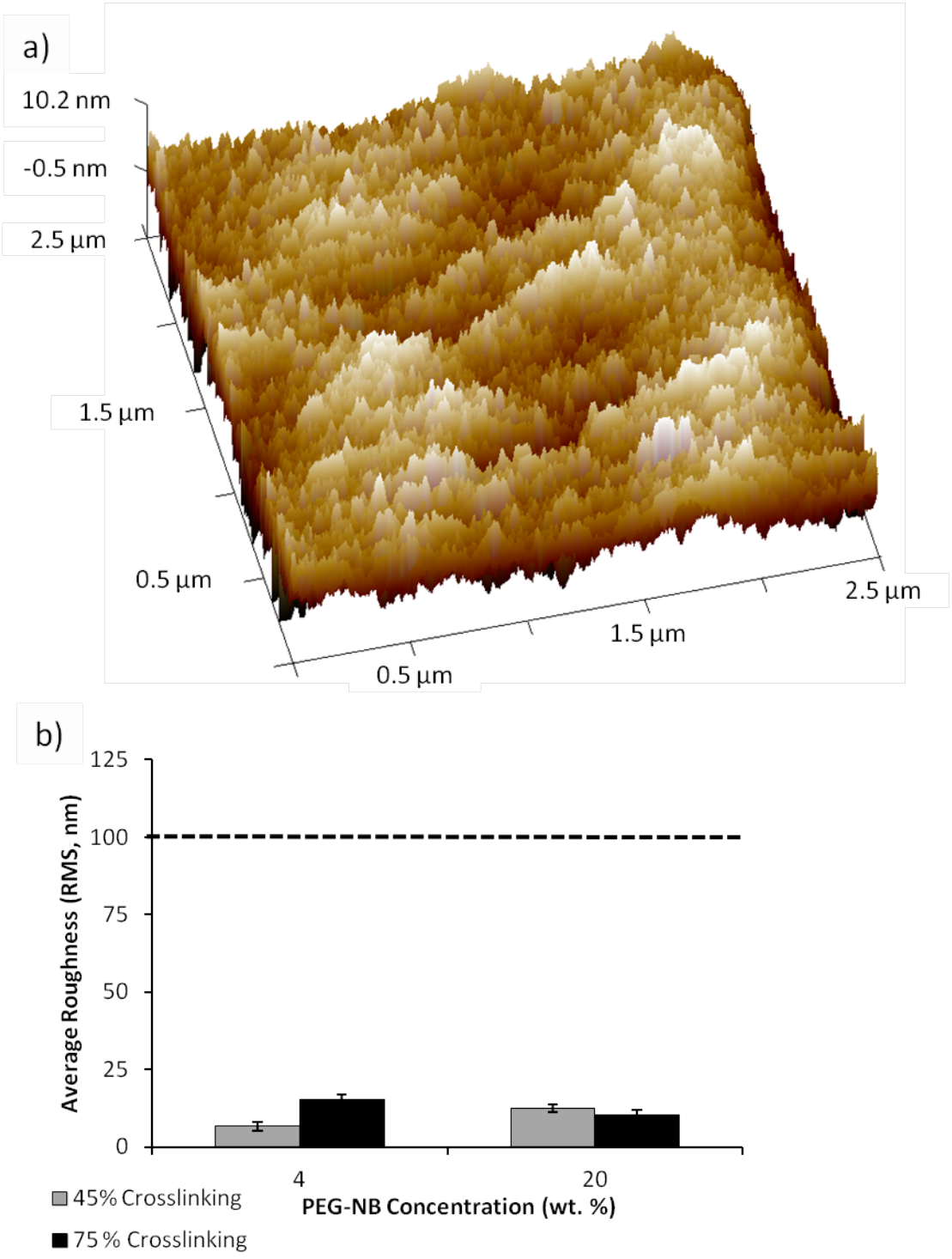

Figure 3.11. Characterization of surface roughness of hydrogels formed using the array formation procedure. (a) Representative AFM height image of hydrogel (shown: 20 wt.%, 45%

crosslinking) in liquid to determine the RMS roughness. (b) The calculated RMS roughness values (6.6-15.1 nm) for hydrogels with the lowest and highest stiffness values formed using this array formation procedure. Dotted line denotes minimum height used in previous studies investigating the influence of nanotopography of compliant surface on hMSC behavior. Sample size: n = 3 (b).

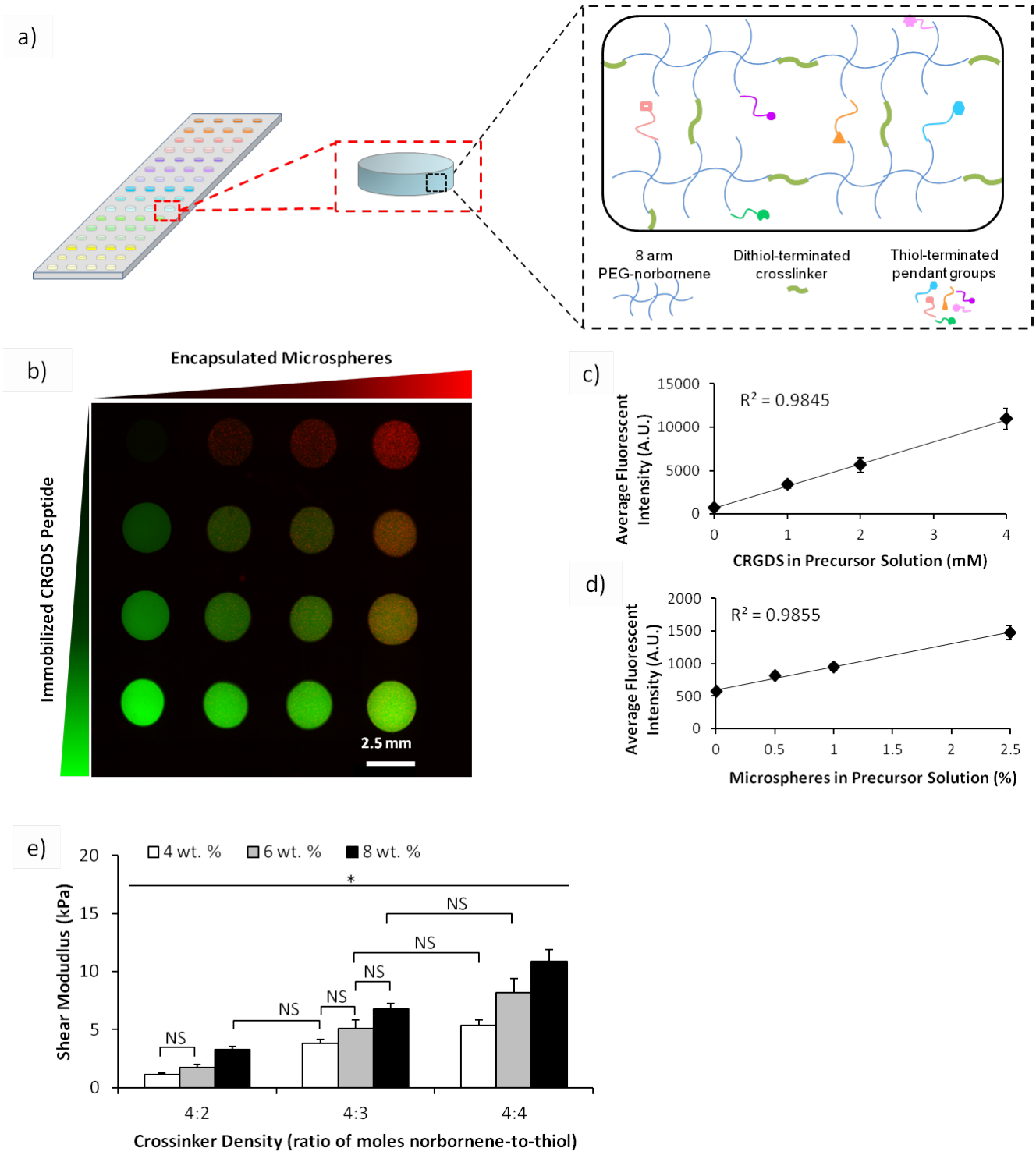

Figure 3.12. Characterization of the chemical and mechanical properties of hydrogel spots in the array. a) Schematic representation of array with hydrogel spots formed using thiolene chemistry. Array with hydrogel spots containing varying concentrations of immobilized CRGDS peptide

(b,c) and encapsulated microspheres (b,d). Hydrogel spots with stiffness varied by changing concentration of PEG-NB or crosslinker density in the hydrogel precursor solution (e). Sample size: n = 4 (c-d) and n = 3 (e). Statistical significance was determined by two-factor ANOVA followed by Tukey HSD test, whereby * denotes statistical significant with $p<0.05$ and “NS” denotes no statistical significance.

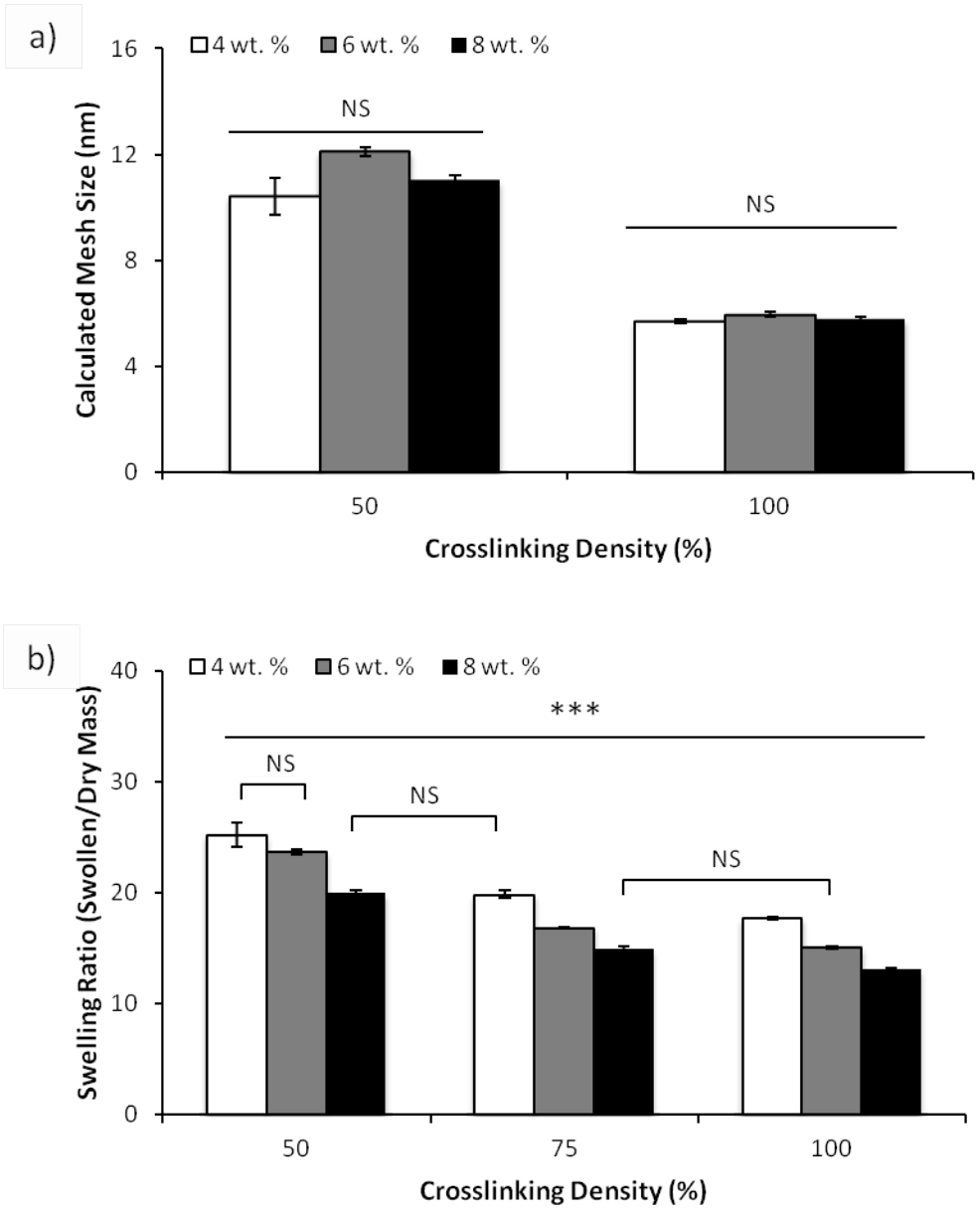

Figure 3.13. Characterization of hydrogel physical properties and network structure. a) Hydrogel network mesh size predicted using calculations based on Flory-Rehner theory. b) Mass equilibrium swelling ratio of bulk hydrogels formed with varying PEG-NB (wt. %) and crosslinker density. Sample size: n = 3 (a-b). Statistical significance was determined by two-

factor ANOVA followed by Tukey HSD test, whereby * denotes statistical significant with $p<0.05$ and “NS” denotes no statistical significance.

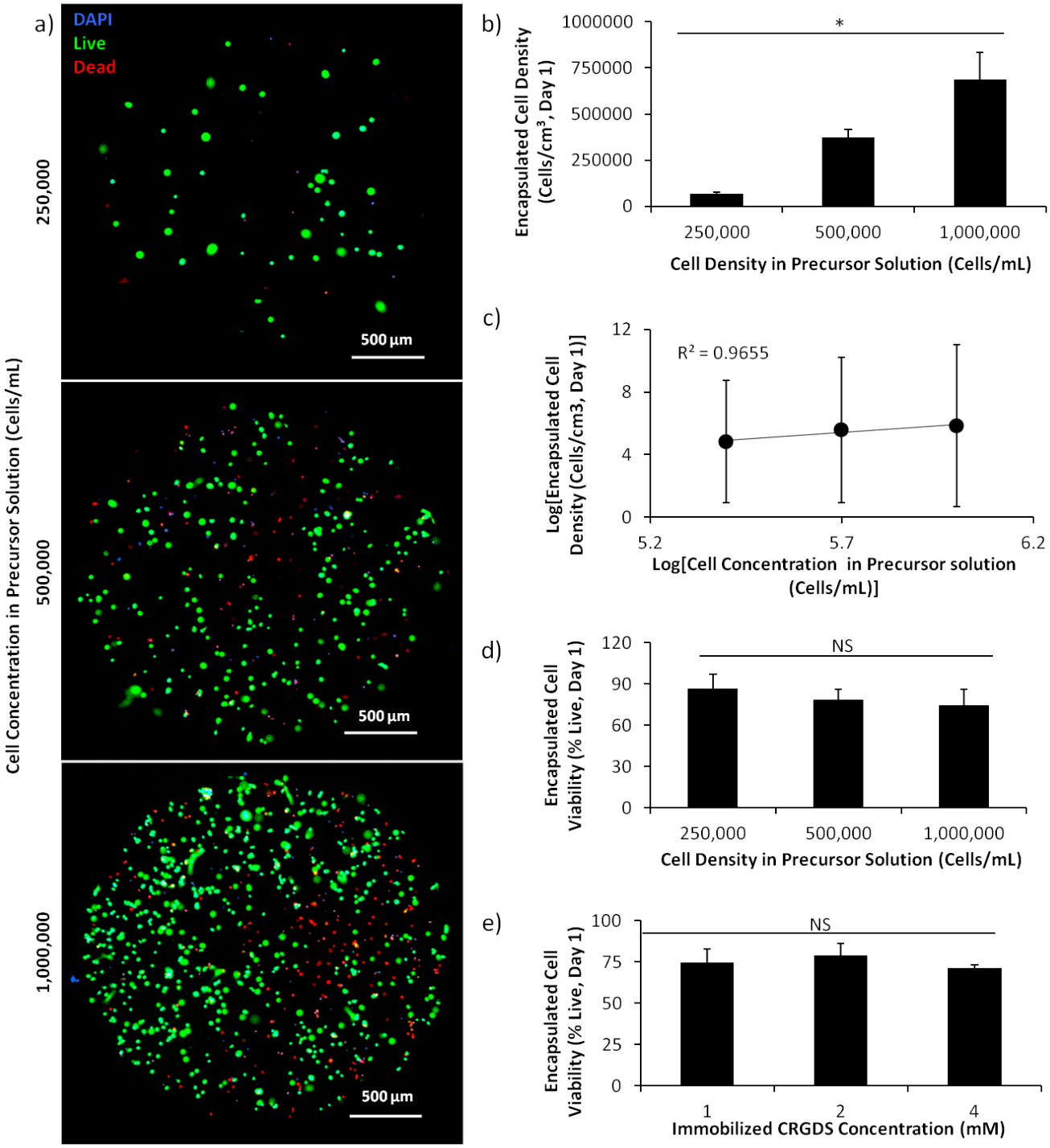

Figure 3.14. Demonstration of hMSC encapsulation in hydrogels formed using differential wettability patterning. All hydrogels presented CRGDS and were crosslinked with a MMP-

degradable peptide. a-d) Viability and density of hMSCs encapsulated in hydrogel spots presenting 2 mM CRGDS and formed using precursor solutions with varying concentrations of hMSC. a) Maximum intensity projection created by stacking images of the hydrogel acquired at 3 different focal planes in the hydrogel. c) Correlation of encapsulated hMSC density with hMSC concentration in precursor solution. e) Viability of ~500,000 hMSCs encapsulated in hydrogels spots containing varying concentrations of immobilized CRGDS peptide. Sample size: $n \geq 5$ (b, d,e), n=3 (c). Statistical significance was determined by ANOVA followed by Tukey-Kramer test, whereby * denotes $p<0.05$ and "NS" denotes no statistical significance.

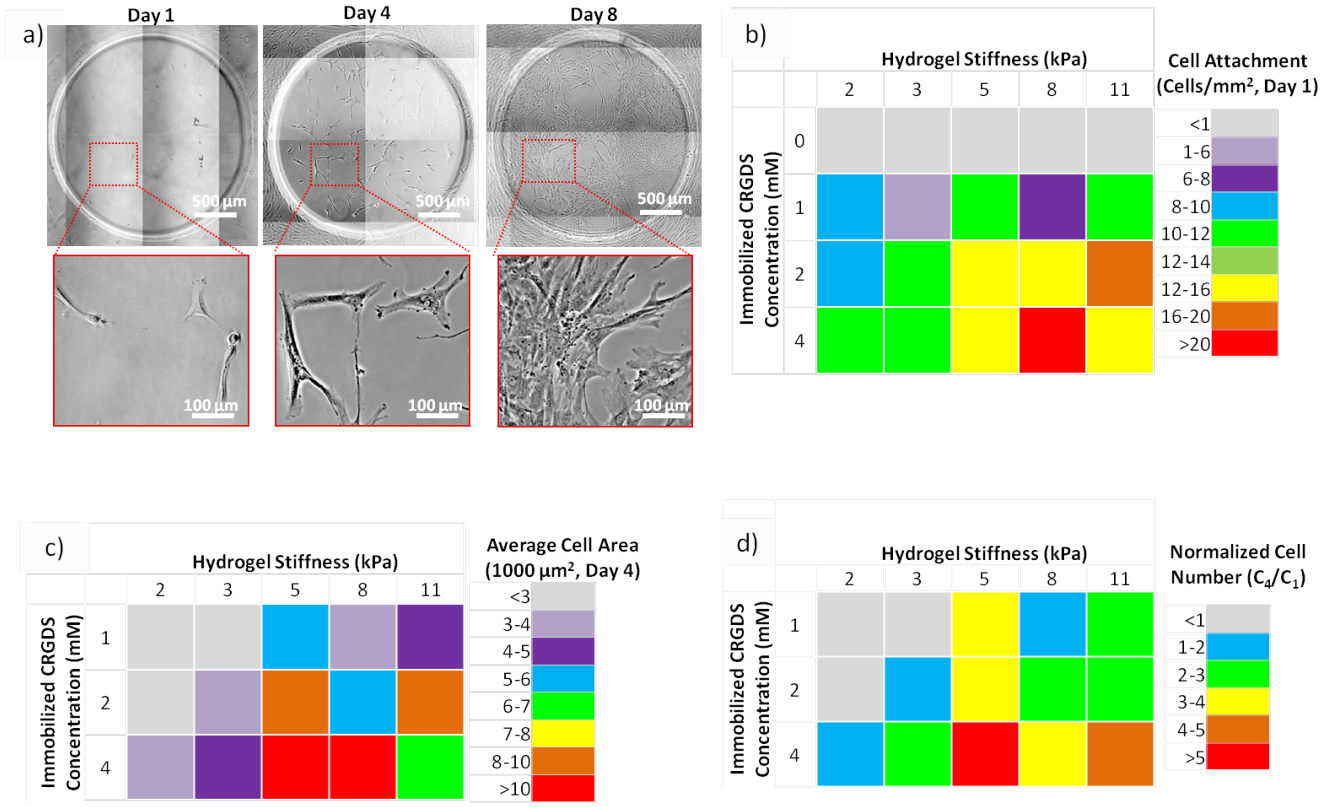

Figure 3.15. Effects of hydrogel spot stiffness and immobilized CRGDS concentration on hMSC behavior. a) hMSC culture on hydrogel spots presenting 4 mM CRGDS over the course of 8 days. hMSC b) cell attachment one day after cell seeding, c) cell spreading four days after cell seeding, and d) cell proliferation (indicated by normalized cell number from day 4 compared to day 1, $C_4/C_1 > 1$) after four days of culture Sample size: n = 4 (b-d).

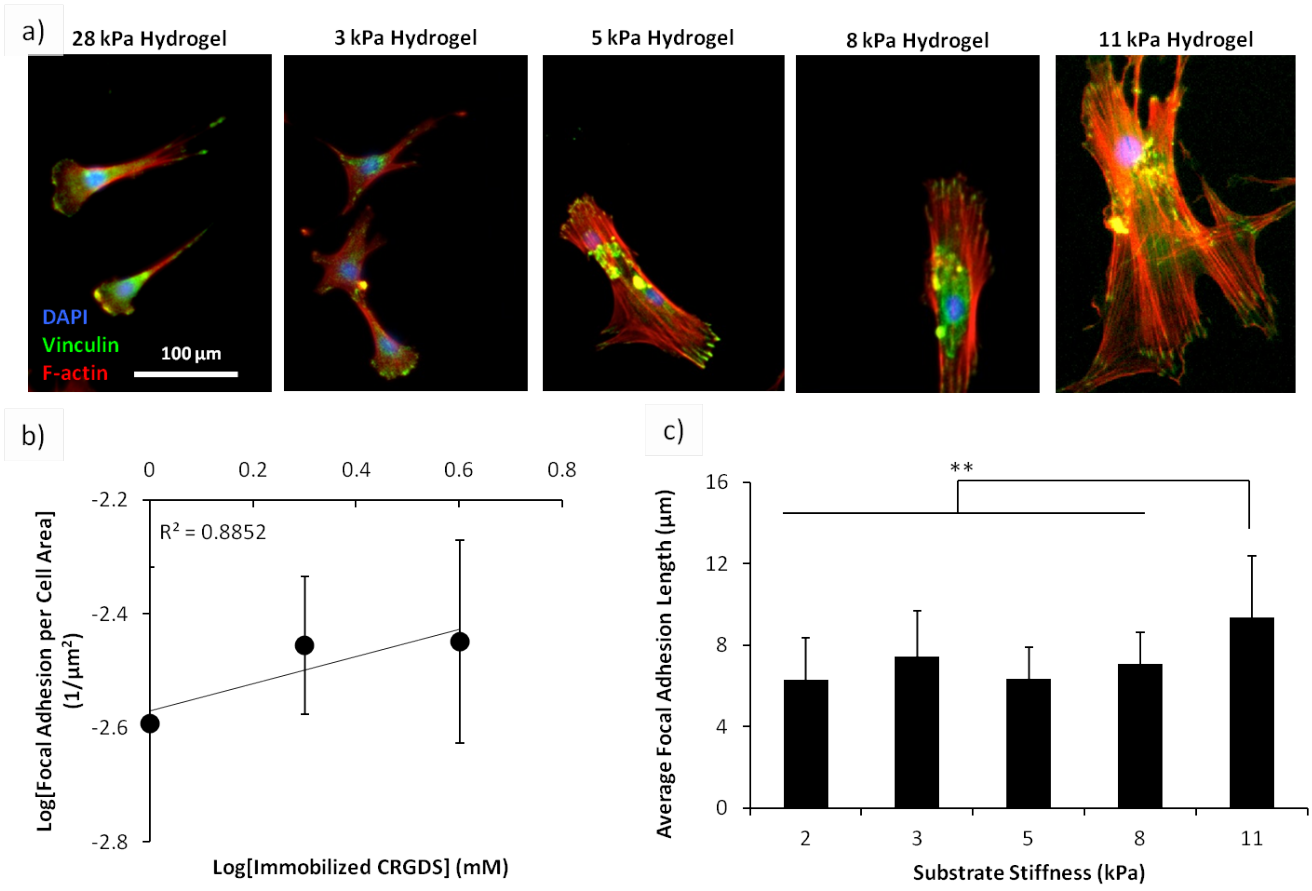

Figure 3.16. Effects of hydrogel spot stiffness and immobilized CRGDS concentration on hMSC cytoskeletal structure. a) Focal adhesion (vinculin, green), stress fiber (F-actin, red), and nuclear (DAPI, blue) stain of hMSCs after 8 days of culture on hydrogel spots with varying stiffness and presenting 4 mM CRGDS. b) Correlation of hMSC focal adhesion density with immobilized CRGDS concentration (calculated by averaging all hydrogel spots with the same CRGDS concentration, regardless of stiffness). c) Average hMSC focal adhesion length on hydrogels of different stiffness values (calculated by averaging all hydrogel spots with the same stiffness values, regardless of CRGDS concentration). Sample size: $n \geq 25$ (b-c). Asterisks denote statistical significance as determined by single factor ANOVA followed by Tukey-Kramer test, whereby ** $p<0.01$.

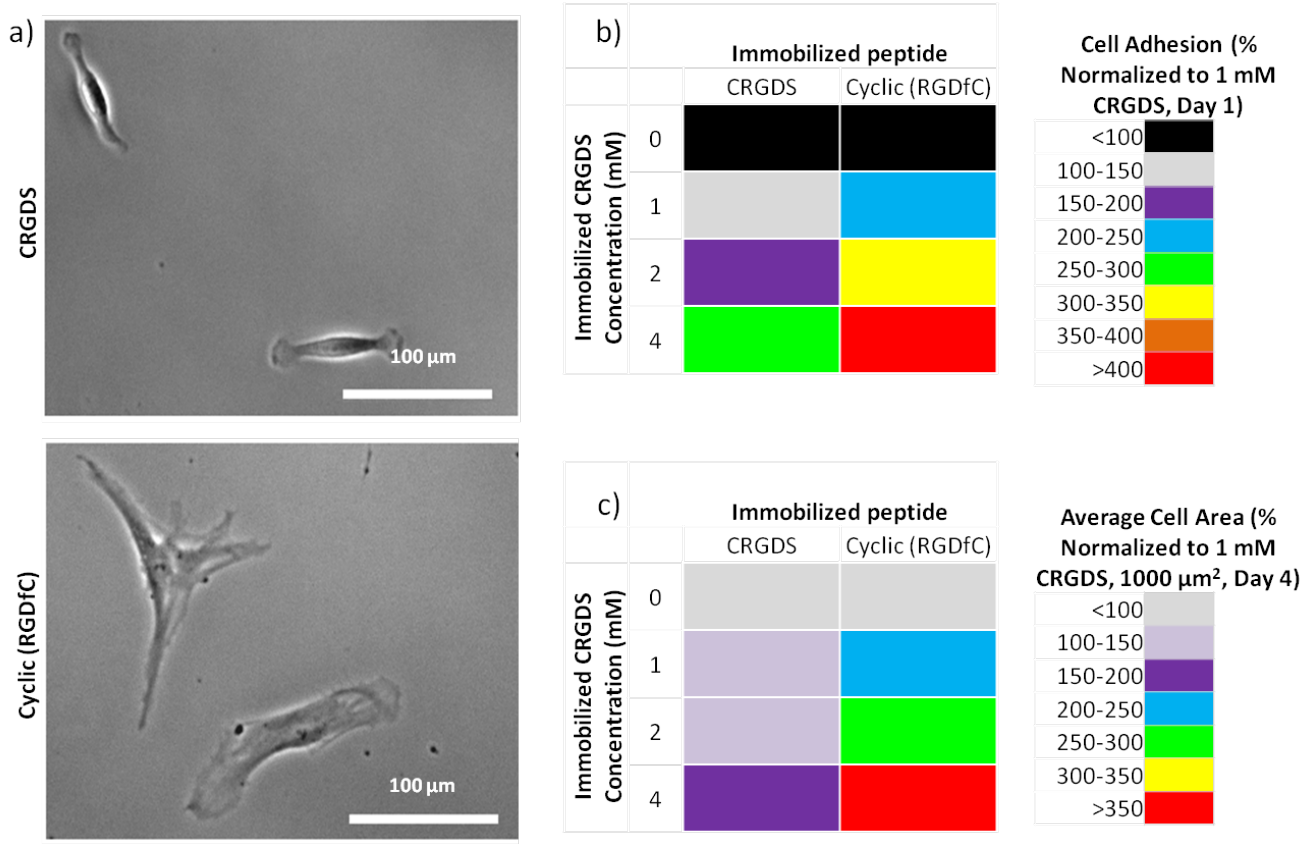

Figure 3.17. Effects of immobilized peptide identity on hMSC behavior. a) hMSC attachment on hydrogels presenting linear CRGDS or cyclic (RGDfC) after 3 days of culture. b) hMSC cell attachment one day after seeding and c) cell spreading after 3 days culture on hydrogel spots presenting 4 mM CRGDS or cyclic (RGDfC). Sample size: n ≥6 (b,c).

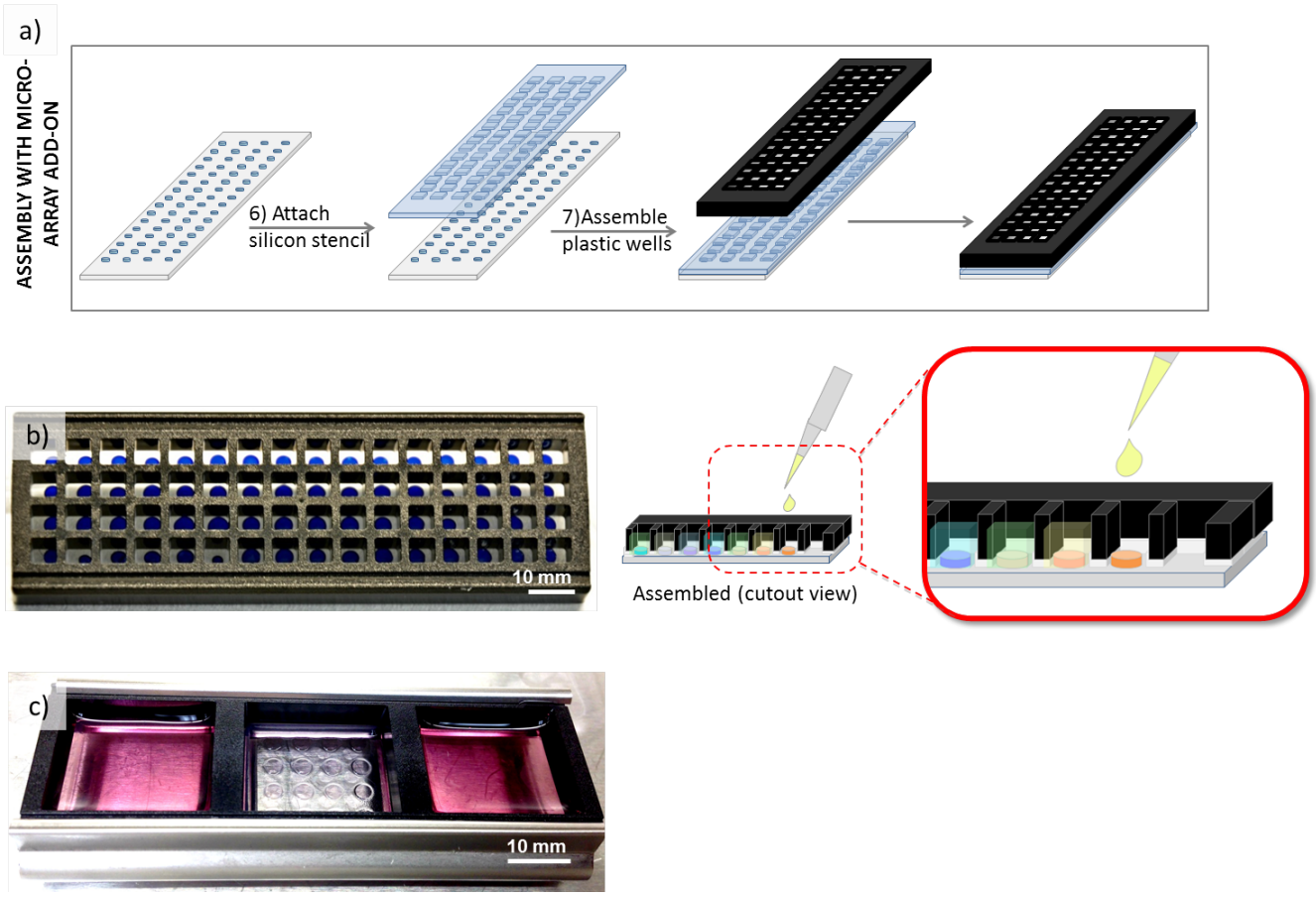

Figure 3.18. Demonstration of hydrogel array setup for soluble media screening. a) Hydrogel array assembly with commercially-available micro-array add-on for ability to introduce different soluble factors to b) each individual spot or c) group of spots in the array. b-c) Hydrogels stained with Trypan blue and media contains phenol red for enhanced contrast and visibility.

3.10 Supporting Information

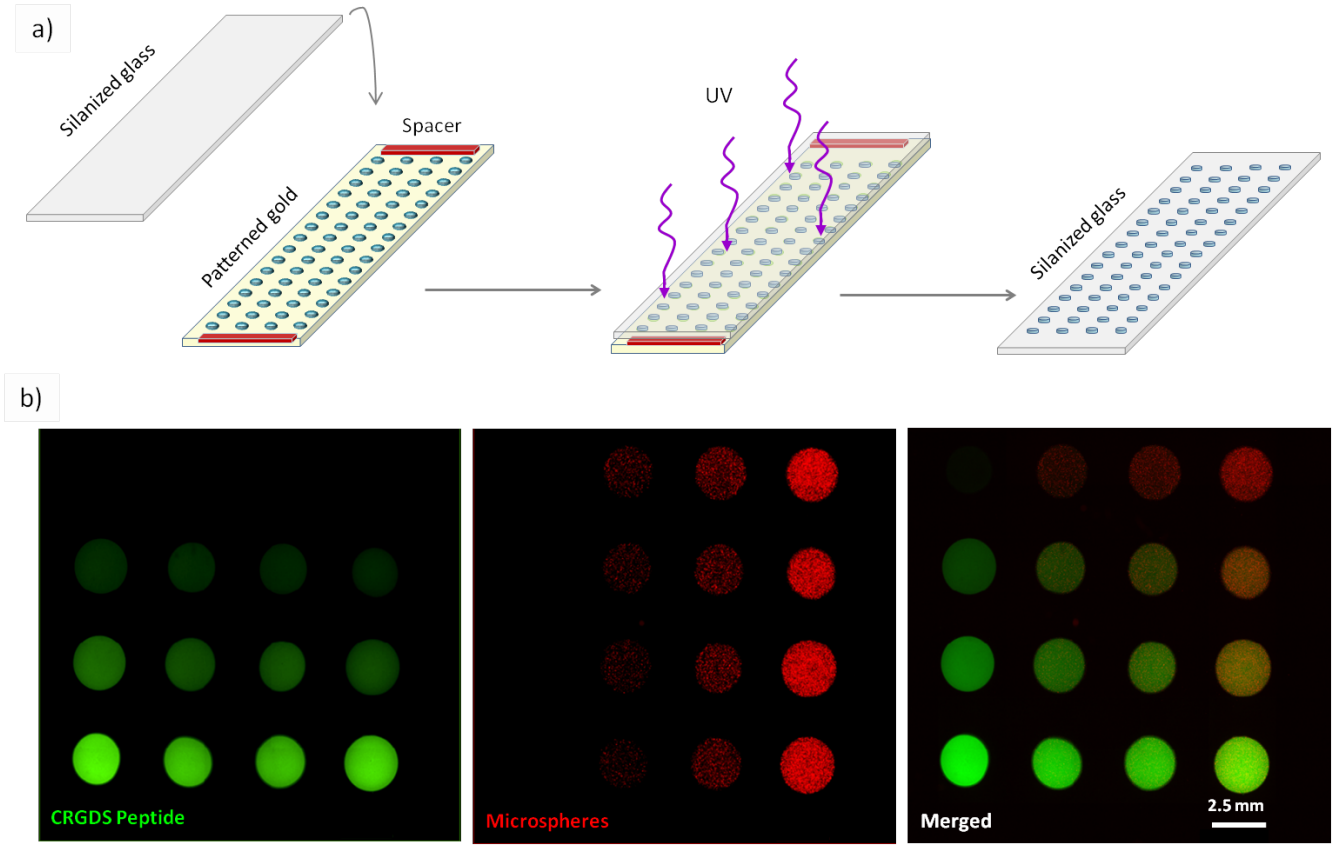

Figure 3.S1. Demonstration of array formation procedure and capabilities. a) During UV polymerization, PEG-NB hydrogels were covalently linked to thiol-presenting silanized glass slides. b) Array with hydrogel spots containing varying concentrations of immobilized CRGDS and encapsulated microspheres.

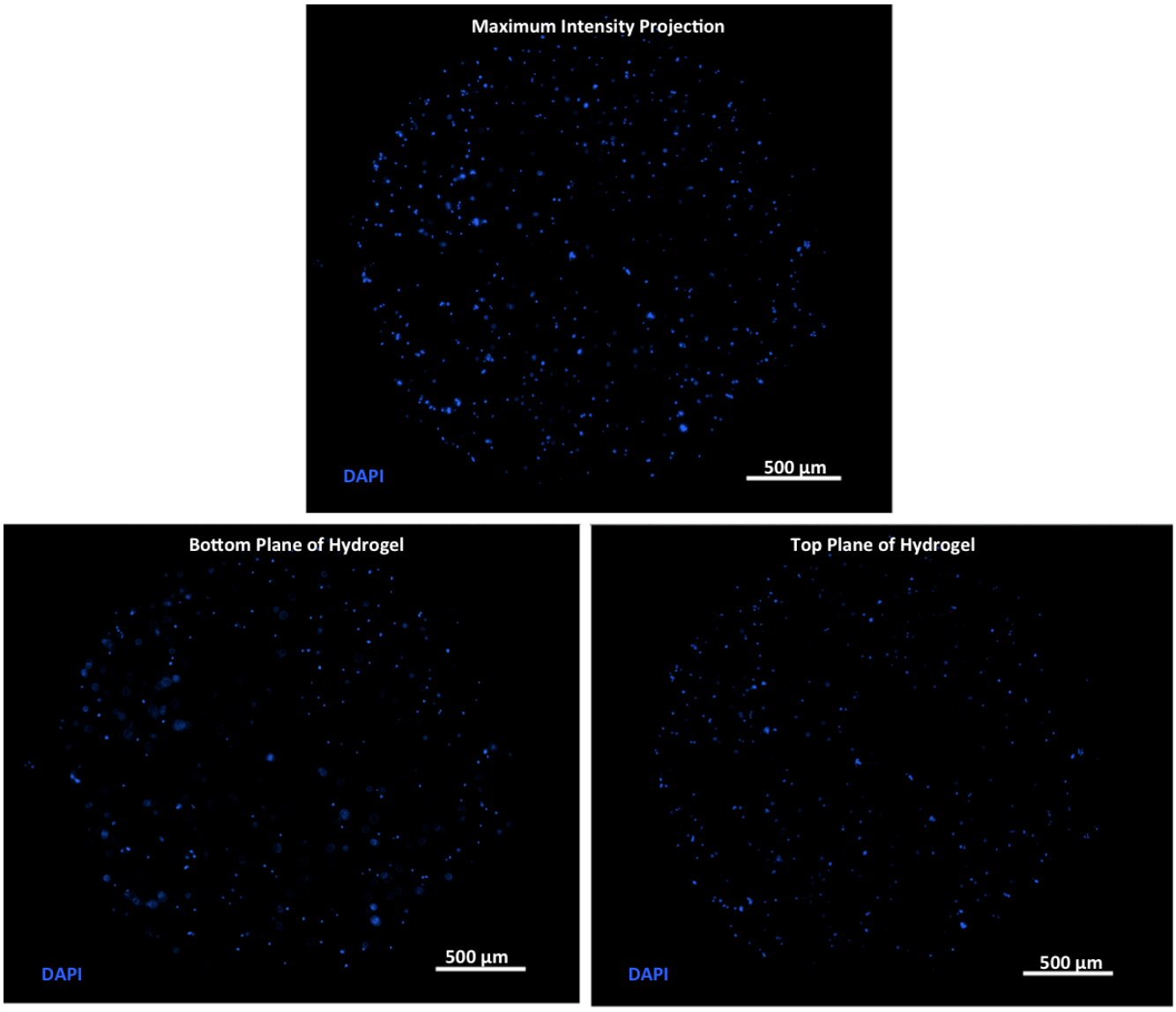

Figure 3.S2. Maximum intensity projection and images acquired at different focal planes reveal uniform distribution of encapsulated hMSC throughout the hydrogel.

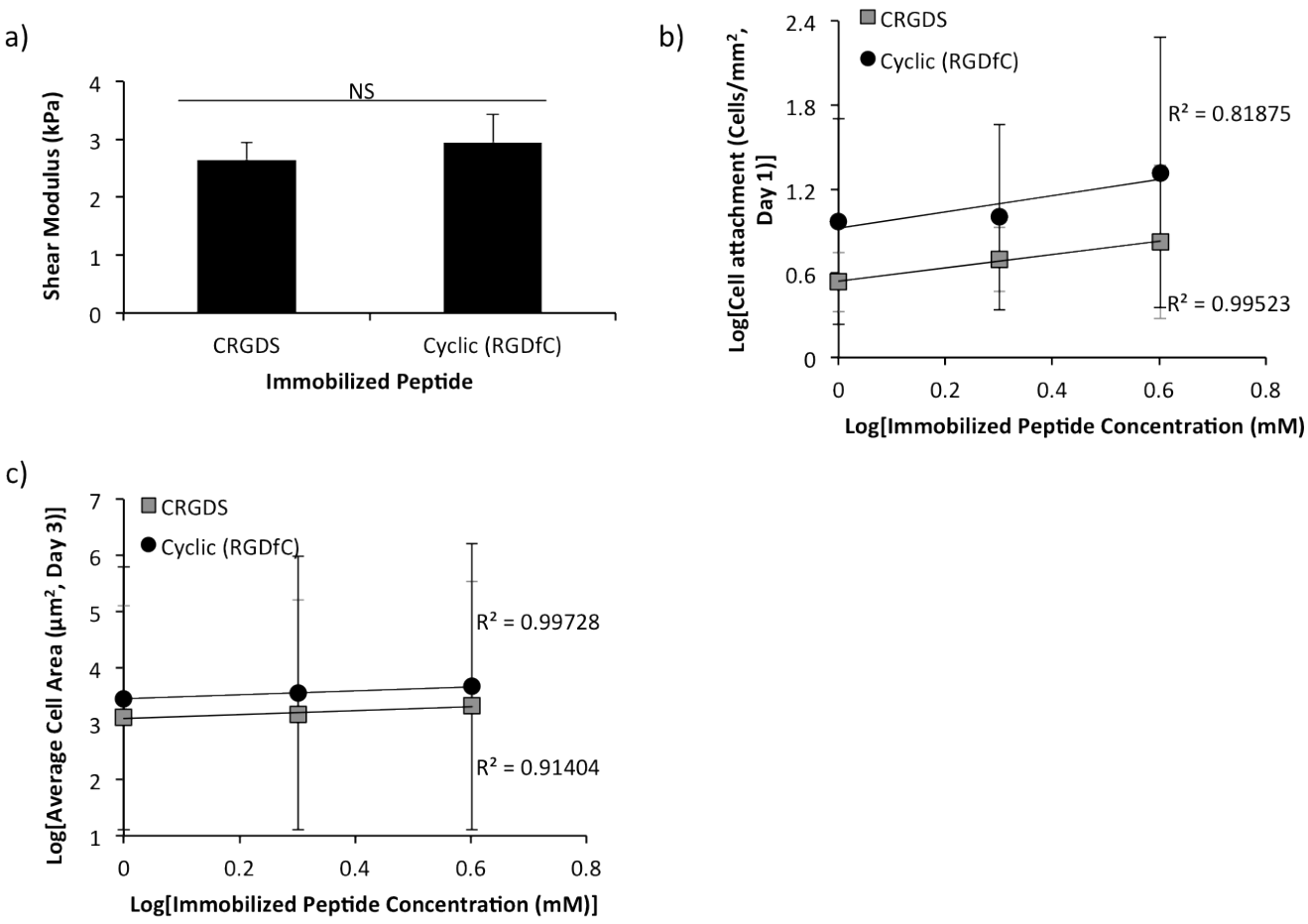

Figure 3.S3. Correlation of hMSC behavior with immobilized CRGDS concentration. hMSC a-b) cell attachment 1 day after cell seeding, c) average cell area 3 days after culture, and d) cell proliferation 3 days after culture on hydrogel spots presenting various concentration of CRGDS. Note that values are averages for hMSCs on hydrogel spots with stiffness from 2 to 11 kPa. Sample size: n $\geq$ 19 (a-d). Asterisks denote statistical significance as determined by two-factor ANOVA followed by Tukey-Kramer test, whereby ** denotes statistical significance with $p<0.01$.

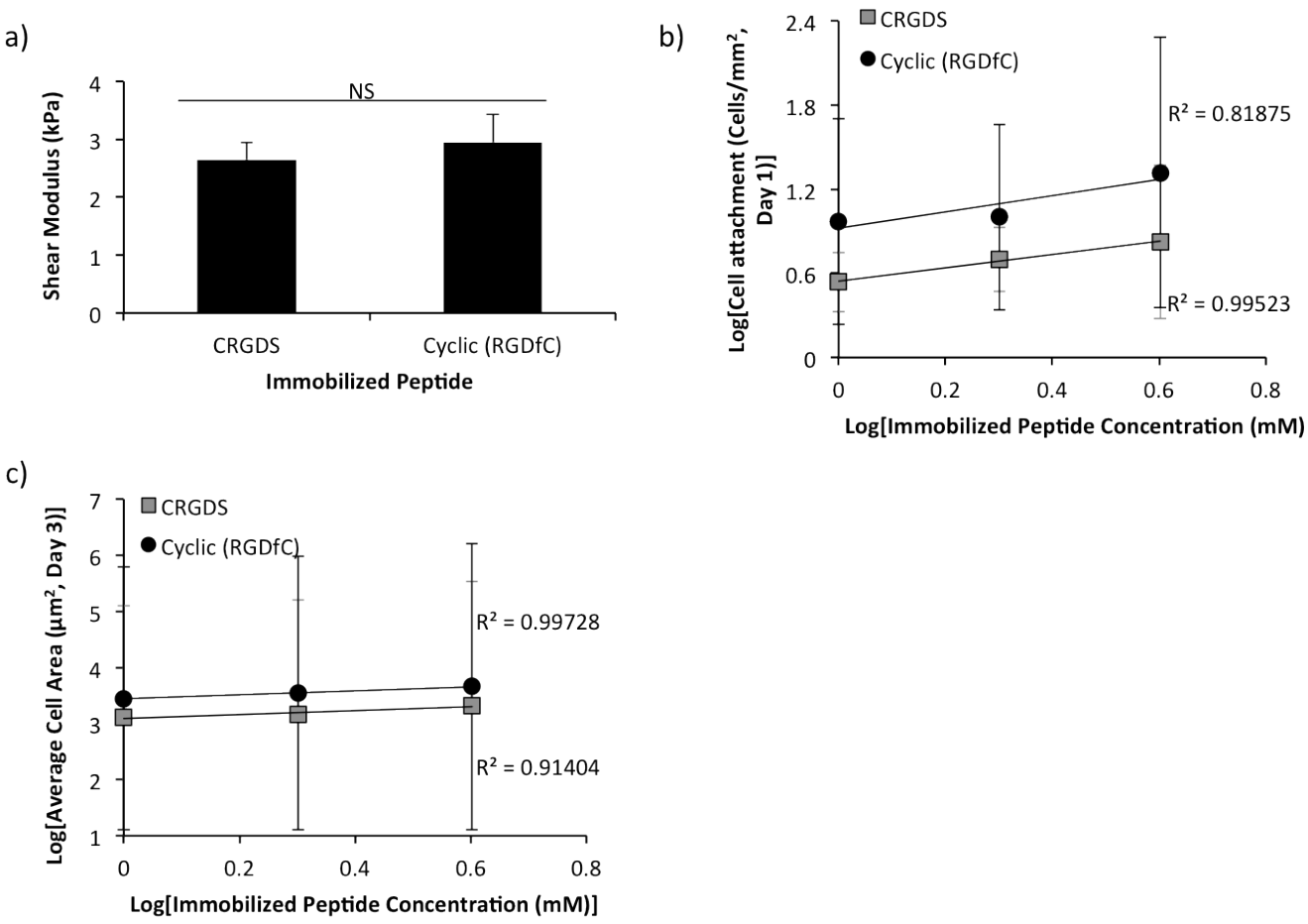

Figure 3.S4. Correlation of hMSC behavior with immobilized RGD-containing peptide concentration. a) Stiffness of 8 wt% PEG-NB, 50% crosslinked hydrogels presenting 4 mM CRGDS or cyclic (RGDfC). hMSC b) initial attachment 1 day after seeding and c) spreading 3 days after culture on hydrogels presenting 1-4 mM RGD-containing peptides. Statistical significance was determined by Student's t-test, whereby "NS" denotes no statistical significance with $\alpha=0.05$. Sample size: n=3 (a), n≥6 (b,c).

3.11. References

[1] Y. Sun, C.S. Chen, J. Fu, Forcing stem cells to behave: a biophysical perspective of the cellular microenvironment, Annual review of biophysics 41 (2012) 519-42.

[2] S. Gobaa, S. Hoehnel, M. Roccio, A. Negro, S. Kobel, M.P. Lutolf, Artificial niche microarrays for probing single stem cell fate in high throughput, Nature methods 8(11) (2011) 949-55.

[3] D.E. Discher, D.J. Mooney, P.W. Zandstra, Growth factors, matrices, and forces combine and control stem cells, Science 324(5935) (2009) 1673-1677.

[4] O.Z. Fisher, A. Khademhosseini, R. Langer, N.A. Peppas, Bioinspired materials for controlling stem cell fate, Accounts of chemical research 43(3) (2010) 419-28.

[5] J. Lee, A.A. Abdeen, D. Zhang, K.A. Kilian, Directing stem cell fate on hydrogel substrates by controlling cell geometry, matrix mechanics and adhesion ligand composition, Biomaterials 34(33) (2013) 8140-8.

[6] L. Jongpaiboonkit, W.J. King, W.L. Murphy, Screening for 3D environments that support human mesenchymal stem cell viability using hydrogel arrays, Tissue Engineering: Part A 15(2) (2009) 11.

[7] A. Ranga, M.P. Lutolf, High-throughput approaches for the analysis of extrinsic regulators of stem cell fate, Current opinion in cell biology 24(2) (2012) 236-44.

[8] W.J. King, L. Jongpaiboonkit, W.L. Murphy, Influence of FGF2 and PEG hydrogel matrix properties on hMSC viability and spreading, Journal of Biomedical Materials Research Part A 93A(3) (2010) 1110-1123.

[9] L. Jongpaiboonkit, W.J. King, G.E. Lyons, A.L. Paguirigan, J.W. Warrick, D.J. Beebe, W.L. Murphy, An adaptable hydrogel array format for 3-dimensional cell culture and analysis, Biomaterials 29(23) (2008) 3346-3356.

[10] A.J. Engler, S. Sen, H.L. Sweeney, D.E. Discher, Matrix elasticity directs stem cell lineage specification, Cell 126(4) (2006) 677-89.

[11] A.J. Engler, L. Bacakova, C. Newman, A. Hategan, M. Griffin, D.E. Discher, Substrate Compliance versus Ligand Density in Cell on Gel Responses, Biophysical journal 86(1) (2004) 617-628.

[12] A.K. Jha, K.E. Healy, Controlling Osteogenic Stem Cell Differentiation via Soft, PLOS ONE 9(6) (2014) 1-11.

[13] K.A. Kilian, M. Mrksich, Directing stem cell fate by controlling the affinity and density of ligand-receptor interactions at the biomaterials interface, Angewandte Chemie 51(20) (2012) 4891-5.

[14] J.H. Wen, L.G. Vincent, A. Fuhrmann, Y.S. Choi, K.C. Hribar, H. Taylor-Weiner, S. Chen, A.J. Engler, Interplay of matrix stiffness and protein tethering in stem cell differentiation, Nature materials (2014).

[15] N.R. Gandavarapu, D.L. Alge, K.S. Anseth, Osteogenic differentiation of human mesenchymal stem cells on alpha5 integrin binding peptide hydrogels is dependent on substrate elasticity, Biomater Science 2(3) (2014) 352-361.

[16] M. Guvendiren, J.A. Burdick, Stiffening hydrogels to probe short- and long-term cellular responses to dynamic mechanics, Nature communications 3 (2012) 792.

[17] S.Y. Tee, J. Fu, C.S. Chen, P.A. Janmey, Cell shape and substrate rigidity both regulate cell stiffness, Biophysical journal 100(5) (2011) L25-7.

[18] J.T. Koepsel, S.G. Loveland, M.P. Schwartz, S. Zorn, D.G. Belair, N.N. Le, W.L. Murphy, A chemically-defined screening platform reveals behavioral similarities between primary human

mesenchymal stem cells and endothelial cells, Integrative biology : quantitative biosciences from nano to macro 4(12) (2012) 1508-21.

[19] C.R. Vistas, A.C.P. Águas, G.N.M. Ferreira, Silanization of glass chips—A factorial approach for optimization, Applied Surface Science 286 (2013) 314-318.

[20] I.E. Dunlop, S. Zorn, G. Richter, V. Srot, M. Kelsch, P.A. van Aken, M. Skoda, A. Gerlach, J.P. Spatz, F. Schreiber, Titanium–silicon oxide film structures for polarization-modulated infrared reflection absorption spectroscopy, Thin Solid Films 517(6) (2009) 2048-2054.

[21] E.H. Nguyen, M.R. Zanotelli, M.P. Schwartz, W.L. Murphy, Differential effects of cell adhesion, modulus and VEGFR-2 inhibition on capillary network formation in synthetic hydrogel arrays, Biomaterials 35(7) (2014) 2149-61.

[22] B.D. Fairbanks, M.P. Schwartz, A.E. Halevi, C.R. Nuttelman, C.N. Bowman, K.S. Anseth, A Versatile Synthetic Extracellular Matrix Mimic via Thiol-Norbornene Photopolymerization, Advanced Materials 21(48) (2009) 5005-5010.

[23] M.W. Toepke, N.A. Impellitteri, J.M. Theisen, W.L. Murphy, Characterization of Thiol-Ene Crosslinked PEG Hydrogels, Macromolecular materials and engineering 298(6) (2013) 699-703.

[24] S. Lin, N. Sangaj, T. Razafiarison, C. Zhang, S. Varghese, Influence of physical properties of biomaterials on cellular behavior, Pharmaceutical research 28(6) (2011) 1422-30.

[25] N.A. Peppas, E.W. Merrill, Poly(vinyl Alcohol) Hydrogels: Reinforcement of radiation-crosslinked networks by crystallization, Journal of Polymer Science 14(2) (1976) 441-457.

[26] T. Canal, N.A. Peppas, Correlation between mesh size and equilibrium degree of swelling of polymeric networks, Journal of Biomedical Materials Research 23(10) (1989) 1183-1193.

[27] J.T. Koepsel, W.L. Murphy, Patterned self-assembled monolayers: efficient, chemically defined tools for cell biology, Chembiochem : a European journal of chemical biology 13(12) (2012) 1717-24.

[28] L.E. McNamara, R.J. McMurray, M.J.P. Biggs, F. Kantawong, R.O.C. Oreffo, M.J. Dalby, Nanotopographical Control of Stem Cell Differentiation, Journal of Tissue Engineering 1(1) (2010).

[29] F. Guilak, D.M. Cohen, B.T. Estes, J.M. Gimble, W. Liedtke, C.S. Chen, Control of Stem Cell Fate by Physical Interactions with the Extracellular Matrix, Cell Stem Cell 5(1) (2009) 17-26.

[30] L.-A. Turner, M. J. Dalby, Nanotopography - potential relevance in the stem cell niche, Biomaterials science 2(11) (2014) 1574-1594.

[31] M.J. Dalby, N. Gadegaard, R.O.C. Oreffo, Harnessing nanotopography and integrin-matrix interactions to influence stem cell fate, Nature materials 13(6) (2014) 558-569.

[32] A. Raza, C.-C. Lin, The Influence of Matrix Degradation and Functionality on Cell Survival and Morphogenesis in PEG-Based Hydrogels, Macromolecular Bioscience 13(8) (2013) 1048-1058.

[33] C.R. Nuttelman, M.C. Tripodi, K.S. Anseth, Synthetic hydrogel niches that promote hMSC viability, Matrix Biology 24(3) (2005) 208-218.

[34] E. Ruoslahti, RGD AND OTHER RECOGNITION SEQUENCES FOR INTEGRINS, Annual Review of Cell and Developmental Biology 12(1) (1996) 697-715.

[35] R. Haubner, D. Finsinger, H. Kessler, Stereoisomeric Peptide Libraries and Peptidomimetics for Designing Selective Inhibitors of the αvβ3 Integrin for a New Cancer Therapy, Angewandte Chemie International Edition in English 36(13-14) (1997) 1374-1389.

[36] A.K. Jha, W.M. Jackson, K.E. Healy, Controlling Osteogenic Stem Cell Differentiation via Soft Bioinspired Hydrogels, PLOS ONE 9(6) (2014) 1-11.

[37] M.J. Wilson, Y. Jiang, B. Yañez-Soto, S. Liliensiek, W.L. Murphy, P.F. Nealey, Arrays of topographically and peptide-functionalized hydrogels for analysis of biomimetic extracellular matrix properties, Journal of Vacuum Science and Technology. B, Nanotechnology & microelectronics : materials, processing, measurement, & phenomena : JVST B 30(6) (2012) 06F903.

[38] B. Trappmann, J.E. Gautrot, J.T. Connelly, D.G. Strange, Y. Li, M.L. Oyen, M.A. Cohen Stuart, H. Boehm, B. Li, V. Vogel, J.P. Spatz, F.M. Watt, W.T. Huck, Extracellular-matrix tethering regulates stem-cell fate, Nat Mater 11(7) (2012) 642-9.

[39] A. Geerligs, G.W. Peters, P.A. Ackermans, C.W. Oomens, Linear viscoelastic behavior of subcutaneous adipose tissue, Biorheology 45(6) (2008) 677-688.

[40] A. Nordez, F. Hug, Muscle shear elastic modulus measured using supersonic shear imaging is highly related to muscle activity level, Journal of applied physiology 108(5) (2010) 1389-94.

[41] S.K. Schmitt, W.L. Murphy, P. Gopalan, Crosslinked PEG mats for peptide immobilization and stem cell adhesion, Journal of Materials Chemistry B 1(9) (2013) 1349.

[42] G. Geiger, A. Bershadsky, R. Pankov, K.M. Yamada, Transmembrane extracellular matrix-cytoskeleton crosstalk, Nature Reviews Molecular Cell Biology 2(11) (2001) 793-805.

[43] J.M. Goffin, P. Pittet, G. Csucs, J.W. Lussi, J.J. Meister, B. Hinz, Focal adhesion size controls tension-dependent recruitment of alpha-smooth muscle actin to stress fibers, Journal of Cell Biology 172(2) (2006) 259-268.

[44] H.J. Kong, T. Boontheekul, D.J. Mooney, Quantifying the relation between adhesion ligand–receptor bond formation and cell phenotype, Proceedings of the National Academy of Sciences 103(49) (2006) 18534-18539.

[45] A. Khademhosseini, R. Langer, J. Borenstein, J.P. Vacanti, Microscale technologies for tissue engineering and biology, Proceedings of the National Academy of Sciences of the United States of America 103(8) (2006) 2480-2487.

3.12 Appendix

3.12.1 Patent (No: US 10,195,313; Issued: February 5, 2019)- Method for forming hydrogel arrays using surfaces with differential wettability


US010195313B2

(12) **United States Patent**
Murphy et al.

(10) **Patent No.: US 10,195,313 B2**
(45) **Date of Patent: Feb. 5, 2019**

(54) **METHOD FOR FORMING HYDROGEL ARRAYS USING SURFACES WITH DIFFERENTIAL WETTABILITY**

(71) Applicant: **Wisconsin Alumni Research Foundation**, Madison, WI (US)

(72) Inventors: **William L. Murphy**, Waunakee, WI (US); **Ngoc Nhi Thi Le**, Madison, WI (US); **Stefan Zorn**, Madison, WI (US); **Michael P. Schwartz**, Madison, WI (US); **Eric Huy Dang Nguyen**, Madison, WI (US)

(73) Assignee: **Wisconsin Alumni Research Foundation**, Madison, WI (US)

(*) Notice: Subject to any disclaimer, the term of this patent is extended or adjusted under 35 U.S.C. 154(b) by 454 days.

(21) Appl. No.: **14/339,938**

(22) Filed: **Jul. 24, 2014**

(65) **Prior Publication Data**

US 2015/0293073 A1 Oct. 15, 2015

Related U.S. Application Data

(60) Provisional application No. 61/978,032, filed on Apr. 10, 2014.

(51) **Int. Cl.**

G01N 33/483	(2006.01)
A61L 31/14	(2006.01)
C12N 5/0735	(2010.01)
G01N 33/50	(2006.01)
A61K 47/42	(2017.01)
A61L 29/16	(2006.01)
B01J 19/00	(2006.01)
G01N 21/64	(2006.01)

(52) **U.S. Cl.**

CPC ***A61L 31/145*** (2013.01); ***A61K 47/42*** (2013.01); ***A61L 29/16*** (2013.01); ***C12N 5/0606*** (2013.01); ***G01N 33/4833*** (2013.01); ***G01N 33/5005*** (2013.01); *A61L 2300/80* (2013.01); *B01J 19/0046* (2013.01); *B01J 2219/00596* (2013.01); *C12N 2533/20* (2013.01); *C12N 2533/30* (2013.01); *C12N 2537/10* (2013.01); *G01N 21/6452* (2013.01); *G01N 2610/00* (2013.01)

(58) **Field of Classification Search**

CPC A61L 31/145
USPC 506/9
See application file for complete search history.

(56) **References Cited**

U.S. PATENT DOCUMENTS

2005/0019843	A1*	1/2005	Chen	G01N 33/56966 435/7.21
2007/0217019	A1*	9/2007	Huang	G02B 3/0031 359/642
2012/0149781	A1	6/2012	Lee et al.	
2012/0225814	A1	9/2012	Hanijaya-Putra et al.	
2013/0210147	A1	8/2013	Jeannin et al.	
2013/0260464	A1	10/2013	Vannier et al.	
2013/0296177	A1	11/2013	Koepsel et al.	
2014/0017284	A1	1/2014	Yang et al.	
2014/0018263	A1*	1/2014	Levkin	C12N 11/08 506/26
2015/0104812	A1*	4/2015	Grevesse	A61L 27/52 435/7.21

FOREIGN PATENT DOCUMENTS

WO	2011156686	A2	12/2011

OTHER PUBLICATIONS

Pishko, M. (Engineering in Medicine and Biology, 27th Annual Conference, Shanghai, China, Sep. 1-4, 2005, pp. 1058-1064).*

Hern et al. (Journal of Biomed Mater Res, 1998, 39(2), pp. 266-276).*

Heller (Annual Reviews of Biomedical Engineering, 2002, 4:129-153) (Year: 2002).*

Kyburz et al., Three-dimensional hMSC motility within peptide-functionalized PEG-based hydrogels of varying adhesivity and crosslinking density, Acta Biomaterialia, vol. 9, No. 5, pp. 6381-6392, 2013.

Leslie-Barbick et al., The promotion of microvasculature formation in poly(ethylene glycol) diacrylate hydrogels by an immobilized VEGF-mimetic peptide, Biomaterials, vol. 32, No. 25, pp. 5782-5789, 2011.

Love et al., Self-Assembled Monolayers of Thiolates on Metals as a Form of Nanotechnology, Chem. Rev. 2005, 105:1103-1169.

Strother et al., Synthesis and Characterization of DNA-Modified Silicon (III) Surfaces, J. Am. Chem. Soc. 2000, 122:1205-1209.

(Continued)

Primary Examiner — Karla A Dines

(74) *Attorney, Agent, or Firm* — Stinson Leonard Street LLP

(57) **ABSTRACT**

Patterned hydrogel arrays and methods of preparing patterned hydrogel arrays are disclosed. Advantageously, the methods used to prepare the patterned hydrogel arrays allow for controlling individual hydrogel spot conditions such as hydrogel spot modulus, hydrogel spot ligand identity and hydrogel spot ligand density, which allows for preparing a wide range of hydrogel spots in a single array format. Patterned hydrogel arrays can also be formed to include hydrogel-free pools surrounded by hydrogel. Additionally, the patterned hydrogel arrays of the present disclosure support the culture of a range of cell types. The patterned hydrogel arrays offer the ability to rapidly screen substrate components for influencing cell attachment, spreading, proliferation, migration, and differentiation.

20 Claims, 14 Drawing Sheets

Specification includes a Sequence Listing.

3.12.2 Patent (No: US 9,694,338; Issued: July 4, 2017) - Covalently-immobilized hydrogel arrays in multi-well plates

US009694338B2

(12) **United States Patent**
Murphy et al.

(10) **Patent No.: US 9,694,338 B2**
(45) **Date of Patent: Jul. 4, 2017**

(54) **COVALENTLY-IMMOBILIZED HYDROGEL ARRAYS IN MULTI-WELL PLATES**

(71) Applicant: **Wisconsin Alumni Research Foundation**, Madison, WI (US)

(72) Inventors: **William Murphy**, Waunakee, WI (US); **Ngoc Nhi Le**, Norcross, GA (US)

(73) Assignee: **Wisconsin Alumni Research Foundation**, Madison, WI (US)

(*) Notice: Subject to any disclaimer, the term of this patent is extended or adjusted under 35 U.S.C. 154(b) by 0 days.

(21) Appl. No.: **14/575,084**

(22) Filed: **Dec. 18, 2014**

(65) **Prior Publication Data**

US 2016/0175800 A1 Jun. 23, 2016

(51) **Int. Cl.**
B01J 19/00 (2006.01)
G01N 33/50 (2006.01)

(52) **U.S. Cl.**
CPC ***B01J 19/0046*** (2013.01); ***G01N 33/5026*** (2013.01); ***G01N 33/5032*** (2013.01); ***G01N 33/5064*** (2013.01); ***G01N 33/5073*** (2013.01); *B01J 2219/0059* (2013.01); *B01J 2219/00315* (2013.01); *B01J 2219/00626* (2013.01); *B01J 2219/00637* (2013.01); *B01J 2219/00644* (2013.01); *B01J 2219/00659* (2013.01); *B01J 2219/00675* (2013.01); *B01J 2219/00711* (2013.01); *B01J 2219/00725* (2013.01); *B01J 2219/00736* (2013.01); *B01J 2219/00756* (2013.01)

(58) **Field of Classification Search**
None
See application file for complete search history.

(56) **References Cited**

U.S. PATENT DOCUMENTS

2004/0029241 A1* 2/2004 Hahn et al. A61K 9/1641 435/174
2005/0244983 A1* 11/2005 Ching G01N 33/52 436/172

OTHER PUBLICATIONS

Cordey et al., "Enhancing the Reliability and Throughput of Neurosphere Culture on Hydrogel Microwell Arrays," Stem Cells 2008, 26:2586-2594.*
Lin et al., "PEG hydrogels formed by thiol-ene photo-click chemistry and their effect on the formation and recovery of insulin-secreting cell spheroids," Biomaterials 2011, 32:9685-9695.*
Polizzotti et al., Three-Dimensional Biochemical Patterning of Click-Based Composite Hydrogels via Thiolene Photopolymerization; Biomacromolecules 2008, 9:1084-1087.
Fairbanks et al., A versatile Synthetic Extracellular Matrix Mimic via Thiol-Norbornene Photopolymerization, (Adv. Mater 2009, 21:5005-5010).

(Continued)

Primary Examiner — Kaijiang Zhang
(74) *Attorney, Agent, or Firm* — Stinson Leonard Street LLP

(57) **ABSTRACT**

Hydrogel arrays, methods for preparing hydrogel arrays and methods for screening cell-substrate interactions using the hydrogel arrays are disclosed. Advantageously, the hydrogel arrays include individual hydrogel posts that are completely isolatable, allowing for systematic and independent control of the chemical composition and physical dimensions of each hydrogel post.

10 Claims, 4 Drawing Sheets
(4 of 4 Drawing Sheet(s) Filed in Color)

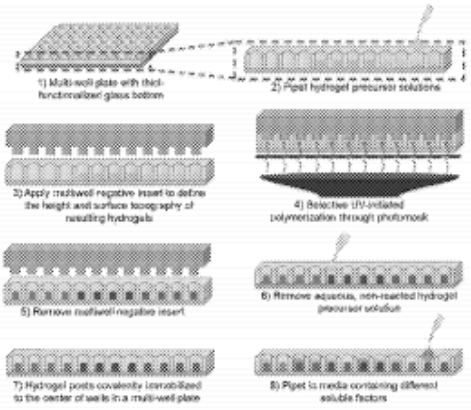

Chapter 4- Customized hydrogel substrates for serum-free expansion of functional hMSCs

Ngoc Nhi T. Le[a], Tianran Leona Liu[b], James Johnston [b], Kayla Marie Templeton[c], Victoria Harms[b], Andrew Dias[b], John Krutty[b], Hau Le[f,g], Padma Gopalan [a,c,d], William L. Murphy[a,b,g*]

[a] Materials Science Program, University of Wisconsin-Madison, Madison, WI USA

[b] Department of Biomedical Engineering, University of Wisconsin-Madison, Madison, WI USA

[c] Department of Material Science and Engineering, University of Wisconsin-Madison, Madison, WI USA

[d] Department of Chemistry, University of Wisconsin-Madison, Madison, WI USA

[e] Department of Chemistry, Humboldt State University, Arcata, CA USA

[f] Department of Surgery, University of Wisconsin-Madison, Madison, WI USA

[g] Department of Orthopedics and Rehabilitation, University of Wisconsin-Madison, Madison, WI USA

* Corresponding author can be contacted at Wisconsin Institute for Medical Research II, 1111 Highland Avenue Room 5405, Madison, WI USA 53705. Phone: (608)265-9978; Email: wlmurphy@wisc.edu

4.1. Preface

The focus of these studies was to develop DOE-driven screening methods and technologies to enable identification of customized substrates for serum-free hMSC culture. Here, the screening approach examined hMSC behavior in response to multiple *in vitro* culture

parameters (substrate stiffness, substrate adhesivity, media composition) in order to identify unique hydrogel substrate compositions that enable hMSC expansion in both serum-containing and serum-free culture. This screening approach combined with MVA enabled understanding of the independent and combinatorial effects each culture parameter had on hMSC behavior *in vitro* and established the importance for moving towards serum-free hMSC biomanufacturing in order to mitigate the confounding effects of serum.

Additionally, reference an issued patent, data published in Nature Biomedical Engineering, and unpublished data in the appendix to demonstrate the commercialization potential for this approach as well as the broader applicability of screening to identify customized substrates for culture of pluripotent stem cells. Our unpublished data indicated the ability to resolve hESC cytoskeletal organization and phenotypes indicative of mechanosensing, thereby further demonstrating the ability to use this approach beyond how we've applied it here.

4.2. Abstract

We describe the development of a screening approach to identify customized substrates for serum-free human mesenchymal stromal cell (hMSC) culture as well as its utility in combining the design of experiment (DOE) screening approach with multivariate analysis (MVA) to survey the effects of culture parameters (namely substrate stiffness, substrate adhesivity, and media composition) on hMSC behavior *in vitro*. This approach enabled the identification of media- and cell-source agnostic hydrogel substrate compositions that supported functional hMSC expansion in multiple serum-containing and serum-free media as well as the expansion of mouse-derived and iPS-derived MSCs. The identified substrates were compatible with standard thaw, seed, and harvest protocols. Finally, we used MVA on the screening data to reveal the importance of serum

and substrate stiffness on hMSC expansion in order to emphasize the need for development of customized culture systems in order to optimize hMSC biomanufacturing processes.

4.3. Statement of Significance

Our DOE-driven screening method enables the ability to rapidly develop customized cell culture substrates for optimizing cell biomanufacturing processes for expansion, differentiation, secretome generation, among many others. The hydrogel array technologies used in this screening approach are benchtop amenable and can be completed without a liquid handling system, thereby increasing the commercial and application translatability of this approach.

4.4. Introduction

Human mesenchymal stromal cells (hMSCs) are powerful tools for research and clinical applications; however, their behavior in culture is poorly understood, resulting in inability to predict subsequent *in vivo* effects. Reliance on poorly-regulated, ill-defined adhesion substrate and growth media during hMSC culture is one contributor to this knowledge gap.

hMSCs are routinely cultured on tissue culture polystyrene (TCPS) in growth factor-supplemented media (most commonly in the form of fetal bovine serum, FBS). Both TCPS and FBS reliance results in poor control of signals presented to the cells and understanding of how extracellular signals influence hMSC behavior. The reliance on TCPS raises concerns due to its supraphysiologically high stiffness and nonspecific protein absorption. TCPS is ~300 Pa while TCPS modulus is six orders of magnitude higher than bone marrow, five orders of magnitude higher than any soft tissue, and long-term hMSC culture on TCPS has been demonstrated to result in increased cellular stress and decreased mechanosensitivity because of cytoskeletal coarsening and stiffening [1-4].. Additionally, TCPS allows nonspecific absorption of hundreds of proteins, therefore it is difficult to parse out and understand the effects of and mechanisms engaged in cell-microenvironmental signaling [3]. Meanwhile, the reliance on FBS raises concerns for both research and clinical applications: potential for xenogenic contamination, large batch-to-batch variability that can reduce manufactured cell quality and efficacy, poorly-characterized composition and protein concentrations that reduces manufactured cell reproducibility, and supply and price volatility that will result in unpredictable supply and costs [5-9].

In efforts to resolve these issues, there has been significant interest in development of chemically defined, xeno-free (XF), serum-free (SF) culture substrates and media formulations [5, 6, 8-10]. Despite the development and commercialization of several SF media formulations, there

have been hurdles to widespread acceptance. First and foremost, the effects of serum-dependence on cell adhesion and proliferation are poorly understood, therefore attempts to remove serum during the development of SF systems have been plagued with performance issues [5-7]. Secondly, transition out of traditional serum-containing (SC) culture often results in suboptimal hMSC attachment and expansion in SF systems [5, 8, 9]. Prior studies evaluating performance of SF systems revealed the need for concurrent optimization of both the media formulation and substrate in order to achieve hMSC growth comparable to levels achieved in SC culture systems [5, 11-14]. Finally, several commercially-available SF media formulations are proprietary and developed to promote optimal growth only when used with proprietary culture substrates, leading to limitations of their utility in research and clinical studies [5, 8, 9, 11-14].

Here, we employed combinatorial high throughput screening technologies to enable rapid identification of chemically-defined substrate for hMSC culture in XF, SF media. Our screening method allowed examination of several variables that, based on prior literature, are likely to influence hMSC behavior: stiffness, adhesivity, and growth medium [15-34]. From this screen, we identified three chemically-defined hydrogel substrates that supported functional hMSC expansion in multiple SC and SF media formulations. Finally, we used these customized substrates to study the influence of culture parameters on hMSC adhesion, expansion, and differentiation.

4.5. Materials and Methods

4.5.1 Hydrogel array formation and characterization

Two hydrogel array formats were utilized in this set of experiments: slide-based hydrogel arrays and multiwell-based hydrogel arrays (Figure 4.S1A). Both array formats utilized Norbornene-functionalized PEG (PEG-NB) hydrogels formed using thiolene chemistry.

PEG-NB was synthesized and characterized as previously described [22, 35-37]. Briefly, 8-arm PEG-OH (20 kDa molecular weight, tripentaerythritol core, 8-arm with terminal OH, JenKem Technology) was dissolved in anhydrous dichloromethane (DCM, Sigma Aldrich) in one round bottom flask while N,N′-dicyclohexylcarbodiimide (DCC, Sigma Aldrich) and 5-Norbornene-2-carboxylic acid (Sigma Aldrich) were dissolved in a second round bottom flask. The PEG and norbornene solutions were combined and stirred overnight, protected from light, to covalently couple the 5-norbornene-2-carboxylic acid to the PEG-OH. The PEG-NB product was filtered through a medium fritted Buchner funnel (to remove urea salts byproduct) and the PEG filtrate was precipitated in 900 mL cold diethyl ether (Sigma Aldrich) and 100 mL hexane (Sigma Aldrich). The PEG solids were collected on qualitative grade filter paper and air dried at room temperature overnight, protected from light. The PEG-NB product was purified by dialysis (SNAKESKIN dialysis tubing, MWCO 3.5K, Sigma Aldrich) to remove residual norbornene acid. PEG-NB product was dialyzed against 4L of dH2O at 4°C for 72 hours, with water change every 8 hours, filtered through a 0.45 µm nylon filter to remove particulates and impurities, and lyophilized. Norbornene functionalization of >90% was confirmed with 1H nuclear magnetic resonance spectroscopy with free induction decay (FID) spectra obtained using spectroscopy services provided by the National Magnetic Resonance Facility at Madison on a Bruker Instruments Avance III 500i spectrometer at 400 MHz and 27°C. Samples were prepared at 6 mg/mL in deuterated chloroform ($CDCl_3$, Sigma Aldrich) with tetramethylsilane (TMS) internal standard.

Silanized glass coverslips were prepared via liquid-phase silanization as previously described [22]. Briefly, clean glass coverslips were activated using oxygen plasma treatment at 40 standard cubic centimeters per minute (sccm) and 50 W for 5 minutes to increase the number

of activated hydroxyl groups on the surface, immersed in 2.5 v./v.% 3-mercaptopropyl trimethoxysilane (3-MPTS, Sigma Aldrich) in toluene for 2 hours, rinsed with ethanol, dried, cured under nitrogen atmosphere at 100 °C for 1 hour, and immersed in 10 mM 1,4-Dithiothreitol (DTT, Sigma Aldrich) in PBS for 30 minutes at 37°C to increase free thiols available for thiolene reaction with PEG-NB.

Hydrogel precursor solutions were prepared by combining PEG-NB (4-20 wt/wt %), PEG-dithiol crosslinker (0.5-1 mole ratio of thiol-to-norbornene), peptides (1-6 mM), and 0.5 wt/wt% Irgacure 2959 photoinitiator (CIBA/BASF) and diluted to desired concentrations with phosphate buffered saline (PBS, pH 7.4) immediately prior to hydrogel array formation. Linear CRGDS, linear CRDGS, CREDV, CRGDSPG, cyclic (RGDfC), CPHSRN-$(SG)_5$-RGD, CRGD-G_{13}-PHSRN, and CIKVAV were purchased from GenScript USA. Note, per the manufacturer, the "f" notation denotes a D-amino acid. Linear PEG-dithiol (PEG-DT, 3.4 kDa) was purchased from Laysan Bio.

Slide-based hydrogel arrays were formed using a patented differential wettability patterning method (US10195313B2) previously described [22].

Multiwell-based hydrogel arrays were formed using a slight modification to the differential wettability patterned method and a patented array formation method (US9694338B2). In this method, hydrogels were immobilized to silanized glass coverslips to provide ease of handling. Briefly, gold-coated slides were cleaned via sonication in ethanol for 1 minute, dried with air, cleaned with oxygen plasma at 40 sccm and 50 W for 1 minute, and immersed in a 0.1 mM solution of $HS–C_{11}–(O–CH_2–CH_2)_3–OH$ (PEG-terminated alkanethiols, ProChimia Surfaces) in ethanol solution for 2 hours to form a hydrophilic alkanethiol SAM layer. 12 mm round coverslips were silanized using the procedure detailed above. Hydrogel precursor solutions were spotted onto the

hydrophilic gold-coated slides, coverslips were used to sandwich the hydrogel precursor solution, hydrogel precursor solutions were crosslinked by UV-initiated photopolymerization through the silanized coverslips with 365 nm wavelength light for <6 seconds at 90 mW/cm^2, the resulting immobilized hydrogels were was immersed in 70% ethanol for ≥ 72 hours, treated with UV-C in a biosafety cabinet for 3 hours to decontaminate, thoroughly washed 3X with PBS, immersed in cell growth medium at 37 °C for 72 hours with media changes every 12 hours, and stored in growth medium at 37 °C until use.

Hydrogel shear storage modulus and compressive modulus were determined using procedures previously published [22, 29, 35, 38-41].

4.5.2 Cell culture

Bone marrow-derived hMSCs (Lonza) were expanded in 10% fetal bovine serum (FBS, Invitrogen) in minimum essential medium alpha formulation (αMEM, MediaTech) supplemented with 1% penicillin/streptomycin (Invitrogen) on tissue culture polystyrene plates at 37 °C in a 5% CO_2 atmosphere until 70% confluence. hMSC (PDL 8-16) were harvested using trypsin (Invitrogen), resuspended in 10% FBS in αMEM, and seeded on sterilized hydrogel arrays or TCPS (for TCPS control). After 24 hours, unattached cells were removed by gently replacing the culture media. Cells on hydrogel arrays were maintained at 37 °C in a 5% CO_2 atmosphere with culture medium changed every 2 days. hMSCs were also cultured in xeno-free and serum-free media: TheraPEAK XF SF (Lonza) with TCPS control, StemPro XF SF (Gibco) with CellStart-coated TCPS control, and RoosterNourish XF (RoosterBio) with TCPS control. All hMSCs used were cryopreserved in αMEM + 10% FBS, thawed into the respective medias of interest, and allowed to recover from cryopreservation for 72 hours prior to harvest and use for hydrogel

experiments. hMSC were seeded onto TCPS and hydrogel substrates at 1000 cell/cm^2 (to prevent significant cell-cell interactions that could mask the effects of cell-substrate interaction) or 3000 cell/cm^2 (based on the media manufacturers' recommended seeding density for optimal growth). For xeno-free harvest, hMSCs were dissociated from the surface using TrypLE (XF trypsin, Thermo Fisher Scientific) and Versene (1X EDTA, Thermo Fisher Scientific).

hMSCs osteogenic and adipogenic differentiation utilized establish protocols previously reported [42, 43]. Briefly, osteogenic medium (0.1 μM dexamethasone, 10 × 10 mM β glycerol phosphate, 50 nM ascorbic acid 2-phosphate) was prepared in αMEM + 10% FBS with penicillin (100 U/mL) and streptomycin (100 μg/mL). Adipogenic medium (1 μM dexamethasone, 500 μM isomethyl isobutyl xanthine, 10 μg/mL insulin) was prepared in 10% FBS in Dulbecco's modification of Eagle's medium high glucose with penicillin (100 U/mL) and streptomycin (100 μg/mL). hMSCs were expanded on TCPS or hydrogels for 8 days, dissociated, and seeded at 5000 cells/cm^2 on 48-well plates (Corning ™ BioCoat™ Collagen I, 48-well multiwell plates, Thermo Fischer Scientific) in αMEM + 10% FBS, allowed to grow until confluent, before media change into osteogenic or adipogenic media for differentiation or αMEM + 2% FBS for no differentiation control. Media was changed every 3 days for 21 days of differentiation.

Immunomodulatory function was assessed using hMSCs expanded on hydrogels or TCPS for 8 days and using instructions based on Miltenyi Biotec's human MSC Suppression Inspector with a ratio of 1:100 hMSCs to activated T cells for 5 days. A CyQUANT Cell Proliferation Assay Kit (Thermo Fisher Scientific) was used to quantify DNA as an indicator of cell proliferation.

Induced pluripotent stem cell- (iPS) derived MSC were provided by Dr. Igor Slukvin's lab at the University of Wisconsin-Madison (Madison, WI) and cultured in complete Vasculife medium (Lifeline Cell Technology, Frederick, MD) supplemented with 10% FBS. Mouse bone

marrow-derived MSCs were collected from bone marrow aspirate using procedures previously published and cultured in αMEM + 10% FBS [44]. Human umbilical vein endothelial cells (HUVECs, Lonza) were cultured in growth medium consisting of medium 199 (M199, Mediatech Inc) supplemented with EGM-2 Bulletkit (Lonza). H1 human embryonic stem cells (hESCs) were purchased from WiCell, expanded on Matrigel-coated TCPS, and cultured in Essential 8 (E8, Stem Cell Technologies) medium.

4.5.3 Data Acquisition and analysis

hMSC viability after harvest was determined by Trypan Blue exclusion assessment. Hydrogel arrays and samples were placed in a heated environmental chamber and imaged on the Nikon Eclipse Ti microscope (Nikon) at each desired time point. Cell number was manually determined using NIS Elements software (Nikon) every 24 hours after seeding, cell area of single cells were determined using NIS Elements' threshold and automated measurement features at 72 hours after seeding, and cell expansion was quantified as previously reported by normalizing cell number at 72 hours relative to 24 hours, where fold change in cell number greater than 1 was used to indicate expansion and proliferation [19].

To assess osteogenic differentiation, cells were fixed with 10% Formalin, stained with Alizarin Red (40 mM, pH 4.1–4.3), washed three times with water, and assessed for mineral-stained red cells as positive indicators of osteogenic differentiation. To assess adipogenic differentiation, cells were fixed with 10% Formalin, incubated in Oil Red O working solution (3 parts of Oil Red O at 3 mg/mL in 99% isopropanol to 2 parts distilled water and filtered with 0.2 μm syringe filter to remove undissolved particulates) for 20 minutes, washed with water until clear, and assessed for lipid vacuoles stained red as positive indicators of adipogenic differentiation.

Additionally, Oil Red O-stained cells were imaged using TxRed fluorescence imaging on the TiEclipse microscope, and lipid droplet size and density was determined using automated thresholding on NIS Elements analysis software.

Design of experiment (DOE) and multivariate analysis (MVA) was performed using JMP statistical analysis software. The multivariate value of each culture parameter was calculated a ratio relative to the total summed effect value for all parameters ($\sum \text{All effects} = 1$). Statistical analysis for significance was performed using the GraphPad Prism software via Student's t-test (2-tailed, α=0.05) or ANOVA with post-hoc Tukey (HSD or Kramer depending on sample size variability) tests as indicated. Error bars denote standard deviation.

4.6. Results

4.6.1 Screening method and platform technologies

We have developed a high throughput screening method utilizing hydrogel array platform technologies with the goal of identifying substrates that support functional hMSC expansion in SF media. Our high throughput screening method employs a design of experiment (DOE)-driven, multistep process, two different hydrogel array platforms, and is amenable for high-content, label-free characterization approaches (Figure 4.1A and Figure 4.S1A,B).

Both the slide-based and multiwell-based array platforms employed in this screening method comprised PEG-DT crosslinked PEG-NB hydrogels with networks formed via thiolene photopolymerization, a step-growth reaction mechanism with rapid gelation time that yields homogeneous polymer networks (Figure 4.1B and Figure 4.S1C) [22, 23]. The composition of each hydrogel spot in the arrays were controlled such that substrate stiffness and adhesivity could

be modified independently (Figure 4.1B,C and Figure 4.S2A,B). Here, hydrogel stiffness could be regulated independent of adhesivity, regardless of total peptide concentration or identity (Figure 4.1C). We controlled identity and concentration of cysteine-terminated moieties incorporated into the network to regulate both stiffness and adhesivity. We controlled the stiffness of each hydrogel spot in the array by changing the concentration of PEG-NB polymer and the molar ratio of crosslinker-to-norbornene in the hydrogel precursor (prepolymer) solution (Figure 4.1C and Figure S1B). We controlled substrate adhesivity through altering peptide identity and concentration in the hydrogel precursor solution. Several fibronectin-, vitronectin-, and laminin-derived integrin-binding peptides were immobilized into the hydrogel network to promote cell adhesion (Figure 4.S2A,B).

Additionally, our high throughput screening arrays and method allowed us to examine the independent and combinatorial effects of substrate stiffness, substrate adhesivity, and media formulation on hMSC behavior to identify combinations of substrates and media that supported hMSC expansion (Figure 4.1A). Each spot in the array could be customized in terms of mechanical stiffness, cell adhesion peptide identity and concentration, GF sequestering molecule identity and concentration, cell type and density, and media formulation.

For the screening workflow, we first use preliminary data from literature and prior experiments to design primary screen(s) on slide-based hydrogel arrays (Figure 4.1A and Figure 4.S3). In this initial screening set, we examined variables that are likely to influence hMSC phenotype: substrate stiffness and adhesivity. First, we performed short-term hMSC culture to identify cytocompatible “hit” hydrogel compositions that support stable hMSC adhesion and spreading. Second, we scale up the hits into multiwell-based arrays for secondary screens to

identify “master hit” hydrogel compositions that support functional hMSC expansion. These steps were iterative and were repeated as needed.

Our screening array platforms and workflow were developed to require no liquid handling systems, be amenable for formation on the benchtop, and produced flat culture surfaces that were compatible with standard imaging techniques.

4.6.2 Customized substrates for functional SF hMSC expansion

We used the aforementioned high throughput screening method to identify customized hydrogel substrates for functional hMSC expansion in SC and SF media.

First, we used slide-based hydrogel arrays to identify integrin-binding adhesion peptides that could support hMSC adhesion in SC and SF media (Figure 4.S2C, Figure 4.S3, and Figure 4.S4). For experiments on slide-based arrays, we seeded hMSCs at 1000 cell/cm^2, a density much lower than recommended for XF SF culture, to prevent significant cell-cell interactions that could mask the effects of cell-substrate interaction. We incorporated 2 mM of several integrin-binding peptides (containing laminin-derived IKVAV, fibronectin-derived RGD, and vitronectin-derived PHSRN sequences) into 8 kPa stiffness hydrogels and examined the ability for each substrate to support stable adhesion, cell spreading, and expansion (a balance between proliferation and cell survival) (Figure 4.S4). Substrates presenting 2 mM cyclic RGDf promoted the highest combination of initial adhesion, cell spreading, and expansion in αMEM + 10% FBS culture; however, regardless of peptide concentration, cyclic RGDf alone was unable to support hMSC adhesion in TheraPEAK XF SF medium at levels comparable to those achieved on the TCPS control (Figure 4.S5A).

Next, we performed a 2nd adhesion-based screen on slide-based hydrogel arrays to examine the influence of increasing cyclic RGDf concentration (8 kPa hydrogels presenting either 2 or 4 mM cyclic RGDf) and the additional of 0.5 mM IKVAV on hMSC adhesion in TheraPEAK XF SF medium (Figure 4.S5). Regardless of cyclic RGDf concentration and media formulation, adding 0.5 mM IKVAV increased hMSC adhesion to levels equal to or greater than those achieved on TCPS controls. In αMEM + 10% FBS culture, increasing cyclic RGD concentration increased hMSC adhesion and the addition of IKVAV provided additive effects to further increase adhesion to levels greater than what was achieved on TCPS. In TheraPEAK XF SF culture, increasing cyclic RGDf concentration alone also increased adhesion, but only the combination of cyclic RGDf and IKVAV promoted adhesion levels comparable to what was achieved on TCPS + CellStart coating.

After we identified adhesion-promoting peptides suitable for supporting hMSC adhesion in both SC and SF media, we performed a 3rd screen on slide-based hydrogel arrays to identify combinations of substrate stiffness and adhesivity that supported hMSC expansion (Figure 4.2 and Figure 4.S6A). We varied hydrogel stiffness (1, 8, or 18 kPa), cyclic RGDf concentration (0 – 6 mM), and IKVAV concentration (0 – 2.5 mM) and examined cell adhesion, spreading, and expansion in SC (αMEM + 2% or 10% FBS) and SF (TheraPEAK XF SF) media. The stiffness range was chosen to reflect stiffness values previously employed for hMSC culture on hydrogel substrates of various other chemistries in SC media [1, 45-50]. Hydrogel compositions that concurrently supported adhesion, spreading, and expansion in both SC and SF media were deemed "hit" compositions.

Of the 48 different hydrogel compositions examined (46 hydrogel substrates, TCPS, and TCPS + CellStart coating), we identified 23 hits (22 hydrogel substrates and TCPS + CellStart coating) that promoted cell adhesion, spreading at levels equal or greater than what was seen on

TCPS controls, and expansion (with > 1 fold change in cell number over 2 days of culture) in TheraPEAK XF SF medium (Figure 4.2 and Figure 4.S6). Note hMSC expansion in TheraPEAK XF SF medium was significantly lower than those seen in αMEM + 2% or 10% FBS culture, regardless of culture substrate. Additionally, regardless of media formulation, culture on TCPS produced higher expansion than those on hydrogel substrates.

Next, we performed a 4th screen on slide-based hydrogel arrays to determine whether the 24 TheraPEAK XF SF hit hydrogel compositions could support hMSC adhesion, spreading, and expansion in other XF and SF media (Figure 4.3). Of the 22 TheraPEAK XF SF hydrogel hit compositions, 3 were "master hits" that supported hMSC culture in αMEM + 2% FBS, RoosterNourish XF, and StemPro XF SF media (Figure 4.4A). Notably, these 3 media-agnostic master hit hydrogel compositions not only supported bone marrow-derived hMSC (BM-hMSC) adhesion, spreading, and expansion, but also supported iPS-derived hMSC and bone marrow-derived mouse MSC adhesion, spreading, and expansion (Figure 4.S6B). Additionally, the screening method was also able to identify customized hydrogel substrates for promoting culture of other cells in XF condition: human embryonic stem cells (hESCs) in Essential 8 (E8) and human umbilical vein endothelial cells (HUVECs) in Endothelial Growth Medium 2 (EGM2) media formulations (Figure 4.S7). Interestingly, the identified master hits or media and cell-source agnostic hMSC culture were also able to support both hESC and HUVEC adhesion and expansion.

Finally, we scaled up the master hits into multiwell-based hydrogel arrays, seeded hMSCs at 3000 cell/cm^2 (per the manufacturers' recommended seeding density for optimal growth), expanded cells for 8 days, and harvested the cells for induced adipogenic differentiation, induced osteogenic differentiation, and activated T-cell co-culture to examine whether the cells retained their function after expansion. hMSCs expanded on master hit hydrogels in SC and SF media

retained their proliferative capacity with expansion levels comparable to those seen on TCPS controls (Figure 4.3B) Notably, hMSCs cultured on "non-hit" hydrogels (18 kPa with varying adhesivity) did expand, but at levels significantly lower than those seen on TCPS controls (Figure 4.S5C).

hMSCs also retained their multipotency and immunosuppressive functions after 8 days of expansion on hit hydrogels. Expanded hMSCs cultured on collagen I-coated TCPS in osteogenic induction medium for 21 days gave rise to mineralized cells (Alizarin Red S+) and those cultured in adipogenic induction medium gave rise to cells with large lipid vacuoles (Oil Red O+) (Figure 4.4A, Figure 4.S8, Figure 4.S9A,B and Figure 4.S10). Expanded hMSCs co-cultured with activated T-cells were able to suppress T-cell proliferation at levels comparable to those expanded on TCPS in αMEM + 10% FBS (Figure 4.S9C).

Finally, to examine master hit hydrogels' compatibility with standard cell culture protocols, we examined the effect of seeding and harvest techniques on cell viability and expansion (Figure 4.S11). hMSCs passaged onto the hydrogels following TCPS expansion (as utilized in the aforementioned experiments) or directly from thaw both maintained adhesion and expansion capabilities similar to cells cultured on TCPS controls (Figure 4.S11A,B). hMSCs dissociated from the surface using enzyme and enzyme-free reagents (trypsin, TrypLE, and Versene) maintained high viability (> 80%, Figure 4.S11C) and multipotency (Figure 4.S8). Additionally, hMSCs could be dissociated off the hydrogels and reseeded onto a fresh hydrogel substrate similar to the repassaging procedure on TCPS (Figure 4.S11D).

4.6.3 The influence of culture parameters on hMSC adhesion, expansion, and differentiation

Next, we performed multivariate analysis (MVA) on the screening data to examine the independent and combinatorial influences of culture parameters (culture media composition, substrate stiffness, and substrate adhesivity via Cyclic RGDf and IKVAV) on hMSC adhesion, expansion, and differentiation (Figure 4.4.B). Independently, media formulation, Cyclic RGDf concentration, and substrate stiffness all were positively correlated with hMSC adhesion and expansion. For combinatorial effects, stiffness and Cyclic RGDf (stiffness x Cyclic RGDf) had the single largest impact on hMSC expansion and their synergistic effect was able to increase expansion 269 % greater than the effect of increasing Cyclic RGDf concentration and 367 % greater than the effect of increasing stiffness alone. Interestingly, the factoring in the effects of IKVAV resulted in the combinatorial effects of stiffness x Cyclic RGDf x IKVAV causing a decrease in both hMSC adhesion and expansion. These results were confirmed via head map of hMSC adhesion and expansion (Figure 4.S11).

Next, we examined the influence of substrate stiffness on adipogenic differentiation of hMSCs following expansion (Figure 4.4A and Figure 4.S10). We use this as a testbed to study substrate-dependent hMSC differentiation in both SC and SF media and to confirm that we are able to generate functional hMSC post culture on hydrogel substrate hits. We use adipogenic differentiation because of the ability to with Oil Red O+ and identify with TxRed fluorescence imaging for a high content data acquisition and analysis method amenable to high throughput approaches [51, 52]. hMSCs were expanded on TCPS, 1 kPa, or 8 kPa master hit hydrogels for 8 days after which the cells were harvested for induced adipogenic differentiation. While the combinatorial effects of stiffness x media formulation were not significant for both adhesion and expansion, there were notable effects on hMSC adipogenic differentiation. Regardless of the XF

SF media formulation used for expansion, hMSCs cultured on master hit hydrogel substrates of decreasing stiffness (8 vs. 1 kPa) possessed increasing adipogenic differentiation potential, as indicated by increasing Oil Red O+ lipid vacuole density, in TheraPEAK XF SF and StemPro XF SF. There was significant difference in lipid vacuole density following induced adipogenic differentiation of hMSC expanded on soft vs stiff substrates in TheraPEAK XF SF media: 364% increase in lipid vacuole density between TCPS controls and 8 kPa hydrogels and 591% increase between TCPS control and 1 kPa hydrogels. These results were consistent with differentiation of hMSCs expanded in StemPro XF SF (+241% between TCPS controls and 8 kPa hydrogels, +285% between TCPS controls and 1 kPa hydrogels). Note, there was no statistically significant difference in hMSC adipogenic potential between hMSCs expanded in TheraPEAK XF SF and StemPro XF SF on TCPS controls (Figure 4.S9B). This substrate stiffness-dependence was not observed when using hMSCs expanded in SC media (αMEM + 10% FBS) for adipogenic differentiation.

4.7. Discussion

Here, we've demonstrated the use of an enhanced screening approach to identify customized substrates for serum-free expansion of functional hMSCs. Of 46 different hydrogel substrate formulations examined, we identified 3 formulations that supported media agnostic, cell-source agnostic, functional MSC expansion. We also demonstrated the ability to integrate the customized substrates into routine culture workflow for thaw, seeding, and harvest.

Consistent with previous studies, our screening results demonstrated the need to optimize the substrate and media combination in order to support hMSC adhesion, survival, and expansion. Miwa *et al.* and Hartman *et al.* demonstrated that the Mesencult-XF system supported attachment when cultured using the manufacturer's proprietary attachment substrate but did not support

attachment when was used in combination with fibronectin-coated TCPS [13, 14]. These two studies suggest that the performance of the medium could be improved by optimizing the culture substrate [5].

Of the 48 different substrate formulations in our screen, 45 and 36 substrates supported hMSC expansion in serum-containing media (10% and 2% FBS-containing media, respectively), but only 23 formulations ("hits") supported hMSC expansion in TheraPEAK XF SF media (Figure 3). Interestingly, we demonstrated the ability to use the screening approach to identify 3 of the 23 media-agnostic hit formulations ("master hits") that supported hMSC expansion in 4 different SC and SF media (Figure 4). Additionally, the master hits also supported cell type-agnostic hMSC culture (iPS-derived and primary, mouse-derived MSC) as well as hESC and HUVEC adhesion and expansion.

Using MVA, we were able to assess the effects of multiple culture parameters on hMSC expansion. Notably, we demonstrated the ability to use combinatorial control of substrate parameters (e.g. concurrent control of substrate adhesivity and media formulation) to yield synergistic increase in hMSC expansion to levels higher than what could be achieved with either parameter alone (Figure 4.4B). This result confirmed the observations reported by Miwa *et al.* and Hartman *et al.* [13, 14].

While we demonstrate the ability to use the screening approach to identify substrates that promoted hMSC adhesion, expansion, and multipotency maintenance, we also observed lowered adhesion and expansion and altered cell morphology in SF, XF media that are consistent with what has been reported in the literature. Previous studies also reported reduced adhesion and expansion in SF, XF media as well as on chemically-defined culture substrates [5-10]. For example, Jung et al. and Chase et al. demonstrated lower initial adhesion and expansion on in XF SF media during

culture on TCPS that could be improved with the use of proprietary culture substrates developed specifically for each media formulation. While culture on the proprietary substrates did improve hMSC adhesion and expansion rates, cell morphology was drastically different than those observed on TCPS or in SC media culture [5, 8-10]. For some media formulations (such as StemPro XF SF), hMSCs were smaller and cells tended to grow in clumps as opposed to the individual, well-spread morphology typical of culture on TCPS in SC media [5, 8-10]. Our results demonstrated some media formulations resulted in smaller, less-spread cells (StemPro XF SF) while other formulations (TheraPEAK XF SF) yielded polygonal, more well-spread cells, even on the same substrates (Figure 4.3A).

In this study, we also demonstrated hMSC expansion and confirmed function via directed differentiation to confirm multipotency maintenance and co-culture with T-cells to confirm immunomodulatory activity (Figure 4.4A and Figures 4.S8-10). Our results and those from literature already suggest that short-term hMSC expansion in different media and substrates produce cell populations with different behavior. We did not examine the effects of morphological differences on long-term cell behavior *in vitro* and *in vivo*; however, based on mechanosensing studies that demonstrated direct correlations between morphology and cell behavior, we predict long-term culture in different media and substrate combinations will lead to differences in hMSC function [1, 2]. For example, our directed differentiation experiment demonstrated hMSCs expanded in TheraPEAK XF SF and StemPro XF SF resulted in higher adipogenic differentiation efficiency than cells expanded in αMEM + 10% FBS media (Figure 4.4A and Figure 4.S10). Interestingly, we were able to observe a priming effect for higher adipogenic differentiation potential from the substrate stiffness in hMSCs expanded in XF SF media but not in αMEM + 10% FBS. Others have also demonstrated different adipogenic and osteogenic differentiation

efficiencies for hMSCs expanded with varying substrates and media, but this is the first demonstration of serum-dependence in the ability to resolve stiffness-dependent hMSC lineage commitment after short-term culture [53].

While the effects of serum dependence are not entirely known, there are previously published reports of serum-dependence on hMSC adhesion and proliferation that's resulted in decreased adhesion and expansion when hMSCs are transitioned from SC to SF culture [5-7]. Additional studies will be needed to examine the long-term effects of varying media and substrates on hMSC behavior and determine the relationship between hMSC phenotype and function.

In conclusion, we used an enhanced throughput screening approach to identify customized hydrogel substrates that support functional SC and SF expansion of MSCs from several sources (human bone marrow-, iPS-, and mouse-derived MSCs). While the formulations themselves are promising for allowing research and clinical studies to compare the effects of biomanufacturing using different media and hMSC cell source, the screening approach can be more broadly applied to develop customized materials for several different cell types (e.g pluripotent stem cells and terminally differentiated cells) and applications (e.g. cell expansion in biomanufacturing, organotypic model development). Additionally, while we screened for "hits" using expansion as a criterion, this screening approach can also be used to identify materials for optimized hMSC biomanufacturing to produce cell populations specifically for adipogenic differentiation, immunomodulatory function, GF secretion, and many other functions.

4.8. Acknowledgements

The authors acknowledge the following funding sources: the National Institutes of Health (grant no. R01HL093282), the National Science Foundation (grant no. 1306482 and EEC-

1648035), the National Science Foundation Graduate Research Fellowships Program (grant no. DGE-0718123), the University of Wisconsin-Madison Graduate Engineering Research Scholars, and the Gates Millennium Scholars Program. The authors also acknowledge support from staff and the use of equipment at the Materials Science Center (National Science Foundation grant no. 1121288) and services from the National Magnetic Resonance Facility at the University of Wisconsin-Madison.

4.9. Figures

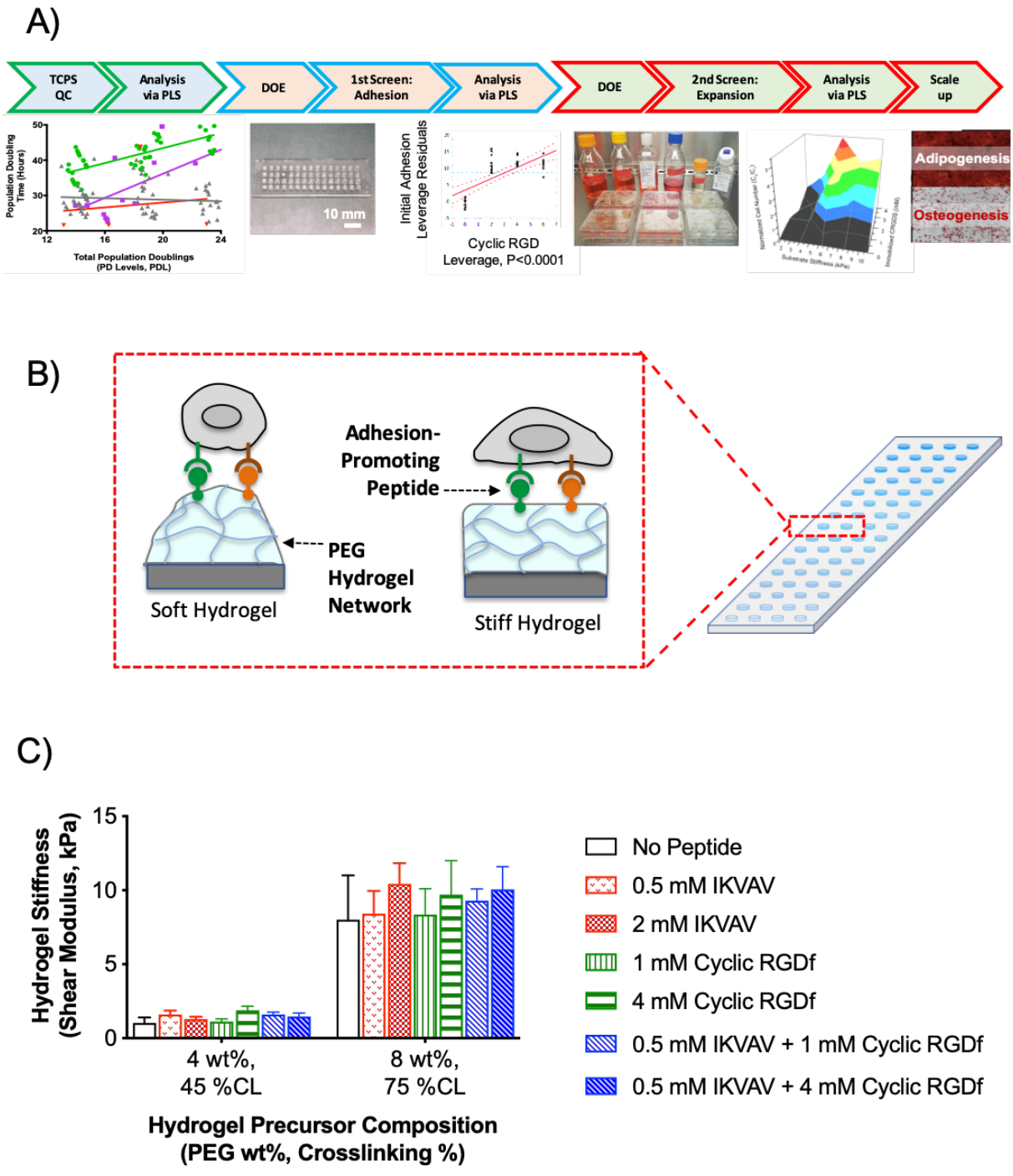

Figure 4.1. Hydrogel array screening. A) Image of workflow for enhanced throughput composition screening on hydrogel arrays formed on glass slide and scale up on bulk hydrogels

formed in 6-well plate for hMSC expansion and long-term culture. B,C) Hydrogel stiffness and adhesivity interpedently tailored by controlling network density, crosslinking, and the identity and concentration of immobilized peptides.

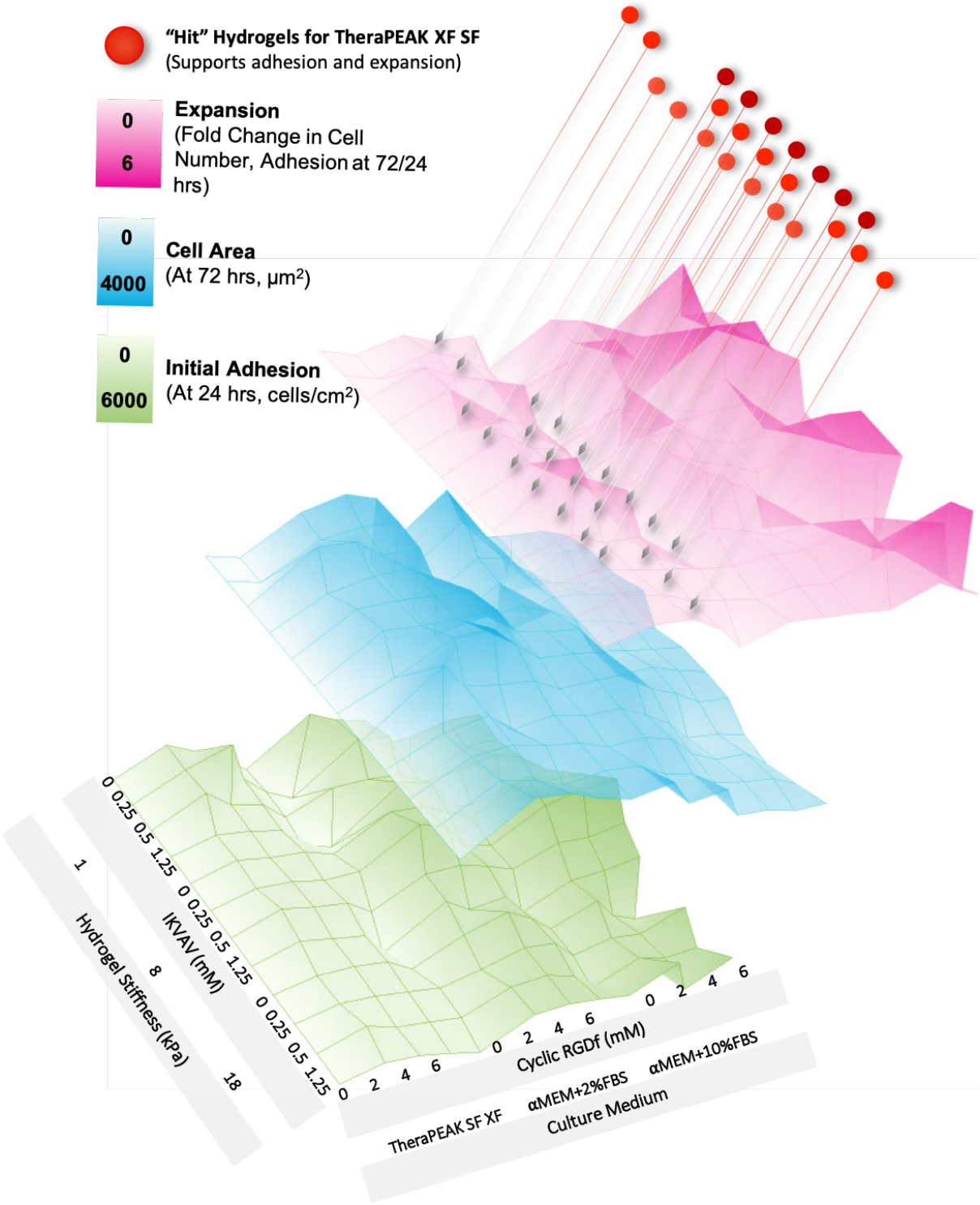

Figure 4.2. Identifying hydrogel compositions for promoting hMSC attachment, expansion, and spreading in TheraPEAK chemically-defined, serum-free, xeno-free medium. A) hMSC

attachment at day 1, expansion over 2 days (C3/C1 = cell number at day 3 normalized to count at day 1), and spreading at day 3.

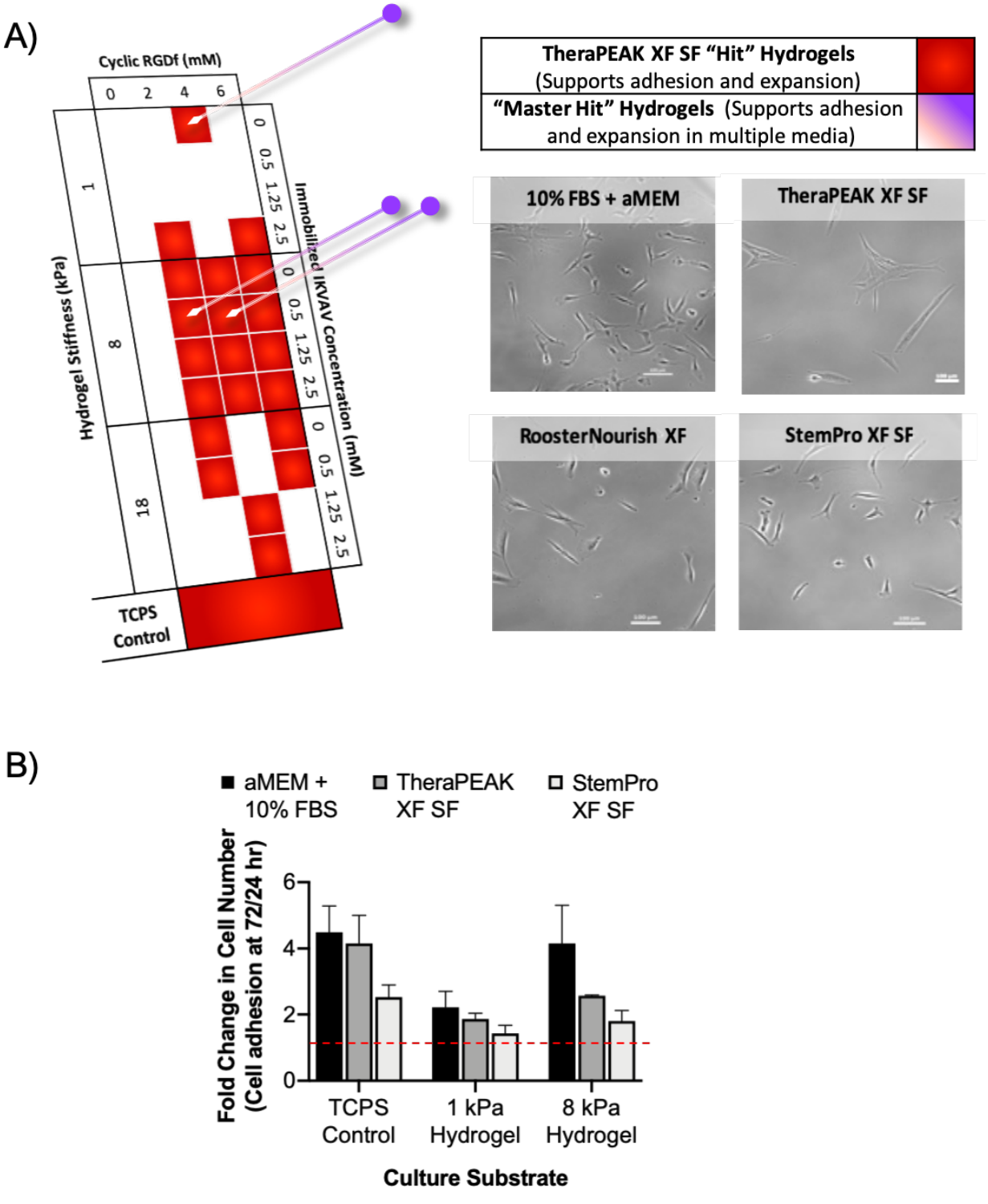

Figure 4.3. Customized "master hit" hydrogel substrates support A) media-agnostic a hMSC adhesion and B) expansion.

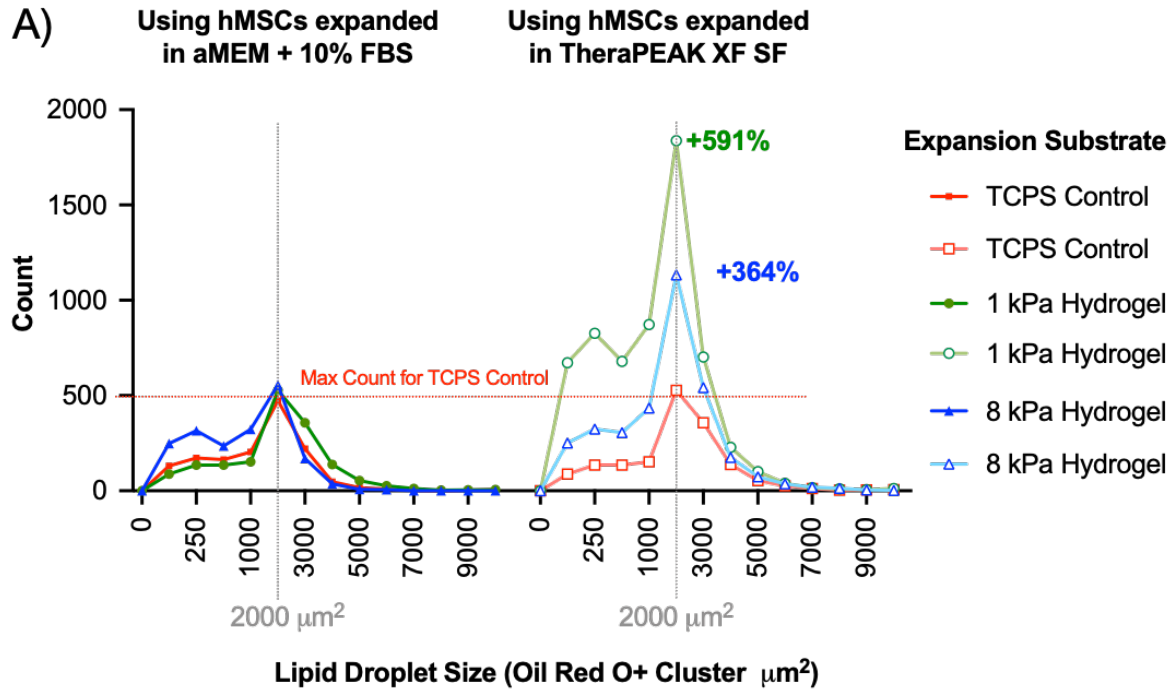

B) Culture Parameters	Effect Magnitude	
	Adhesion (at 24 hrs)	Expansion (at 72/24 hrs)
Stiffness x Cyclic RGDf x IKVAV	-0.036	-0.239
Stiffness x Cyclic RGDf x IKVAV x Media Formulation	-0.0828	-0.0549
Cyclic RGDf x IKVAV x Media Formulation	-0.0598	-0.0397
Cyclic RGDf x IKVAV	-0.0205	-0.0136
IKVAV	-0.0057	-0.0038
IKVAV x Media Formulation	0.0012	0.0008
Stiffness x Cyclic RGDf x Media Formulation	0.0124	0.0082
Stiffness x Media Formulation	0.035	0.0232
Stiffness x IKVAV x Media Formulation	0.0531	0.0352
Stiffness x IKVAV	0.0673	0.0447
Stiffness	0.1328	0.0881
Cyclic RGDf x Media Formulation	0.1476	0.098
Cyclic RGDf	0.1803	0.1197
Serum in Media Formulation	0.4561	0.3027
Stiffness x Cyclic RGDf	0.0486	0.323

Figure 4.4. Culture parameters and their effects on hMSC adhesion, expansion, and differentiation. A) Directed adipogenic differentiation potential of hMSCs following 8-day

expansion on hydrogel substrates in TheraPEAK XF SF or in αMEM + 10% FBS culture media. B) MVA of the independent and combinatorial effects of culture parameters (e.g. media formulation, substrate stiffness, and substrate adhesivity) on hMSC adhesion and expansion.

4.10 Supporting Information

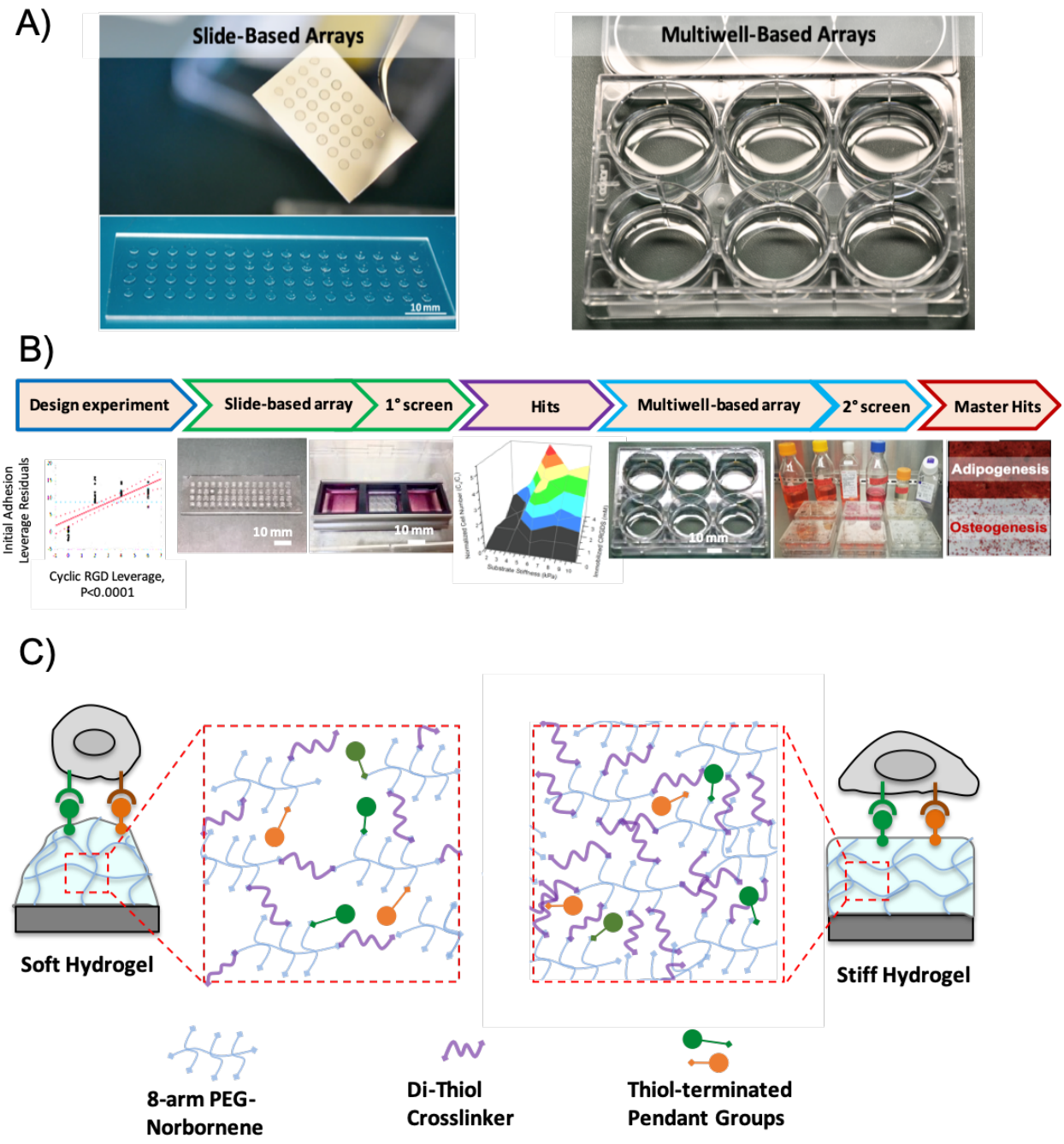

Figure 4.S1. Screening workflow and platforms. A) Slide- and multiwell-based hydrogel arrays for screening. B) Image of workflow for enhanced throughput composition screening on hydrogel arrays formed on glass slide and scale up on bulk hydrogels formed in 6-well plate for

hMSC expansion and long-term culture. C) Hydrogel networks formed using thiolene chemistry with an 8-arm PEG-norbornene polymer backbone, PEG-dithiol crosslinker, and thiol-terminated peptide pendant groups to promote adhesion. Stiffness is modulated using control of PEG-norbornene and PEG-dithiol crosslinker density in the unpolymerized hydrogel precursor solution.

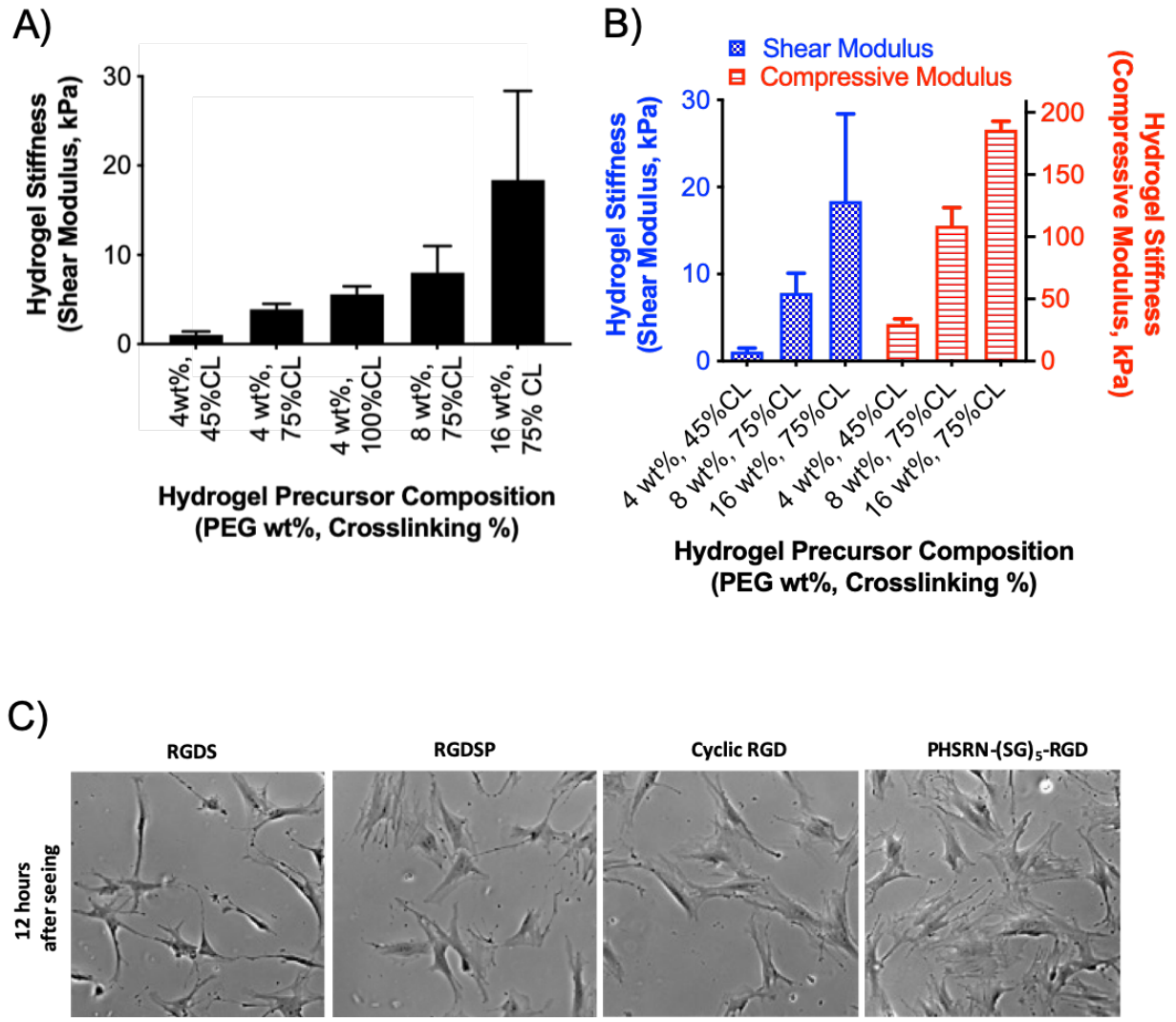

Figure 4.S2. Controllable hydrogel substrate stiffness and adhesivity. A,B) Hydrogel stiffness is tunable by changing the polymer concentration (wt/wt %) and crosslinking density (total percentage of norbornene arms crosslinked). C) Adhesivity is controlled by changing the identity and concentration of integrin-binding peptides.

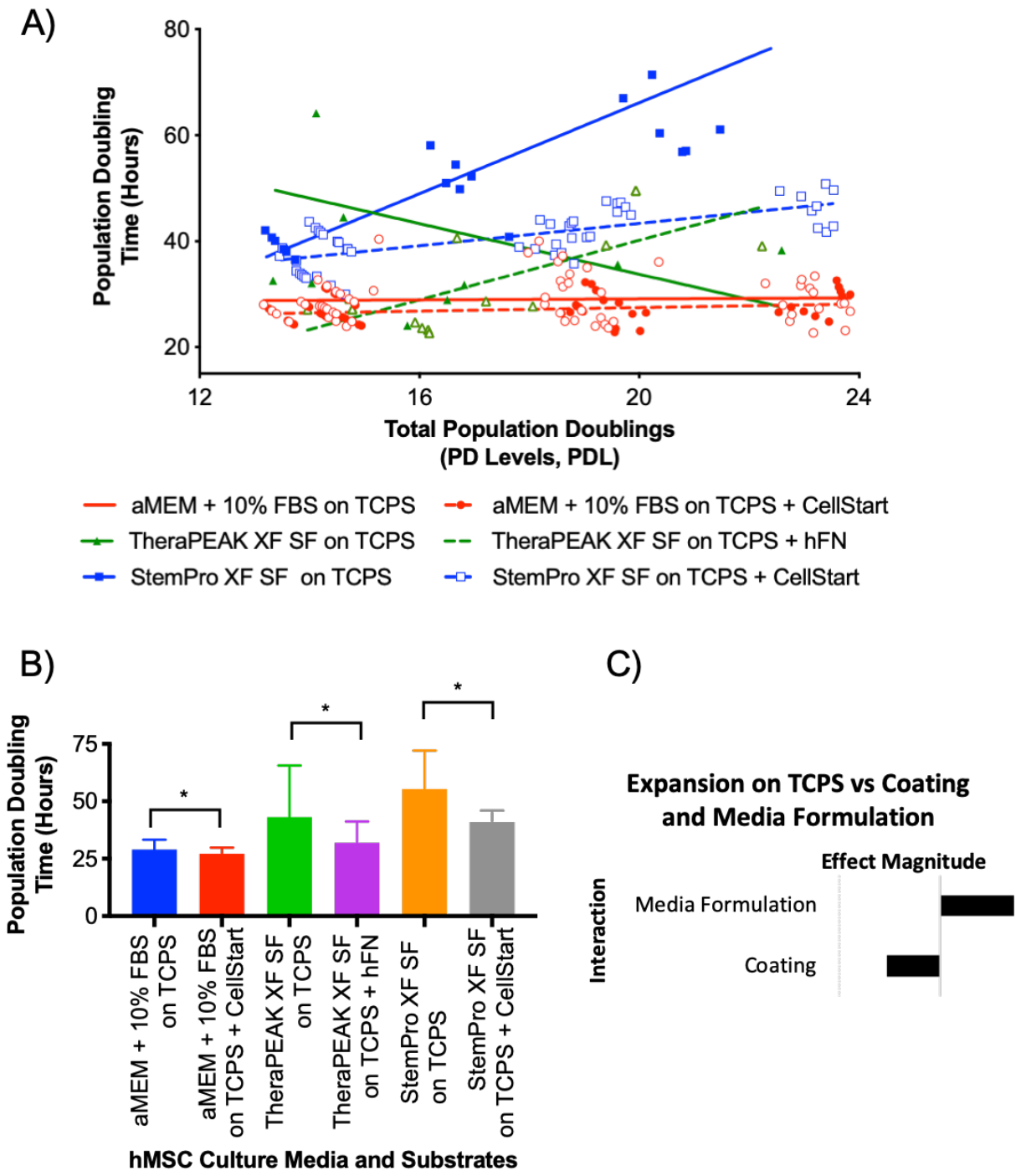

Figure 4.S3. hMSC growth and maintenance in different xeno-free (XF) and serum-free (XF) media and protein-coated tissue-culture polystyrene (TCPS) substrates. A,B) Media and substrate properties independently and combinatorially affect age-dependent hMSC reduction in

proliferative capacity. C) Multivariate analysis of previous quality control data reveals the importance of both media formulation and substrate adhesivity on hMSC adhesion.

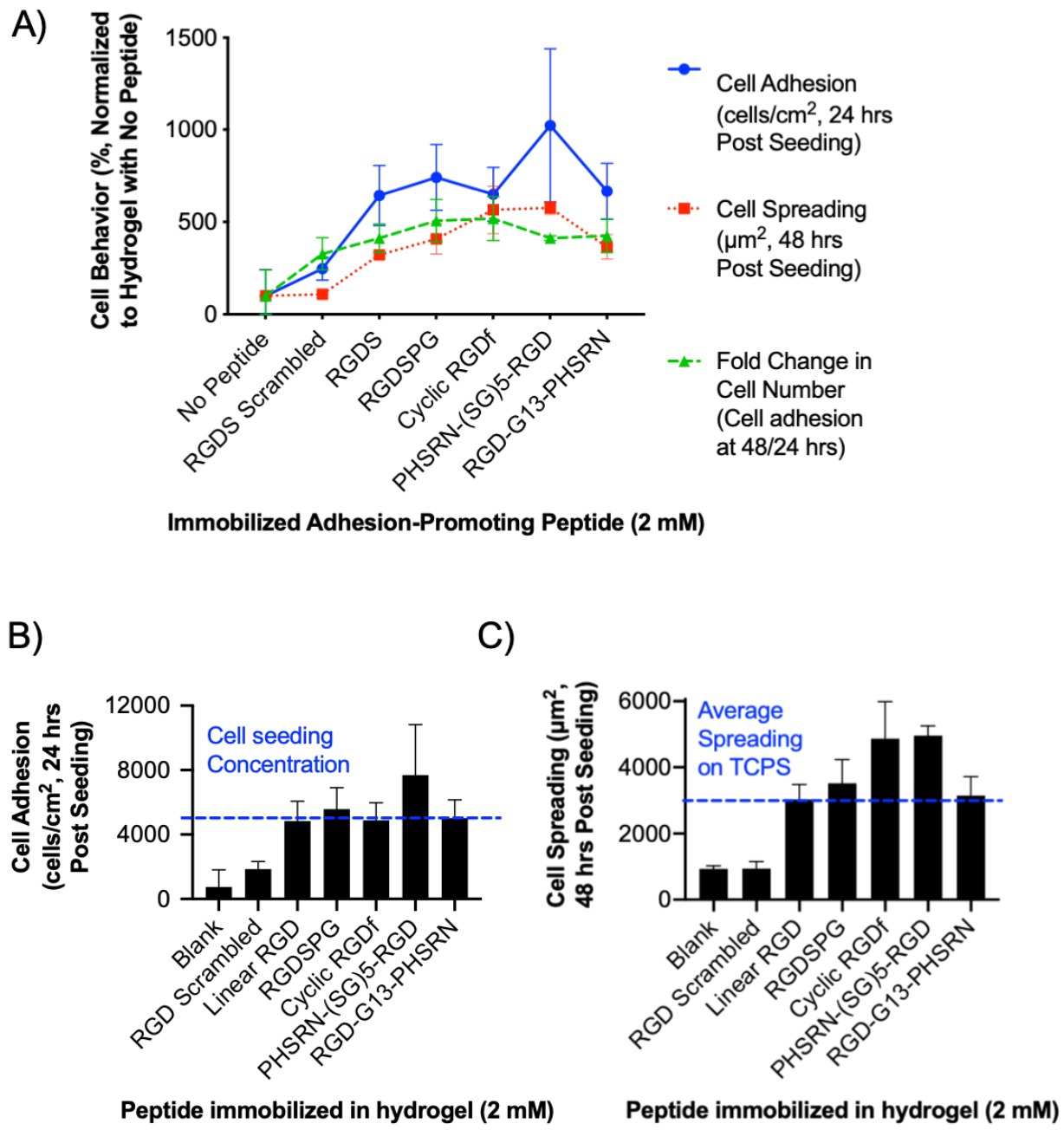

Figure 4.S4. First screen of hydrogels containing various RGD-containing adhesion-promoting peptides and their effects on hMSC A,B) adhesion, A,C) spreading, and A) expansion.

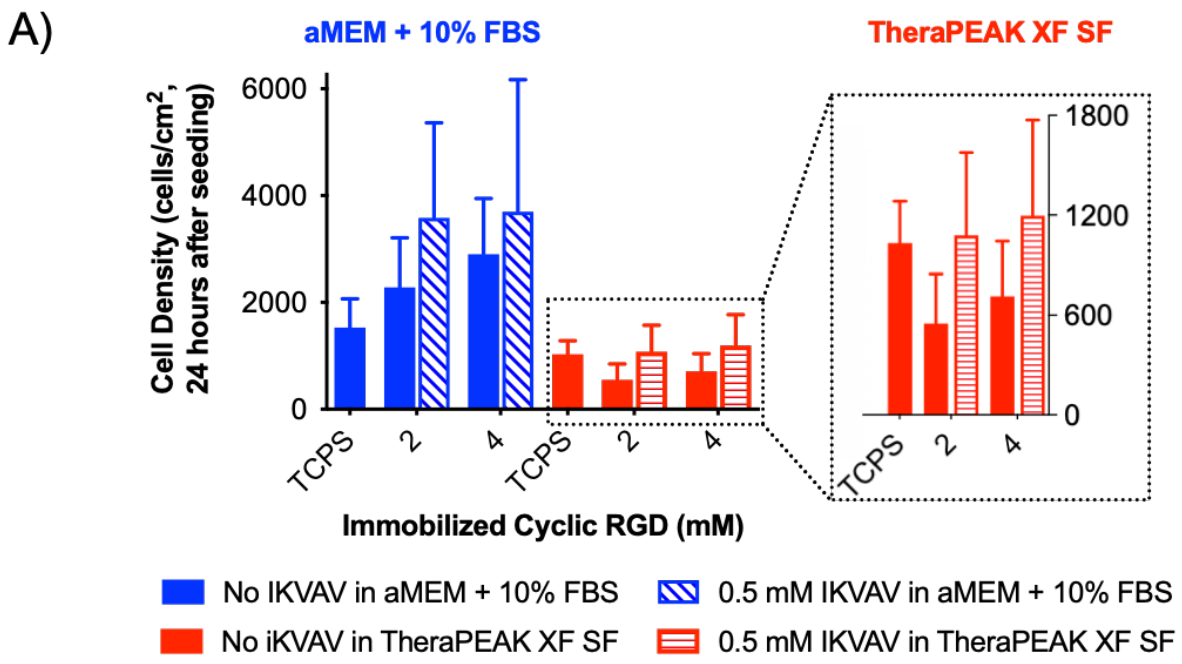

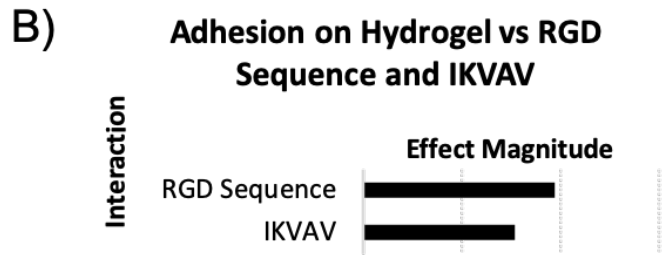

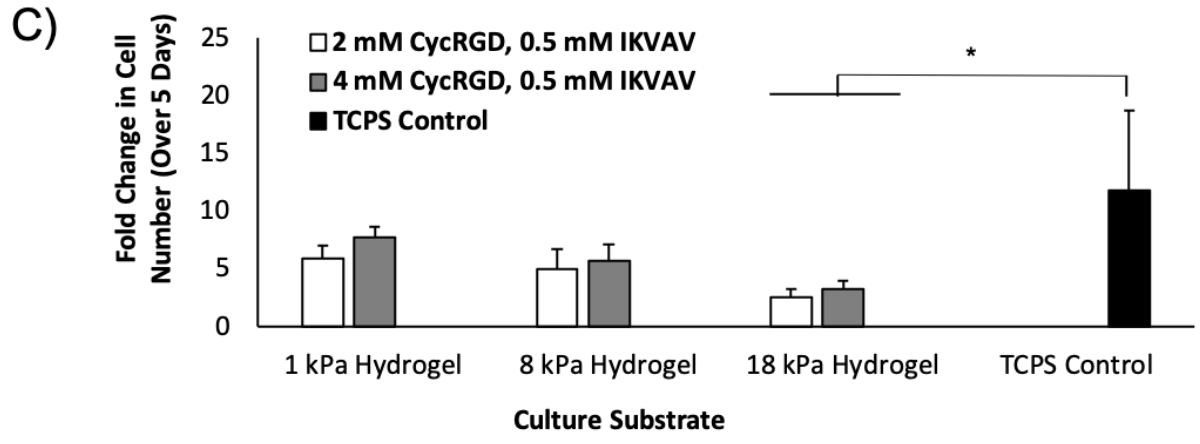

Figure 4.S5. Second screen of the effects of hydrogels with immobilized A) Cyclic RGDf and IKVAV on hMSC adhesion in SC and SF media. B) MVA of RGD and IKVAV and their effects

on hMSC adhesion. A,C) The combinatorial effects of adding IKVAV to Cyclic RGDf-containing hydrogels on stable hMSC adhesion and long-term expansion in SF culture.

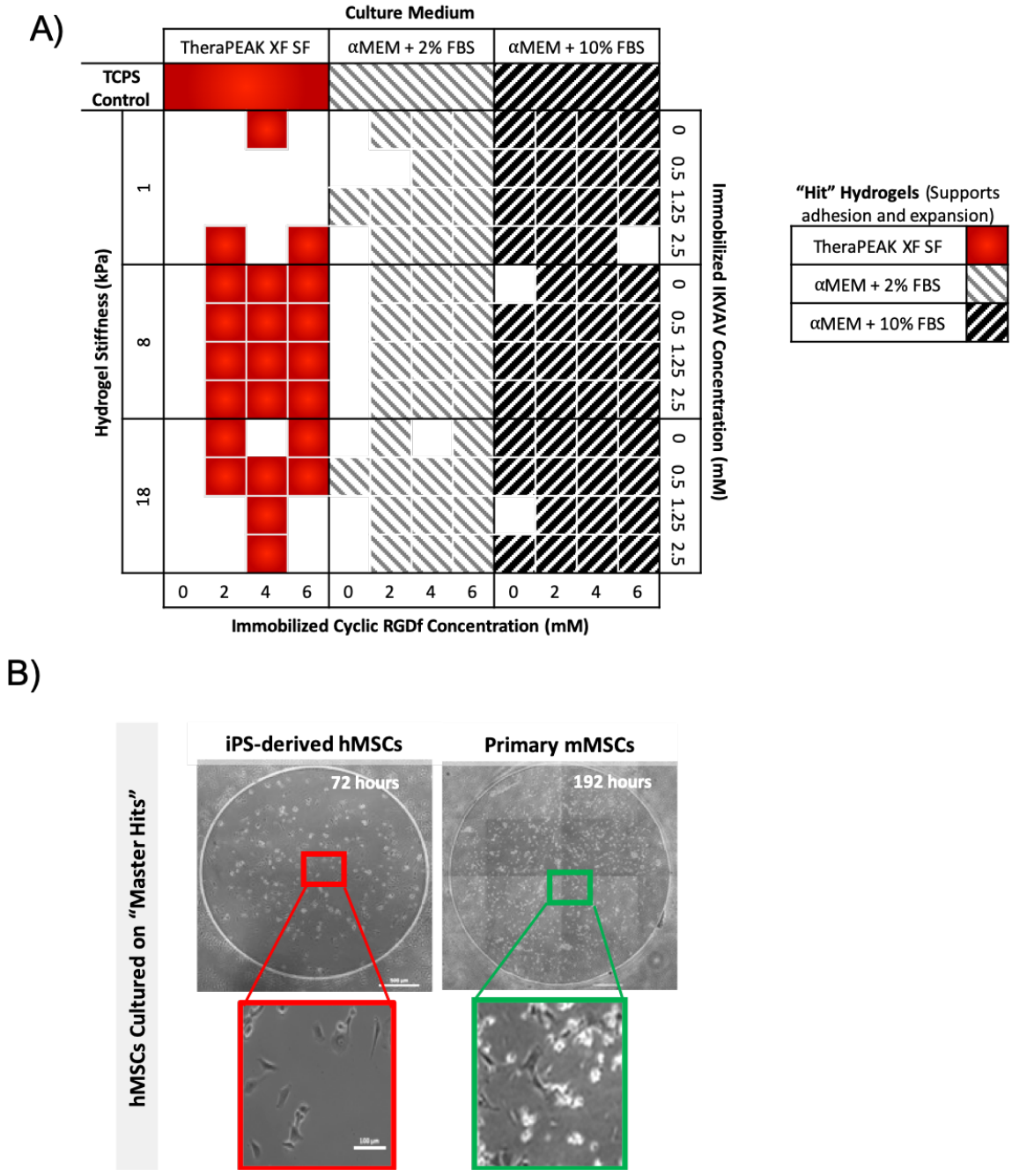

Figure 4.S6. Screening for A) hydrogel substrates that support hMSC adhesion and expansion in TheraPEAK XF SF, αMEM + 2% FBS, and αMEM + 10% FBS media ("hits") and B) "master hits" that support media- and cell source-agnostic hMSC culture.

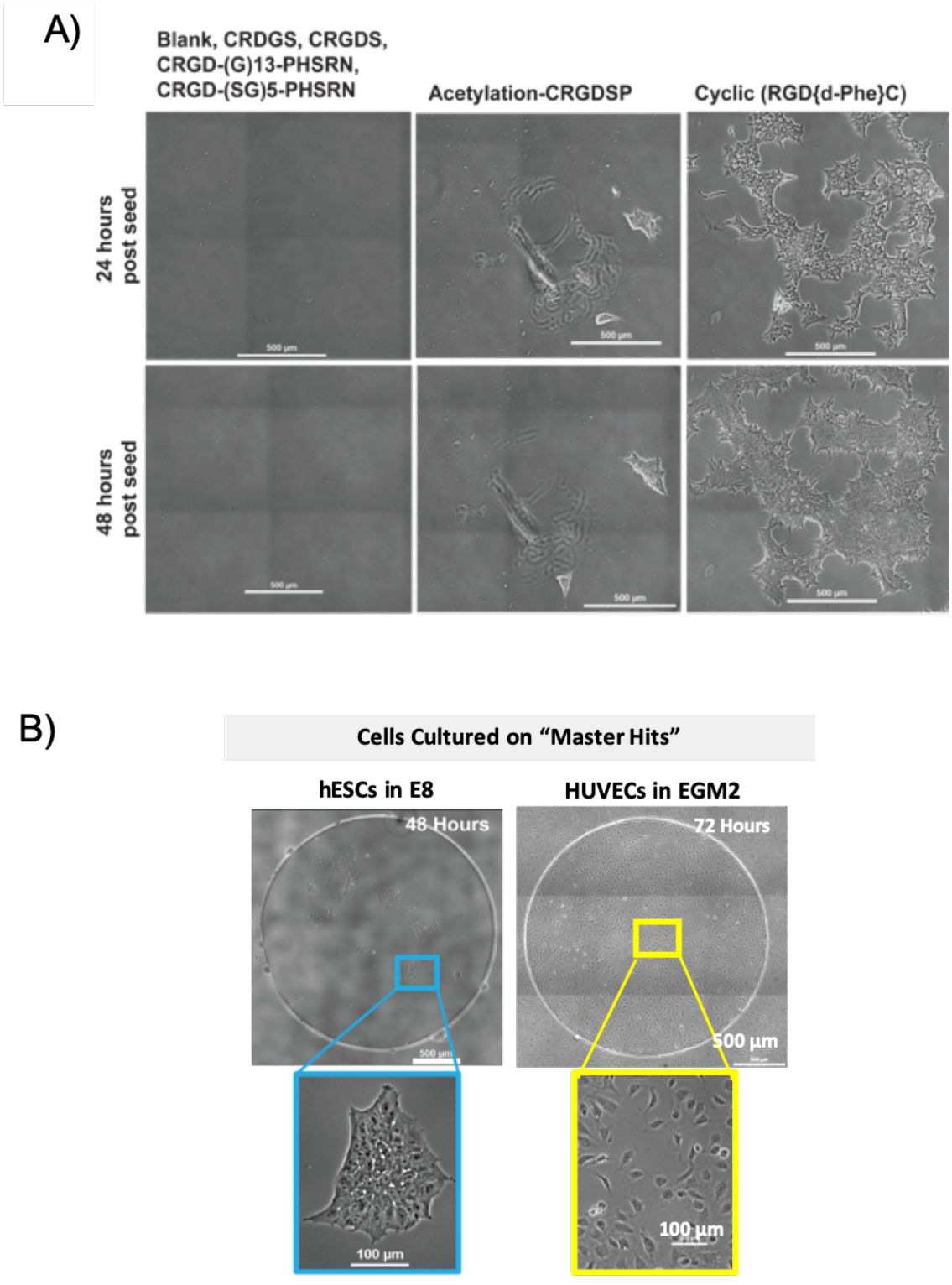

Figure 4.S7. Screening workflow for use in identifying substrates for serum-free hESC and -HUVEC attachment and proliferation

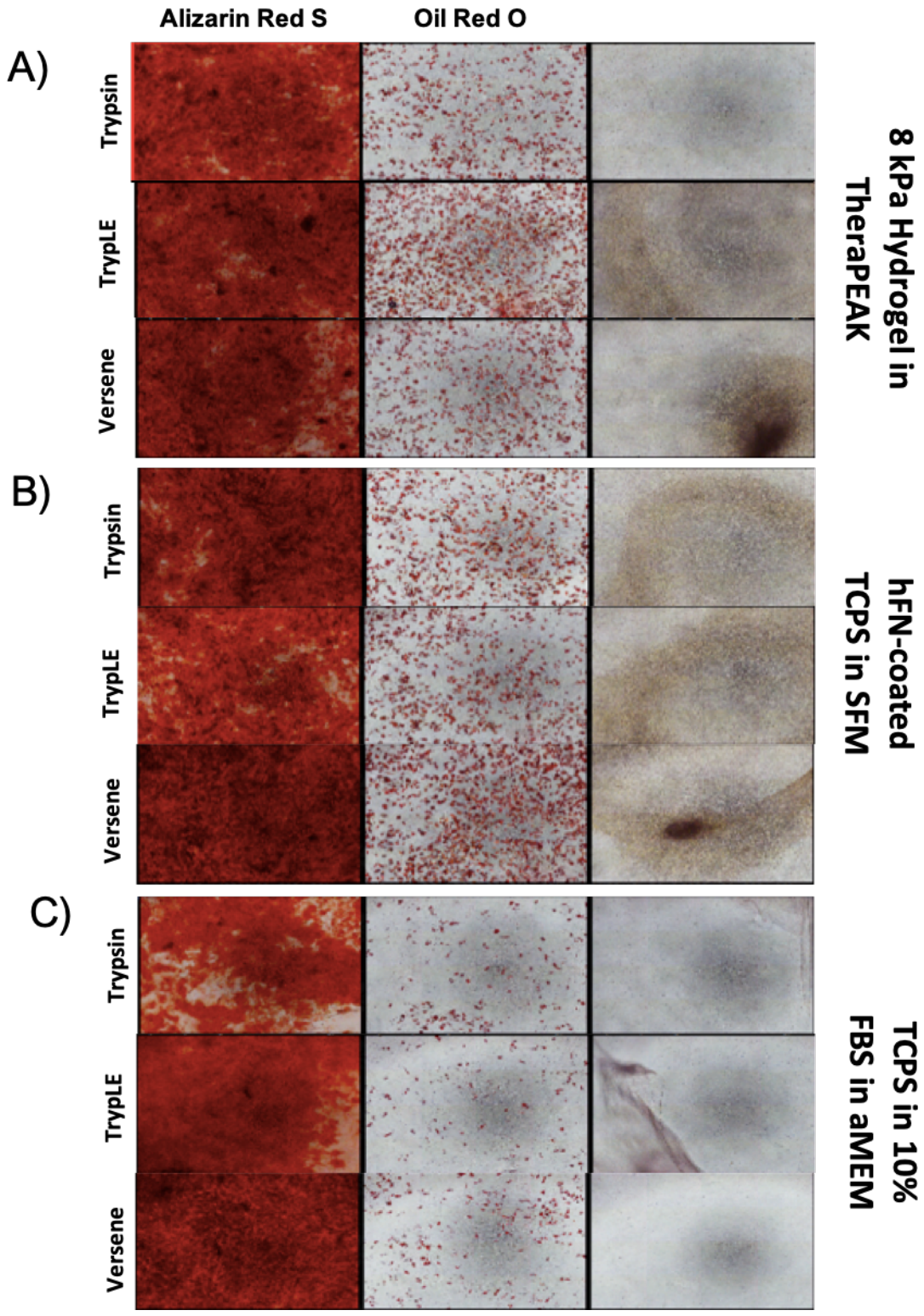

Figure 4.S8. hMSC multipotency analysis after 8 days of culture on A) 8 kPa hydrogel in SFM, B) hFN-coated TCPS in SFM, or C) TCPS in 10% FBS in a αMEM and dissociated with trypsin,

trypLE, or versene during harvest. All differentiation experiments conducted on collagen-coated TCPS. Osteogenic differentiation and no differentiation control (culture in αMEM + 2% FBS) assessed with Alizarin Red S staining and adipogenic differentiation staining assessed with Oil Red O staining after 28 days of culture in differentiation media.

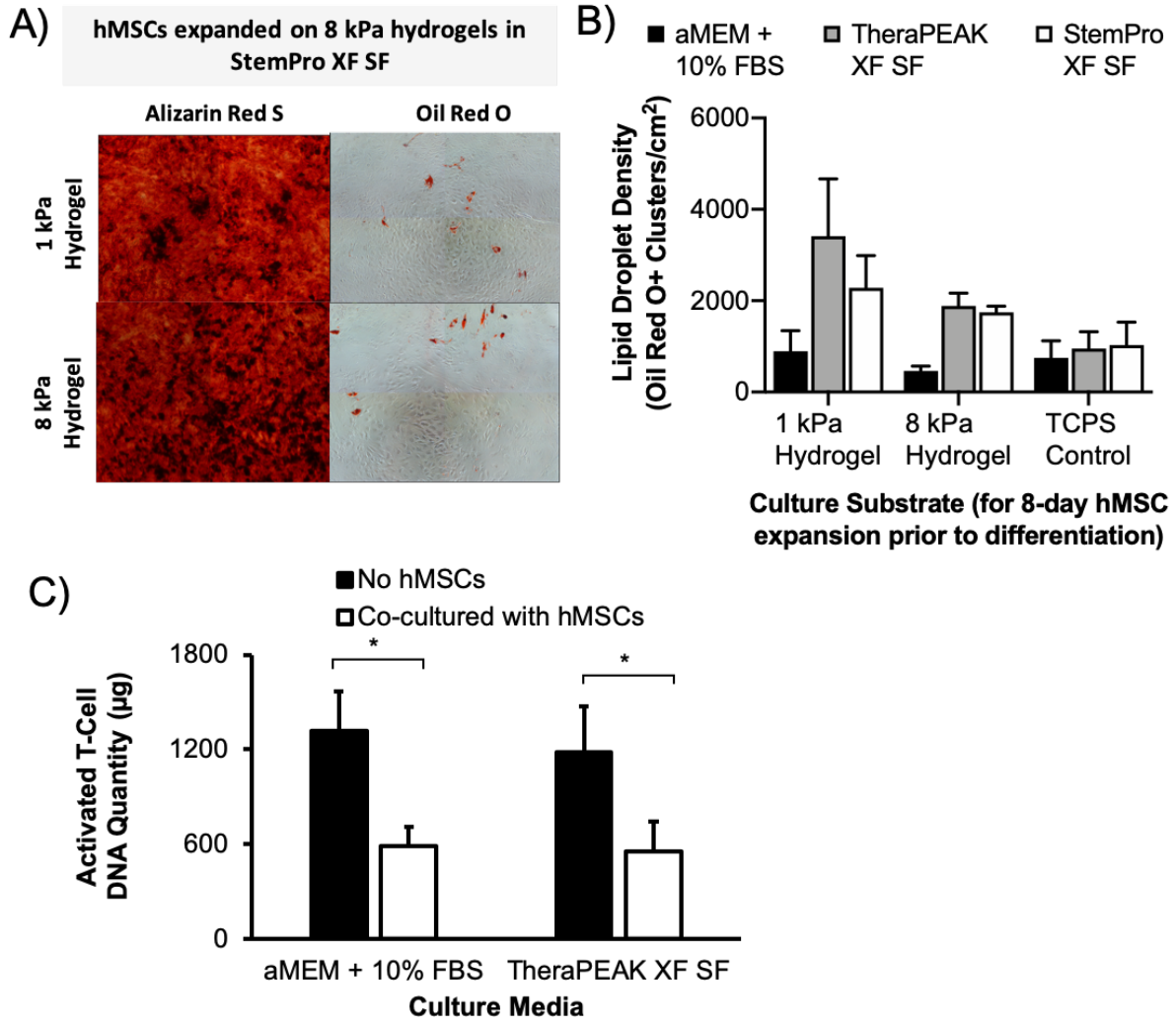

Figure 4.S9. Confirmation of functional hMSCs after 8-days of expansion on hydrogels in SC and SF media. A,B) Directed differentiation and C) immunomodulatory activity by controlling T-cell proliferation.

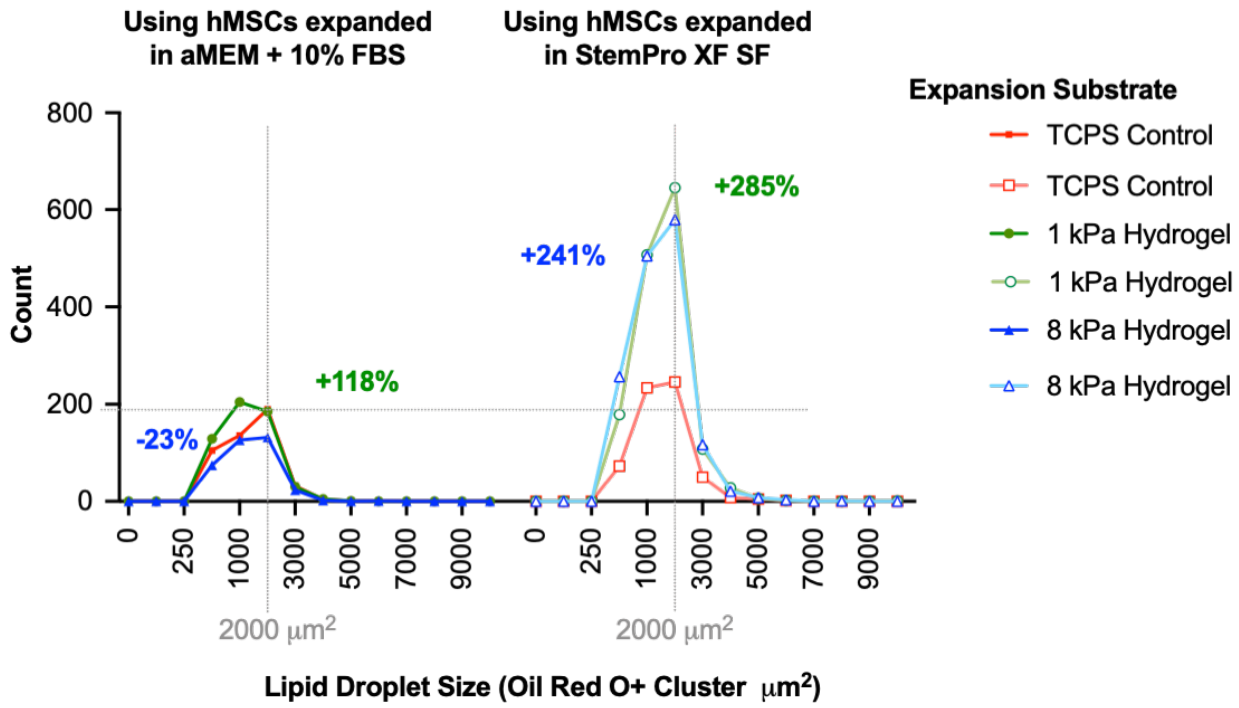

Figure 4.S10. Directed hMSC adipogenic differentiation and Oil Red O+ quantification of hMSCs expanded for 8 days in αMEM + 10% FBS or StemPro XF SF media on TCPS controls or hydrogels of varying stiffness. Note TCPS control for αMEM + 10% FBS is uncoated TCPS and for StemPro XF SF is CellStart-coated TCPS.

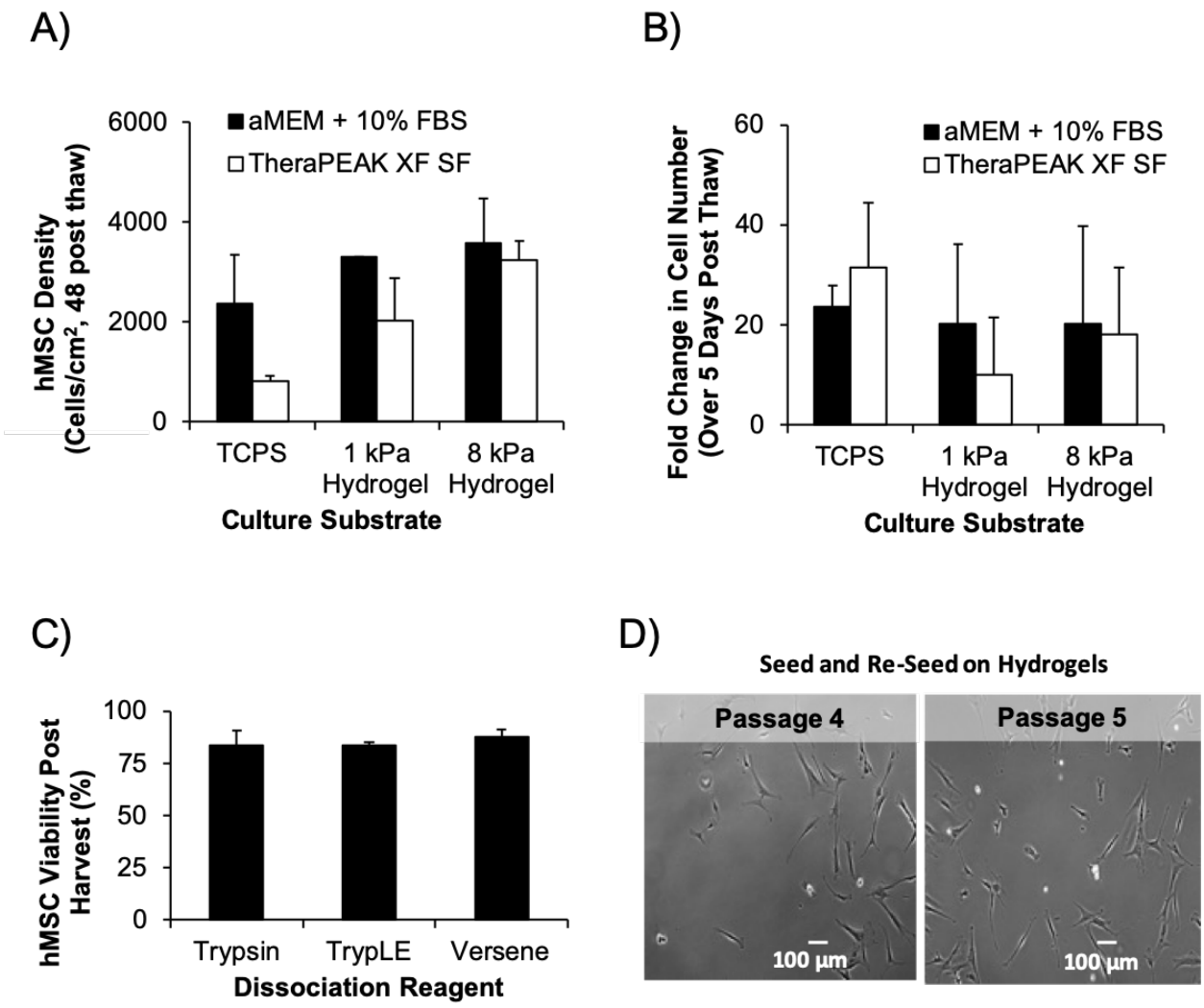

Figure 4.S11. Integration of "hit" hydrogel substrates into standard hMSC culture workflow. A) hMSC adhesion and B) expansion following thaw directly onto hydrogels. hMSC C) viability following harvest with varying enzymatic and non-enzymatic dissociation reagents and D) after re-seeding onto new hydrogel substrates for continued expansion.

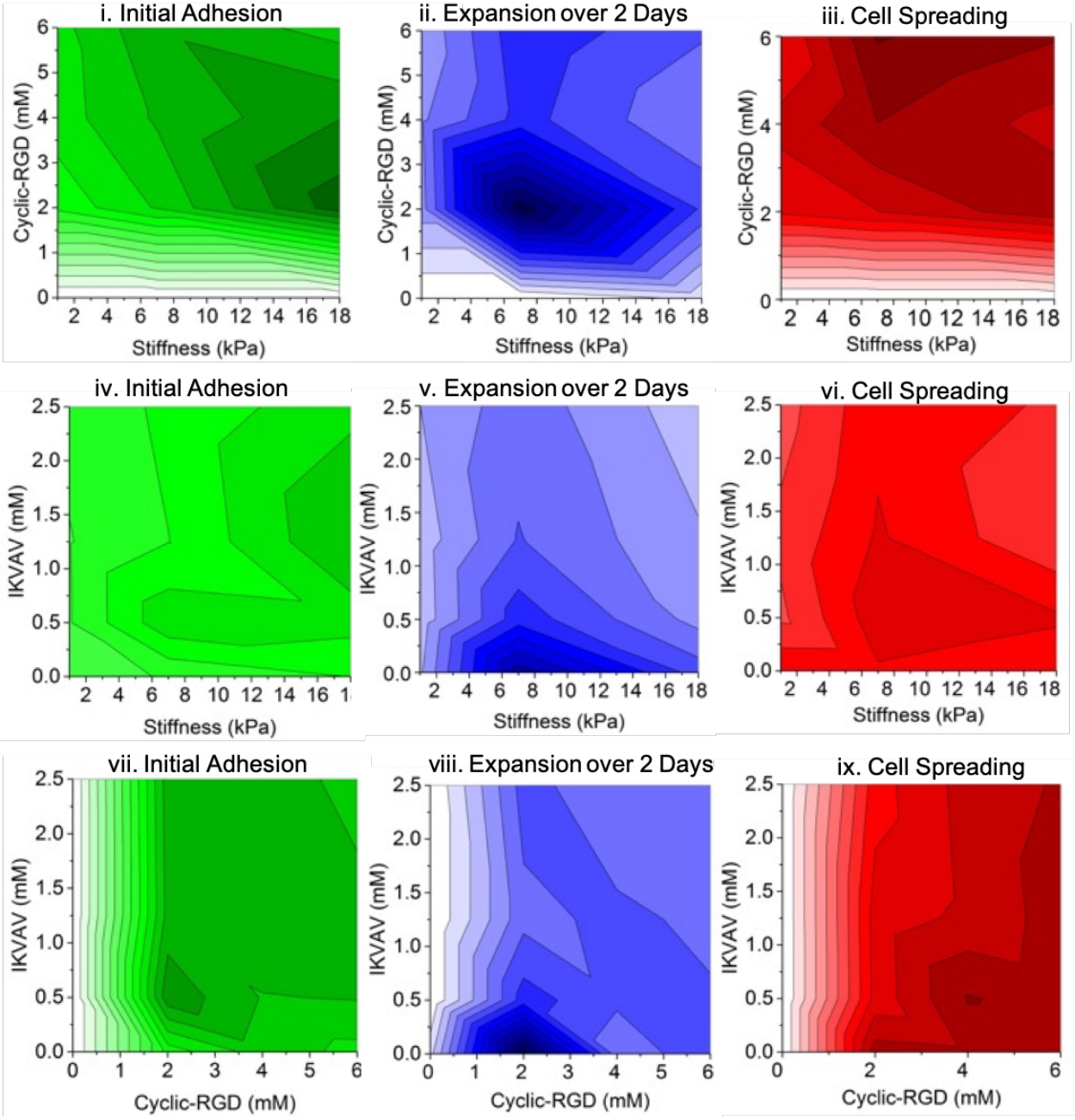

Figure 4.S12. Heat map of hMSC i, iv, vii) adhesion, ii, v, viii) expansion and ii, vi, ix) spreading in TheraPEAK chemically-defined XF SF medium. Increasing color intensity indicates increasing adhesion, expansion, or spreading.

4.11. References

[1] V.V. Rao, M.K. Vu, H. Ma, A.R. Killaars, K.S. Anseth, Rescuing mesenchymal stem cell regenerative properties on hydrogel substrates post serial expansion, Bioengineering & Translational Medicine (2018).

[2] M. Raab, J.-W. Shin, D.E. Discher, Matrix elasticity in vitro controls muscle stem cell fate in vivo, Stem Cell Research & Therapy 1(5) (2010) 38-38.

[3] S. VandeVondele, J. Voros, J.A. Hubbell, RGD-grafted poly-L-lysine-graft-(polyethylene glycol) copolymers block non-specific protein adsorption while promoting cell adhesion, Biotechnol Bioeng 82(7) (2003) 784-90.

[4] J.M. Maloney, D. Nikova, F. Lautenschlager, E. Clarke, R. Langer, J. Guck, K.J. Van Vliet, Mesenchymal stem cell mechanics from the attached to the suspended state, Biophys J 99(8) (2010) 2479-87.

[5] S. Jung, K.M. Panchalingam, L. Rosenberg, L.A. Behie, Ex Vivo Expansion of Human Mesenchymal Stem Cells in Defined Serum-Free Media, Stem Cells International 2012 (2012) 21.

[6] K. Crapnell, R. Blaesius, A. Hastings, D.P. Lennon, A.I. Caplan, S.P. Bruder, Growth, differentiation capacity, and function of mesenchymal stem cells expanded in serum-free medium developed via combinatorial screening, Exp Cell Res 319(10) (2013) 1409-18.

[7] G. Chamberlain, J. Fox, B. Ashton, J. Middleton, Concise Review: Mesenchymal Stem Cells: Their Phenotype, Differentiation Capacity, Immunological Features, and Potential for Homing, STEM CELLS 25(11) (2007) 2739-2749.

[8] L.G. Chase, S. Yang, V. Zachar, Z. Yang, U. Lakshmipathy, J. Bradford, S.E. Boucher, M.C. Vemuri, Development and characterization of a clinically compliant xeno-free culture medium in

good manufacturing practice for human multipotent mesenchymal stem cells, Stem Cells Transl Med 1(10) (2012) 750-8.

[9] L.G. Chase, U. Lakshmipathy, L.A. Solchaga, M.S. Rao, M.C. Vemuri, A novel serum-free medium for the expansion of human mesenchymal stem cells, Stem Cell Research & Therapy 1(1) (2010) 8-8.

[10] C. Tekkatte, G.P. Gunasingh, K.M. Cherian, K. Sankaranarayanan, "Humanized" stem cell culture techniques: the animal serum controversy, Stem cells international 2011 (2011) 504723-504723.

[11] K.Y. Tan, K.L. Teo, J.F.Y. Lim, A.K.L. Chen, S. Reuveny, S.K.W. Oh, Serum-free media formulations are cell line–specific and require optimization for microcarrier culture, Cytotherapy 17(8) (2015) 1152-1165.

[12] P.J. Dolley-Sonneville, L.E. Romeo, Z.K. Melkoumian, Synthetic Surface for Expansion of Human Mesenchymal Stem Cells in Xeno-Free, Chemically Defined Culture Conditions, PLoS ONE 8(8) (2013) e70263.

[13] H. Miwa, Y. Hashimoto, K. Tensho, S. Wakitani, M. Takagi, Xeno-free proliferation of human bone marrow mesenchymal stem cells, Cytotechnology 64(3) (2012) 301-308.

[14] I. Hartmann, T. Hollweck, S. Haffner, M. Krebs, B. Meiser, B. Reichart, G. Eissner, Umbilical cord tissue-derived mesenchymal stem cells grow best under GMP-compliant culture conditions and maintain their phenotypic and functional properties, Journal of Immunological Methods 363(1) (2010) 80-89.

[15] Y. Sun, C.S. Chen, J. Fu, Forcing stem cells to behave: a biophysical perspective of the cellular microenvironment, Annual review of biophysics 41 (2012) 519-42.

[16] S. Gobaa, S. Hoehnel, M. Roccio, A. Negro, S. Kobel, M.P. Lutolf, Artificial niche microarrays for probing single stem cell fate in high throughput, Nature methods 8(11) (2011) 949-55.

[17] D.E. Discher, D.J. Mooney, P.W. Zandstra, Growth factors, matrices, and forces combine and control stem cells, Science 324(5935) (2009) 1673-1677.

[18] A.J. Engler, L. Bacakova, C. Newman, A. Hategan, M. Griffin, D.E. Discher, Substrate Compliance versus Ligand Density in Cell on Gel Responses, Biophysical journal 86(1) (2004) 617-628.

[19] J.T. Koepsel, S.G. Loveland, M.P. Schwartz, S. Zorn, D.G. Belair, N.N. Le, W.L. Murphy, A chemically-defined screening platform reveals behavioral similarities between primary human mesenchymal stem cells and endothelial cells, Integrative biology : quantitative biosciences from nano to macro 4(12) (2012) 1508-21.

[20] K.A. Kilian, M. Mrksich, Directing stem cell fate by controlling the affinity and density of ligand-receptor interactions at the biomaterials interface, Angewandte Chemie 51(20) (2012) 4891-5.

[21] J. Lee, A.A. Abdeen, D. Zhang, K.A. Kilian, Directing stem cell fate on hydrogel substrates by controlling cell geometry, matrix mechanics and adhesion ligand composition, Biomaterials 34(33) (2013) 8140-8.

[22] N.N.T. Le, S. Zorn, S.K. Schmitt, P. Gopalan, W.L. Murphy, Hydrogel arrays formed via differential wettability patterning enable combinatorial screening of stem cell behavior, Acta Biomaterialia (2015).

[23] A.K. Jha, K.E. Healy, Controlling Osteogenic Stem Cell Differentiation via Soft, PLOS ONE 9(6) (2014) 1-11.

[24] A.A. Abdeen, J.B. Weiss, J. Lee, K.A. Kilian, Matrix Composition and Mechanics Direct Proangiogenic Signaling from Mesenchymal Stem Cells, Tissue Engineering. Part A 20(19-20) (2014) 2737-2745.

[25] D.S. Benoit, K.S. Anseth, Heparin functionalized PEG gels that modulate protein adsorption for hMSC adhesion and differentiation, Acta Biomater 1(4) (2005) 461-70.

[26] D.G. Belair, N.N. Le, W.L. Murphy, Design of growth factor sequestering biomaterials, Chem Commun (Camb) 50(99) (2014) 15651-68.

[27] W.L. Murphy, T.C. McDevitt, A.J. Engler, Materials as stem cell regulators, Nat Mater 13(6) (2014) 547-557.

[28] S.K. Schmitt, W.L. Murphy, P. Gopalan, Crosslinked PEG mats for peptide immobilization and stem cell adhesion, Journal of Materials Chemistry B 1(9) (2013) 1349.

[29] S. Lin, N. Sangaj, T. Razafiarison, C. Zhang, S. Varghese, Influence of physical properties of biomaterials on cellular behavior, Pharmaceutical research 28(6) (2011) 1422-30.

[30] M.M.L. Deckers, M. Karperien, C. van der Bent, T. Yamashita, S.E. Papapoulos, C.W.G.M. Löwik, Expression of Vascular Endothelial Growth Factors and Their Receptors during Osteoblast Differentiation, Endocrinology 141(5) (2000) 1667-1674.

[31] I.A. Potapova, G.R. Gaudette, P.R. Brink, R.B. Robinson, M.R. Rosen, I.S. Cohen, S.V. Doronin, Mesenchymal Stem Cells Support Migration, Extracellular Matrix Invasion, Proliferation, and Survival of Endothelial Cells In Vitro, STEM CELLS 25(7) (2007) 1761-1768.

[32] H. Mayer, H. Bertram, W. Lindenmaier, T. Korff, H. Weber, H. Weich, Vascular endothelial growth factor (VEGF-A) expression in human mesenchymal stem cells: Autocrine and paracrine role on osteoblastic and endothelial differentiation, Journal of Cellular Biochemistry 95(4) (2005) 827-839.

[33] T. Furumatsu, Z.N. Shen, A. Kawai, K. Nishida, H. Manabe, T. Oohashi, H. Inoue, Y. Ninomiya, Vascular Endothelial Growth Factor Principally Acts as the Main Angiogenic Factor in the Early Stage of Human Osteoblastogenesis, Journal of Biochemistry 133(5) (2003) 633-639.

[34] S.B. Traphagen, I. Titushkin, S. Sun, K.K. Wary, M. Cho, Endothelial invasive response in a co-culture model with physically-induced osteodifferentiation, Journal of Tissue Engineering and Regenerative Medicine 7(8) (2013) 621-630.

[35] E.H. Nguyen, M.R. Zanotelli, M.P. Schwartz, W.L. Murphy, Differential effects of cell adhesion, modulus and VEGFR-2 inhibition on capillary network formation in synthetic hydrogel arrays, Biomaterials 35(7) (2014) 2149-61.

[36] B.D. Fairbanks, M.P. Schwartz, A.E. Halevi, C.R. Nuttelman, C.N. Bowman, K.S. Anseth, A Versatile Synthetic Extracellular Matrix Mimic via Thiol-Norbornene Photopolymerization, Advanced Materials 21(48) (2009) 5005-5010.

[37] M.W. Toepke, N.A. Impellitteri, J.M. Theisen, W.L. Murphy, Characterization of Thiol-Ene Crosslinked PEG Hydrogels, Macromolecular materials and engineering 298(6) (2013) 699-703.

[38] N.A. Peppas, E.W. Merrill, Poly(vinyl Alcohol) Hydrogels: Reinforcement of radiation-crosslinked networks by crystallization, Journal of Polymer Science 14(2) (1976) 441-457.

[39] T. Canal, N.A. Peppas, Correlation between mesh size and equilibrium degree of swelling of polymeric networks, Journal of Biomedical Materials Research 23(10) (1989) 1183-1193.

[40] M. Parlato, S. Reichert, N. Barney, W.L. Murphy, Poly(ethylene glycol) Hydrogels with Adaptable Mechanical and Degradation Properties for Use in Biomedical Applications, Macromolecular Bioscience 14(5) (2014) 687-698.

[41] E. Nguyen, W. Daly, N.N. Le, M. Farnoodian, D. Belair, M. Schwartz, C. S. Lebakken, G. E. Ananiev, M.A. Saghiri, T. Knudsen, N. Sheibani, W. Murphy, Versatile synthetic alternatives to Matrigel for vascular toxicity screening and stem cell expansion, 2017.

[42] A.D. Dias, J.M. Elicson, W.L. Murphy, Microcarriers with Synthetic Hydrogel Surfaces for Stem Cell Expansion, Adv Healthc Mater 6(16) (2017).

[43] P.T. Brown, M.W. Squire, W.-J. Li, Characterization and evaluation of mesenchymal stem cells derived from human embryonic stem cells and bone marrow, Cell and tissue research 358(1) (2014) 149-164.

[44] P. Tropel, D. Noël, N. Platet, P. Legrand, A.-L. Benabid, F. Berger, Isolation and characterisation of mesenchymal stem cells from adult mouse bone marrow, Experimental Cell Research 295(2) (2004) 395-406.

[45] A. Geerligs, G.W. Peters, P.A. Ackermans, C.W. Oomens, Linear viscoelastic behavior of subcutaneous adipose tissue, Biorheology 45(6) (2008) 677-688.

[46] A. Nordez, F. Hug, Muscle shear elastic modulus measured using supersonic shear imaging is highly related to muscle activity level, Journal of applied physiology 108(5) (2010) 1389-94.

[47] F.P. Seib, M. Prewitz, C. Werner, M. Bornhäuser, Matrix elasticity regulates the secretory profile of human bone marrow-derived multipotent mesenchymal stromal cells (MSCs), Biochemical and Biophysical Research Communications 389(4) (2009) 663-667.

[48] T.H. Qazi, D.J. Mooney, G.N. Duda, S. Geissler, Biomaterials that promote cell-cell interactions enhance the paracrine function of MSCs, Biomaterials 140 (2017) 103-114.

[49] F.P. Seib, M. Prewitz, C. Werner, M. Bornhauser, Matrix elasticity regulates the secretory profile of human bone marrow-derived multipotent mesenchymal stromal cells (MSCs), Biochem Biophys Res Commun 389(4) (2009) 663-7.

[50] R.A. Marklein, D.E. Soranno, J.A. Burdick, Magnitude and presentation of mechanical signals influence adult stem cell behavior in 3-dimensional macroporous hydrogels, Soft Matter 8(31) (2012) 8113-8120.

[51] R. Koopman, G. Schaart, M.K. Hesselink, Optimisation of oil red O staining permits combination with immunofluorescence and automated quantification of lipids, Histochemistry and Cell Biology 116(1) (2001) 63-68.

[52] S.D. Fowler, P. Greenspan, Application of Nile red, a fluorescent hydrophobic probe, for the detection of neutral lipid deposits in tissue sections: comparison with oil red O, Journal of Histochemistry & Cytochemistry 33(8) (1985) 833-836.

[53] B. Gharibi, F.J. Hughes, Effects of Medium Supplements on Proliferation, Differentiation Potential, and In Vitro Expansion of Mesenchymal Stem Cells, Stem Cells Translational Medicine 1(11) (2012) 771-782.

4.12 Appendix

4.12.1 Patent (No: US 9,683,213; Issued: June 10, 2017)- Hydrogel compositions for use in cell expansion and differentiation

US 20170246357A1

(19) **United States**

(12) **Patent Application Publication** (10) **Pub. No.: US 2017/0246357 A1**

Murphy et al. (43) **Pub. Date: Aug. 31, 2017**

(54) **HYDROGEL COMPOSITIONS FOR USE IN CELL EXPANSION AND DIFFERENTIATION**

(71) Applicant: **Wisconsin Alumni Research Foundation**, Madison, WI (US)

(72) Inventors: **William L. Murphy**, Waunakee, WI (US); **Matthew Brian Parlato**, Madison, WI (US); **James A Molenda**, Madison, WI (US); **Ngoc Nhi Le**, Norcross, GA (US)

(21) Appl. No.: **15/596,529**

(22) Filed: **May 16, 2017**

Related U.S. Application Data

(63) Continuation of application No. 14/684,120, filed on Apr. 10, 2015, now Pat. No. 9,683,213.

(60) Provisional application No. 61/978,032, filed on Apr. 10, 2014.

Publication Classification

(51) **Int. Cl.**

A61L 31/14	(2006.01)
A61L 29/16	(2006.01)
A61K 47/42	(2006.01)

(52) **U.S. Cl.**

CPC ***A61L 31/145*** (2013.01); ***A61K 47/42*** (2013.01); ***A61L 29/16*** (2013.01); *A61L 2300/80* (2013.01)

(57) **ABSTRACT**

Hydrogel compositions and methods of using hydrogel compositions are disclosed. Advantageously, the hydrogel compositions offer the ability to promote cellular expansion and/or cellular differentiation of various cells.

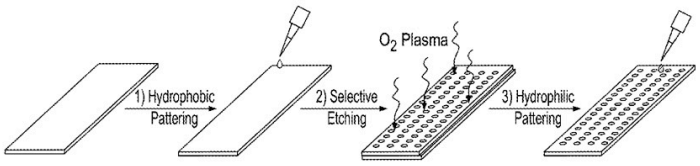

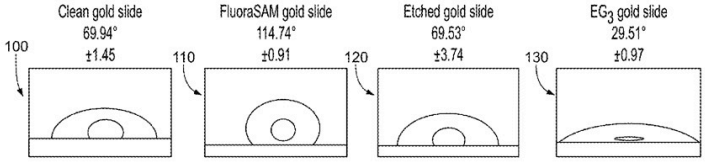

4.12.2 Figures: Customized biomaterials for chemically-defined short-term pluripotent stem cell culture

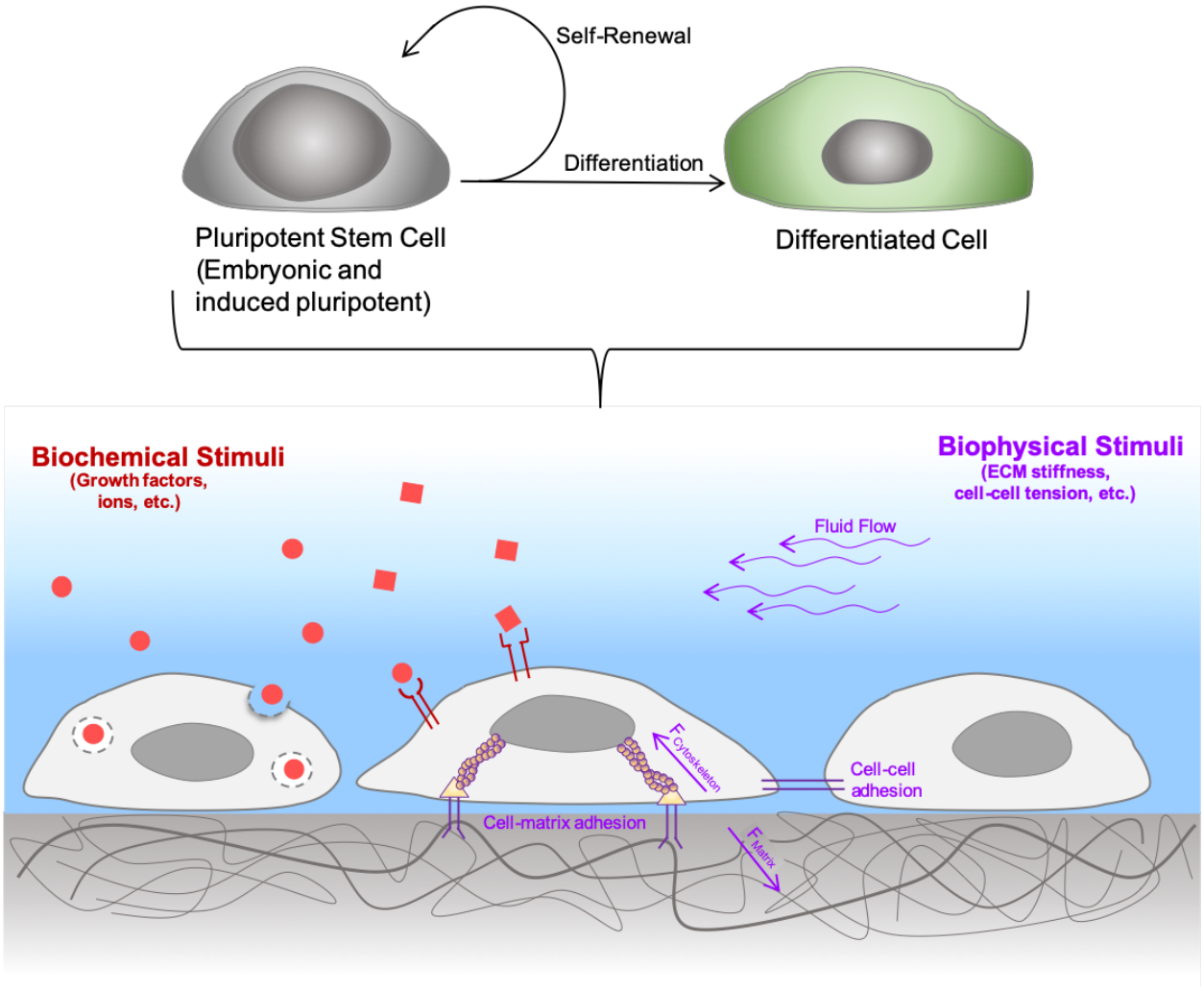

Figure 4.12.2.1. Human pluripotent stem cell self-renewal and differentiation are tightly regulated by intrinsic genes (e.g. Sox2, Oct3/4) as well as extrinsic biochemical and biophysical signals from the cell's microenvironment.

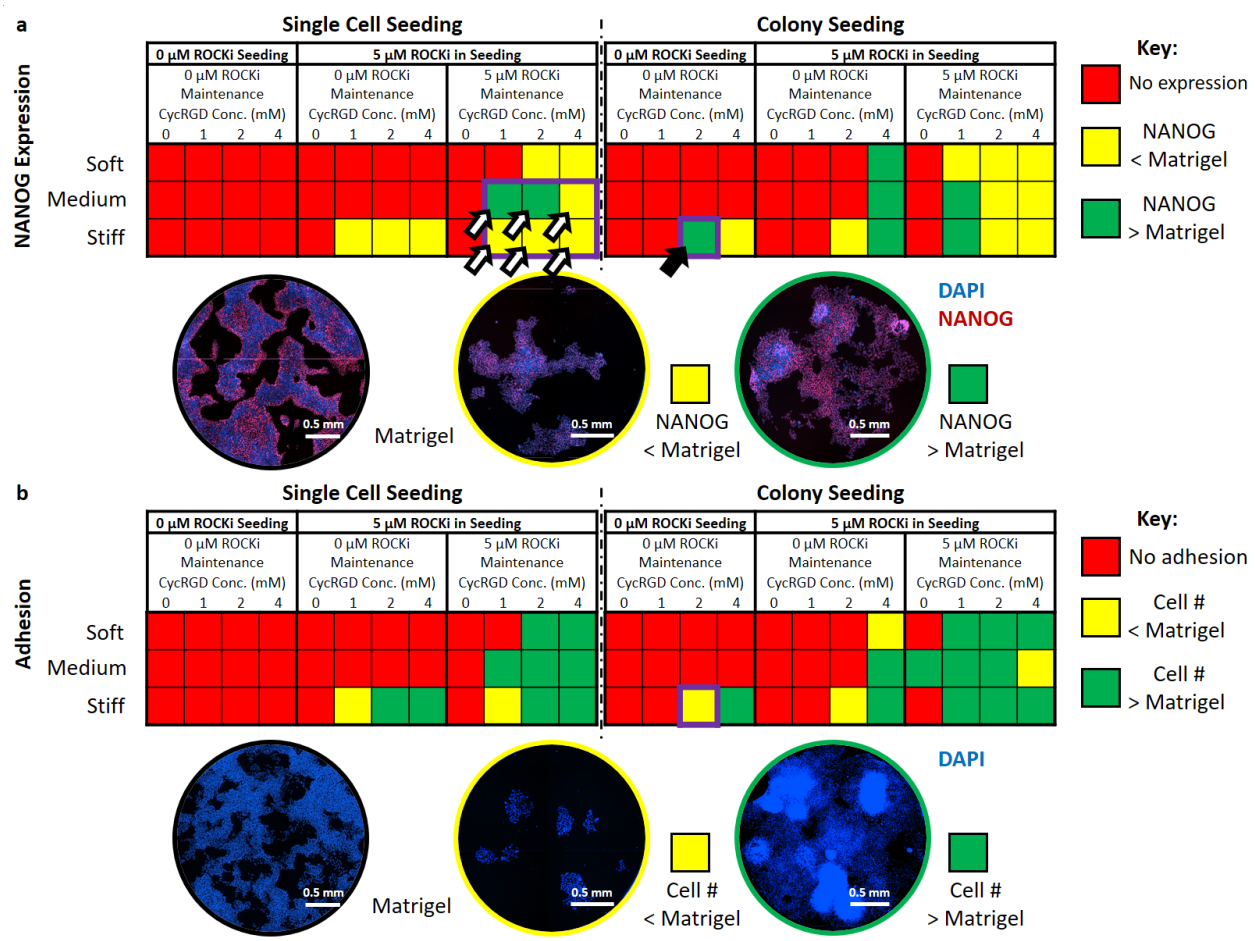

Figure 4.12.2.2. Enhanced throughput screening approach applied to identify substrates for hESC short-term culture and pluripotency maintenance. Figure and caption as previously published in Nature Biomedical Engineering [41]. "Material-dependent maintenance of hESC pluripotency. (a) Quantitative heat map of hESC NANOG expression relative to Matrigel in varying synthetic hydrogel-based culture conditions (n=3, n=5 in colony seeding conditions where ROCK inhibitor was removed, n=10 in single-cell seeding conditions where ROCK inhibitor was removed). The screen was performed twice over the course of these studies. Conditions highlighted with a black arrowhead denote environments that maintained both hESC pluripotency and cell attachment over a 96-hour culture period without the use of ROCK Inhibitor. Conditions highlighted with a white arrowhead denote conditions that were further

investigated for OCT3/4 expression in addition to NANOG expression. (b) Quantitative heat map of hESC attachment in varying culture conditions. and spreading on PEG hydrogel substrates (n=3, n=5 in colony seeding conditions where ROCK inhibitor was removed, n=10 in single-cell seeding conditions where ROCK inhibitor was removed.) The screen was performed once over the course of these studies."

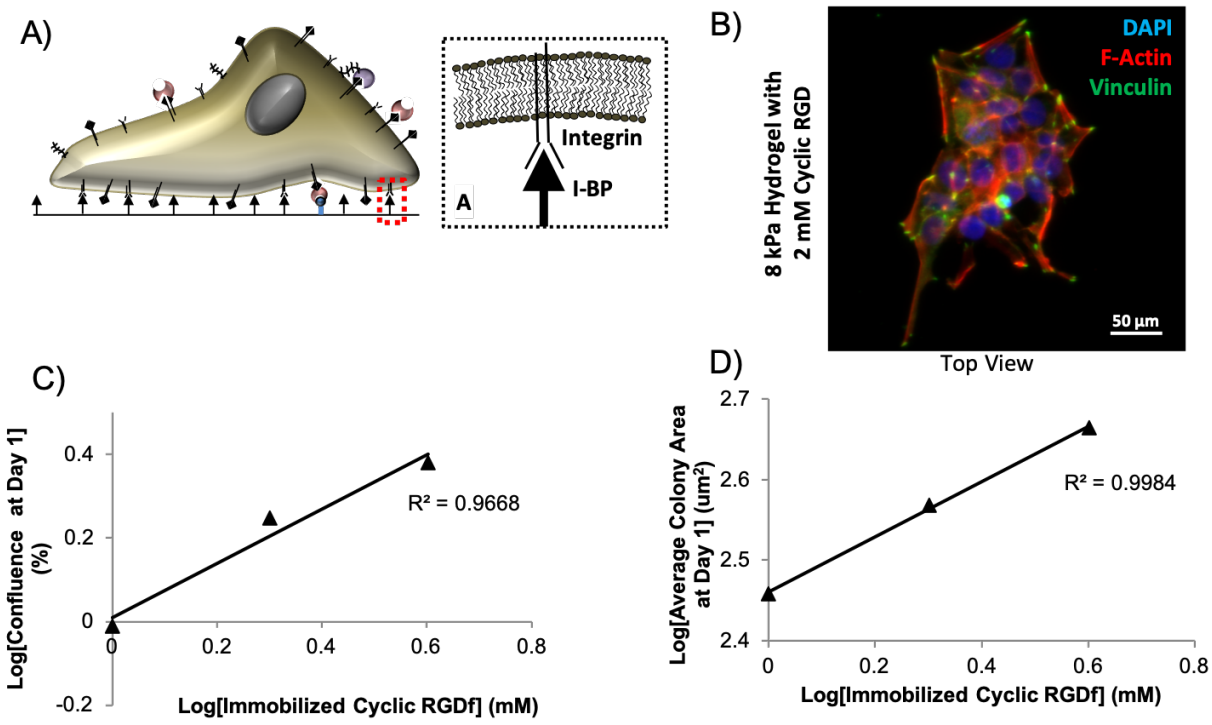

Figure 4.12.2.3. hESCs culture on customized hydrogel substrates with varying A) substrate adhesivity express B) cytoskeletal organization suggestive of hESC mechanosensitivity. A) Hydrogels presenting immobilized Cyclic RGDf, a fibronectin-derived integrin-binding peptide, supports hESC C) attachment and D) colony-based spreading in a manner directly correlated to the concentration of immobilized adhesion-promoting peptide.

Chapter 5- VEGF sequestering hydrogels enhance hMSC expansion without need for additional GF supplementation

Ngoc Nhi T. Le[a], Tianran Leona Liu[b], James Johnston [b], John Krutty[b], Padma Gopalan [a,c,d], William L. Murphy[a,b,e*]

[a] Materials Science Program, University of Wisconsin-Madison, Madison, WI USA

[b] Department of Biomedical Engineering, University of Wisconsin-Madison, Madison, WI USA

[c] Department of Material Science and Engineering, University of Wisconsin-Madison, Madison, WI USA

[d] Department of Chemistry, University of Wisconsin-Madison, Madison, WI USA

[e] Department of Orthopedics and Rehabilitation, University of Wisconsin-Madison, Madison, WI USA

* Corresponding author can be contacted at Wisconsin Institute for Medical Research II, 1111 Highland Avenue Room 5405, Madison, WI USA 53705. Phone: (608)265-9978; Email: wlmurphy@wisc.edu

5.1 Preface

The purpose of these studies was to examine the influence of substrate stiffness, adhesivity, and vascular endothelial growth factor (VEGF) sequestering on human mesenchymal stromal cell (hMSC) behavior in order to probe the potential for developing instructive biomaterials for cell culture that could induce and control changes in cell behavior without the need for expensive, additionally-supplemented growth factors. Here, hydrogel substrates presenting VEGF-binding peptide (VBP) were able to sequester recombinant human VEGF as

well as hMSC-secreted VEGF. These studies demonstrated the ability to use VBP-mediated VEGF regulation for autocrine VEGF signaling to enhance hMSC expansion and paracrine VEGF signaling to promote human umbilical vein endothelial cell (HUVEC) proliferation without the need for induction with supplemented growth factors.

Additionally, we provide reference to an issued patent in the appendix in order to demonstrate the commercial applicability of this approach. We also provide unpublished data demonstrating the utility of this approach to 1) create different biomaterials for applications in sequestering and delivery beyond the 2D culture demonstrated here and 2) control the sequestration via immobilization of varying bioactive GF-regulating molecules (such a heparin or heparin-binding peptides).

5.2 Abstract

We describe development of customized hydrogels that enabled sequestering of endogenous human mesenchymal stromal cell (hMSC)-secreted vascular endothelial growth factor (VEGF) as well as exogenous, supplemented recombinant human VEGF for autocrine regulation of hMSC expansion and paracrine promotion of human umbilical vein endothelial cell (HUVEC) proliferation, all without the need for induction with additionally supplemented growth factors.

5.3 Statement of Significance

Our growth factor sequestering biomaterials developed in this work is the first demonstration of the ability to use instructive biomaterials to “autocatalyze” and control cell behavior changes *in vitro* without the need to rely on induction via additionally supplemented growth factors. This approach could be utilized to explore cost-reduction strategies associated with

the development of biomaterials for cell biomanufacturing that either reduce or completely eliminate the reliance on expensive growth factor supplementation.

5.4 Introduction

Human mesenchymal stromal cells (hMSCs) are appealing candidates for cell therapies and tissue engineering because they possess potent immunomodulatory properties to regulate immune function and secrete an array of paracrine factors capable of supporting tissue regeneration [1-3]. hMSC-secreted paracrine factors help promote wound healing *in vivo* that in turn recruit stem and immune cells, promote survival and proliferation, and stimulate organization and remodeling [4-7].

Less than 1% of hMSCs engraft and survive 24 hours after transplantation, therefore vascular endothelial growth factor A (VEGF)-priming (pre-treatment) and co-delivery has been employed to increase hMSC survival and retention at the transplantation site. VEGF priming during hMSC culture has been shown to promote hMSC expansion by synergistically increasing proliferation and decreasing apoptosis [8, 9]. Priming hMSCs with rhVEGF increased Erk ½ phosphorylation-mediated proliferation accompanied by increased cyclin B1 (regulator of S/G2 cell entry during mitosis) and decreased $p16^{INK}$ (cell cycle inhibitor). Additionally, rhVEGF provided an Akt phosphorylation-mediated protective effect via decreased Bax (pro-apoptotic protein) production, reduced Caspase-3 (a pro-apoptotic protease enzyme) activation, increased Bcl-2 (anti-apoptotic survival protein kinase) biosynthesis, and increased Bcl-xL (anti-apoptotic survival protein kinase) activation [9, 10].

These VEGF-priming protocols require high concentrations of supplemented rhVEGF (up to 20 ng/10^6 hMSCs); however, culture materials are expensive and the reliance on high concentrations of growth factors results in protocols that are cost prohibitive for large-scale manufacturing. Studies estimate that up to 20% of the total materials cost of goods in the hMSC biomanufacturing process can be attributed to the media cost alone [8-11]. There is ample

evidence that hMSCs secrete detectable levels of VEGF in routine culture and increase endogenous VEGF secretion during osteogenic differentiation, both of which are accompanied by increased VEGF receptor gene expression needed for autocrine signaling [5, 7, 12-17]. In addition, hMSCs VEGF secretion can also be regulated by biophysical cues through hMSC mechanosensing of the substrate stiffness and subsequent actomyosin contractility-mediated intracellular signaling to regulate gene expression [6, 18-21].

While there a small number of studies that have examined the relationship between matrix mechanics and GF production, the results were inconsistent and contradictory [18, 22]. Seib *et al.* and Abdeen *et al.* showed hMSCs cultured on stiffer substrates produced higher concentrations of secreted VEGF, but Marklein *et al.* and others demonstrated increasing substrate stiffness resulted in decreased VEGF secretion in a time-dynamic manner [6, 18-22]. The existing studies have predominantly relied on culture media supplemented with fetal bovine serum (FBS) with varying substrate chemistries and mechanics. These contradictory results might be due to several factors: 1) lack of reproducibility due to FBS variability, 2) temporal differences, and 3) differences in culture substrate chemistry. Nonnis *et al.* examined the effects of FBS on the hMSC secretome and revealed that increasing FBS (from 0 to 10%) concentration in culture media reduced detection sensitivity and accuracy needed for characterizing hMSC protein production [33].

Here, we examine the effects of substrate mechanics on hMSC VEGF production in xeno-free (XF) culture and investigated potential mechanisms for regulating these effects. We explore the use of biomaterials that mimic the combinatorial adhesivity, matrix stiffness, and VEGF-sequestering functions of the cell microenvironment to simultaneously induce hMSC behavior changes, harness and localize cell-secreted VEGF at the cell-material interface to amplify VEGF

signaling, and subsequently provide a positive feedback loop to autocatalyze hMSC expansion without the need for additionally-supplemented rhVEGF.

5.5 Materials and methods

5.5.1 Materials

PEG-OH (20 kDa molecular weight, tripentaerythritol core, 8-arm with terminal OH) was purchased from JenKem Technology. Anhydrous dichloromethane, 5-Norbornene-2-carboxylic acid, N,N′-dicyclohexylcarbodiimide, diethyl ether, hexane, SNAKESKIN dialysis tubing with MWCO 3.5K, deuterated chloroform with tetramethylsilane internal standard, 1,4-Dithiothreitol (DTT), 3-mercaptopropyl trimethoxysilane (3-MPTS), Rho associated protein kinase (ROCK) inhibitor (Y27632), and SU5416 (an inhibitor of VEGF receptor activity) were purchased from Sigma Aldrich. Linear 3.4 kDa PEG-dithiol (PED-DT) crosslinker was purchased from Laysan Bio. Irgacure 2959 photoinitiator was purchased from CIBA/BASF. All peptides were purchased from GenScript USA. Bone marrow-derived hMSCs, TheraPEAK XF SF medium, human umbilical vein endothelial cells (HUVECs), and endothelial growth medium 2 (EGM-2) Bulletkit were purchased from Lonza. Fetal bovine serum (FBS), penicillin/streptomycin and trypsin were purchased from Invitrogen. Minimum essential medium alpha formulation (αMEM) and medium 199 (M199) were purchased from MediaTech. Versene 1X EDTA, TrypLE, and Click-iT EdU cell proliferation kits were purchased from Thermo Fisher Scientific. StemPro XF SF medium and CellStart coating were purchased from Gibco. RoosterNourish XF medium was purchased from RoosterBio. 96-well Angiogenesis plates were purchased from Ibidi. Alexa-Fluor 488 goat anti-human IgG antibody against endothelial transmembrane marker Platelet-Endothelial Cell Adhesion Molecule-1 (PECAM-1/CD31), Alexa Fluor 647 rabbit anti -human IgG antibody

against alpha smooth muscle actin (SMA), diamidino-2-phenylindole (DAPI), and all Quantikine ELISA kits were purchased from R&D Systems. Nuclear magnetic resonance spectroscopy services were provided by the National Magnetic Resonance Facility at the University of Wisconsin-Madison.

5.5.2 Hydrogel formation and characterization

Norbornene-functionalized PEG (PEG-NB) hydrogels were formed using thiolene chemistry as previously reported [34-37]. PEG-NB was synthesized and characterized as previously described [34-37]. In brief, PEG-OH was dissolved in a round-bottom flask with anhydrous dichloromethane while 5-Norbornene-2-carboxylic acid was dissolved in a second flask with N,N′-dicyclohexylcarbodiimide. Contents of both flasks were combined and stirred overnight to allow for 5-norbornene-2-carboxylic acid to covalently couple to the PEG-OH and form a PEG-NB precipitate. The PEG-NB was filtered through a medium fritted Buchner funnel to remove urea salts byproduct and subsequently further precipitated from the residual salts in 900 mL cold diethyl ether and 100 mL hexane. The PEG-NB solids were filtered through qualitative grade filter paper in a porcelain Buchner Funnel, collected on the filter paper, and allowed to air dry overnight at room temperature. The dried PEG-NB product was dissolved in distilled water at 1 g/mL, purified via dialysis against distilled water for 72 hours at 4 °C using SNAKESKIN dialysis tubing with molecular weight cutoff of 3.5 kDa to remove residual norbornene acids, and lyophilized. The resulting PEG-NB product was dissolved at 6 mg/mL in deuterated chloroform with tetramethylsilane internal standard and norbornene functionalization was confirmed to be >90% via 1H nuclear magnetic resonance spectroscopy on a Bruker Instruments Avance III 500i spectrometer at 400 MHz and 27°C.

Hydrogel precursor solutions were prepared by combining PEG-NB (4 or 8 wt/wt %), PEG-dithiol crosslinker (0.5 or 0.75 mole ratio of thiol-to-norbornene), adhesion-promoting Cyclic RGDfC peptides (2 or 4 mM), adhesion-promoting CIKVAV peptide (0.5 mM), VEGF-binding peptide (VBP, $CEF_dA_dY_dL_dIDFNWEYPASK$) or the scrambled control (VBPscr, $CDA_dPYNF_dEFAWEY_dVISL_dK$) peptide (0, 0.067, 0.13, or 0.27 mM), and Irgacure 2959 photoinitiator (0.5 wt/wt%) and diluted to the desired concentrations with phosphate buffered saline (PBS) at pH 7.4 immediate prior to hydrogel network photopolymerization using UV initiation at 365 nm wavelength.

For experiments quantifying hMSC-secreted VEGF, 1 mL of hydrogels precursor solutions were spotted onto the bottom of 6-well plates and photopolymerized with 365 nm UV light with 90 mW/cm^2 intensity for 6 seconds. For rhVEGF and hMSC-secreted VEGF binding experiments, hydrogel networks were formed via spotting 8 uL/well of hydrogel precursor solution into the well bottoms of 96-well Angiogenesis plates and photopolymerizing with 365 nm UV light with 4.5 mW/cm^2 intensity for 8 minutes [38]. For experiments assessing hMSC and HUVEC expansion in response to hMSC-secreted VEGF, hydrogel arrays were formed using a patented differential wettability patterning method as previously reported [37, 38]. Briefly, hydrogel precursor solutions were spotted onto hydrophilic-patterned regions of alkanethiol self-assembled monolayers formed on gold-coated sample slides, a DTT-treated 3-MPTS-silanized glass coverslip was placed on top to sandwich the hydrogel precursor solutions, and hydrogel precursor solutions were photopolymerized with 365 nm UV light for 90 mW/cm^2 for <6 seconds, and the gold-coated slide was separated from the silanized coverslip. The result is a hydrogel array composed of glass-immobilized hydrogel spots. Arrays were formed in a biosafety cabinet and additionally decontaminated with UV-C in the biosafety cabinet for 3

hours, thoroughly washed with PBS, immersed in the desired media for 48 hours at 37 °C until use.

Hydrogel shear storage modulus was determined using procedures previously published [34, 37, 39-42].

5.5.3 Cell Culture

All hMSCs used were cryopreserved in αMEM + 10% FBS, thawed into the respective medias of interest, and allowed to recover from cryopreservation at 37 °C in a 5% CO_2 atmosphere for 72 hours prior to harvest and use for hydrogel experiments. hMSCs were expanded as needed (before 75 % confluence or until used for experiments) with total population doubling level <16. The following growth media formulations and substrates were used for hMSC culture: 1) minimum essential medium alpha formulation with 1% penicillin/streptomycin and supplemented with 10% fetal bovine serum (αMEM +10% FBS) on uncoated TCPS, 2) TheraPEAK XF SF on uncoated TCPS, 3) StemPro XF SF on CellStart-coated TCPS, and RoosterNourish XF on uncoated TCPS. For repassage and hydrogel experiments, hMSC were seeded onto TCPS and hydrogel substrates at 1000 cell/cm^2 to reduce the amount of cell-cell interactions that could mask the effects of cell-substrate interaction. Human umbilical vein endothelial cells (HUVECs)) were cultured in growth medium consisting of medium 199 (M199) supplemented with the complete EGM-2 Bulletkit (Full EGM2), without the rhVEGF supplement from the Bulletkit (EGM2, no VEGF), without the rhFGF-2 supplement from the Bulletkit (EGM2, no FGF-2), or without both the rhVEGF and rhFGF-2 supplements from the Bulletkit (EGM2, no VEGF no FGF-2). All cells were harvested using trypsin.

5.5.4 Data acquisition and analysis

Immunofluorescence staining for PECAM-1, and SMA were performed manufacturer's instructions with 1:200 dilutions. Nuclear counterstain was performed using 1:5000 dilution of DAPI. Click-iT EdU proliferation assay to identify cells in S-Phase were performed per the manufacturer's instructions with 8 hours of EdU incubation for hMSCs and 12 hours of EdU incubation for HUVECs.

Samples were placed in a heated environmental chamber and imaged on the Nikon Eclipse Ti microscope (Nikon) at the desired times. Cell number was manually determined using NIS Elements software (Nikon) and expansion was determined as fold change in cell number (cell adhesion density at 72 hours divided by count at 24 or 48 hours) with a fold change >1 indicating proliferation.

hMSC-secreted growth factors were quantified by seeding hMSCs at high density (3000 cells/cm^2), collecting cell culture supernatant following 3 days of hMSC culture on hydrogels or TCPS controls, and performing Quantikine ELISAs per the manufacturer's instructions. Quantified protein amounts were normalized against cell number at the time of supernatant collection. Cell culture supernatant collected also was used as hMSC conditioned media for HUVEC studies.

hMSC proliferation studies were performed by seeding hMSCs at 1000 cells/cm^2 on hydrogel arrays in the growth medium of interest, removing unattached cells via media change after 24 hours of attachment, and replacing the media with the experimental condition (with or without inhibitors) indicated. Samples were imaged every 24 hours with experiments lasting 72 hours total after media change. Note, for hMSC proliferation experiments, ROCK inhibitor was

supplemented to the experimental media conditions to help prevent dissociation-associated cell death.

HUVEC proliferation studies using hMSC-conditioned media were performed by seeding HUVECs at 5000 cells/cm^2 in EGM-2 without VEGF or FGF-2 on hydrogels previously incubated in hMSC-conditioned media and removing unattached cells via media change after 24 hours of attachment. After 72 hours of culture, HUVECs were fixed, immunostained or labeled using the Click-iT EdU kit, and imaged. Percent of cells in S-Phase was determined by normalizing the number of EdU stained cells against all DAPI counterstained cells.

Statistical analysis for significance was performed using the GraphPad Prism software via Student's t-test (2-tailed, α=0.05) or ANOVA with post-hoc Tukey (HSD or Kramer depending on sample size variability) tests as indicated. Error bars denote standard deviation.

5.6 Results

5.6.1 Customized hydrogels for combinatorial control of substrate stiffness, adhesivity, and VEGF sequestering.

PEG-NB hydrogels presenting VEGF-binding peptide (VBP) enabled the ability to sequester rhVEGF without compromising the capability to regulate hydrogel stiffness (Figure 5.1 and Figure 5.S1A). Hydrogels without VBP and those presenting the VBPscr control, a peptide containing a different sequence organization of same amino acid residues found in VBP, were not able to sequester rhVEGF at levels comparable to VBP-hydrogels (Figure 5.S1B).

Note that hydrogels presenting 0.27 mM VBP did not sequester more rhVEGF than 0.13 mM VBP-hydrogels. Additionally, regardless of the concentration of rhVEGF loaded into the

hydrogels, the maximum potentially bound by the VBP-hydrogels is approximately 70-80% of available rhVEGF (Figure 5.S1B).

5.6.2 Stiffness- and adhesion-dependent hMSC-secreted VEGF production

hMSCs cultured on hydrogels with decreasing stiffness secreted higher concentrations of VEGF than those cultured on stiffer hydrogels or on TCPS controls; however, this stiffness-dependence was observed in TheraPEAK XF SF culture but not in αMEM + 10% FBS (Figure 5.2A). hMSCs cultured on substrates with increasing adhesivity secreted higher concentrations of VEGF (Figure 5.2B) and, similar to stiffness dependence, this adhesion-dependent differential VEGF secretion was only observed in TheraPEAK XF SF culture and not in αMEM + 10% FBS. hMSCs cultured on hydrogel substrates, regardless of stiffness or adhesivity, secreted higher concentrations of VEGF than those cultured on TCPS. Note FGF-2 and TGFβ1 secretion was not affected by stiffness in either TheraPEAK XF SF or αMEM + 10% FBS culture (Figure 5.S2 and Figure 5.S3).

5.6.3 VBP-hydrogels sequestered hMSC-secreted VEGF

Hydrogels presenting higher concentrations of VBP bound higher concentrations of hMSC-secreted VEGF from hMSC supernatant. Hydrogels presenting adhesion-promoting Cyclic RGDf and VBPscr did not sequester significant amounts of VEGF (Figure 5.3). Note that, a small amount of FGF-2 was sequester by hydrogels containing VBPscr (Figure 5.S4).

5.6.4 VBP-hydrogels enhanced hMSC expansion without additionally supplemented growth factors

Soft, 1 kPa hydrogels presenting 0.27 mM VBP promoted higher hMSC expansion than all other hydrogel surfaces for culture in TheraPEAK XF SF, RoosterNourish XF, and αMEM + 10% FBS media (Figure 5.4 and Figure 5.S5). Note that, while VBP incorporation into 8 kPa hydrogels promoted increased hMSC expansion, the differential increase was smaller than what's achievable via hMSCs culture on 1 kPa hydrogels presenting VBP. Note that these increased expansion rates occurred without any additional supplemented recombinant growth factors.

5.6.5 VBP-hydrogels sequester bioactive hMSC-secreted VEGF for paracrine signaling

VBP-hydrogels incubated in hMSC-conditioned media supported HUVEC expansion in culture without supplemented rhVEGF (Figure 5.5 and Figure 5.S8). The addition of VBP also enabled HUVEC proliferation even in the absence of both rhVEGF and rhFGF-2. Notably, in the presence of VEGF signaling inhibitor (SU5416), HUVEC proliferation rescue was mitigated.

5.7 Discussion and Conclusions

Here, we have developed customized hydrogels for VEGF sequestering using a published VEGF-binding peptide identified by biomimicry of the VEGF-VEGFR2 active binding domain [38, 43-47]. VBP-hydrogels sequestered exogenously supplemented recombinant VEGF (rhVEGF) and endogenous hMSC-secreted VEGF with high specificity without binding several mitogenic GFs commonly found in growth media (e.g. FGF-2 and TGFβ1) (Figure 5.1, Figure 5.3, and Figure 5.S1B). These results are consistent with previously-

published data from our lab indicating the ability to sequester both recombinant human VEGF as well as serum-borne, activated-platelet-derived VEGF [38, 44, 45, 47]. Interestingly, VBP- and VBPscr-hydrogel incubation in hMSC-conditioned media suggested higher concentrations of hMSC-secreted FGF-2 from cell populations cultured on 1 kPa hydrogels presenting 0.27 mM VBPscr (Figure 5.S4B). While the VBPscr was developed as a negative binding control for VEGF sequestering, future experiments should examine the influence of VBP and VBPscr on FGF-2 secretion and other growth factors in order to accommodate previously-published reports of multiple GFs' dynamic, combinatorial, and convergent ability to regulate hMSC behavior [4, 23-32].

In this work, we have also demonstrated the ability to use previously-published thiolene chemistry to develop customized hydrogel with systematically controlled VEGF sequestering via increasing concentration of VBP in the hydrogel precursor solution (Figure 5.1B) [34-37]. VEGF sequestering capabilities were engineered into the hydrogel substrates without compromising the ability to customize substrate stiffness (via increasing PEG-NB backbone polymer and PEG-DT crosslinker concentrations in the hydrogel precursor solution) and adhesivity (via increasing Cyclic RGDf and IKVAV adhesion-promoting peptide concentrations in the hydrogel precursor solution) (Figure 5.2 and Figure 5.S1).

Using previously-published hydrogel array screening techniques, we examined the effect of substrate stiffness, adhesivity, and VBP concentration on hMSC expansion and growth factor secretion over the course of 72 hours (Figure 5.2, Figure 5.4, Figures 5.S1-S2, and Figures 5.S5-S6) [37, 38, 44, 48]. We discovered hydrogel substrates able to sequester hMSC-secreted VEGF to promote hMSC and HUVEC proliferation, potentially through autocrine and paracrine signaling (Figures 5.3-5 and Figure 5.S5-S9). Soft hydrogels of 1 kPa presenting 0.27 mM of

VBP supported increased hMSC expansion in multiple different serum-containing and serum-free growth media (when compared to surfaces without VEGF regulation) (Figure 5.4 and Figure 5.S5). Notably, hMSC expansion was increased without induction through additionally-supplemented recombinant growth factors, potentially suggestive of either VBP-mediated harnessing of hMSC-secreted VEGF or localization and amplification of VEGF present in the growth media (Figure 5.S9). When we inhibit VEGF signaling via the use of VEGF receptor inhibitor SU5416, we see mitigation of the VBP-mediated increase in hMSC expansion (Figure 5.S5). In addition to the potential regulation of autocrine signaling, we demonstrated the ability to use VBP-hydrogels for paracrine signaling by sequestering hMSC-secreted VEGF to rescue VEGF-starved HUVEC proliferation (Figure 5.5, Figure 5.S8, and Figure 5.S9). Our results suggest VEGF-signaling mediated this potential paracrine effect as VBP-mediated HUVEC proliferation was also mitigated in the presence of VEGF signaling inhibitors.

While we do see VBP-mediated increase in hMSC expansion on hydrogels of 8 kPa stiffness, the increase is much larger for hMSCs cultured on soft hydrogels (Figure 5.5, Figure 5.S5, and Figure 5.S7). There are several potential mechanisms involved in this stiffness dependence. First and foremost, we showed increased hMSC VEGF secretion for cells cultured on softer substrates accompanied by, albeit not statistically significant, a slight increase in secreted FGF-2; all of which potentially suggests increased hMSC autocrine regulation on softer substrates (Figure 5.2 and Figure 5.S2). This is consistent with the stiffness-dependent VEGF production relationships previously reported by Seib *et al.* and Abdeen *et al.*, but contradictory to Marklein *et al.*'s conclusions [6, 18-22]. The trends reported here robust in its consistency across this work and those published by Seib *et al.* and Abdeen *et al.*, independent of substrate chemistry and media composition.

To further explore the mechanisms involved in stiffness-dependent VEGF secretion and amplified VEGF signaling, we use ROCK inhibitor to disrupt cytoskeletal tension (and potentially mitigate mechanosensing effects transduced through actomyosin contractility). In the presence of ROCK inhibitor, we saw increased hMSC retention and survival on all hydrogels (regardless of VBP concentration or stiffness) in RoosterNourish XF media and for hMSCs on 8 kPa hydrogels in αMEM + 10% FBS (Figure 5.S6). We previously reported stiffness-dependent hMSC adhesion and expansion, therefore the protective effects of ROCK inhibitor could potentially suggest low survival on soft hydrogels resulting from low adhesion stability [48]. Our insights from DOE- and MVA-driven screening in chapter 4 of this work suggests that culture parameters can combinatorially affect cell response to their microenvironment. In this chapter, we used hydrogel compositions with substrate stiffness, Cyclic RGDf, and IKVAV concentrations that were previously identified to support hMSC expansion in multiple growth media; however, those experiments did not factor in the effects of VEGF sequestering as an additional, potentially synergistic culture parameter. To better understand the combinatorial effects of stiffness and VEGF sequestering, additional optimization screens should be performed to identify compositions suitable for supporting hMSC survival and expansion in the presence of VBP.

Combined, the aforementioned results suggest that we have developed customized biomaterials that can both induce hMSC differential VEGF secretion (through control of substrate stiffness) and sequester endogenous VEGF for autocrine signaling (through controlling VEGF-binding peptide concentration) for a positive feedback loop that amplifies the initial substrate-induced hMSC behavior change in an seemingly “autocatalytic” manner.

Notably, we demonstrated the use of these “autocatalytic” biomaterial substrates can enable enhanced hMSC expansion without the need for additionally supplemented growth factors. Future work on these “autocatalytic” biomaterials could potentially be used as a cost-reduction strategy for cell biomanufacturing in order to either reduce the concentration of supplemented growth factors or completely eliminate the need for protocols relying on growth factor-induced cell behavior control.

5.8 Acknowledgements

The authors acknowledge the following funding sources: the National Institutes of Health (grant no. R01HL093282), the National Science Foundation (grant no. 1306482), the National Science Foundation Graduate Research Fellowships Program (grant no. DGE-0718123), the National Science Foundation Engineering Research Center for Cell Manufacturing Technologies (CMaT, NSF grant no. 1648035), the University of Wisconsin-Madison Graduate Engineering Research Scholars, and the Gates Millennium Scholars Program. The authors also acknowledge support from staff and the use of equipment at the Materials Science Center (National Science Foundation grant no. 1121288) and services from the National Magnetic Resonance Facility at the University of Wisconsin-Madison.

5.9 Figures

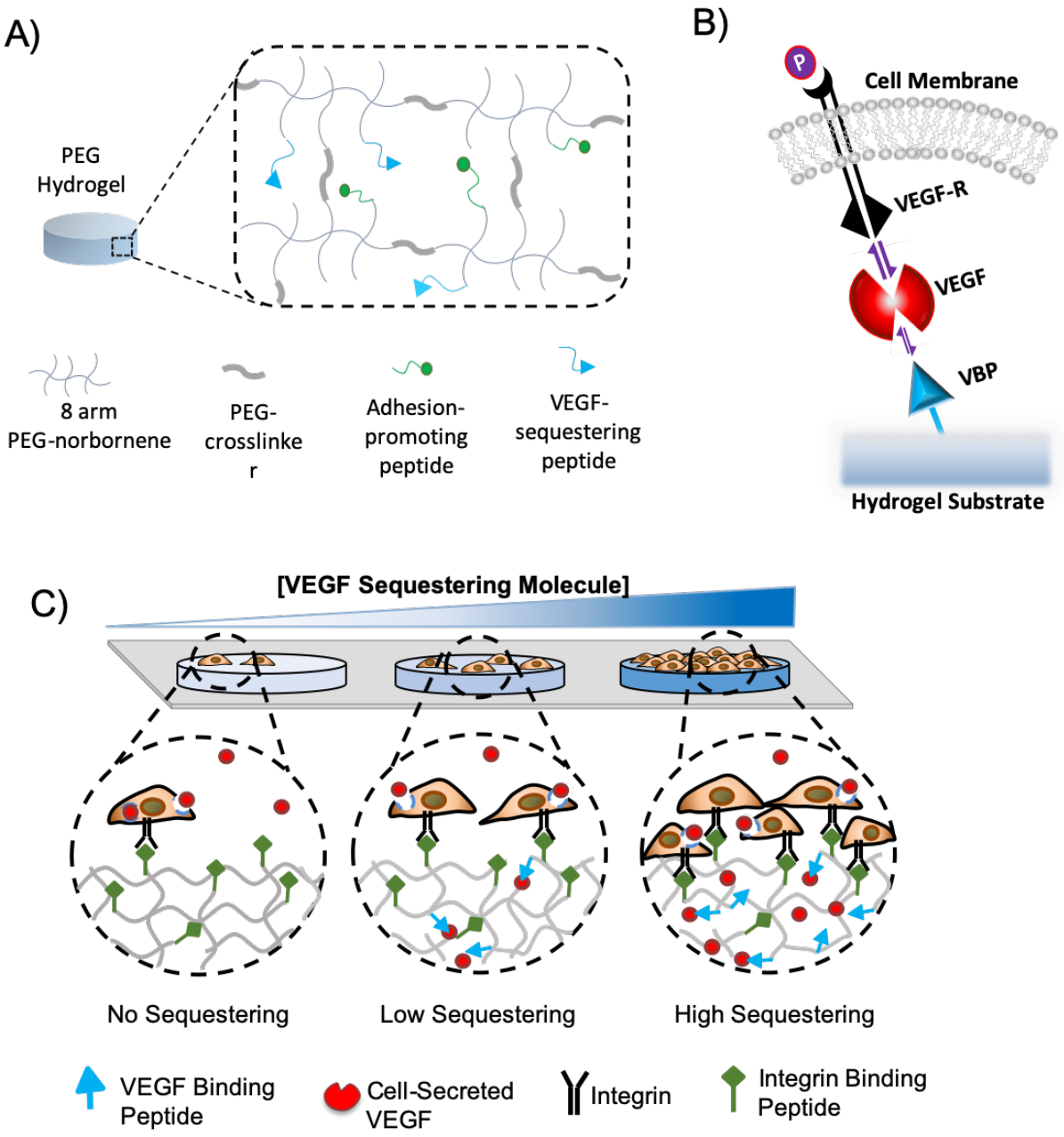

Figure 5.1. VEGF sequestering biomaterials developed using A) VEGF-binding peptides (VBP) immobilized inside a PEG-NB hydrogel network formed via thiolene photopolymerization. B) VEGF sequestering capability of the hydrogel substrates can be tailored by controlling the concentration of immobilized VBP incorporated into the hydrogel network.

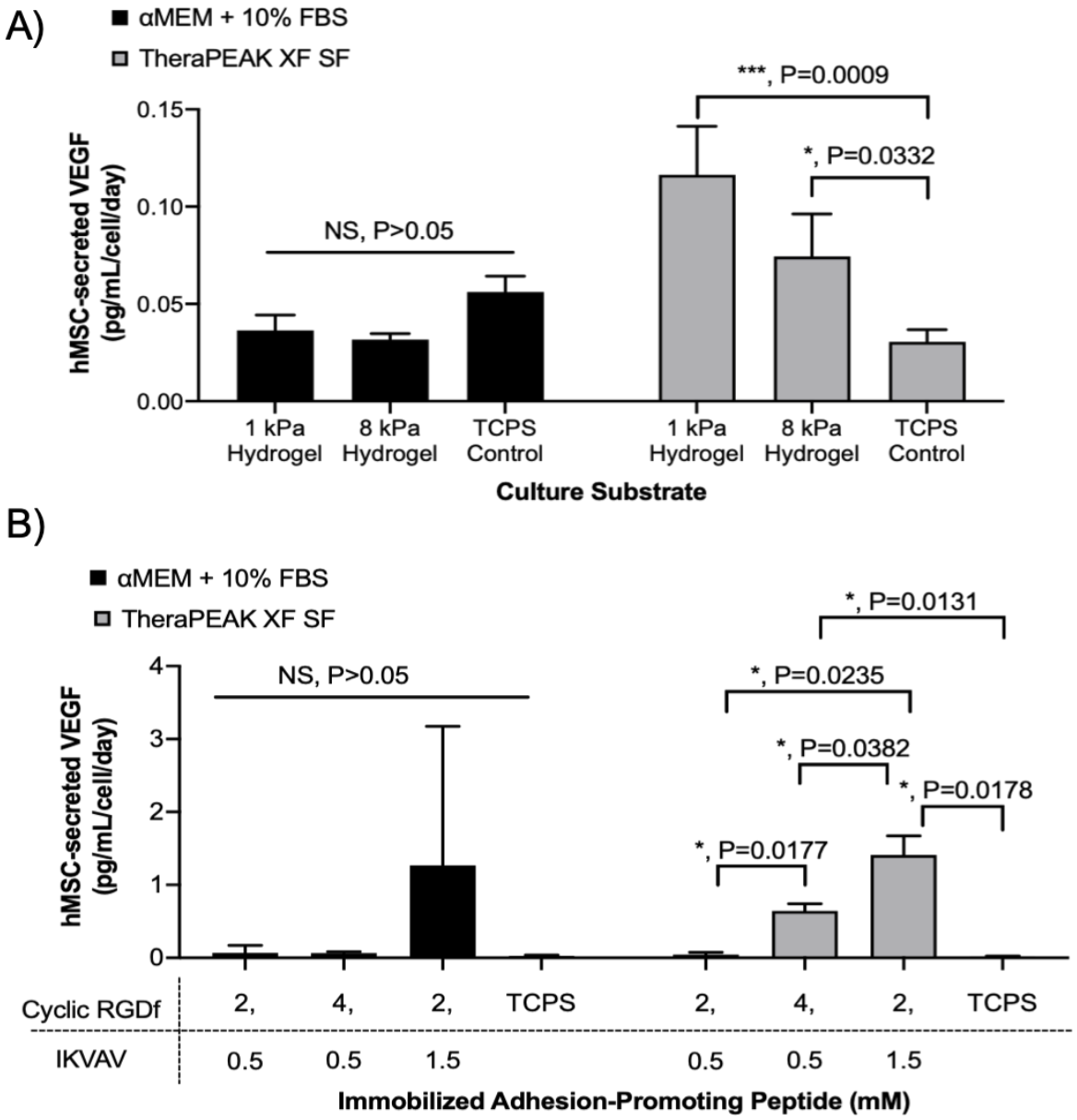

Figure 5.2. Differential hMSC VEGF secretion induced via A) control of hydrogel stiffness or B) adhesivity for culture in TheraPEAK XF SF media. A) Increasing substrate stiffness decreased hMSC VEGF secretion while B) increasing substrate adhesivity increased hMSC VEGF secretion.

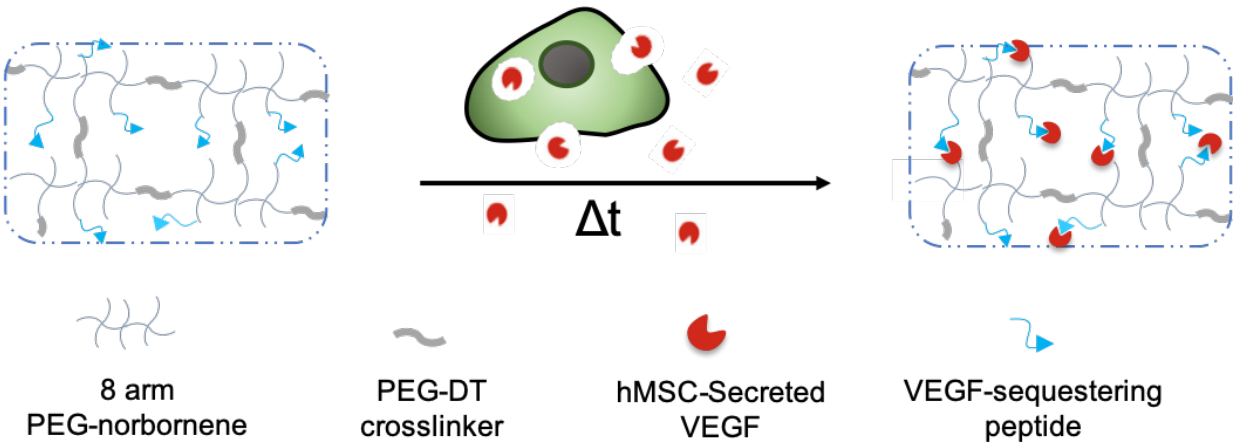

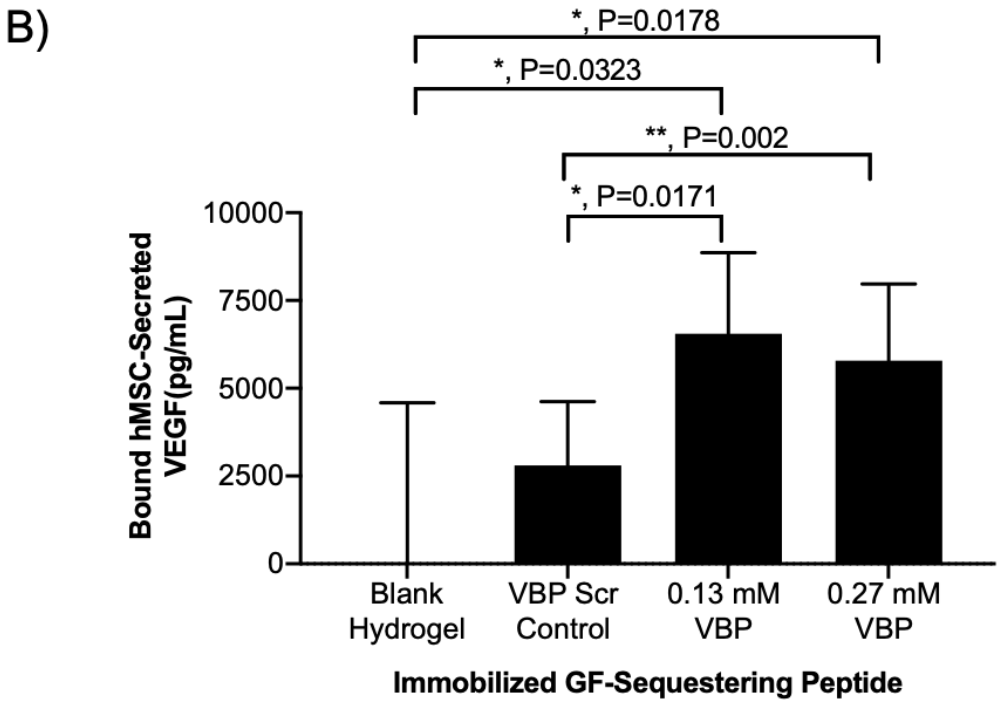

Figure 5.3. Hydrogels presenting VBP A) incubated in hMSC-conditioned medium B) bound hMSC-secreted VEGF. VEGF binding occurred in a A) diffusion-limited, time-dependent manner and the degree of VEGF sequestering directly correlated to B) the concentration of VBP immobilized in the hydrogel network.

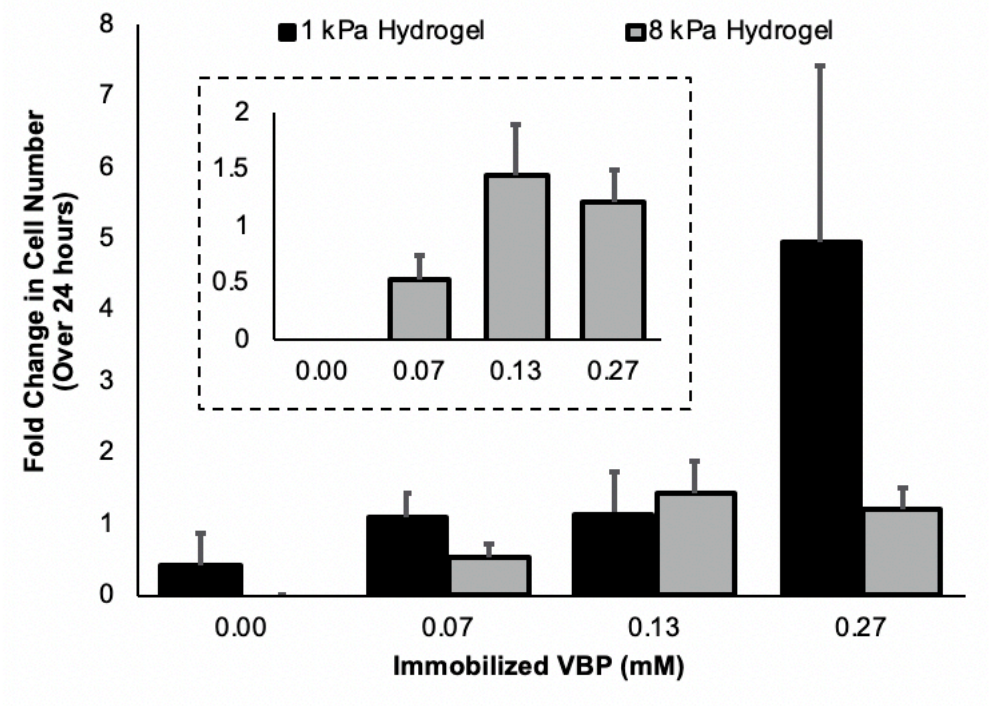

Figure 5.4. Hydrogels presenting 0.27 mM VBP increased hMSC expansion (indicated by fold change in cell number) on both soft 1 kPa and stiff 8 kPa hydrogel substrates in TheraPEAK XF SF culture. Note this increased expansion was not induced by growth factors additionally supplemented in the growth medium.

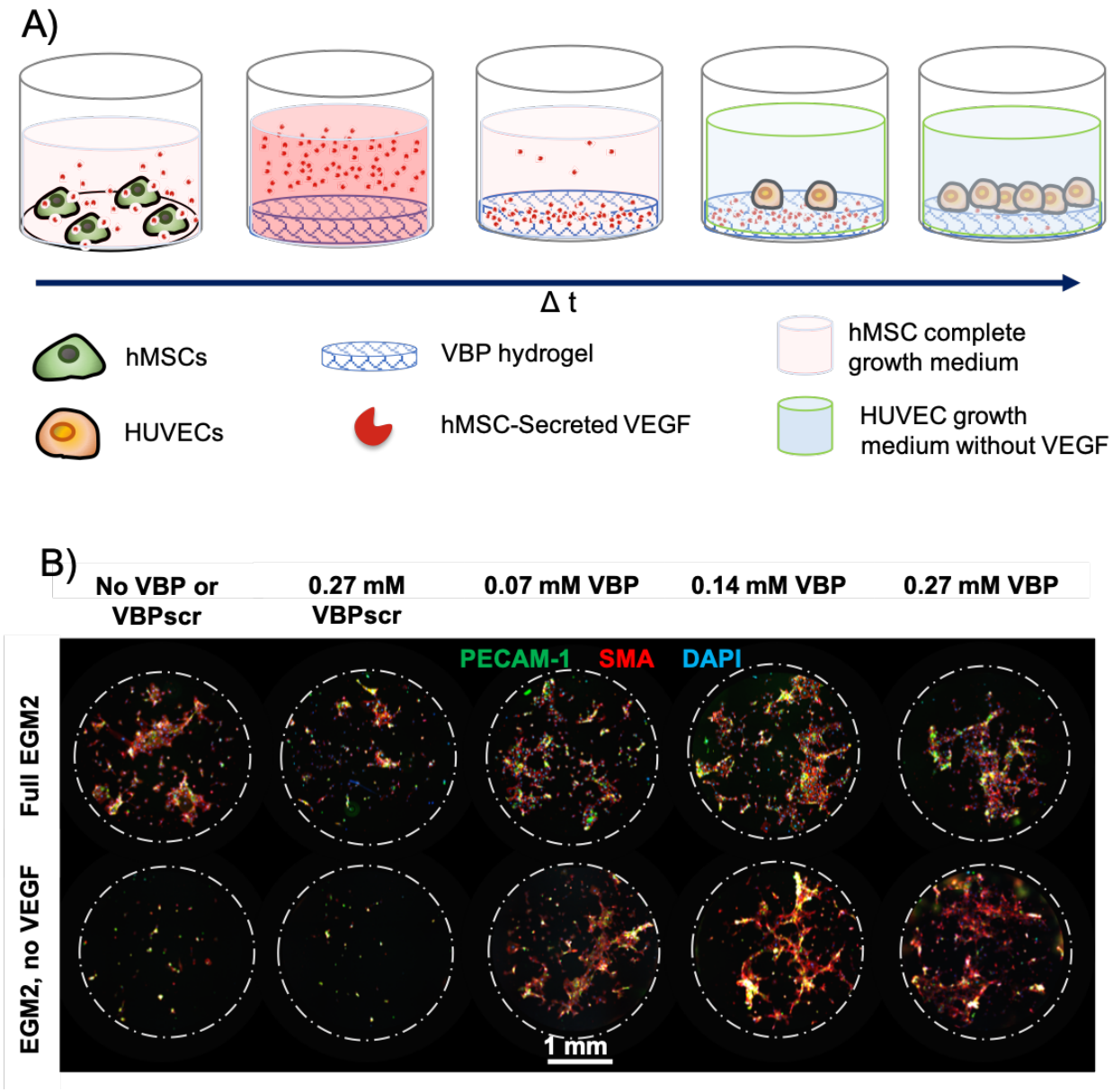

Figure 5.5. Hydrogels presenting VBP A) sequestered hMSC-secreted VEGF from hMSC-conditioned media for B) paracrine regulation of HUVEC proliferation in VEGF-starved culture.

5.10 Supporting Information

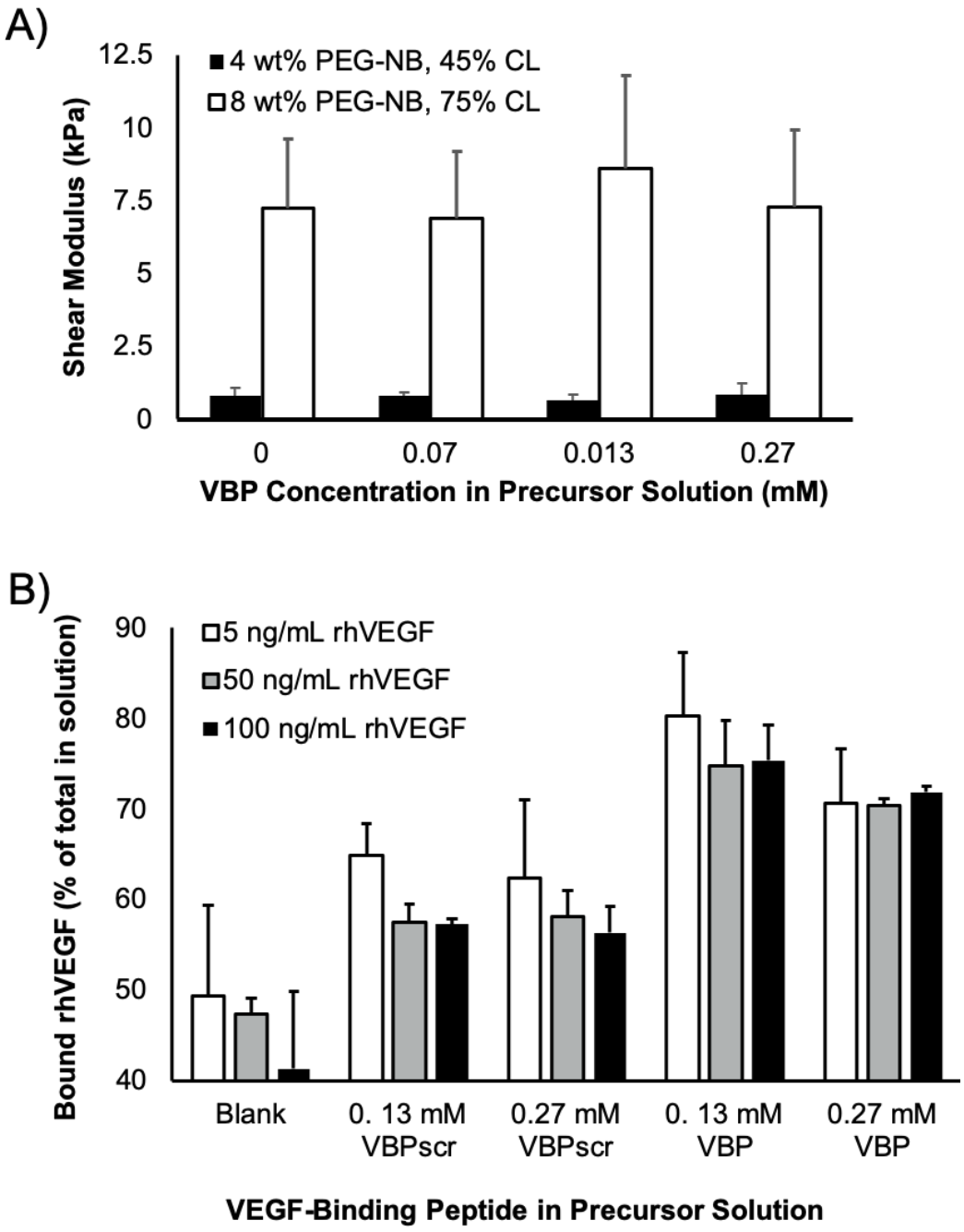

Figure 5.S1. VBP incorporated into the hydrogel network A) did not alter the ability the control substrate stiffness, but did B) enable rhVEGF sequestering to levels above what could be achieved with blank Cyclic RGDf- and negative binding control VBPscr-containing hydrogel substrates.

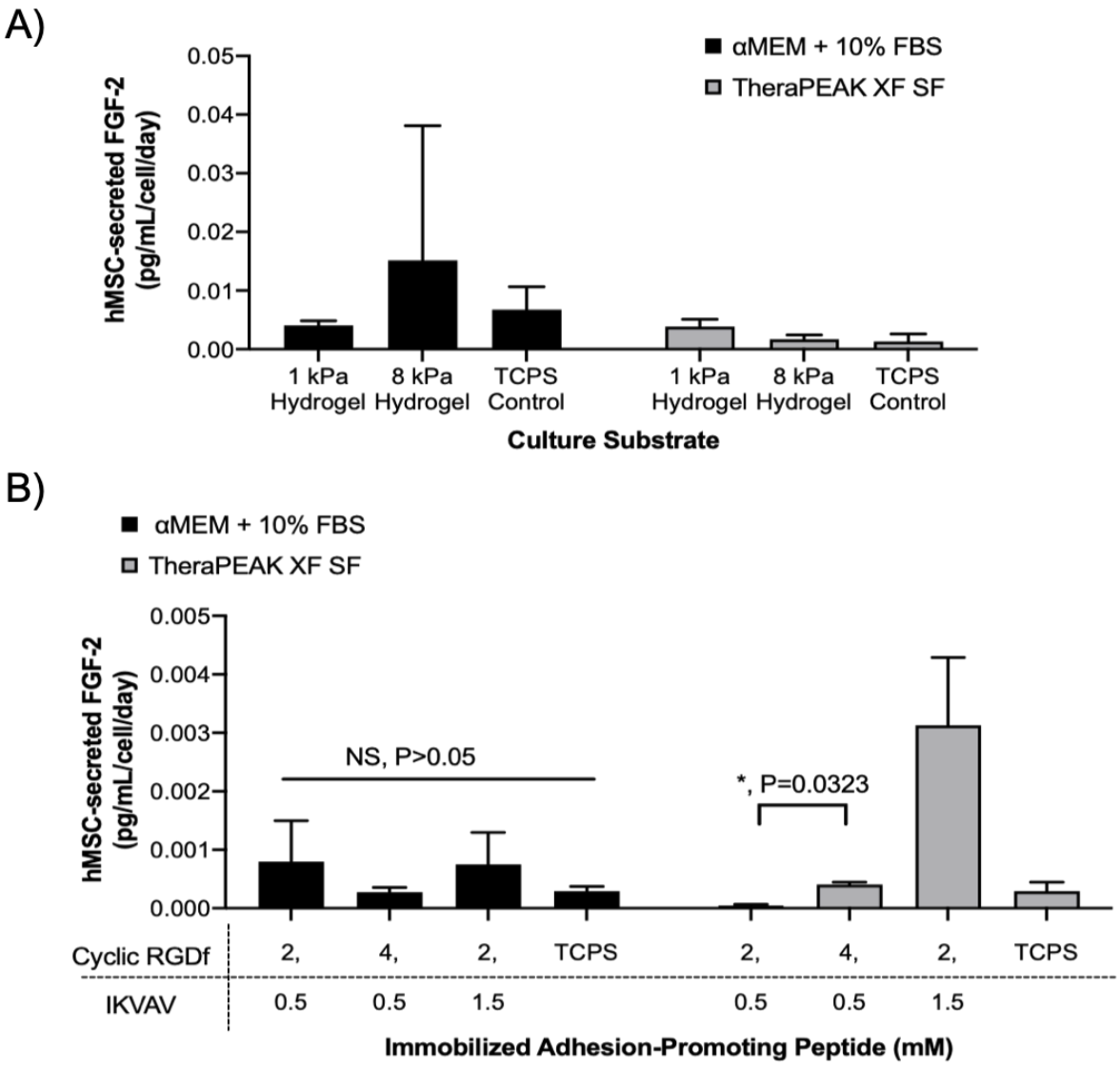

Figure 5.S2. Changing hydrogel substrate A) stiffness and B) adhesivity did not significantly affect hMSC-secreted FGF-2 concentration detected in hMSC-conditioned media.

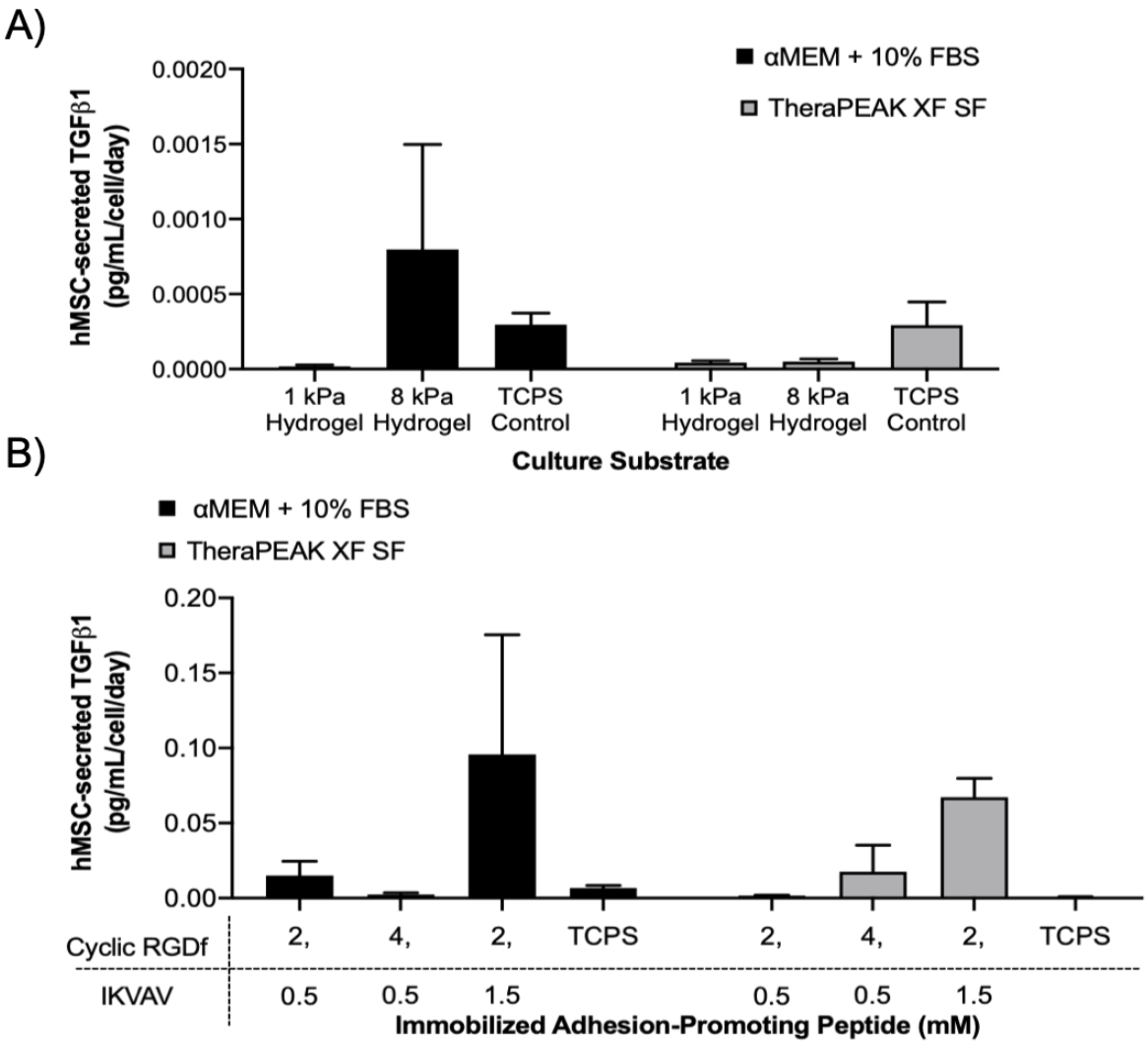

Figure 5.S3. Changing hydrogel substrate A) stiffness and B) adhesivity did not significantly affect hMSC-secreted TGFβ1 concentration detected in hMSC-conditioned media.

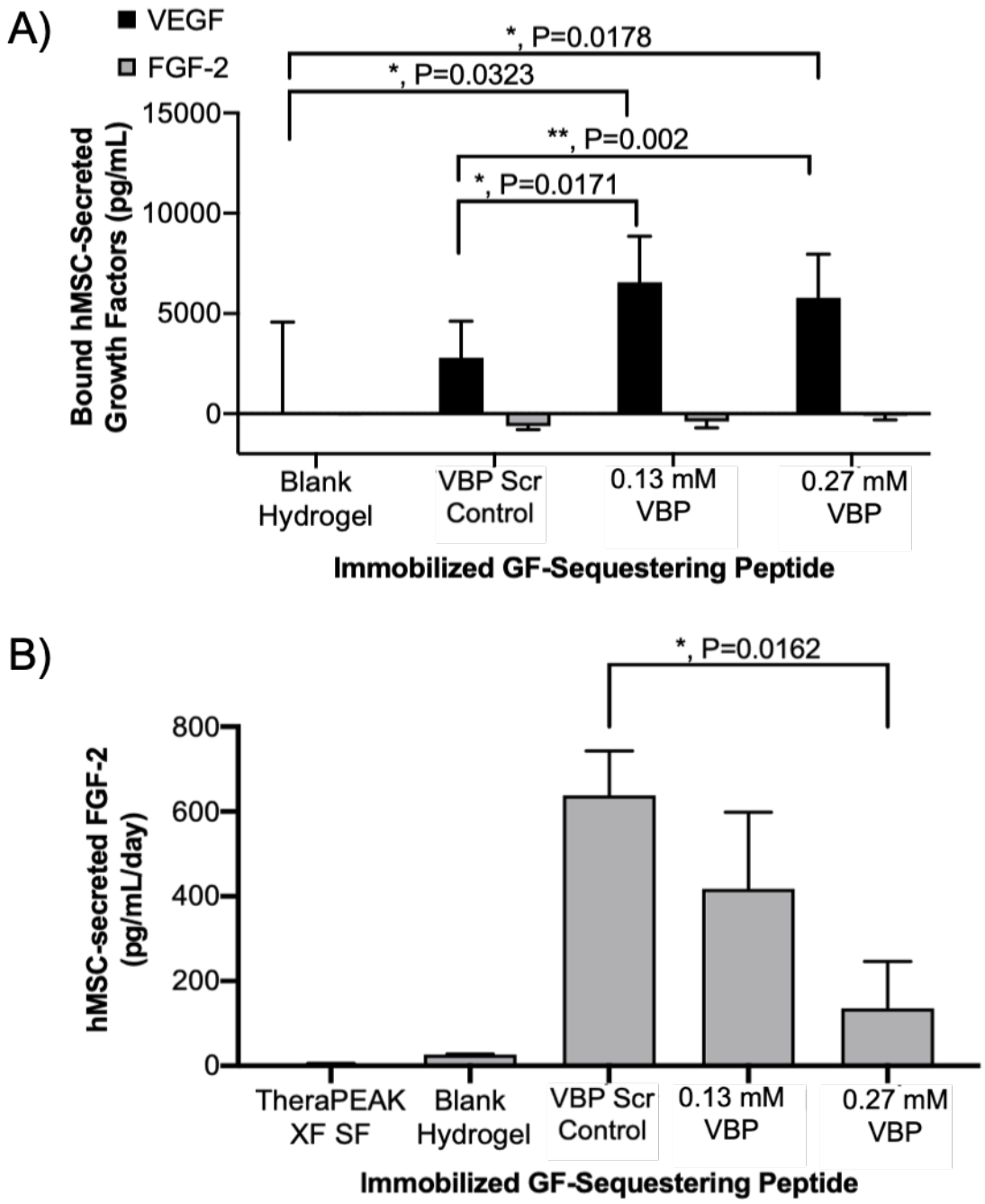

Figure 5.S4. Hydrogels presenting increasing concentrations of VBP A) sequestered increasing concentrations of hMSC-secreted VEGF but not FGF-2. B) Increasing VBPscr concentrations in hydrogel substrates resulted in increased FGF-2 secretion.

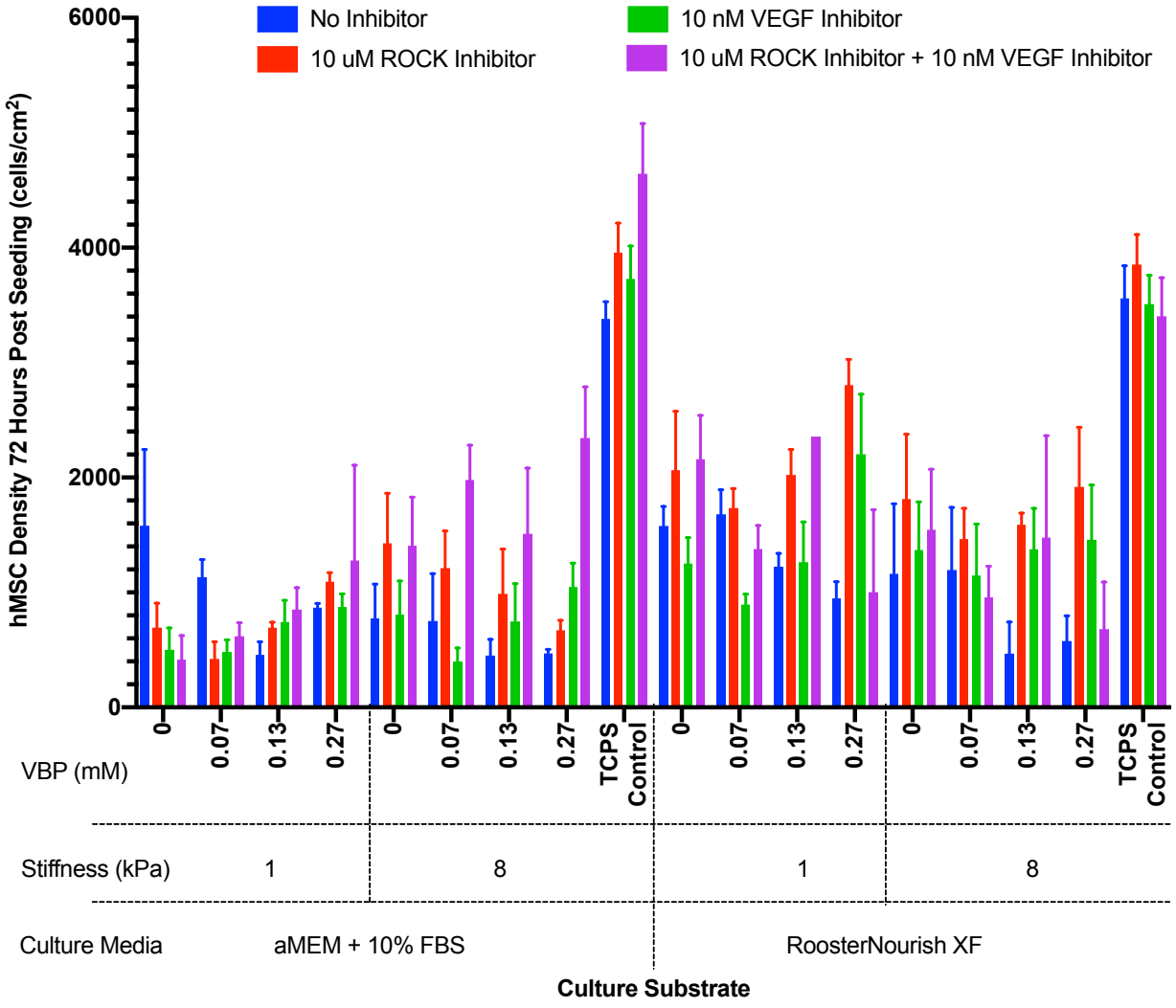

Figure 5.S5. Addition of ROCK inhibitor increased hMSC retention at 72 hours after seeding for all hydrogel substrates (regardless of substrate stiffness or VBP concentration) in RoosterNourish XF media.

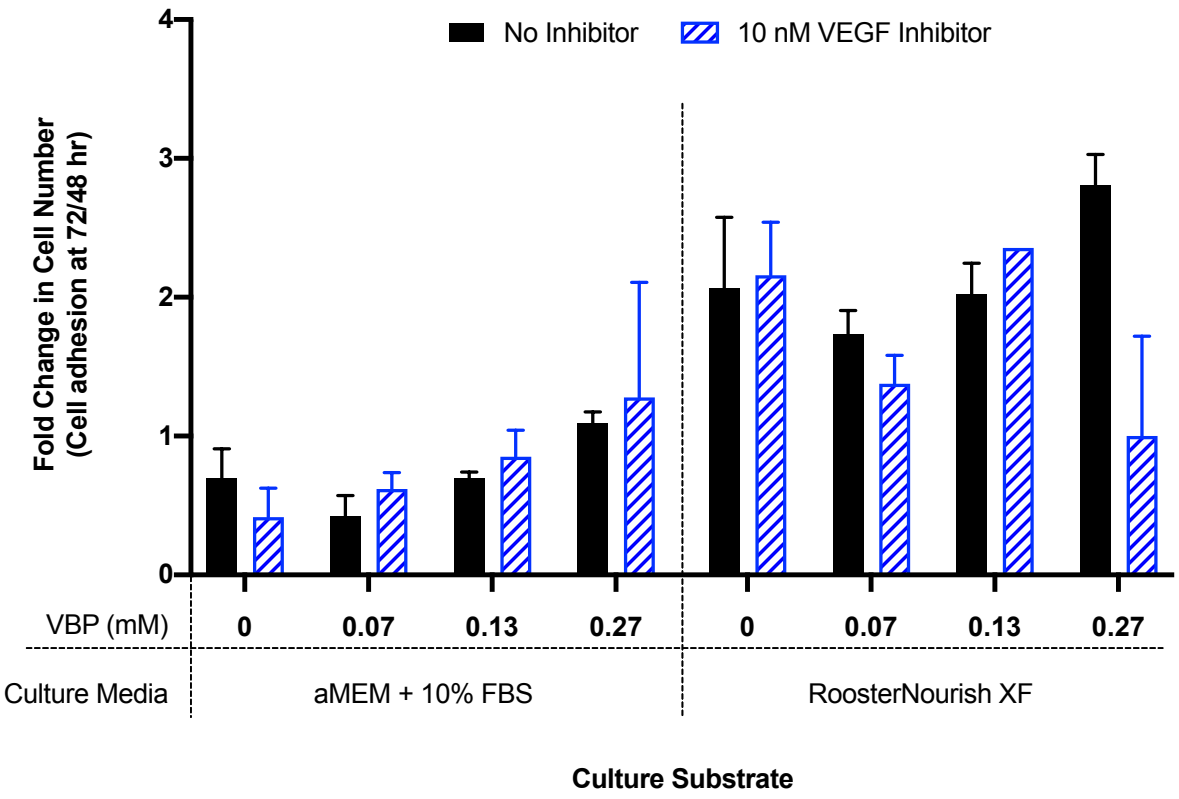

Figure 5.S6. VBP-mediated increase in hMSC expansion on 1 kPa hydrogels culture in RoosterNourish XF medium was mitigated in the presence of VEGF receptor signaling inhibitor (SU5416).

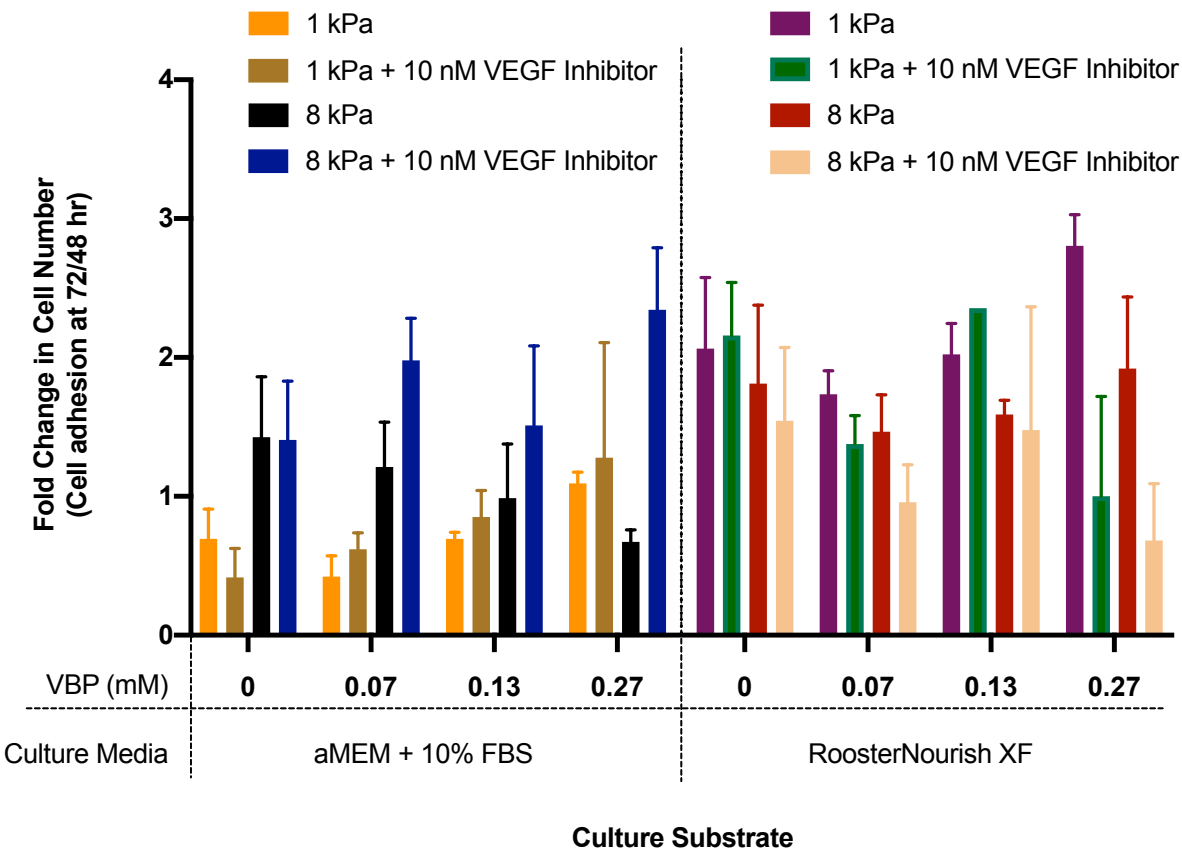

Figure 5.S7. VBP-mediated increase in hMSC expansion was more pronounced for hMSCs cultured on 1 kPa hydrogel stiffness. VEGF signaling dependence was observed in RoosterNourish XF culture but not in αMEM + 10% FBS culture.

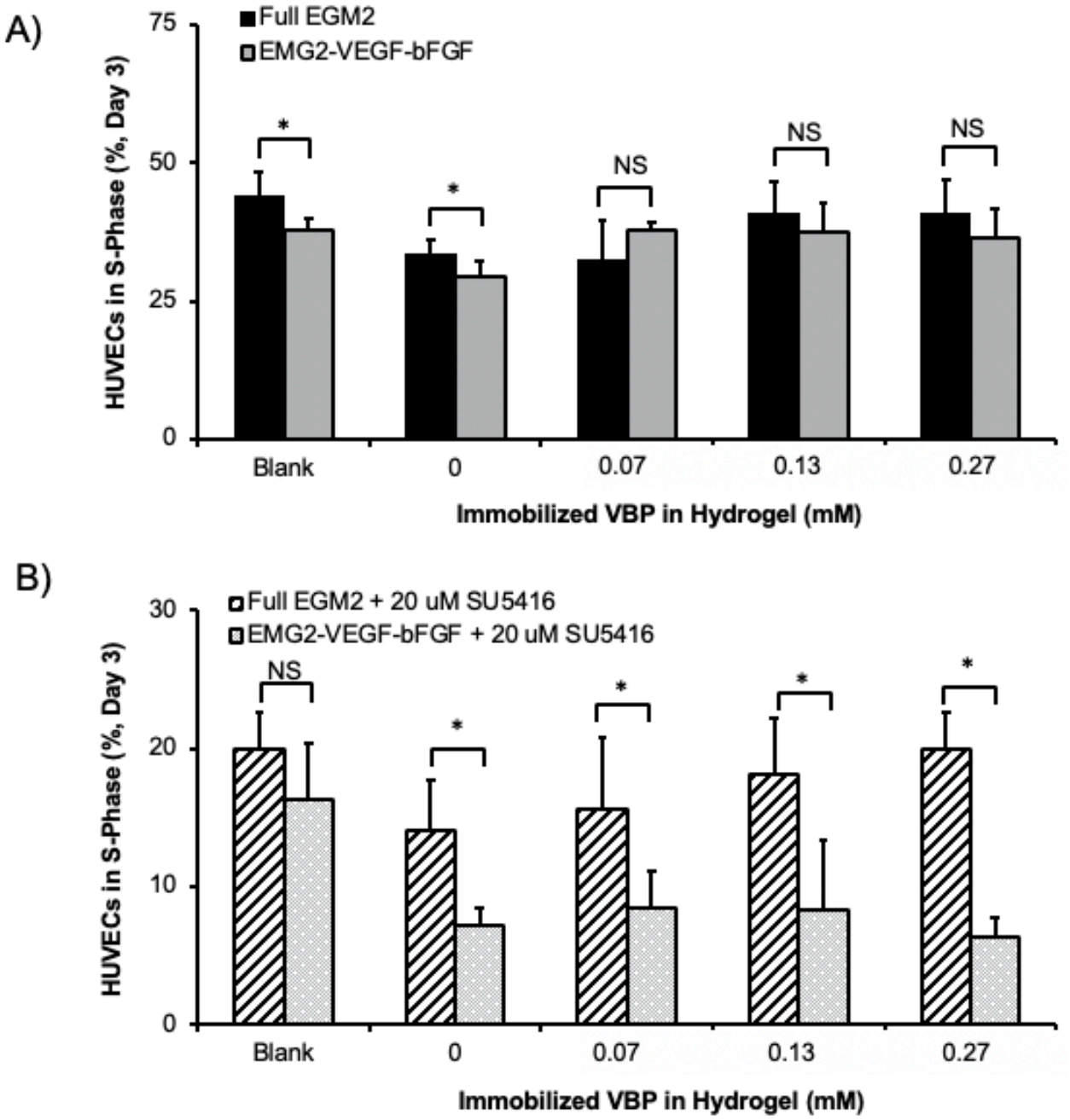

Figure 5.S8. Hydrogels presenting VBP A) rescued HUVEC proliferation during VEGF and FGF-2 starvation. B) VBP-mediated HUVEC proliferation was mitigated in the presence of VEGF receptor signaling inhibitor (SU5416).

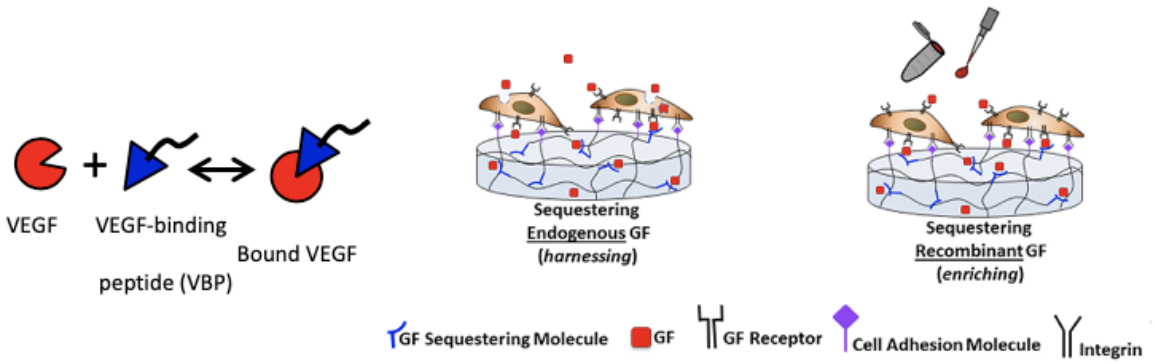

Figure 5.S9. Hydrogels presenting VBP potentially harnessed endogenous, cell-secreted VEGF or enriched recombinant VEGF already found in the growth media.

5.11 References

[1] M. Rodrigues, L.G. Griffith, A. Wells, Growth factor regulation of proliferation and survival of multipotential stromal cells, Stem Cell Research & Therapy 1(4) (2010) 32-32.

[2] M.F. Pittenger, A.M. Mackay, S.C. Beck, R.K. Jaiswal, R. Douglas, J.D. Mosca, M.A. Moorman, D.W. Simonetti, S. Craig, D.R. Marshak, Multilineage Potential of Adult Human Mesenchymal Stem Cells, Science 284(5411) (1999) 143-147.

[3] G. Chamberlain, J. Fox, B. Ashton, J. Middleton, Concise Review: Mesenchymal Stem Cells: Their Phenotype, Differentiation Capacity, Immunological Features, and Potential for Homing, STEM CELLS 25(11) (2007) 2739-2749.

[4] K. Wingate, M. Floren, Y. Tan, P.O.N. Tseng, W. Tan, Synergism of Matrix Stiffness and Vascular Endothelial Growth Factor on Mesenchymal Stem Cells for Vascular Endothelial Regeneration, Tissue Engineering. Part A 20(17-18) (2014) 2503-2512.

[5] S.B. Traphagen, I. Titushkin, S. Sun, K.K. Wary, M. Cho, Endothelial invasive response in a co-culture model with physically-induced osteodifferentiation, Journal of Tissue Engineering and Regenerative Medicine 7(8) (2013) 621-630.

[6] A.A. Abdeen, J.B. Weiss, J. Lee, K.A. Kilian, Matrix Composition and Mechanics Direct Proangiogenic Signaling from Mesenchymal Stem Cells, Tissue Engineering. Part A 20(19-20) (2014) 2737-2745.

[7] I.A. Potapova, G.R. Gaudette, P.R. Brink, R.B. Robinson, M.R. Rosen, I.S. Cohen, S.V. Doronin, Mesenchymal Stem Cells Support Migration, Extracellular Matrix Invasion, Proliferation, and Survival of Endothelial Cells In Vitro, STEM CELLS 25(7) (2007) 1761-1768.

[8] G. Adas, B. Koc, M. Adas, G. Duruksu, C. Subasi, O. Kemik, A. Kemik, D. Sakiz, M. Kalayci, S. Purisa, S. Unal, E. Karaoz, Effects of mesenchymal stem cells and VEGF on liver regeneration following major resection, Langenbecks Arch Surg 401(5) (2016) 725-40.

[9] C. Penna, M.-G. Perrelli, J.-P. Karam, C. Angotti, C. Muscari, C.N. Montero-Menei, P. Pagliaro, Pharmacologically active microcarriers influence VEGF-A effects on mesenchymal stem cell survival, Journal of Cellular and Molecular Medicine 17(1) (2013) 192-204.

[10] J. Pons, Y. Huang, J. Arakawa-Hoyt, D. Washko, J. Takagawa, J. Ye, W. Grossman, H. Su, VEGF improves survival of mesenchymal stem cells in infarcted hearts, Biochemical and Biophysical Research Communications 376(2) (2008) 419-422.

[11] Y.Y. Lipsitz, W.D. Milligan, I. Fitzpatrick, E. Stalmeijer, S.S. Farid, K.Y. Tan, D. Smith, R. Perry, J. Carmen, A. Chen, C. Mooney, J. Fink, A roadmap for cost-of-goods planning to guide economic production of cell therapy products, Cytotherapy 19(12) (2017) 1383-1391.

[12] M.M.L. Deckers, M. Karperien, C. van der Bent, T. Yamashita, S.E. Papapoulos, C.W.G.M. Löwik, Expression of Vascular Endothelial Growth Factors and Their Receptors during Osteoblast Differentiation, Endocrinology 141(5) (2000) 1667-1674.

[13] H. Mayer, H. Bertram, W. Lindenmaier, T. Korff, H. Weber, H. Weich, Vascular endothelial growth factor (VEGF-A) expression in human mesenchymal stem cells: Autocrine and paracrine role on osteoblastic and endothelial differentiation, Journal of Cellular Biochemistry 95(4) (2005) 827-839.

[14] T. Furumatsu, Z.N. Shen, A. Kawai, K. Nishida, H. Manabe, T. Oohashi, H. Inoue, Y. Ninomiya, Vascular Endothelial Growth Factor Principally Acts as the Main Angiogenic Factor in the Early Stage of Human Osteoblastogenesis, Journal of Biochemistry 133(5) (2003) 633-639.

[15] I. Aizman, D. Vinodkumar, M. McGrogan, D. Bates, Cell Injury-Induced Release of Fibroblast Growth Factor 2: Relevance to Intracerebral Mesenchymal Stromal Cell Transplantations, Stem Cells and Development 24(14) (2015) 1623-1634.

[16] B. Johnstone, T.M. Hering, A.I. Caplan, V.M. Goldberg, J.U. Yoo, In VitroChondrogenesis of Bone Marrow-Derived Mesenchymal Progenitor Cells, Experimental Cell Research 238(1) (1998) 265-272.

[17] P.T. Lee, W.-J. Li, Chondrogenesis of Embryonic Stem Cell-Derived Mesenchymal Stem Cells Induced by TGFβ1 and BMP7 Through Increased TGFβ Receptor Expression and Endogenous TGFβ1 Production, Journal of Cellular Biochemistry (2016) n/a-n/a.

[18] F.P. Seib, M. Prewitz, C. Werner, M. Bornhauser, Matrix elasticity regulates the secretory profile of human bone marrow-derived multipotent mesenchymal stromal cells (MSCs), Biochem Biophys Res Commun 389(4) (2009) 663-7.

[19] F.P. Seib, M. Prewitz, C. Werner, M. Bornhäuser, Matrix elasticity regulates the secretory profile of human bone marrow-derived multipotent mesenchymal stromal cells (MSCs), Biochemical and Biophysical Research Communications 389(4) (2009) 663-667.

[20] V.V. Rao, M.K. Vu, H. Ma, A.R. Killaars, K.S. Anseth, Rescuing mesenchymal stem cell regenerative properties on hydrogel substrates post serial expansion, Bioengineering & Translational Medicine (2018).

[21] T.H. Qazi, D.J. Mooney, G.N. Duda, S. Geissler, Biomaterials that promote cell-cell interactions enhance the paracrine function of MSCs, Biomaterials 140 (2017) 103-114.

[22] R.A. Marklein, D.E. Soranno, J.A. Burdick, Magnitude and presentation of mechanical signals influence adult stem cell behavior in 3-dimensional macroporous hydrogels, Soft Matter 8(31) (2012) 8113-8120.

[23] S. Nonnis, E. Maffioli, L. Zanotti, F. Santagata, A. Negri, A. Viola, S. Elliman, G. Tedeschi, Effect of fetal bovine serum in culture media on MS analysis of mesenchymal stromal cells secretome, EuPA Open Proteomics 10 (2016) 28-30.

[24] E.H. Nguyen, M.R. Zanotelli, M.P. Schwartz, W.L. Murphy, Differential effects of cell adhesion, modulus and VEGFR-2 inhibition on capillary network formation in synthetic hydrogel arrays, Biomaterials 35(7) (2014) 2149-61.

[25] B.D. Fairbanks, M.P. Schwartz, A.E. Halevi, C.R. Nuttelman, C.N. Bowman, K.S. Anseth, A Versatile Synthetic Extracellular Matrix Mimic via Thiol-Norbornene Photopolymerization, Advanced Materials 21(48) (2009) 5005-5010.

[26] M.W. Toepke, N.A. Impellitteri, J.M. Theisen, W.L. Murphy, Characterization of Thiol-Ene Crosslinked PEG Hydrogels, Macromolecular materials and engineering 298(6) (2013) 699-703.

[27] N.N.T. Le, S. Zorn, S.K. Schmitt, P. Gopalan, W.L. Murphy, Hydrogel arrays formed via differential wettability patterning enable combinatorial screening of stem cell behavior, Acta Biomaterialia (2015).

[28] E. Nguyen, W. Daly, N.N. Le, M. Farnoodian, D. Belair, M. Schwartz, C. S. Lebakken, G. E. Ananiev, M.A. Saghiri, T. Knudsen, N. Sheibani, W. Murphy, Versatile synthetic alternatives to Matrigel for vascular toxicity screening and stem cell expansion, 2017.

[29] S. Lin, N. Sangaj, T. Razafiarison, C. Zhang, S. Varghese, Influence of physical properties of biomaterials on cellular behavior, Pharmaceutical research 28(6) (2011) 1422-30.

[30] N.A. Peppas, E.W. Merrill, Poly(vinyl Alcohol) Hydrogels: Reinforcement of radiation-crosslinked networks by crystallization, Journal of Polymer Science 14(2) (1976) 441-457.

[31] T. Canal, N.A. Peppas, Correlation between mesh size and equilibrium degree of swelling of polymeric networks, Journal of Biomedical Materials Research 23(10) (1989) 1183-1193.

[32] M. Parlato, S. Reichert, N. Barney, W.L. Murphy, Poly(ethylene glycol) Hydrogels with Adaptable Mechanical and Degradation Properties for Use in Biomedical Applications, Macromolecular Bioscience 14(5) (2014) 687-698.

[33] M.W. Toepke, N.A. Impellitteri, S.K. Lan Levengood, D.S. Boeldt, I.M. Bird, W.L. Murphy, Regulating specific growth factor signaling using immobilized branched ligands, Advanced healthcare materials 1(4) (2012) 457-460.

[34] D.G. Belair, N.N. Le, W.L. Murphy, Regulating VEGF signaling in platelet concentrates via specific VEGF sequestering, Biomaterials Science 4(5) (2016) 819-825.

[35] D.G. Belair, M.J. Miller, S. Wang, S.R. Darjatmoko, B.Y.K. Binder, N. Sheibani, W.L. Murphy, Differential regulation of angiogenesis using degradable VEGF-binding microspheres, Biomaterials 93 (2016) 27-37.

[36] N.A. Impellitteri, M.W. Toepke, S.K. Lan Levengood, W.L. Murphy, Specific VEGF sequestering and release using peptide-functionalized hydrogel microspheres, Biomaterials 33(12) (2012) 3475-3484.

[37] D.G. Belair, W.L. Murphy, Specific VEGF sequestering to biomaterials: influence of serum stability, Acta biomaterialia 9(11) (2013) 8823-8831.

[38] Y. Bai, P. Li, G. Yin, Z. Huang, X. Liao, X. Chen, Y. Yao, BMP-2, VEGF and bFGF synergistically promote the osteogenic differentiation of rat bone marrow-derived mesenchymal stem cells, Biotechnol Lett 35(3) (2013) 301-308.

[39] Y. Yang, Q.H. Chen, A.R. Liu, X.P. Xu, J.B. Han, H.B. Qiu, Synergism of MSC-secreted HGF and VEGF in stabilising endothelial barrier function upon lipopolysaccharide stimulation via the Rac1 pathway, Stem Cell Res Ther 6 (2015) 250.

[40] D. Krakora, P. Mulcrone, M. Meyer, C. Lewis, K. Bernau, G. Gowing, C. Zimprich, P. Aebischer, C.N. Svendsen, M. Suzuki, Synergistic effects of GDNF and VEGF on lifespan and disease progression in a familial ALS rat model, Mol Ther 21(8) (2013) 1602-10.

[41] K. Ogata, M. Matsumura, M. Moriyama, W. Katagiri, H. Hibi, S. Nakamura, Cytokine Mixtures Mimicking Secretomes From Mesenchymal Stem Cells Improve Medication-Related Osteonecrosis of the Jaw in a Rat Model, JBMR Plus 2(2) (2018) 69-80.

[42] H.M. Kwon, S.M. Hur, K.Y. Park, C.K. Kim, Y.M. Kim, H.S. Kim, H.C. Shin, M.H. Won, K.S. Ha, Y.G. Kwon, D.H. Lee, Y.M. Kim, Multiple paracrine factors secreted by mesenchymal stem cells contribute to angiogenesis, Vascul Pharmacol 63(1) (2014) 19-28.

[43] M. Papetti, J. Shujath, K.N. Riley, I.M. Herman, FGF-2 Antagonizes the TGF-β1-Mediated Induction of Pericyte α-Smooth Muscle Actin Expression: A Role for Myf-5 and Smad-Mediated Signaling Pathways, Investigative Opthalmology & Visual Science 44(11) (2003).

[44] R. Chinnadurai, D. Rajan, M. Qayed, D. Arafat, M. Garcia, Y. Liu, S. Kugathasan, L.J. Anderson, G. Gibson, J. Galipeau, Potency Analysis of Mesenchymal Stromal Cells Using a Combinatorial Assay Matrix Approach, Cell Rep 22(9) (2018) 2504-2517.

[45] A. De Boeck, A. Hendrix, D. Maynard, M. Van Bockstal, A. Daniëls, P. Pauwels, C. Gespach, M. Bracke, O. De Wever, Differential secretome analysis of cancer-associated fibroblasts and bone marrow-derived precursors to identify microenvironmental regulators of colon cancer progression, PROTEOMICS 13(2) (2013) 379-388.

[46] D.E. Discher, D.J. Mooney, P.W. Zandstra, Growth Factors, Matrices, and Forces Combine and Control Stem Cells, Science 324(5935) (2009) 1673.

[47] L.F. Mendes, W.L. Tam, Y.C. Chai, L. Geris, F.P. Luyten, S.J. Roberts, Combinatorial Analysis of Growth Factors Reveals the Contribution of Bone Morphogenetic Proteins to

Chondrogenic Differentiation of Human Periosteal Cells, Tissue Engineering Part C: Methods 22(5) (2016) 473-486.

[48] W.L. Murphy, N.N. Le, S. Zorn, M.P. Schwartz, E.H.N. Nguyen, Method for forming hydrogel arrays using surfaces with differential wettability, in: USPTO (Ed.) Wisconsin Alumni Research Foundation, United States, 2019, p. 9.

[49] G.A. Hudalla, J.T. Koepsel, W.L. Murphy, Surfaces That Sequester Serum-Borne Heparin Amplify Growth Factor Activity, Advanced Materials 23(45) (2011) 5415-5418.

[50] G.A. Hudalla, N.A. Kouris, J.T. Koepsel, B.M. Ogle, W.L. Murphy, Harnessing endogenous growth factor activity modulates stem cell behavior, Integrative Biology 3(8) (2011) 832-842.

5.12 Appendix

5.12.1 Patent (No: US 9,688,957; Issued: June 27, 2017)- Hydrogel compositions for use in promoting tubulogenesis

US009688957B2

(12) **United States Patent**
Murphy et al.

(10) **Patent No.: US 9,688,957 B2**
(45) **Date of Patent: *Jun. 27, 2017**

(54) **HYDROGEL COMPOSITIONS FOR USE IN PROMOTING TUBULOGENESIS**

(71) Applicant: **Wisconsin Alumni Research Foundation**, Madison, WI (US)

(72) Inventors: **William L. Murphy**, Waunakee, WI (US); **Ngoc Nhi Le**, Norcross, GA (US); **Michael P. Schwartz**, Madison, WI (US); **Eric Huy Dang Nguyen**, Madison, WI (US); **Stefan Zorn**, Madison, WI (US); **Hamisha Ardalani**, Madison, WI (US); **Matthew Zanotelli**, Muskego, WI (US); **Matthew Brian Parlato**, Madison, WI (US); **David Gregory Belair**, Madison, WI (US); **William T. Daly**, Madison, WI (US)

(73) Assignee: **Wisconsin Alumni Research Foundation**, Madison, WI (US)

(*) Notice: Subject to any disclaimer, the term of this patent is extended or adjusted under 35 U.S.C. 154(b) by 0 days.

This patent is subject to a terminal disclaimer.

(21) Appl. No.: **14/684,062**

(22) Filed: **Apr. 10, 2015**

(65) **Prior Publication Data**

US 2015/0291929 A1 Oct. 15, 2015

Related U.S. Application Data

(60) Provisional application No. 61/978,032, filed on Apr. 10, 2014.

(51) **Int. Cl.**

C12N 5/00	(2006.01)
C12N 5/0735	(2010.01)
G01N 33/483	(2006.01)
B01J 19/00	(2006.01)
G01N 21/64	(2006.01)

(52) **U.S. Cl.**

CPC ***C12N 5/0606*** (2013.01); ***G01N 33/4833*** (2013.01); *B01J 19/0046* (2013.01); *B01J 2219/00596* (2013.01); *C12N 2533/20* (2013.01); *C12N 2533/30* (2013.01); *C12N 2537/10* (2013.01); *G01N 21/6452* (2013.01); *G01N 2610/00* (2013.01)

(58) **Field of Classification Search**

CPC C12N 5/0606

See application file for complete search history.

(56) **References Cited**

U.S. PATENT DOCUMENTS

2005/0019843	A1	1/2005	Chen et al.
2012/0149781	A1	6/2012	Lee et al.
2012/0225814	A1	9/2012	Hanjaya-Putra et al.
2013/0210147	A1	8/2013	Jeannin et al.
2013/0260464	A1	10/2013	Vannier et al.
2013/0296177	A1	11/2013	Koepsel et al.
2014/0017284	A1	1/2014	Yang et al.
2014/0018263	A1	1/2014	Levkin et al.
2015/0104812	A1	4/2015	Grevesse et al.

OTHER PUBLICATIONS

Shih et al. Biomacromolecules, 2012, 13:2003-2012.*

Kyburz et al., Three-dimensional hMSC motility within peptide-functionalized PEG-based hydrogels of varying adhesivity and crosslinking density, Acta Biomaterialia, vol. 9, No. 5, pp. 6381-6392, 2013.

Leslie-Barbick et al., The promotion of microvasculature formation in poly(ethylene glycol) diacrylate hydrogels by an immobilized VEGF-mimetic peptide, Biomaterials, vol. 32, No. 25, pp. 5782-5789, 2011.

Love et al., Self-Assembled Monolayers of Thiolates on Metals as a Form of Nanotechnology, Chem. Rev. 2005, 105:1103-1169.

Strolher et al., Synthesis and Characterization of DNA-Modified Silicon (III) Surfaces, J. Am. Chem. Soc. 2000, 122:1205-1209.

Schwartz et al., , Chemical modification of silicon surfaces for biological applications, 2005 Phys. Stat. Sol. (a) 202 (8):1380-1384.

Strother et al., Photochemical Functionalization of Diamond Films, Langmuir, 2002, 18:968-971.

Polizzotti et al., Three-Dimensional Biochemical Patterning of Click-Based Composit Hydrogels via Thiolene Photopolymerization, Biomacromolecules 2008, 9:1084-1087.

Fairbanks et al., A Versatile Synthetic Extracellular Matrix Mimic via Thiol-Norbornene Photopolymerization, Adv. Mater. 2009, 21:5005-5010.

Nagase and Fields, Human Matrix Metalloproteinase Specificity Studies Using Collagen Sequence-Based Synthetic Peptides, Biopolymers 1996, 40:399-416.

Toepke et al., Characterization of Thiol-Ene Crosslinked PEG Hydrogels, 2013, Macromol. Mater. Eng., 298:699-703.

Impellitteri et al., Specific VEGF sequestering and release using peptide-functionalized hydrogel microspheres, Biomaterials 2012, 33:3475-84.

Belair and Murphy, Specific VEGF sequestering to biomaterials: Influence of serum stability, Acta Biomater, 2013.

Gould et al., Small Peptide Functionalized Thiol-Ene Hydrogels as Culture Substrates for Understanding Valvular Interstitial Cell Activation and de novo Tissue Deposition, Acta Biomater 2012, 8:3201-3209.

Seo et al., Attachment of hydrogel microstructures and proteins to glass via thiol-terminated silanes, Colloids Surf B Biointerfaces 2012, 98:1-6.

(Continued)

Primary Examiner — Bin Shen

(74) *Attorney, Agent, or Firm* — Stinson Leonard Street LLC

(57) **ABSTRACT**

Hydrogel Compositions and methods of using hydrogel compositions are disclosed. Advantageously, the hydrogel compositions offer the ability to rapidly screen substrate components for influencing cell attachment, spreading, proliferation, migration, and differentiation. In particularly suitable embodiments, the hydrogel compositions of the present disclosure may be used to promote tubulogenesis of endothelial cells.

19 Claims, 52 Drawing Sheets
(19 of 52 Drawing Sheet(s) Filed in Color)

5.12.2 Patent (No: US 10,183,079; Issued: January 22, 2019)- Hydrogel microspheres containing peptide ligands for growth factor regulation in blood products

(12) **United States Patent**
Belair et al.

(10) **Patent No.: US 10,183,079 B2**
(45) **Date of Patent: Jan. 22, 2019**

(54) **HYDROGEL MICROSPHERES CONTAINING PEPTIDE LIGANDS FOR GROWTH FACTOR REGULATION IN BLOOD PRODUCTS**

(71) Applicant: **Wisconsin Alumni Research Foundation**, Madison, WI (US)

(72) Inventors: **David Belair**, Madison, WI (US); **Ngoc Nhi Le**, Norcross, GA (US); **Michael W. Toepke**, Midland, MI (US); **Nicholas Impellitteri**, Madison, WI (US); **Connie Sue Chamberlain**, Monona, WI (US); **William Leo Murphy**, Waunakee, WI (US)

(73) Assignee: **Wisconsin Alumni Research Foundation**, Madison, WI (US)

(*) Notice: Subject to any disclaimer, the term of this patent is extended or adjusted under 35 U.S.C. 154(b) by 0 days.

(21) Appl. No.: **15/074,493**

(22) Filed: **Mar. 18, 2016**

(65) **Prior Publication Data**

US 2017/0266318 A1 Sep. 21, 2017

(51) **Int. Cl.**

A61K 38/17	(2006.01)
A61K 47/48	(2006.01)
A61K 47/60	(2017.01)
A61K 47/69	(2017.01)

(52) **U.S. Cl.**

CPC ***A61K 47/48784*** (2013.01); ***A61K 38/179*** (2013.01); ***A61K 47/48215*** (2013.01); ***A61K 47/60*** (2017.08); ***A61K 47/6903*** (2017.08); ***A61K 47/6927*** (2017.08); *C07K 2319/30* (2013.01); *C07K 2319/32* (2013.01)

(58) **Field of Classification Search**

None

See application file for complete search history.

(56) **References Cited**

PUBLICATIONS

Holmes et al. ("Vascular endothelial growth factor receptor-2: Structure, function, intracellular signaling and therapeutic inhibition" Cellular Signaling 19 (2007) 2003-2012).*

Of Sigma-Aldrich (8arm-PEG20K-Norbornene, tripentaerythritol core, Dec. 11, 2014).*

Parlato et al. (Acta biomater. Dec. 2013; 9(12):9270-9280).*

Belair et al., Serum-Dependence of Affintiy-Mediated VEGF Release from Biomimetic Microspheres, American Chemical Society, 2014, pp. 2038-2048.

Fairbanks et al., A Versatile Synthetic Extracellular Matrix Mimic via Thiol-Norbornene Photopolymerization, Adv Mater, 2009, vol. 21, No. 48, pp. 5005-5010.

Impellitteri et al., Specific VEGF sequestering and release using peptide-functionalized hydrogel microspheres, Biomaterials, 2012, vol. 33, No. 12, pp. 2475-3484.

Toepke et al., Regulating specific growth factor signaling using immobilized branched ligands, Adv Healthc Mater., 2012, vol. 1, No. 4, pp. 457-460.

* cited by examiner

Primary Examiner — Jennifer Pitrak McDonald
Assistant Examiner — Tara L Martinez
(74) *Attorney, Agent, or Firm* — Stinson Leonard Street LLP

(57) **ABSTRACT**

Vascular endothelial growth factor VEGF-sequestering hydrogel microspheres that have been prepared to selectively bind VEGF from blood products are disclosed herein. In one particular embodiment, the microspheres bind VEGF as part of an intra-operative process such that the growth factor can be removed from the blood products before the products are used in a clinical procedure.

13 Claims, 21 Drawing Sheets

Specification includes a Sequence Listing.

5.12.3 Figures: Hydrogel substrates presenting heparin and heparin-binding peptides for promiscuous GF sequestering

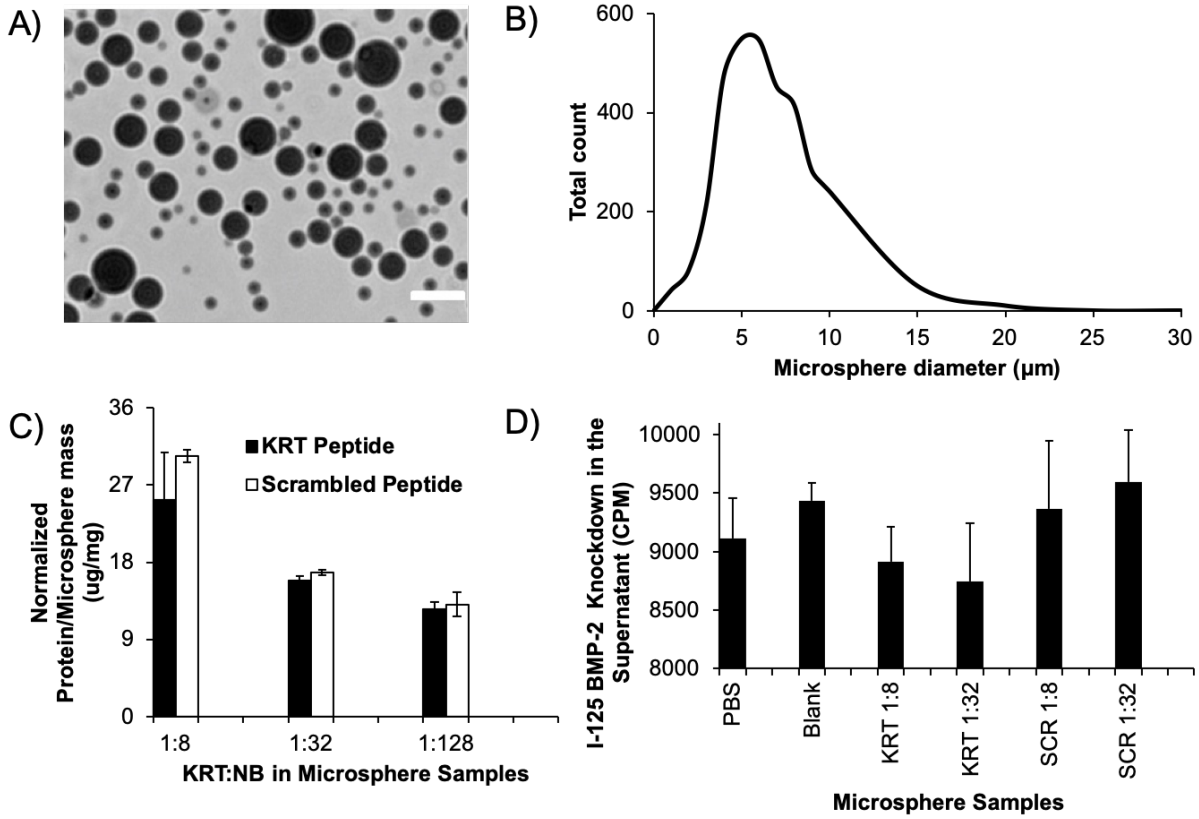

Figure 5.12.3.1. Hydrogel microspheres formed with a previously-published water-in-water emulsion technique using PEG-NB thiolene chemistry with immobilized heparin-binding peptide (KRT). A,B) Water-in-water emulsion technique resulted in micron-sized hydrogel microspheres for potential cell and/or growth factor sequestering and delivery applications. C) The concentration of immobilized peptide can be controlled by changing the concentration of molar ratios of KRT to total available norbornene groups in the precursor solution. D) Increasing molar ratio of KRT:NB in the precursor solution resulted in increasing KRT immobilization into the hydrogel microsphere network and, subsequently, increased ability to sequester BMP-2, a known heparin-binding growth factor, in the presence of heparin-containing FBS. This work built upon

microsphere formation techniques [47] and KRT-mediated GF sequestering insights previously published by our lab [49, 50].

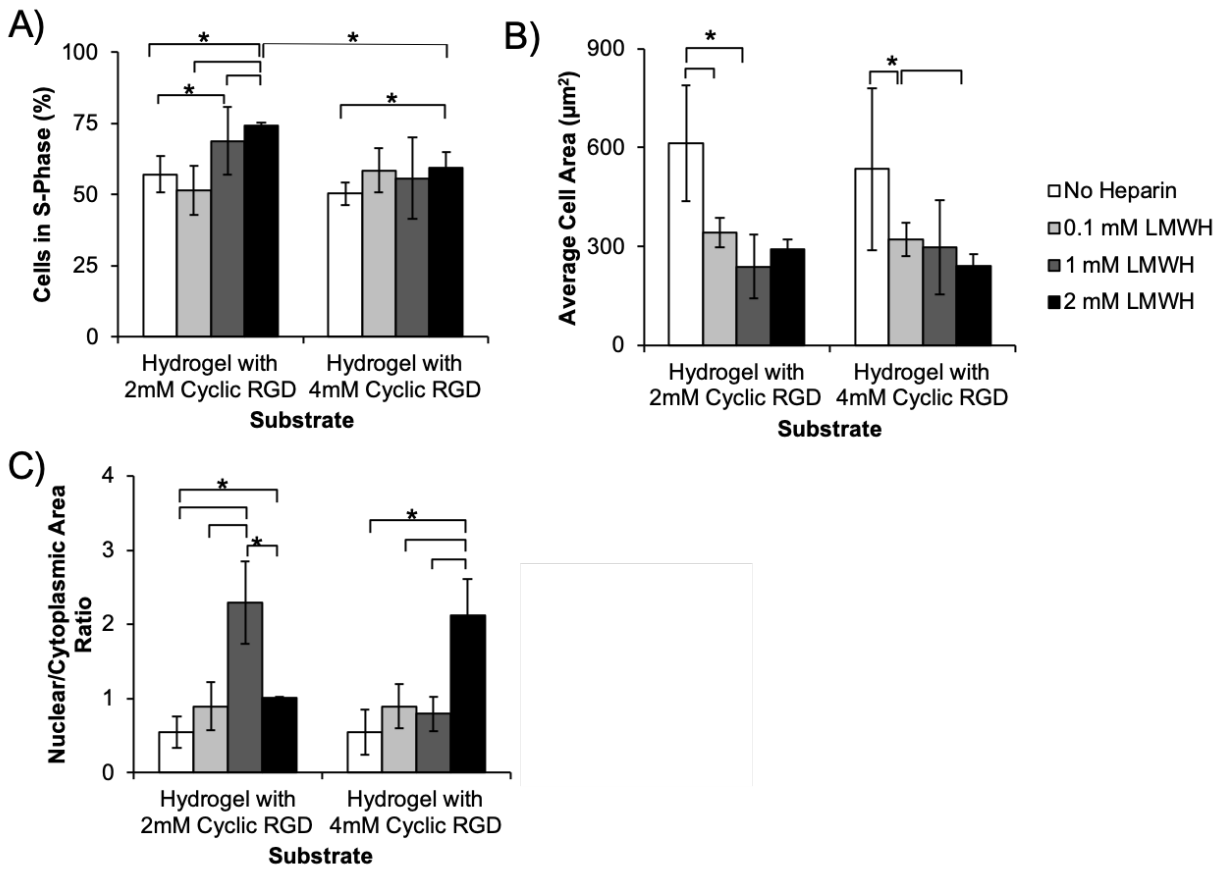

Figure 5.12.3.2. H1 hESC A) proliferation, B) cell area, and C) nuclear/cytoplasmic area ratio after 3 days of culture on Matrigel or PEG-NB hydrogels containing 2 or 4 mM immobilized Cyclic RGDf and varying concentrations of immobilized thiolated, low molecular weight heparin (LMWH). Asterisks indicate statistical significance as determined from two-tailed Student's t-test with α=0.05.

Chapter 6 – Conclusion and future outlook

6.1 Conclusion

In this thesis, we developed and utilized enhanced throughput screening methods and hydrogel array platform technologies for identifying customized biomaterials for cell culture. We demonstrated the ability to use a patented, benchtop-amenable hydrogel array formation approach to create screening arrays without need for liquid handling systems in order to decrease the barrier-to-entry for commercial translation to industry and dissemination to other researchers. We additionally employed that array technology in a design of experiment (DOE)-driven screening workflow to examine multiple bioinspired materials parameters (e.g. stiffness, adhesion, growth factor sequestering) to identify customized biomaterials substrates for functional serum-containing and serum-free human mesenchymal stromal cell (hMSC) expansion. Through screening, we identified several media- and cell-source agnostic hydrogel substrate compositions that support human-, mouse-, and iPS-derived MSC expansion using routine thaw, seed, and harvest protocols in order to increase potential for translation to and utility in hMSC biomanufacturing processes. Finally, we demonstrated the ability to use multivariate analysis (MVA) to determine the independent and combinatorial effects of culture parameters on hMSC expansion and used this insight to develop customized, growth factor sequestering biomaterials for inducing and controlling hMSC expansion without the need for additionally supplemented growth factors. While this “autocatalytic” material is currently not optimized for hMSC expansion at levels greater than what we can achieve on standard TCPS in fetal bovine serum (FBS)-containing media, this preliminary work demonstrated the potential to use the screening approach to develop and optimized customized growth factor sequestering materials for cell expansion as well as other biomanufacturing processes (e.g. secretome

generation, differentiation). Collectively, the studies detailed in this thesis demonstrated the ability to combine DOE-driven high throughput screening with what we currently understand about how cells interact with their environment in order to optimize materials for more robust, efficient, and effective cell biomanufacturing.

6.2 Future outlook

The screening approach and hydrogel array platform technologies employed here may be applied more broadly to design of materials for cell biomanufacturing, development of self-assembled organs-on-a-chip, and for materials that can be transplanted and/or co-delivered with cells for clinical applications. These specific broader applicability examples are chosen based on the preliminary works explored in current collaborations between our lab, several federal agencies (e.g. EPA, NIH, and NSF), as well as through consulting with Stem Pharm, a Madison-based startup that spun out of our lab and has licensed the patented technologies developed through this thesis work and mentioned in this document.

The current collaborations we have engaged in have revealed several additional steps needed to increase feasibility for broader translation of the platform technologies and customized substrates developed in this thesis. In this work, we have designed the studies and technologies in order to improve our fundamental understanding of how cells interact with and respond to their microenvironment. From this research-driven experimental and technological design, we have considered translatability and cost, but we are still far from the cost and scale needed for both commercial and clinical translation. For example, we currently rely on expensive peptides in order to confer bioactivity to our inert PEG-NB hydrogel networks. Though the use of peptides allows us to tightly regulate the signals presented to cells, thereby enabling the ability to

parse out the effects of individual culture parameters, the cost associated with these peptides, at the concentration in which we are using them, will limited their appeal. While we have been able to demonstrate that our chemically-defined substrates can perform several functions as well as TCPS standards, our materials are currently 10-fold more expensive than TCPS and are not likely to be widely utilized due to high switching cost.

Finally, while this work has produced some insights into the individual and combinatorial effects of culture parameters on cell behavior, the parameters, cell types, and cell behavior outputs explored here are limited. As mentioned in Chapter 2, cell signaling is context-dependent, therefore insights discussed here can be used to guide the development of other experiments but should not be applied literally and directly without consideration of context. Additionally, the work on inductive, autocatalytic biomaterials discussed in Chapter 5 is extremely preliminary and we have not explored the mechanisms underlying the behavior changes.

In the appendix of each chapter, we have presented published and unpublished work to demonstrate the broader applicability of the approaches and concepts discussed. Immediate steps for future work should expand upon the work in the appendices as well as emphasize understanding of the mechanisms regulating the substrate-mediated cell behavior changes explored here.